Particle identification in HEP experiments

Samo Korpar

University of Maribor and J. Stefan Institute, Ljubljana

ICFA School on Instrumentation in Elementary Particle & Nuclear Physics
TIFR, Mumbai, India, February 12th-25th, 2023

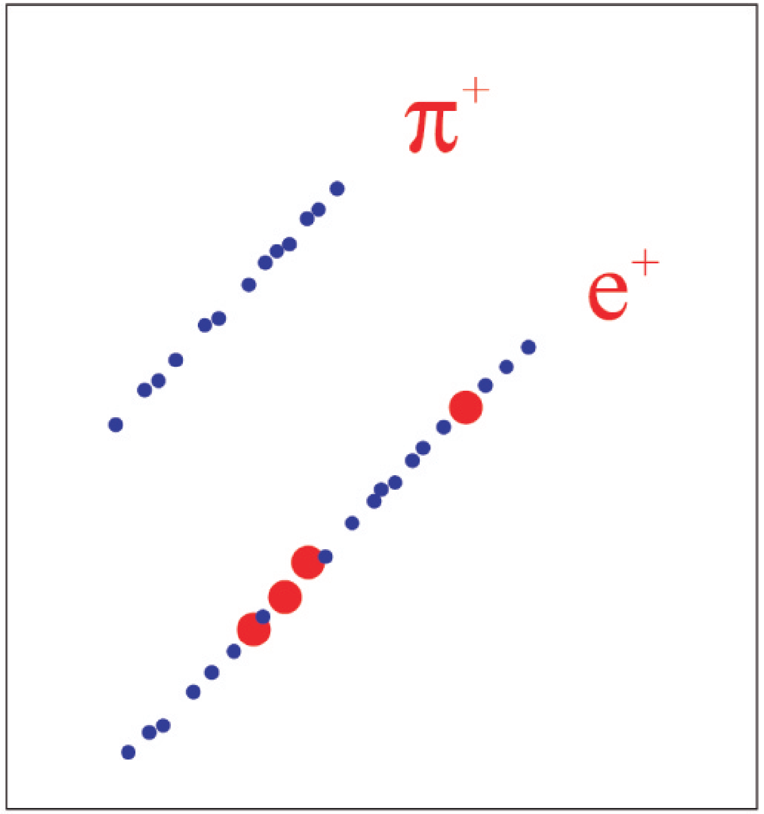

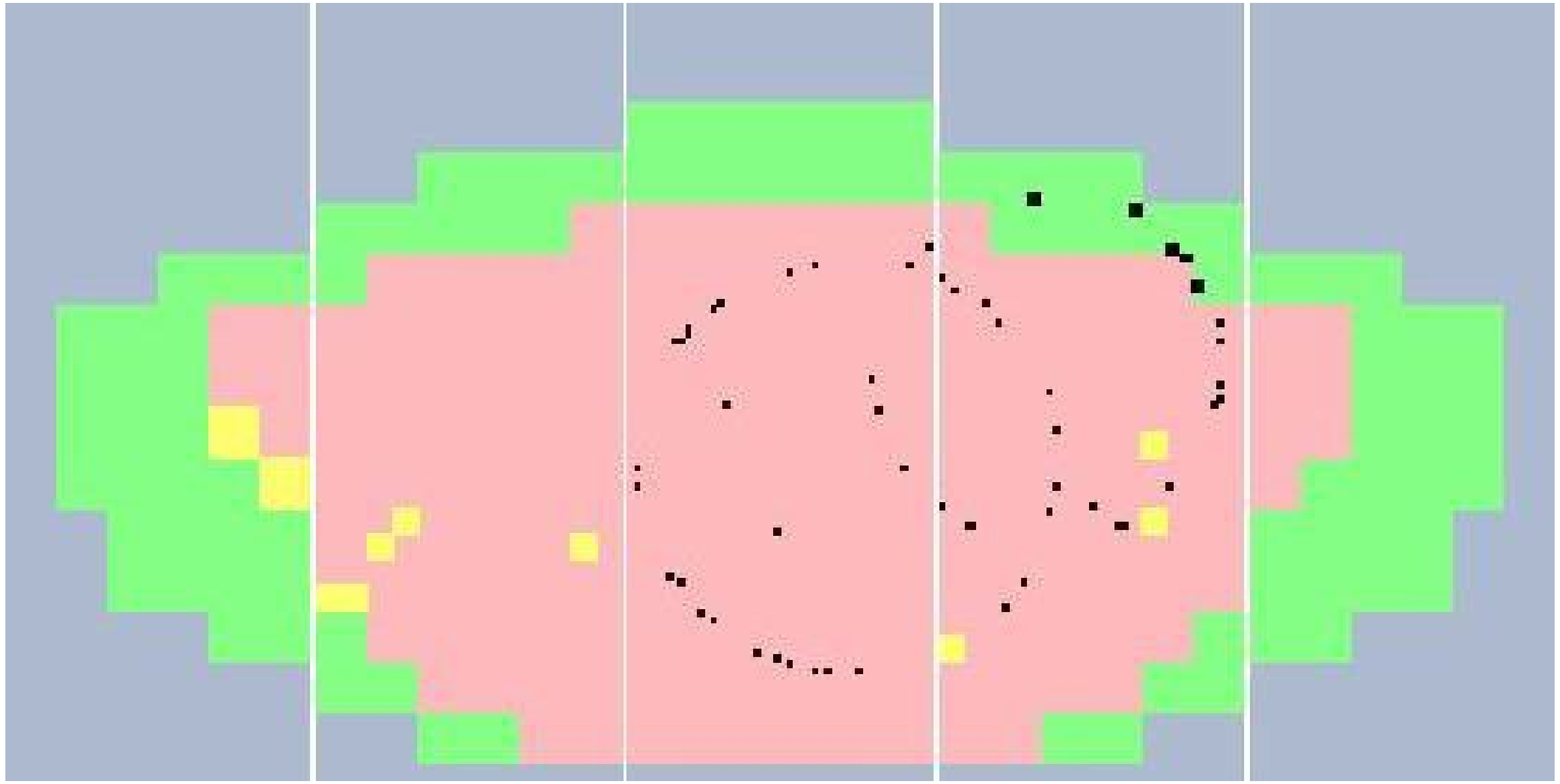

Outline:

- Why PID?
- TOF detectors
- Specific ionization loss - dE/dx
- Transition radiation detectors (TRD)
- **Cherenkov based PID devices**
  - **Threshold detectors**
  - **RICH detectors**
  - **DIRC type detectors**

PART I

Outline:

- **Why PID?**
- TOF detectors
- Specific ionization loss - dE/dx
- Transition radiation detectors (TRD)
- Cherenkov based PID devices
  - Threshold detectors
  - RICH detectors
  - DIRC type detectors

Why we need PID?

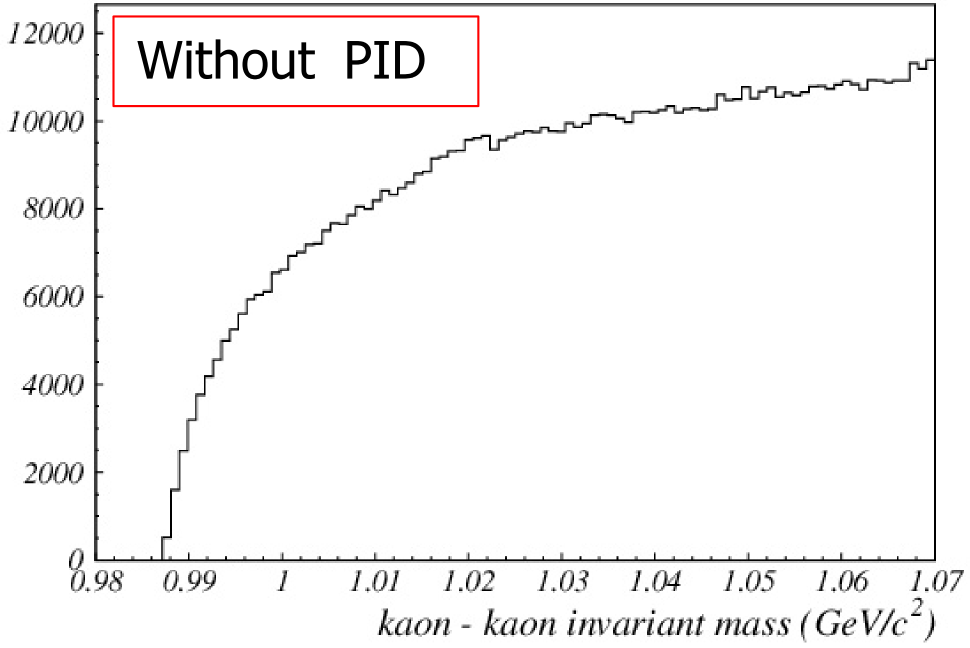

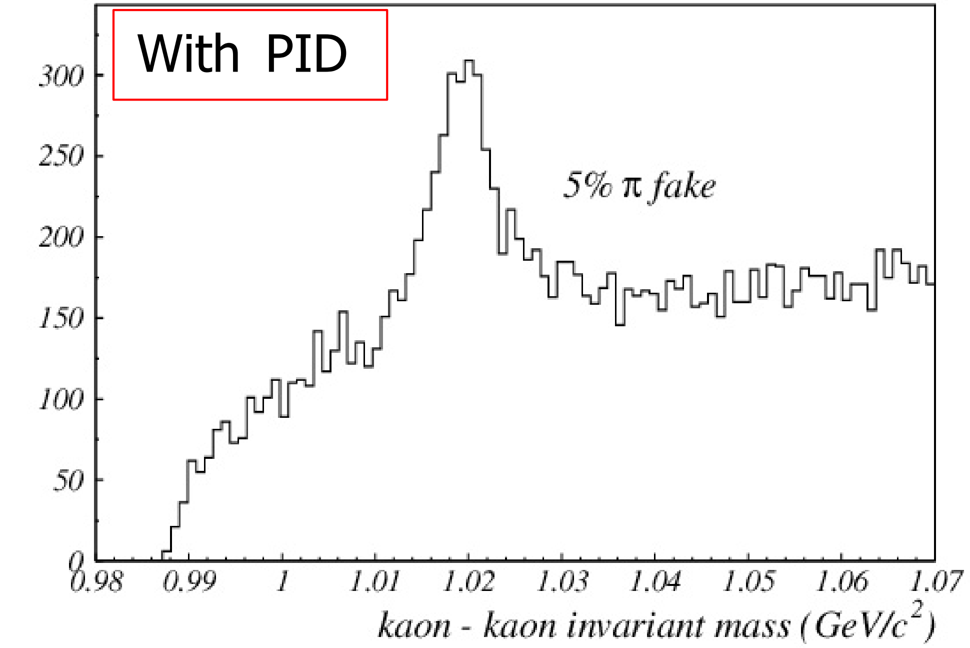

Example: HERA-B

K^+K^- invariant mass.

The $\Phi \to K^+K^-$ decay only becomes visible after the use of the particle identification, strong suppression of pions was required

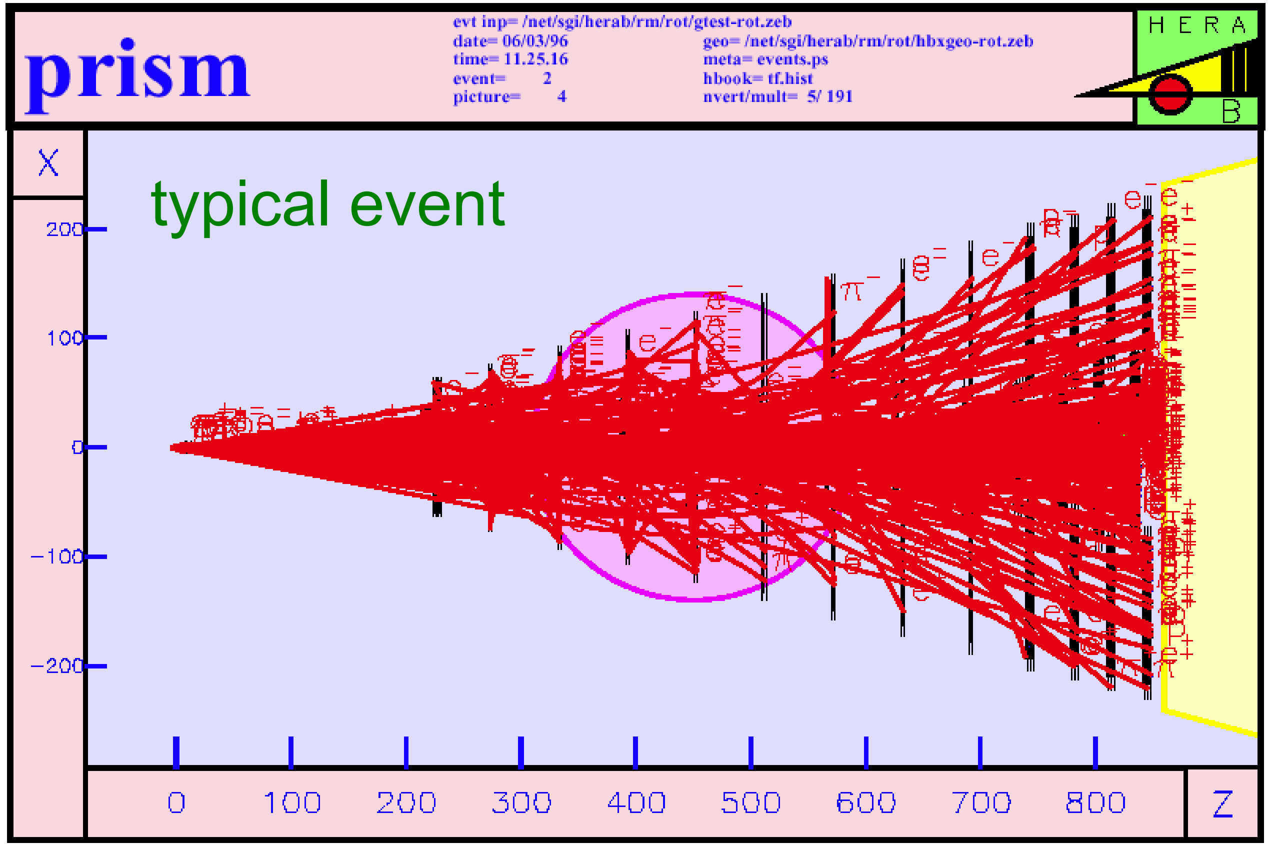

Why we need PID?

Example 2: LHCb

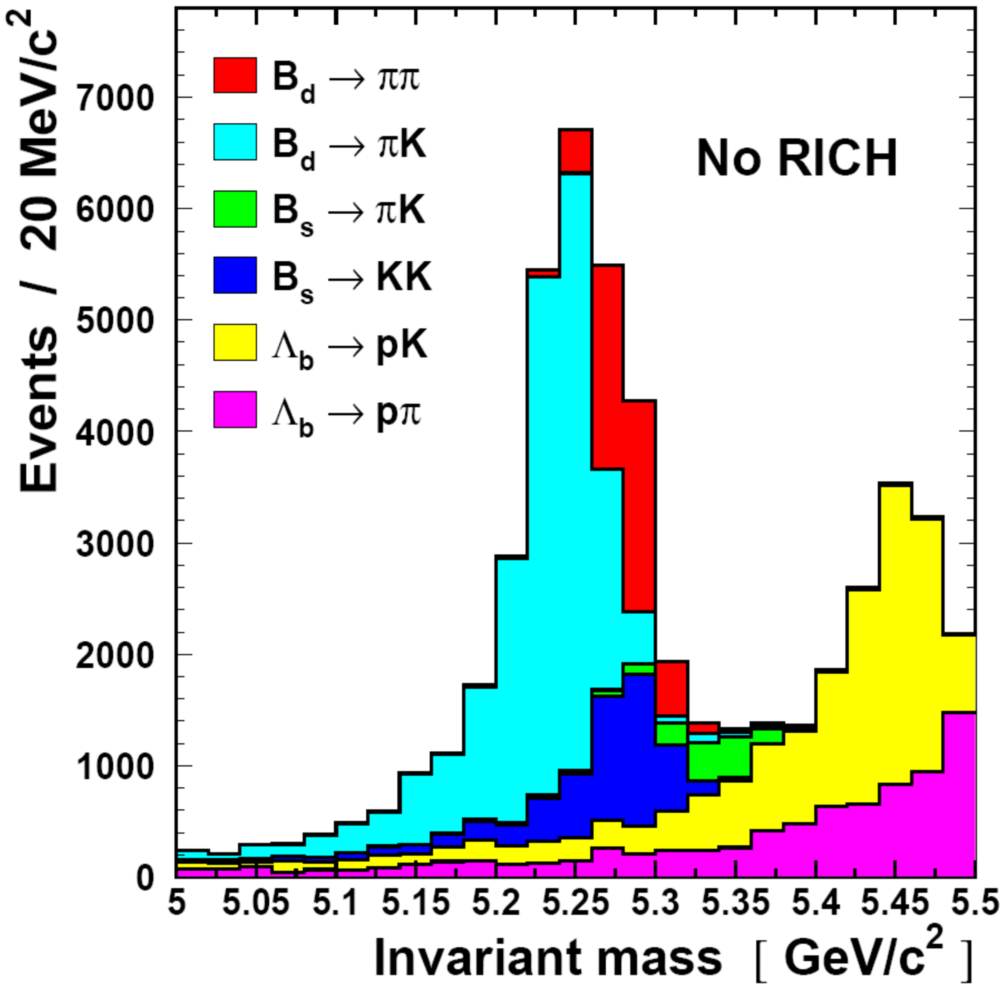

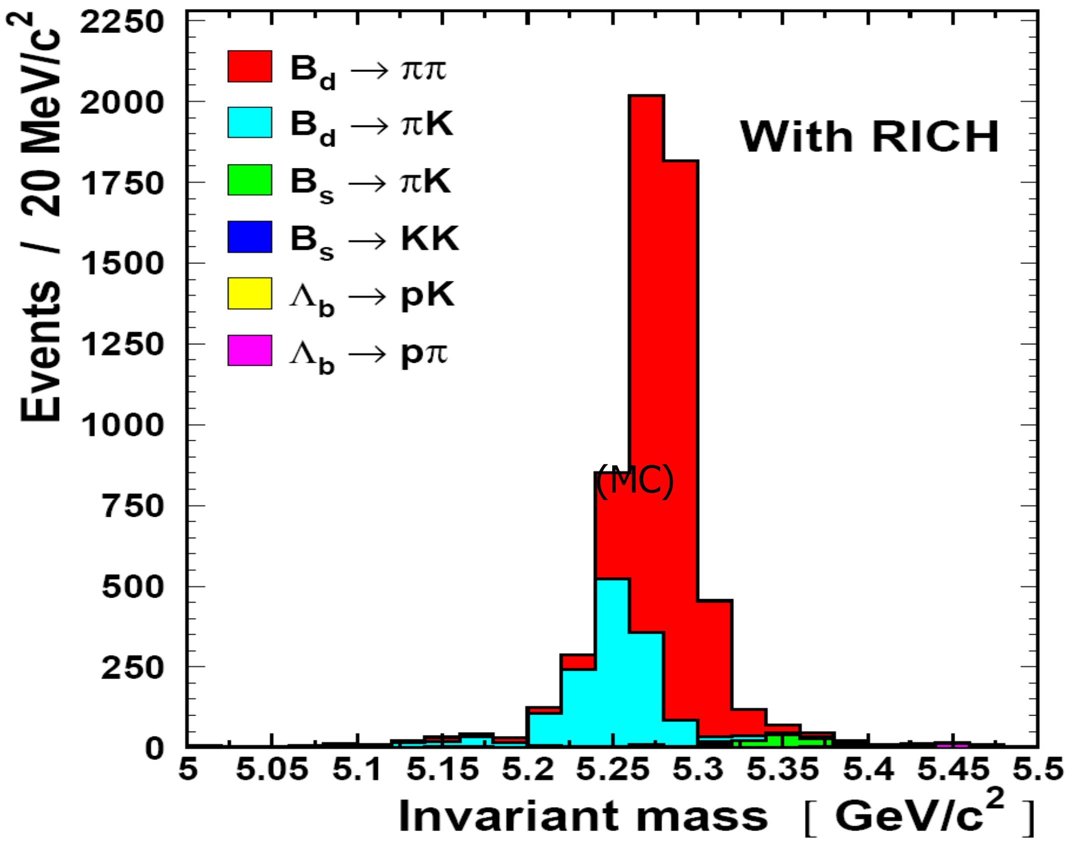

Need to distinguish $B_d \to \pi^+\pi^-$ from other similar topology 2-body decays and to distinguish B from anti-B using K tag.

Event reconstruction

- Most of the particles are short-lived and decay before reaching the detectors
- Their detection is based on decay products, detected in the spectrometer

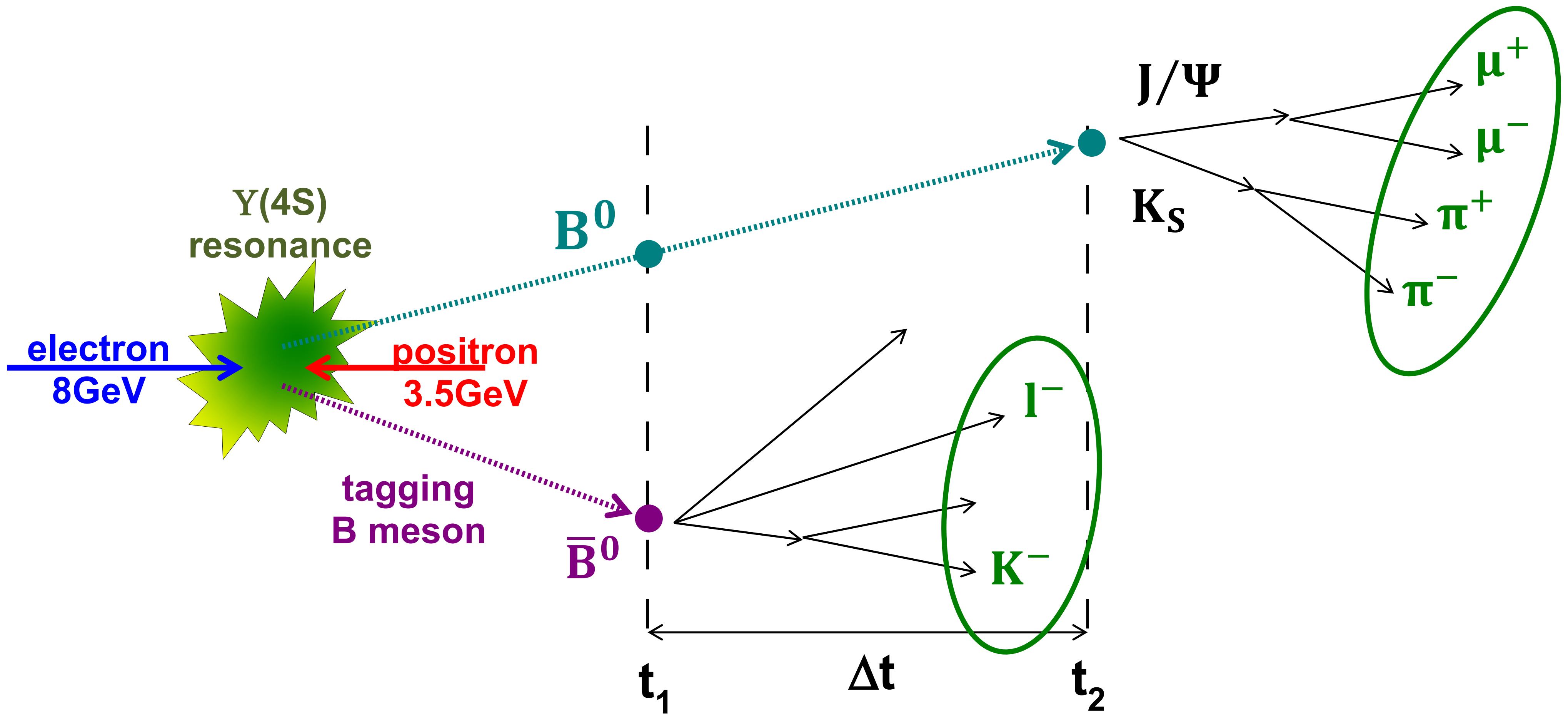

Spectrometer Belle

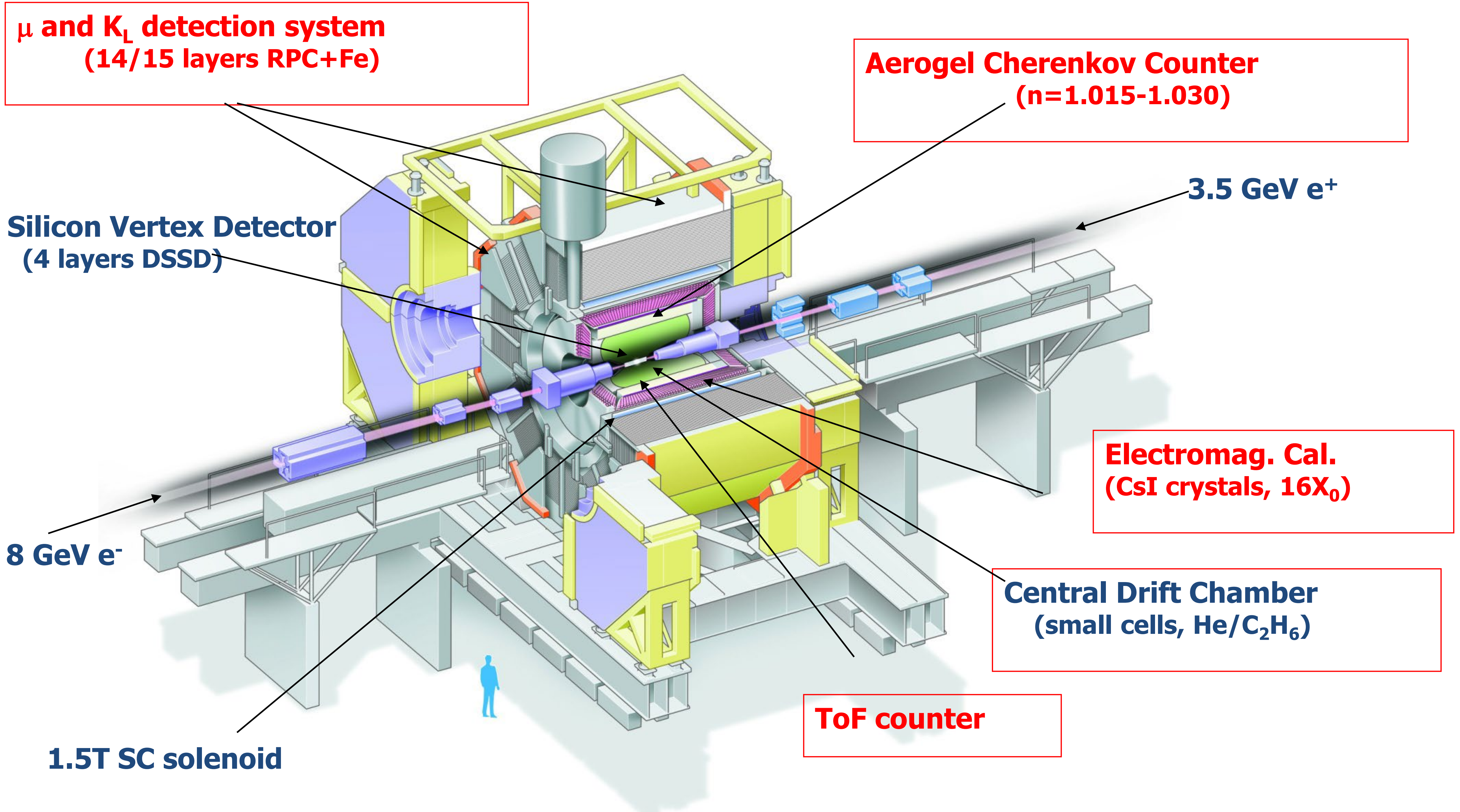

Masses and lifetimes for some particles

Particle		Mass $[MeV/c^2]$	Lifetime t_0 $[s]$	Range estimate ct_0 [m]
electron (positron)	e^-/e^+	0,511	stable	--
muon	μ^-/μ^+	105,7	$2{,}2 \times 10^{-6}$	660
tau lepton	τ^-/τ^+	1777	$2{,}9 \times 10^{-13}$	$8{,}7 \times 10^{-5}$
neutral pion	π^0	135	$8{,}4 \times 10^{-17}$	$2{,}5 \times 10^{-8}$
charged **pion**	π^+/π^-	139,6	$2{,}6 \times 10^{-8}$	7,8
short-lived kaon	K_S	498	$9{,}0 \times 10^{-11}$	$2{,}7 \times 10^{-2}$
long-lived **kaon**	K_L	498	$5{,}1 \times 10^{-8}$	15,3
charged **kaon**	K^+/K^-	494	$1{,}2 \times 10^{-8}$	3,6
neutral B meson	$B^0/\bar{B}^0$	5279,6	$1{,}5 \times 10^{-12}$	$4{,}5 \times 10^{-4}$
charged B meson	B^+/B^-	5279,3	$1{,}5 \times 10^{-12}$	$4{,}5 \times 10^{-4}$
J/Ψ meson	J/Ψ	3097	$7{,}2 \times 10^{-21}$	$2{,}2 \times 10^{-12}$
proton (antiproton)	$p/\bar{p}$	938,2	stable	--
neutron	$n/\bar{n}$	939,6	885,7	$2{,}7 \times 10^{11}$

Particle IDentification - PID

- particles are identified by their mass or interaction
- charged and neutral particles that live long enough to rich detectors:

  $e, \mu, \pi, K, p, \mathrm{d}, \gamma, K_L, n$

- momentum is measured by track curvature in magnetic field
- in addition we can measure velocity:
  - Time Of Flight - TOF
  - ionization loss – dE/dx, dN/dx
  - Cherenkov radiation (threshold, RICH, DIRC …)
  - transition radiation
- or identify by specific interaction:
  - electrons → EM calorimeters
  - muons → muon detectors

$$p = \beta\gamma mc$$

$$\mathrm{E} = \gamma mc^2$$

$$\frac{E}{pc} = \beta \approx 1$$

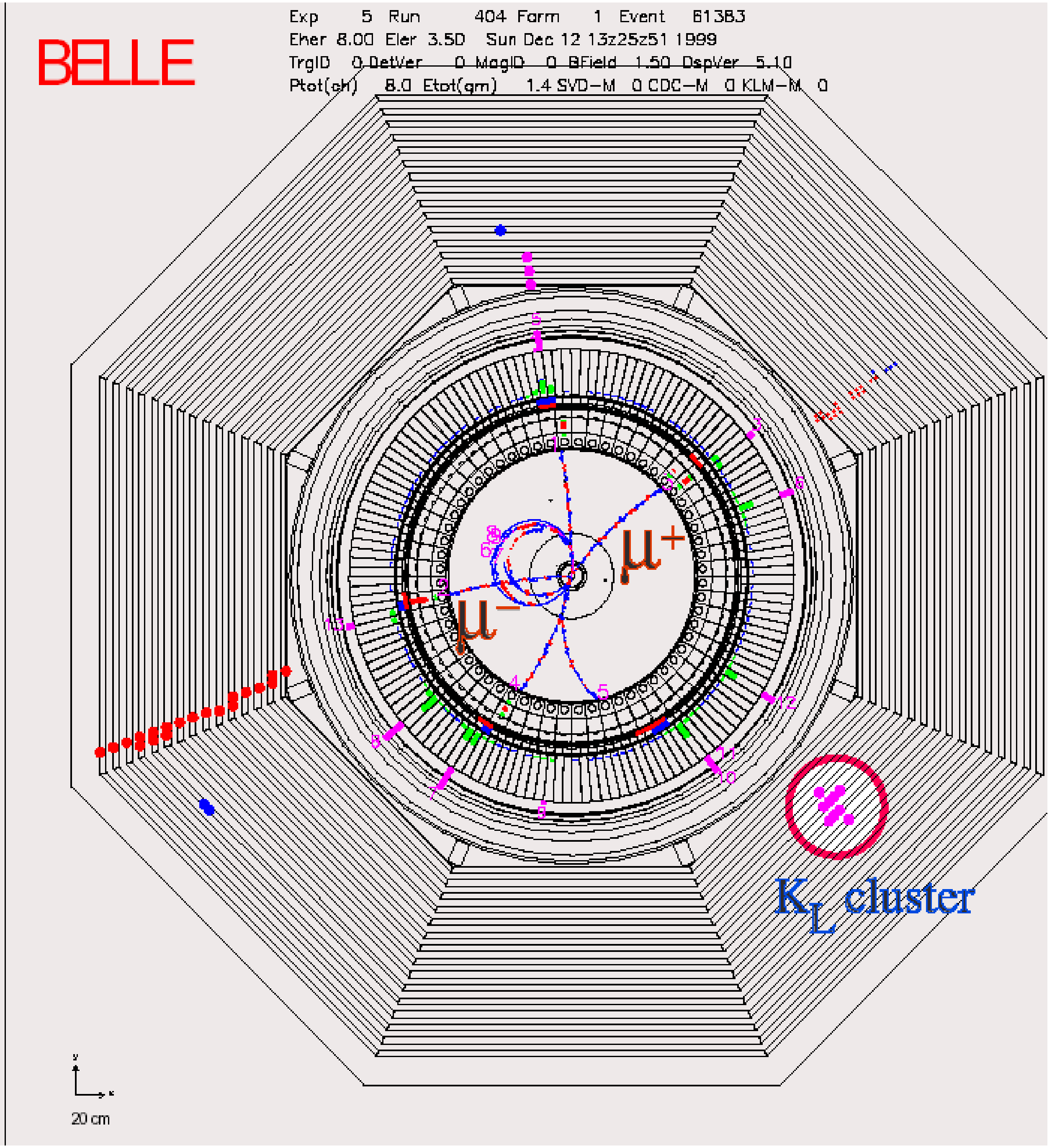

K/π separation at B factories

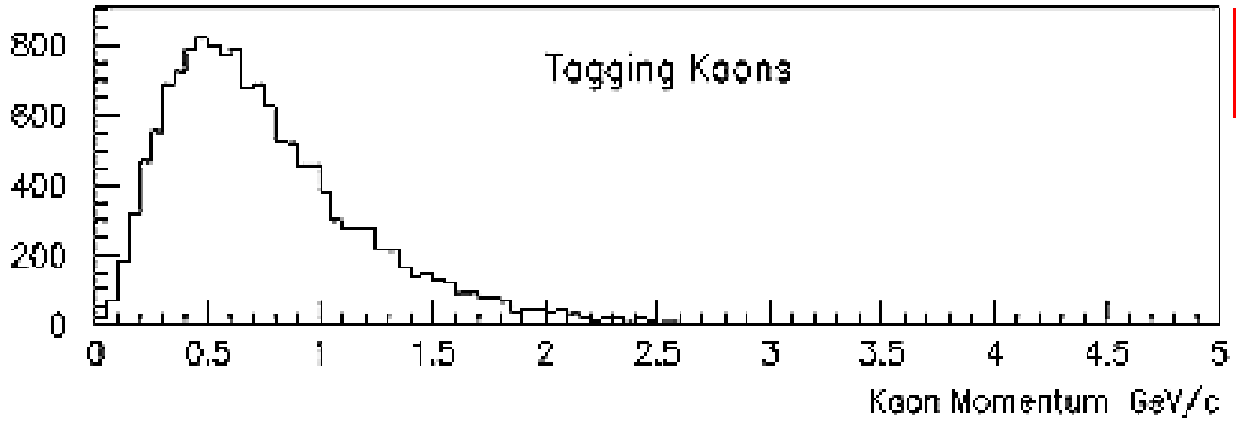

Tagging Kaons

Relatively soft

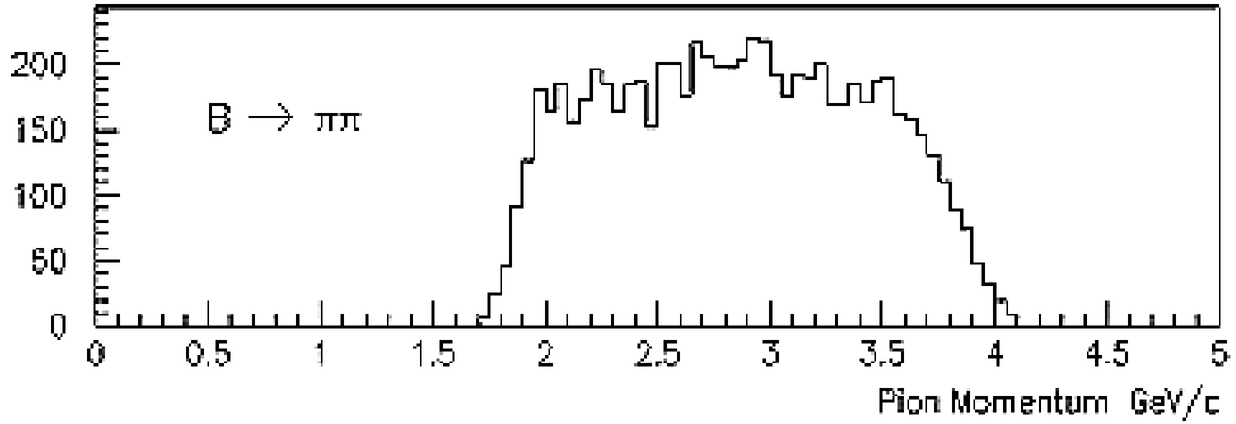

$B \to \pi\pi$

Requires dedicated PID

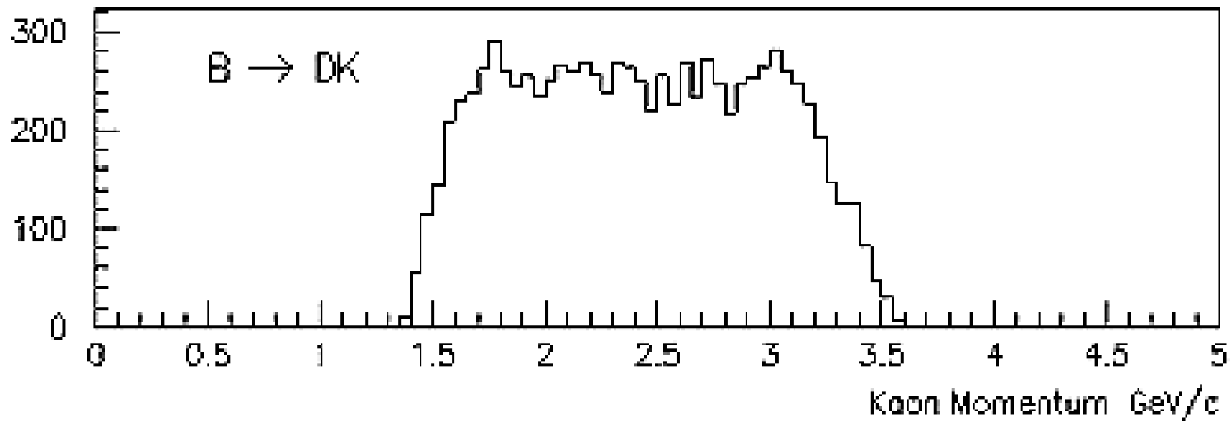

$B \to DK$

Requires dedicated PID

K/π PID at Belle

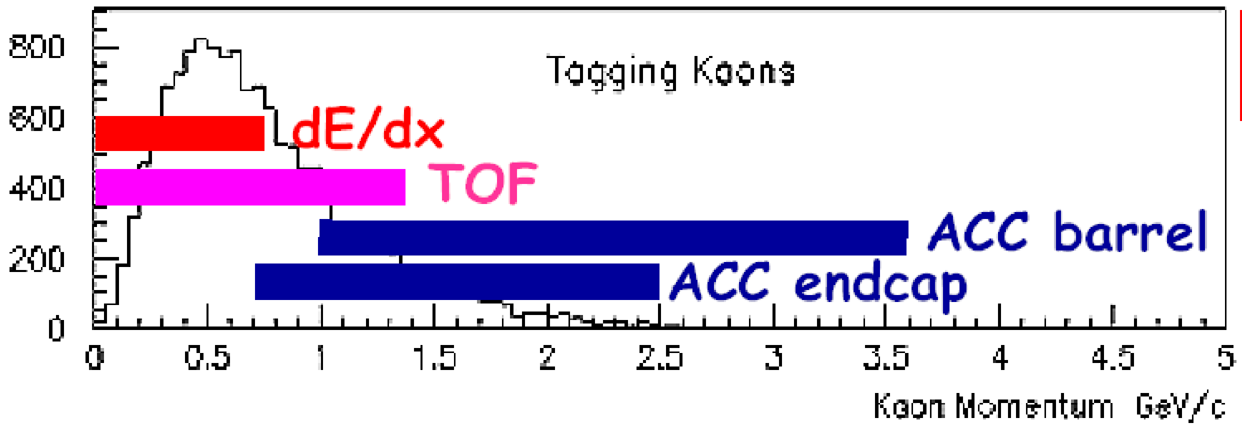

Tagging Kaons

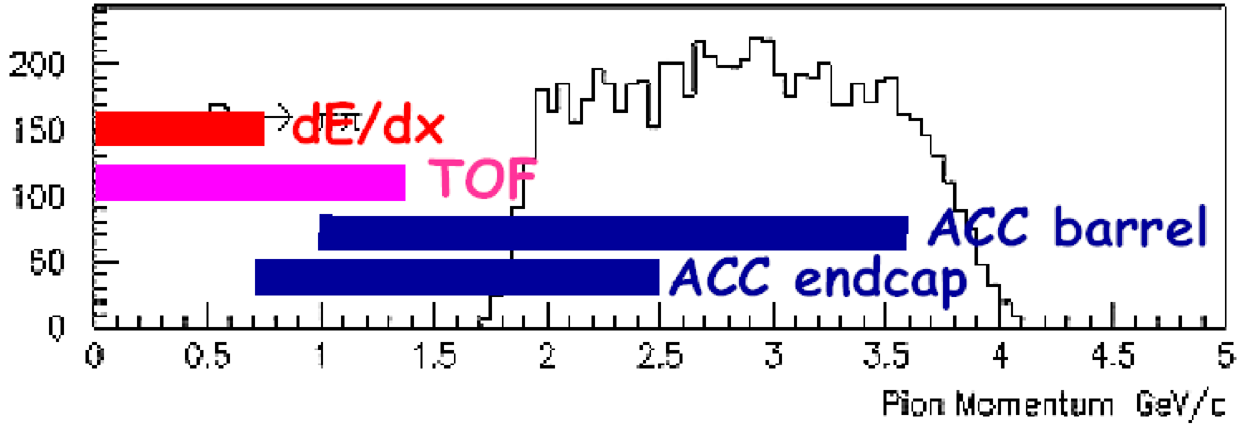

$B \to \pi\pi$

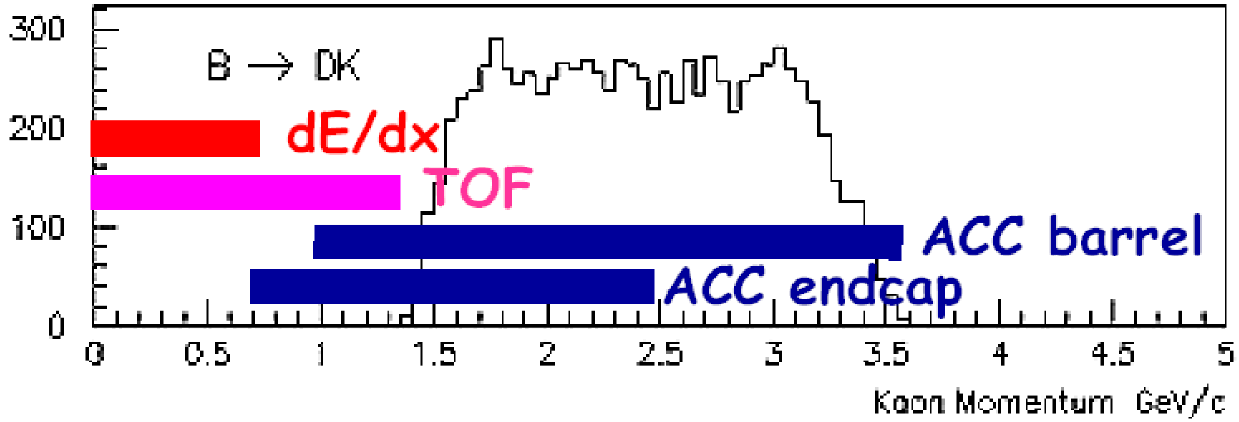

$B \to DK$

K/π PID at BaBar

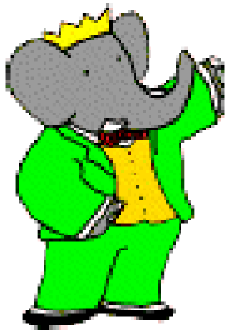

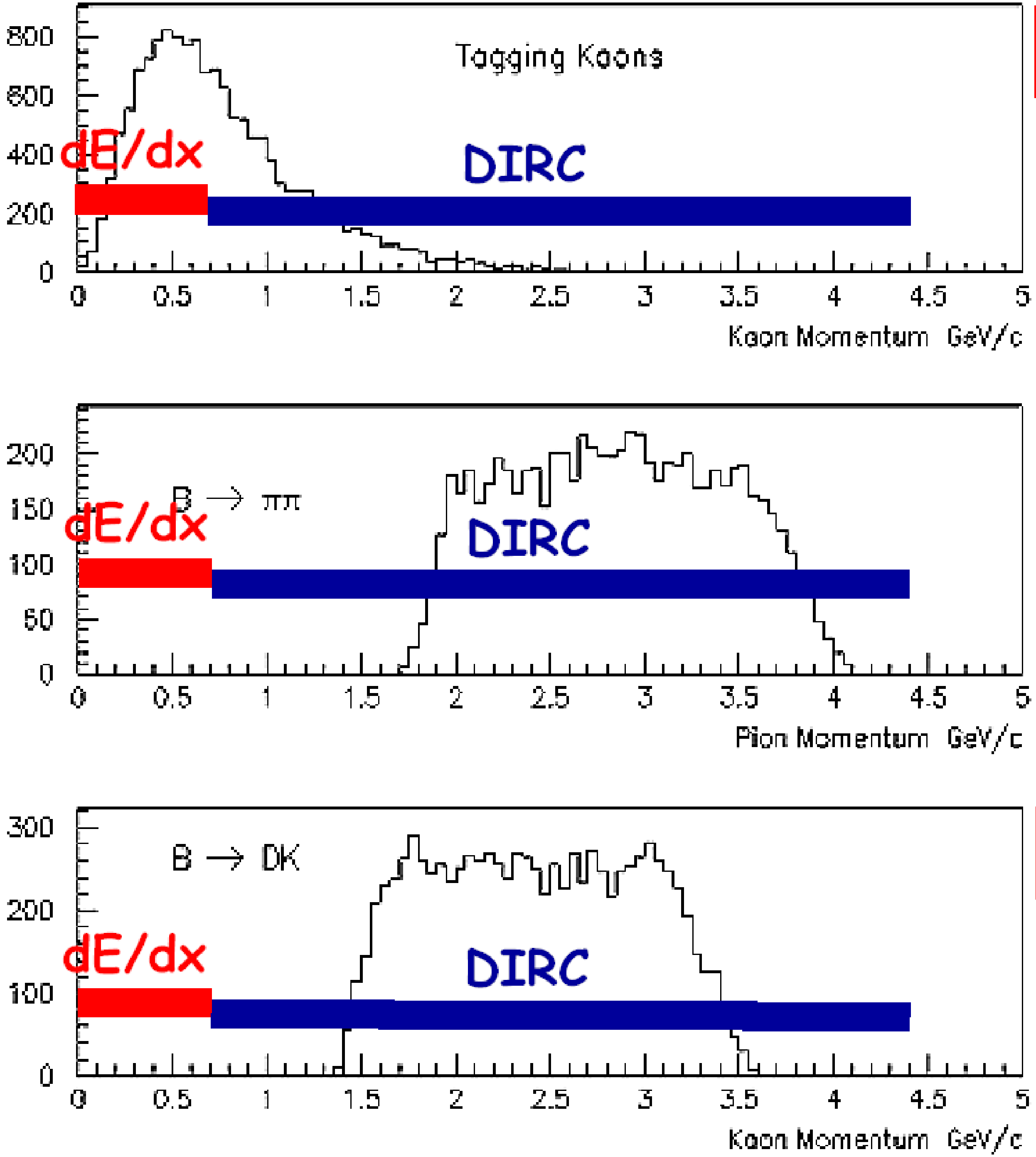

Tagging Kaons

B → ππ

B → DK

Momentum range for different PID methods at ALICE

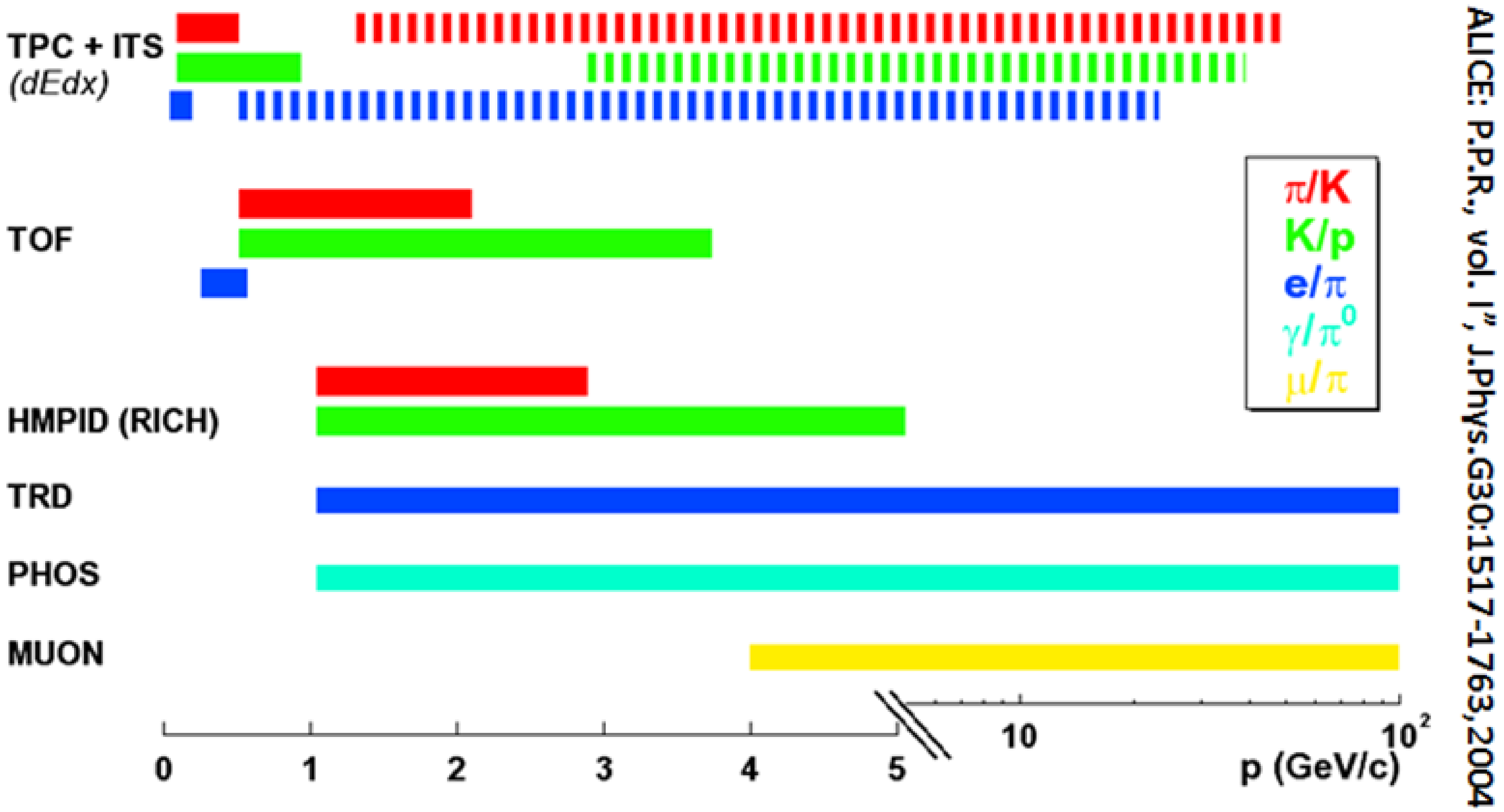

Efficiency and misidentification probability

Efficiency and purity are tightly coupled!

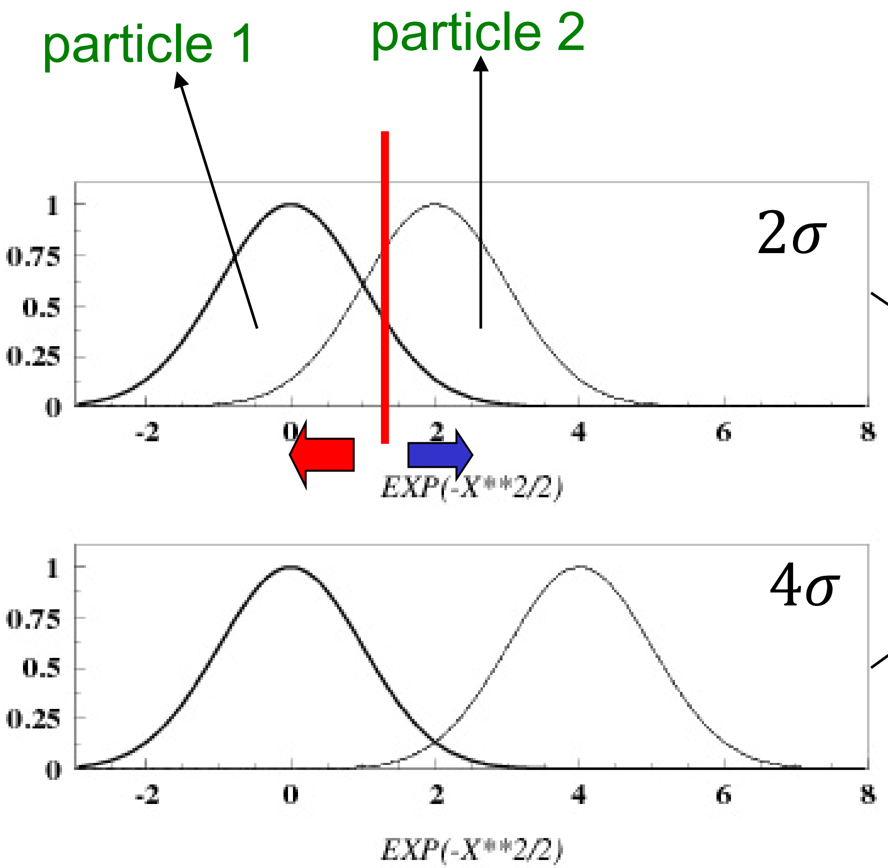

some discriminating variable
(eg., time of flight, likelihood ...)

Efficiency vs. misidentification probability

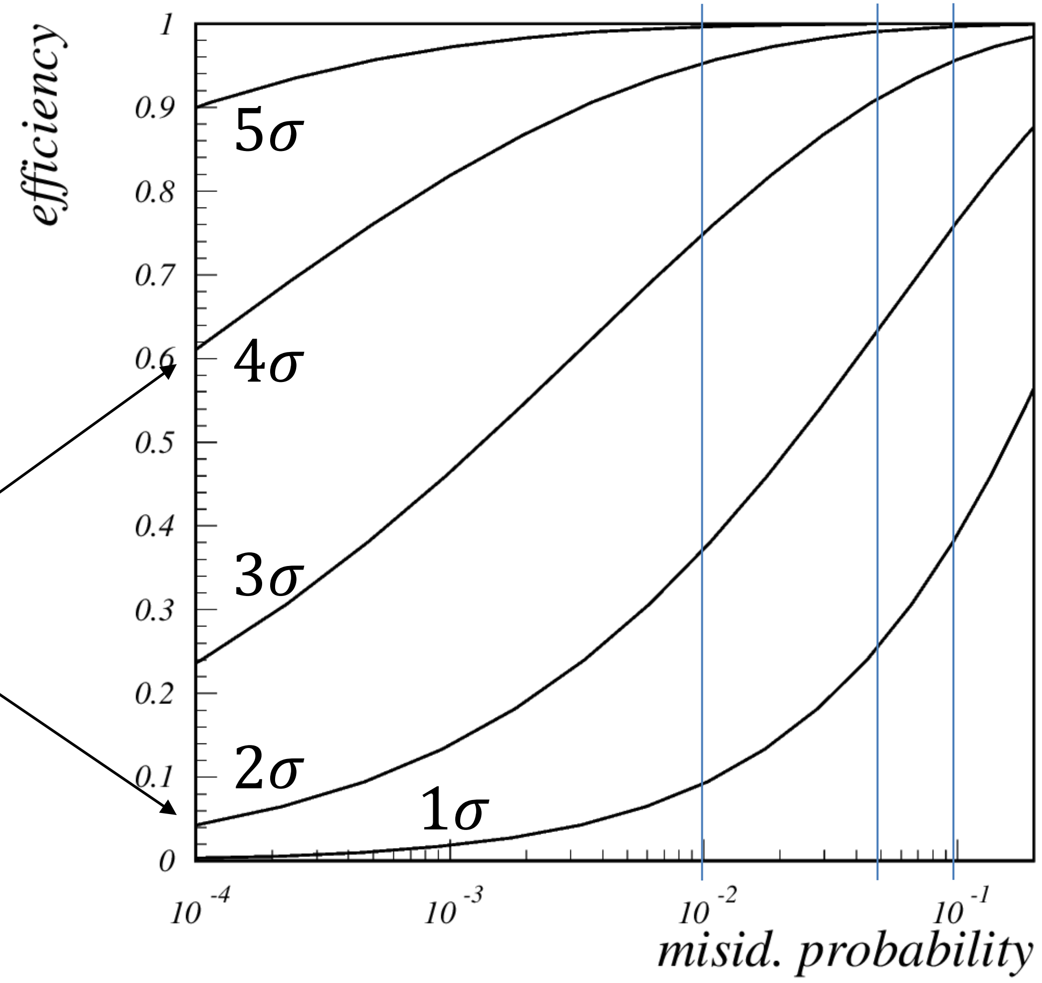

(A variation of a Receiver Operating Characteristic (ROC) curve for binary classification parameter that shows efficiency vs. misid. probability as parameter is varied.)

Outline:

- Why PID?
- **TOF detectors**
- Specific ionization loss - dE/dx
- Transition radiation detectors (TRD)
- Cherenkov based PID devices
  - Threshold detectors
  - RICH detectors
  - DIRC type detectors

Time-Of-Flight (TOF)

- measure particle travel time over known distance
- typical resolution $\sigma_t \approx$100 ps

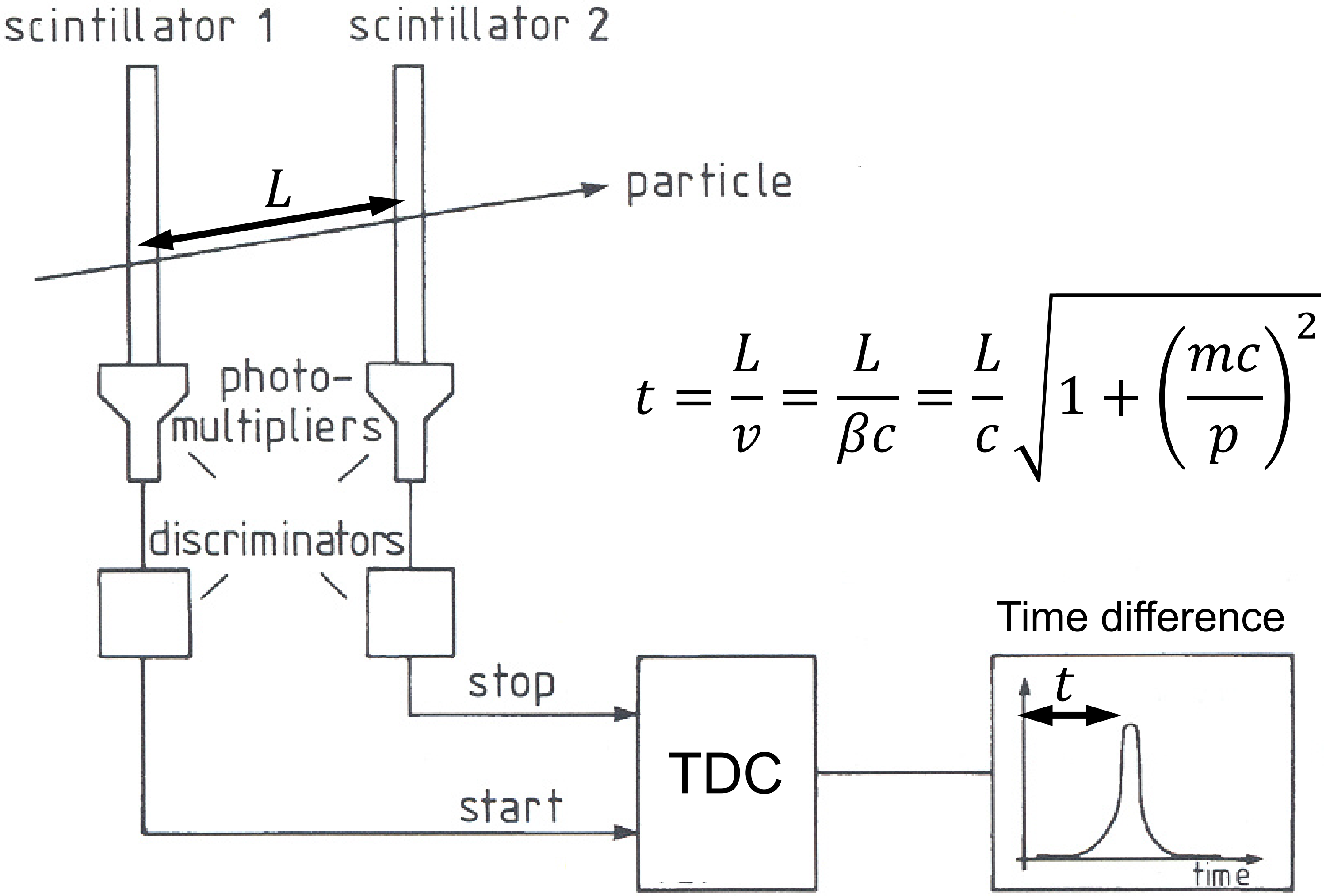

$$t = \frac{L}{v} = \frac{L}{\beta c} = \frac{L}{c}\sqrt{1 + \left(\frac{mc}{p}\right)^2}$$

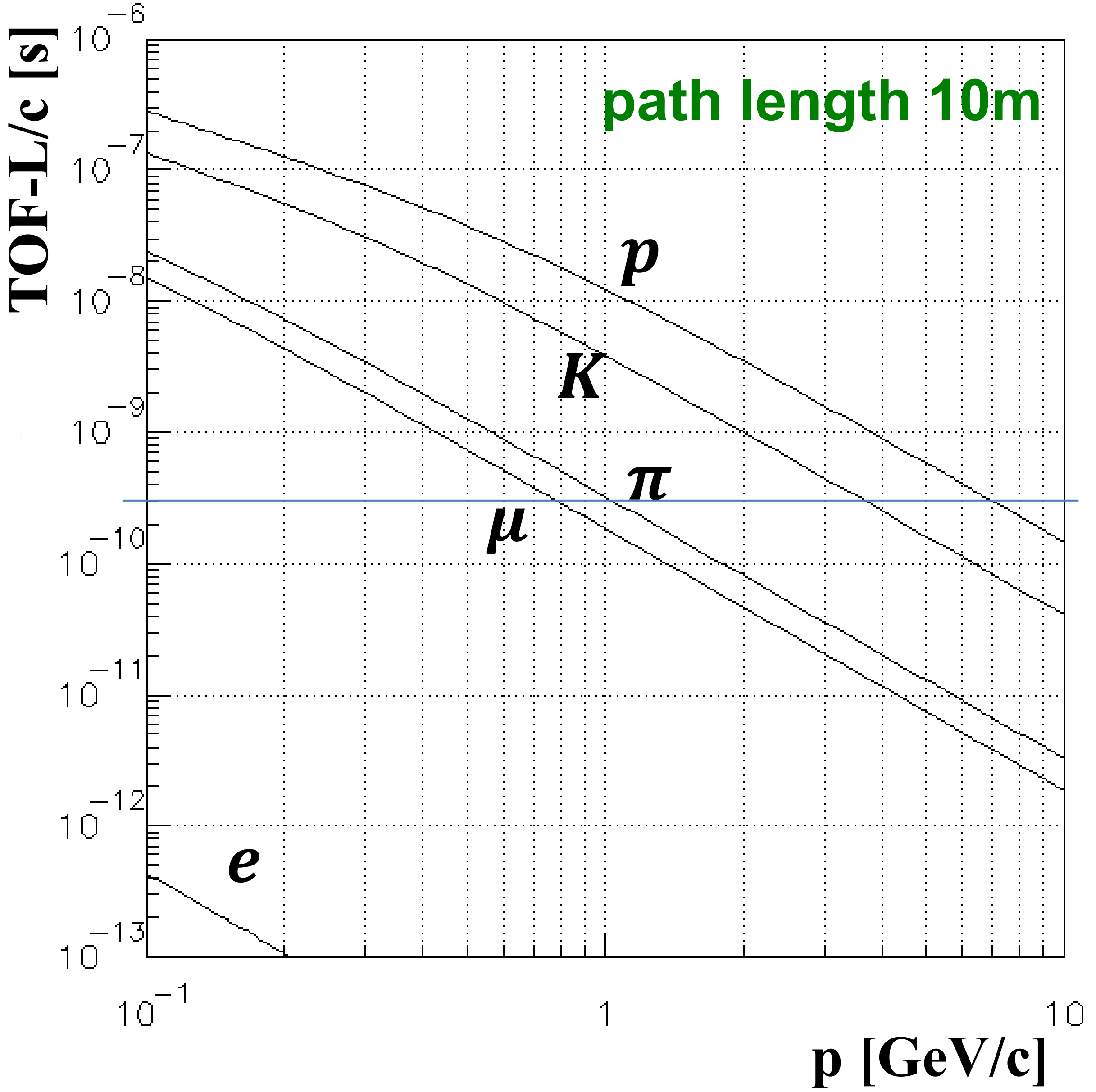

Time-Of-Flight (TOF)

- measured TOF difference

$$t = \frac{L}{v} = \frac{L}{\beta c} = \frac{L}{c}\sqrt{1+\left(\frac{mc}{p}\right)^2}$$

$$\Delta t = \frac{L}{c}\left(\sqrt{1+\left(\frac{m_1 c}{p}\right)^2} - \sqrt{1+\left(\frac{m_2 c}{p}\right)^2}\right) \approx \frac{Lc}{2p^2}(m_1^2 - m_2^2)$$

- typical time resolution $\sigma_t \approx 100$ ps
- $5\sigma\ \pi/K$ separation up to ≈ 1.2 GeV/c for $L = 2$ m

- mass resolution ($m = \frac{p}{c}\sqrt{\left(\frac{ct}{L}\right)^2 - 1}$)

$$\frac{\sigma_m}{m} = \frac{\sigma_p}{p} \oplus \gamma^2\left(\frac{\sigma_L}{L} \oplus \frac{\sigma_t}{t}\right) \approx \gamma^2 \frac{\sigma_t}{t}$$

- mainly determined by time resolution

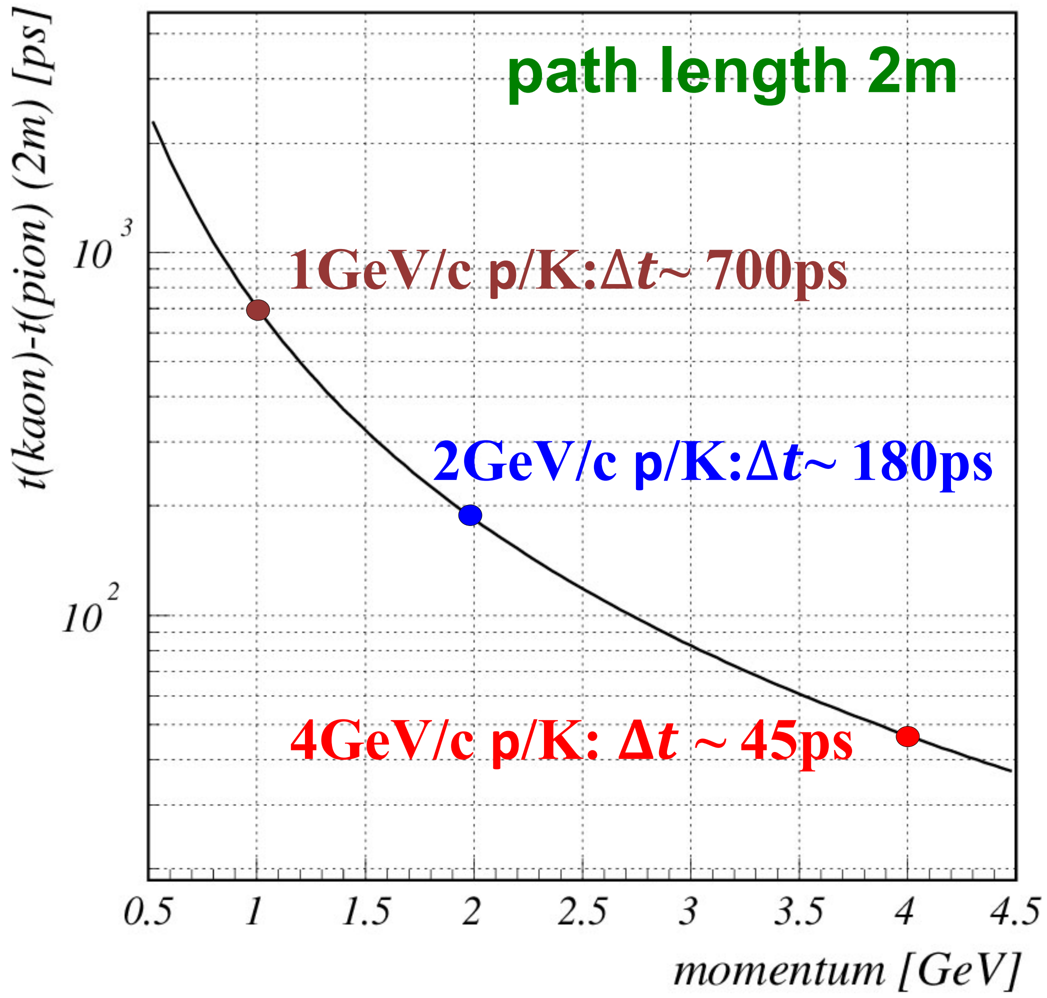

Belle TOF with scintillator counters

TOF based on scintillation counters:

- 128 255 cm long scintillator bars (BC408), 4x6 cm^2
- read out on both sides by finemesh PMT (Hamamatsu R6680)
- start time from collision time t_0 , σ_{t_0}~25 ps
- ~ 100 ps timing resolution
- 2σ K/π separation up to ~1.25 GeV

NIM A453(2000)315

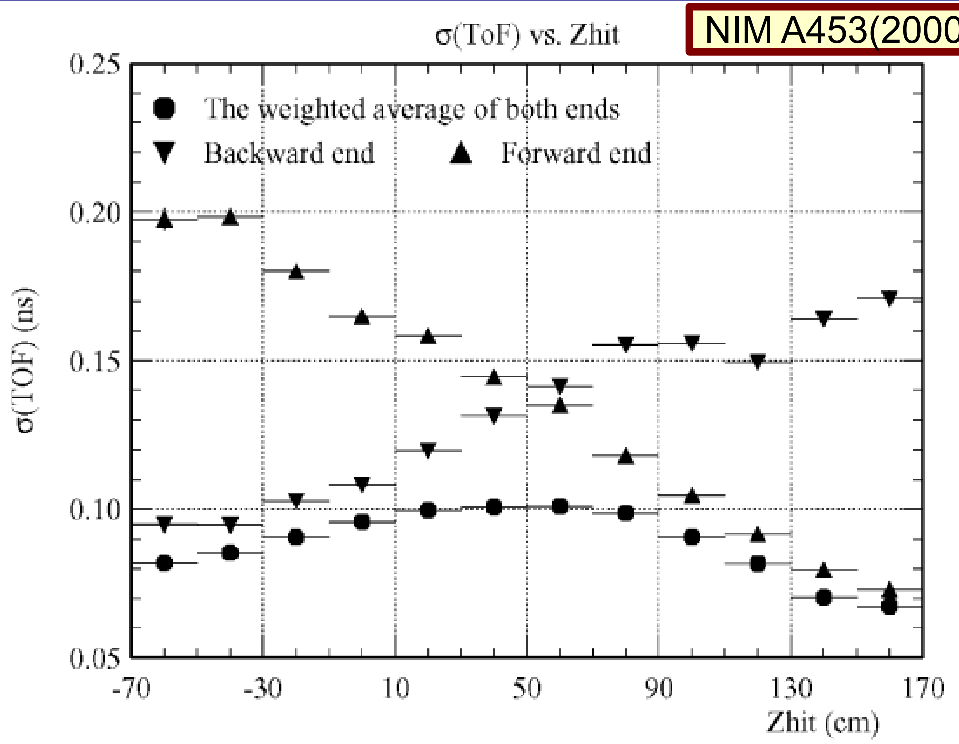

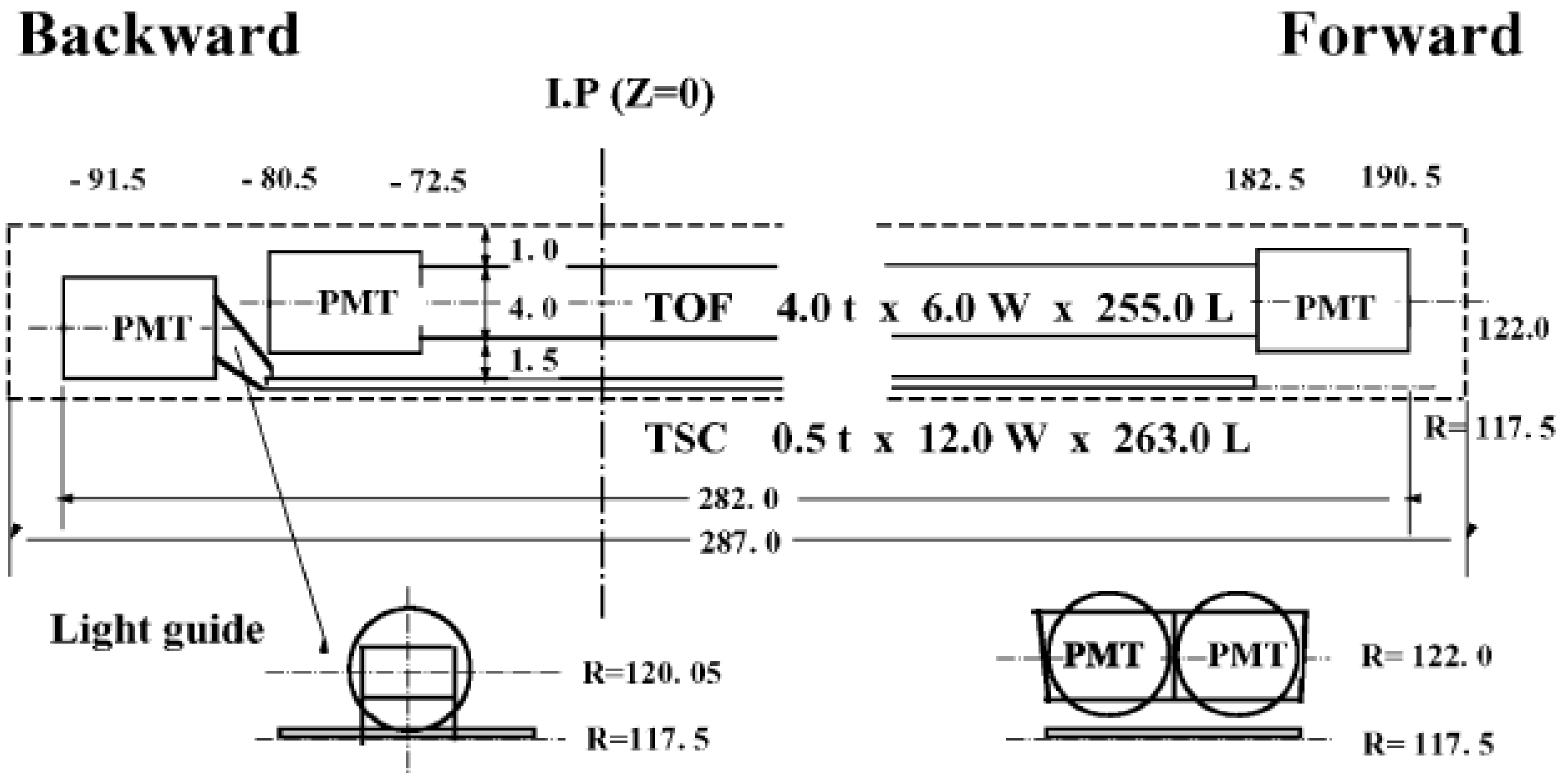

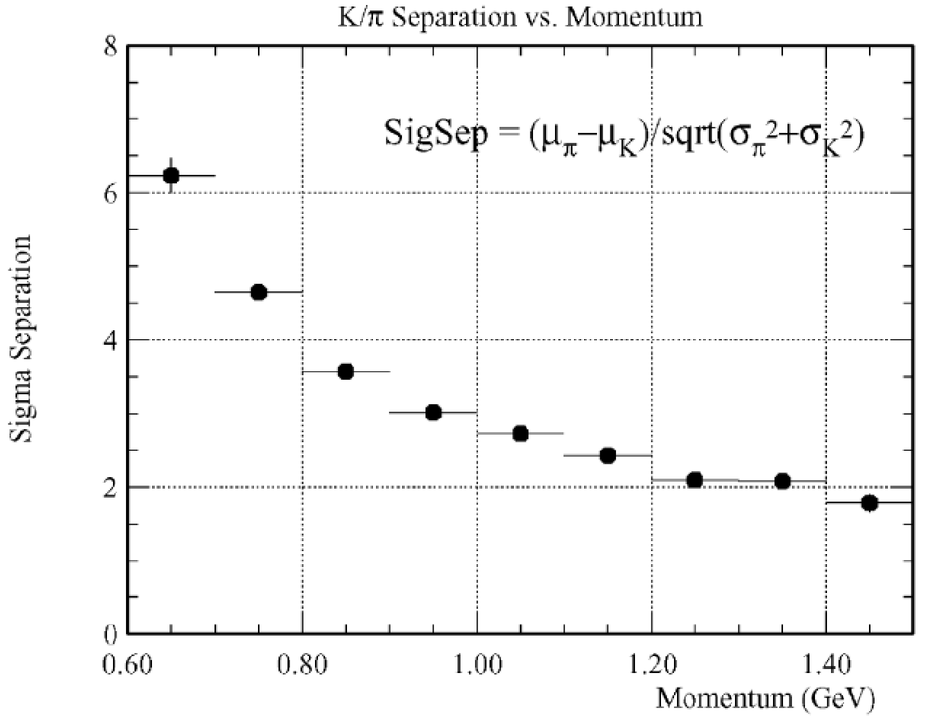

ALICE TOF with MRPCs

Multi-gap Resistive Plate Chambers:

- 2 x 5 gaps – 250um
- ~ 80 ps timing resolution
- K/π separation up to ~2.5 GeV
- requires many tracks for accurate t_0

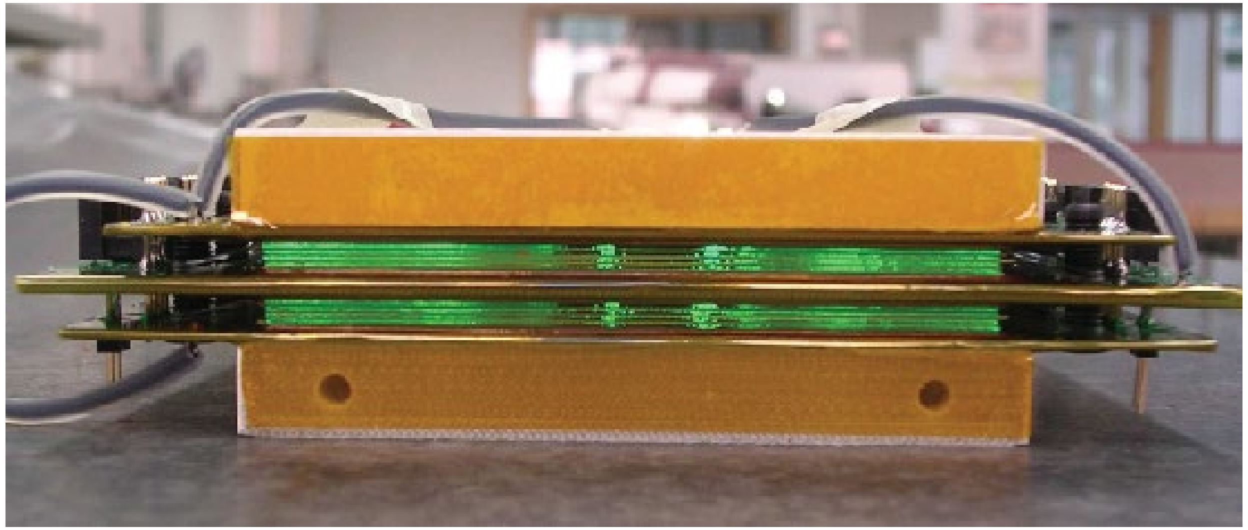

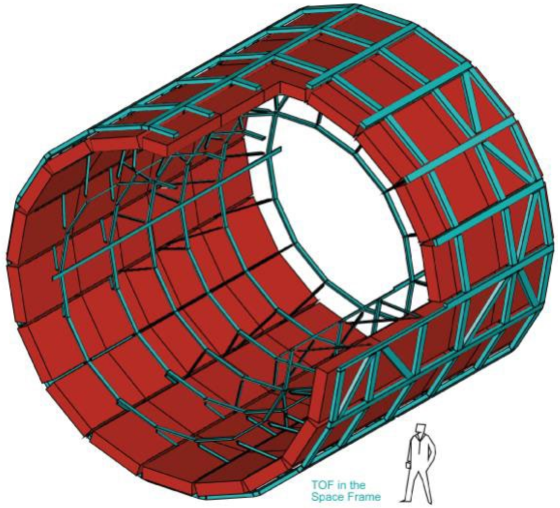

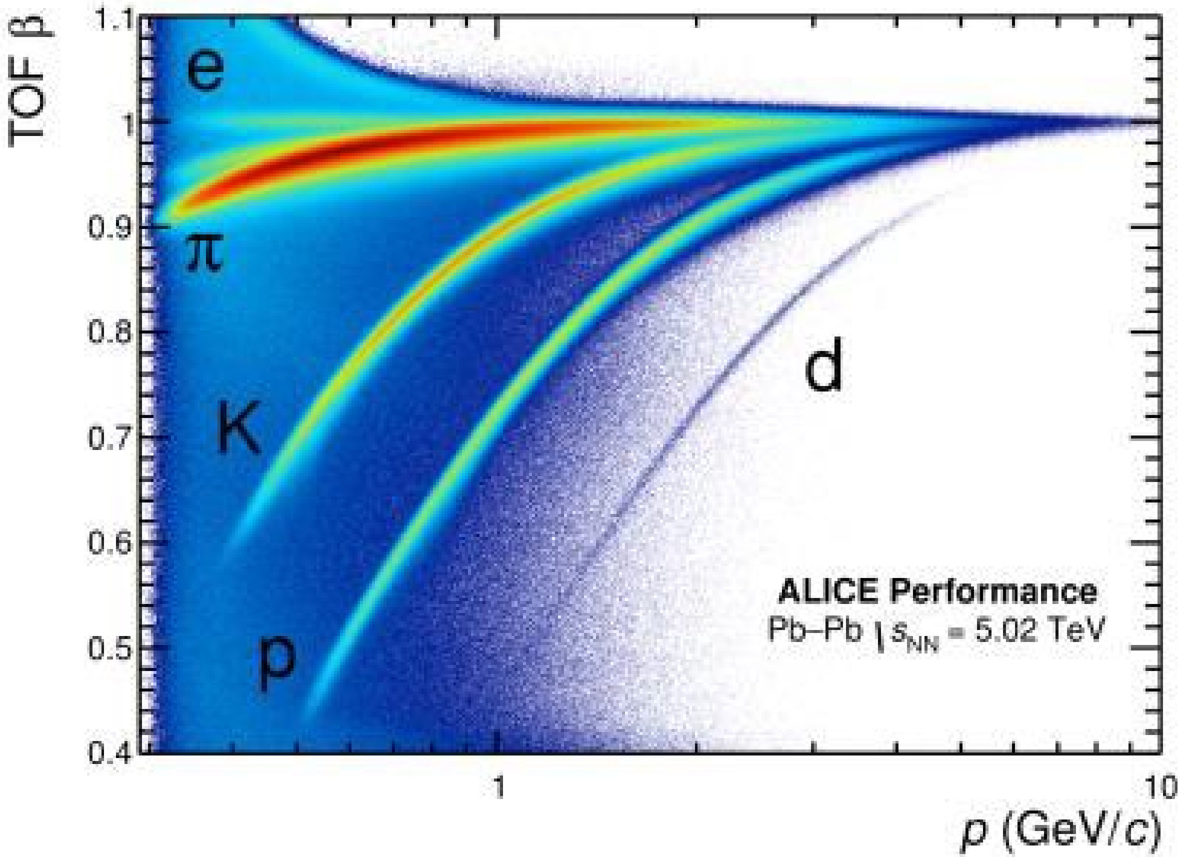

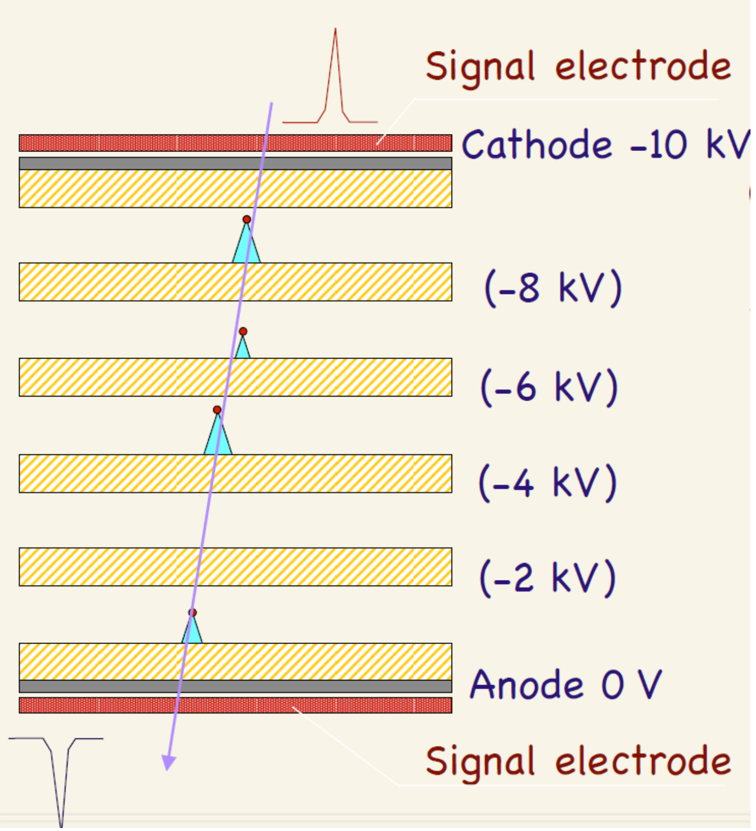

Eur.Phys.J.Plus 128(2013)44

ALICE TOF

A Large Ion Collider Experiment

t_0 resolution depends on the number of tracks in the event

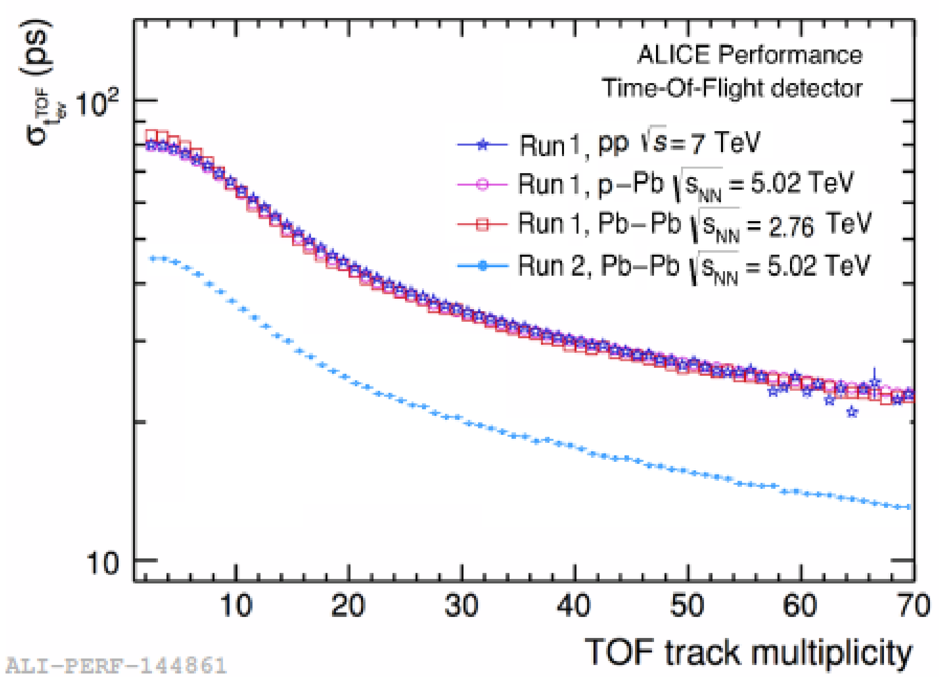

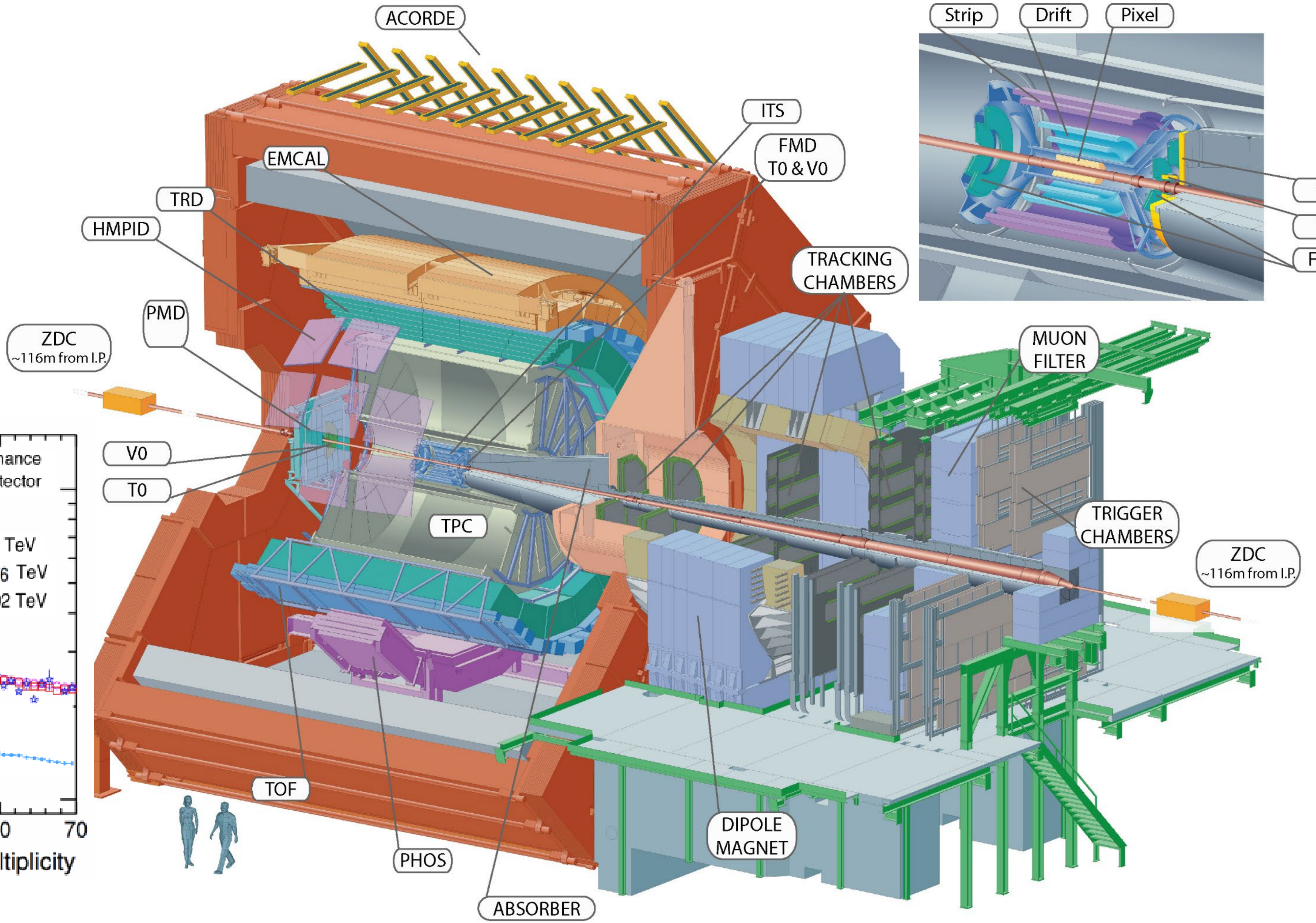

TOF – where are the limits?

- Excellent timing properties require fast light source → Cherenkov radiator
- Small prototypes based on MCP-PMT directly attached to the radiator show TOF in the range of ~10 ps may be possible

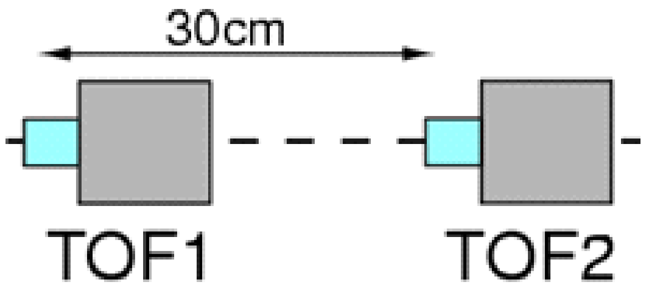

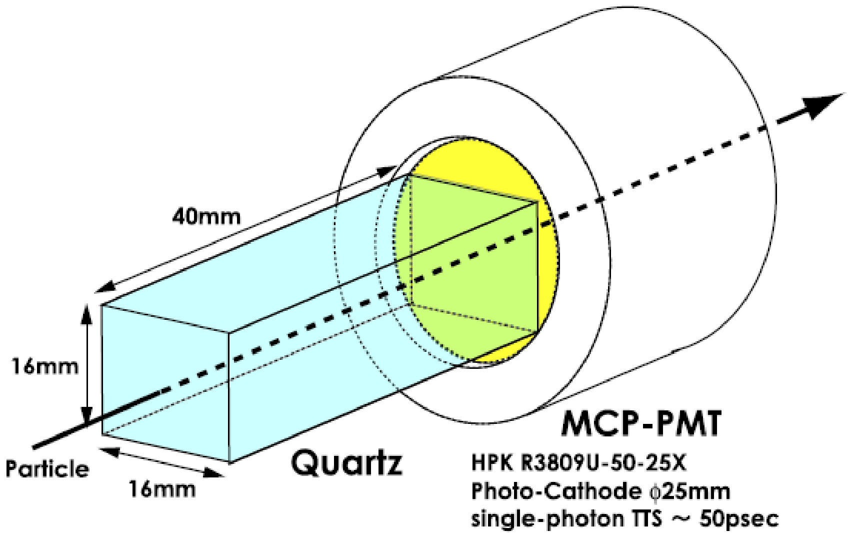

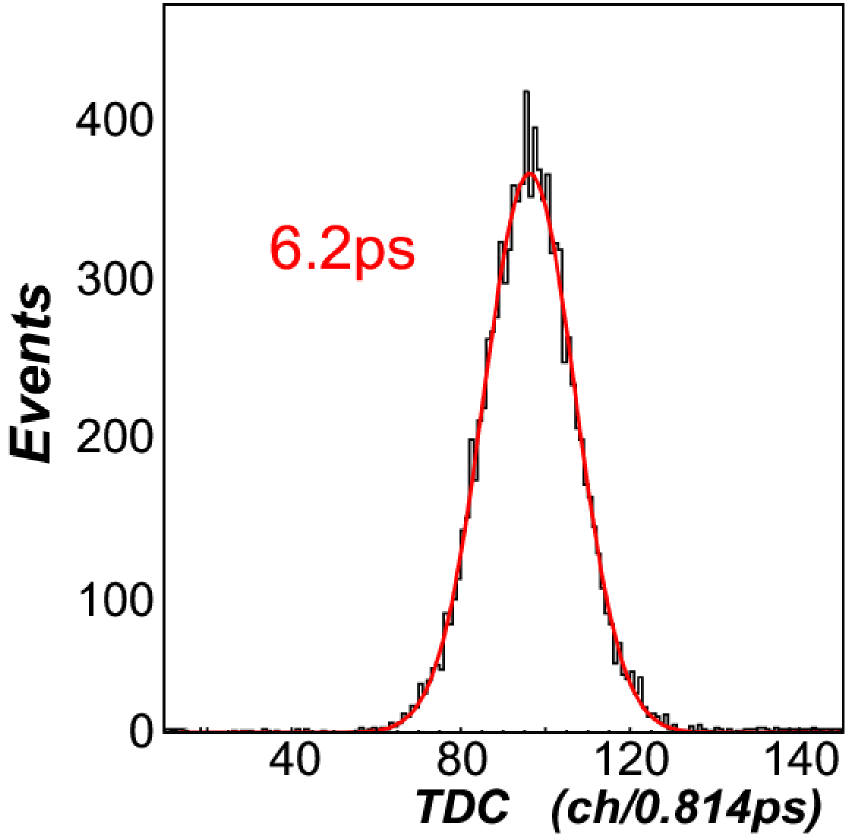

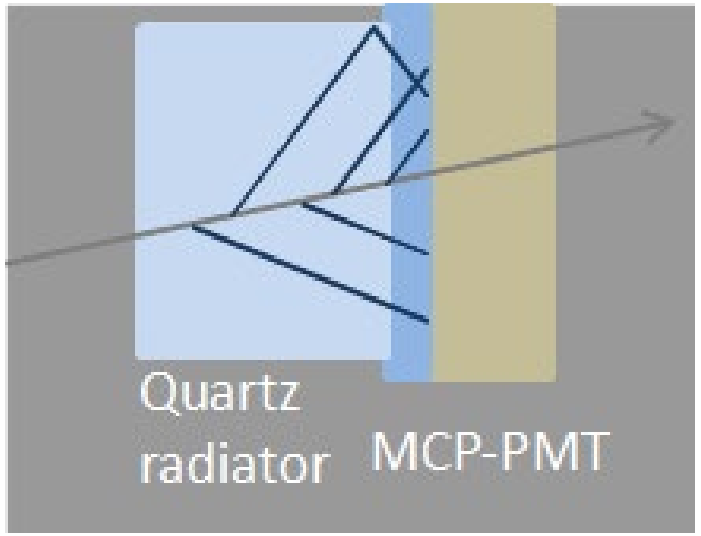

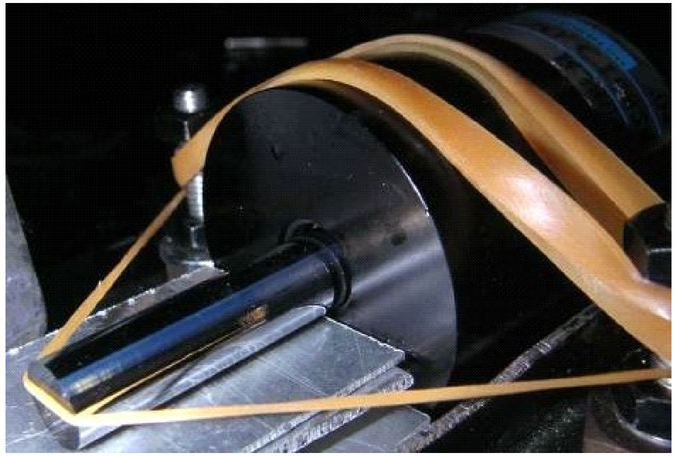

Excellent timing resolution 6.2 ps obtained in the pion beam (includes contribution from electronics).

K.Inami@PD07

Outline:

- Why PID?
- TOF detectors
- **Specific ionization loss - dE/dx**
- Transition radiation detectors (TRD)
- Cherenkov based PID devices
  - Threshold detectors
  - RICH detectors
  - DIRC type detectors

Ionization loss – dE/dx

- dE/dx is a function of particle velocity

- Separation is possible in low momentum region up to about $\approx 1\ GeV$
- With a good resolution partial separation is available also at higher momenta

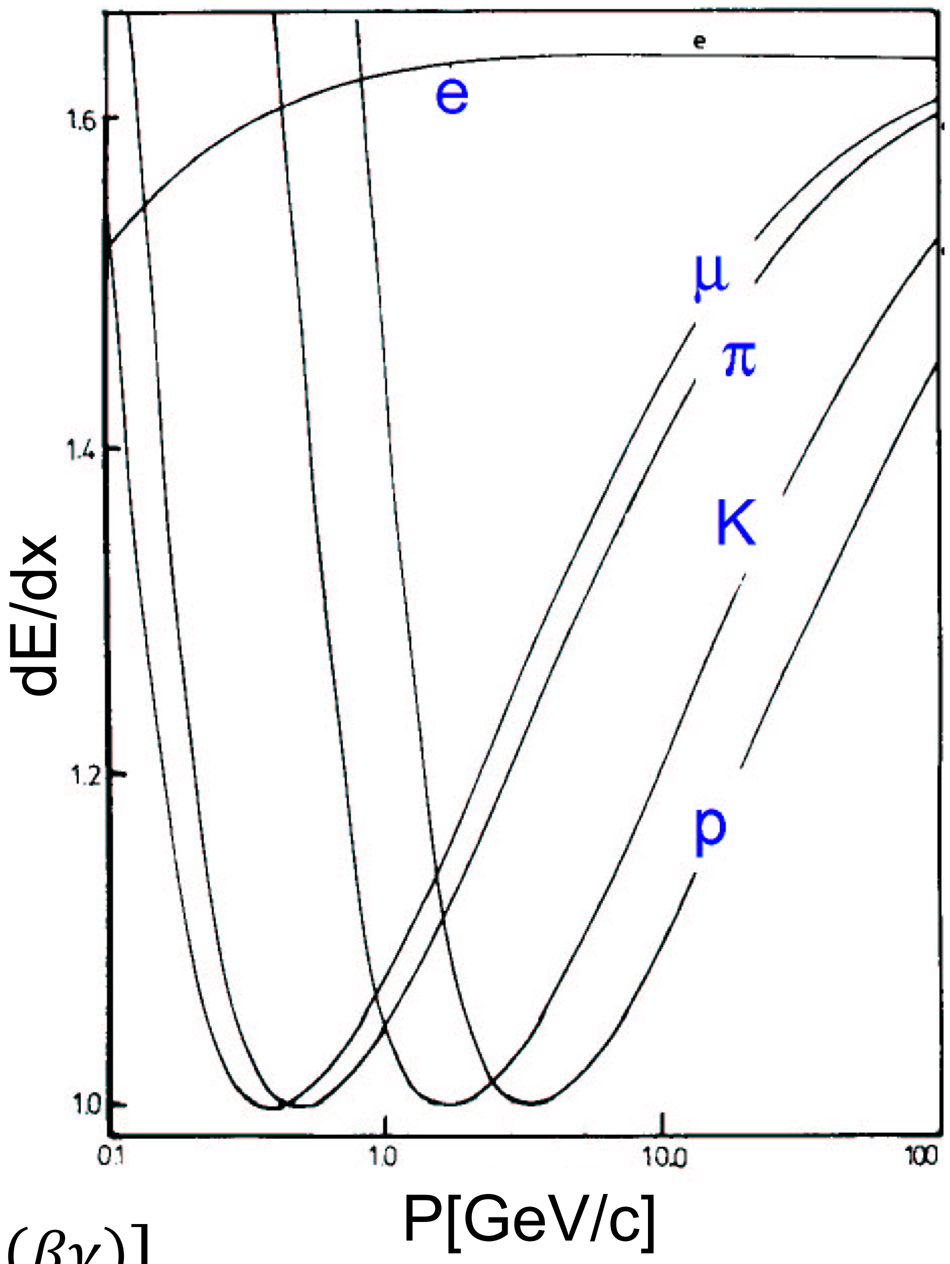

$$\left\langle -\frac{dE}{dx} \right\rangle = 4\pi N_A r_e^2 m_e c^2 \frac{Z}{A} z^2 \frac{1}{\beta^2} \left[\frac{1}{2} \ln \frac{2 m_e c^2 \beta^2 \gamma^2 W_{max}}{I} - \beta^2 - \frac{\delta(\beta\gamma)}{2} \right]$$

Central drift chamber - Belle

- tracking in magnetic field → momentum
- ionization loss measurement → charged particle identification

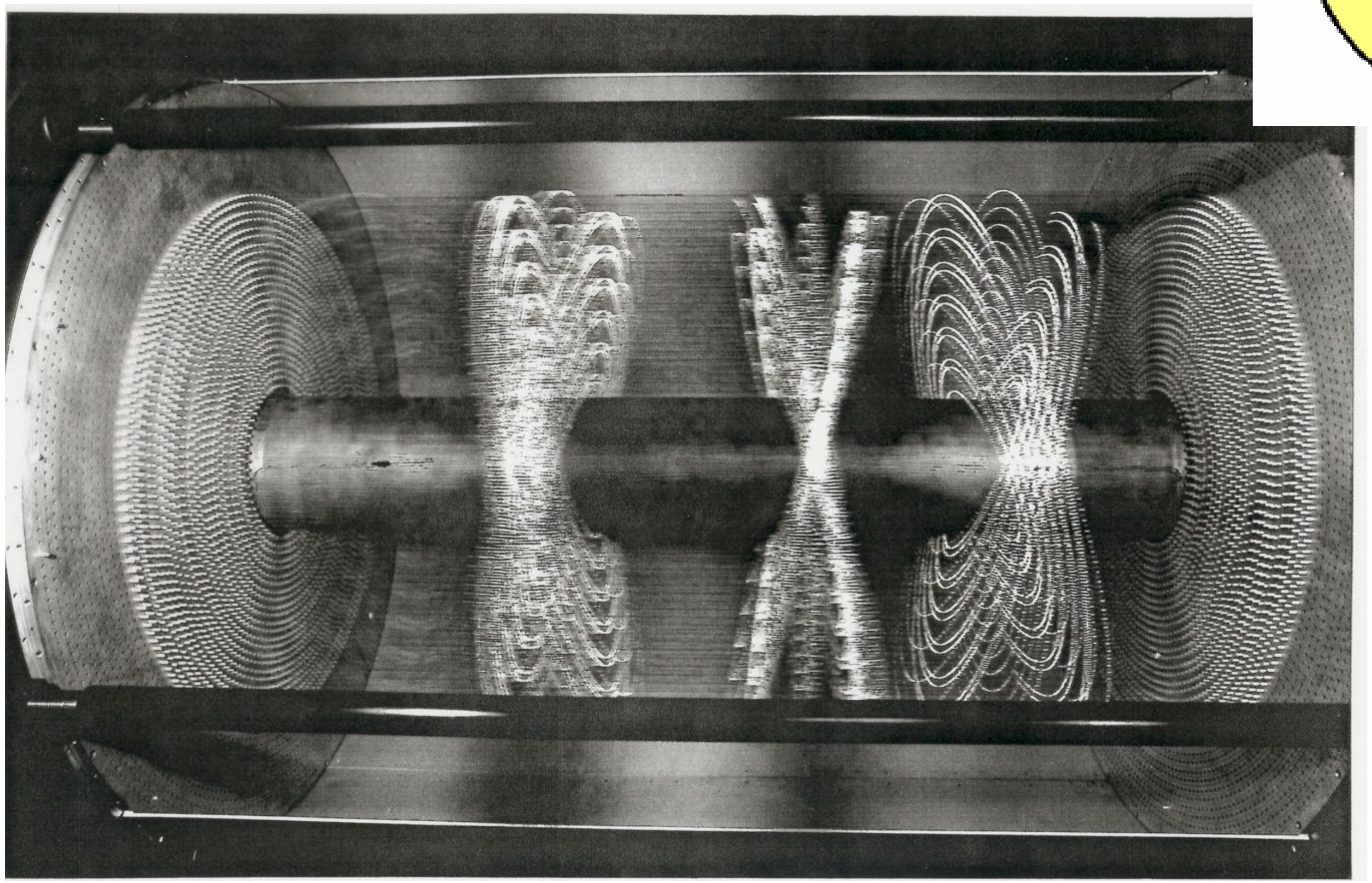

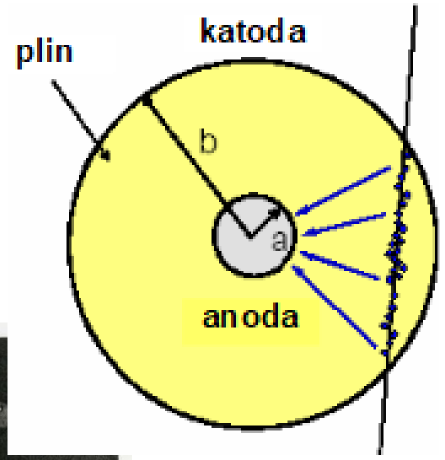

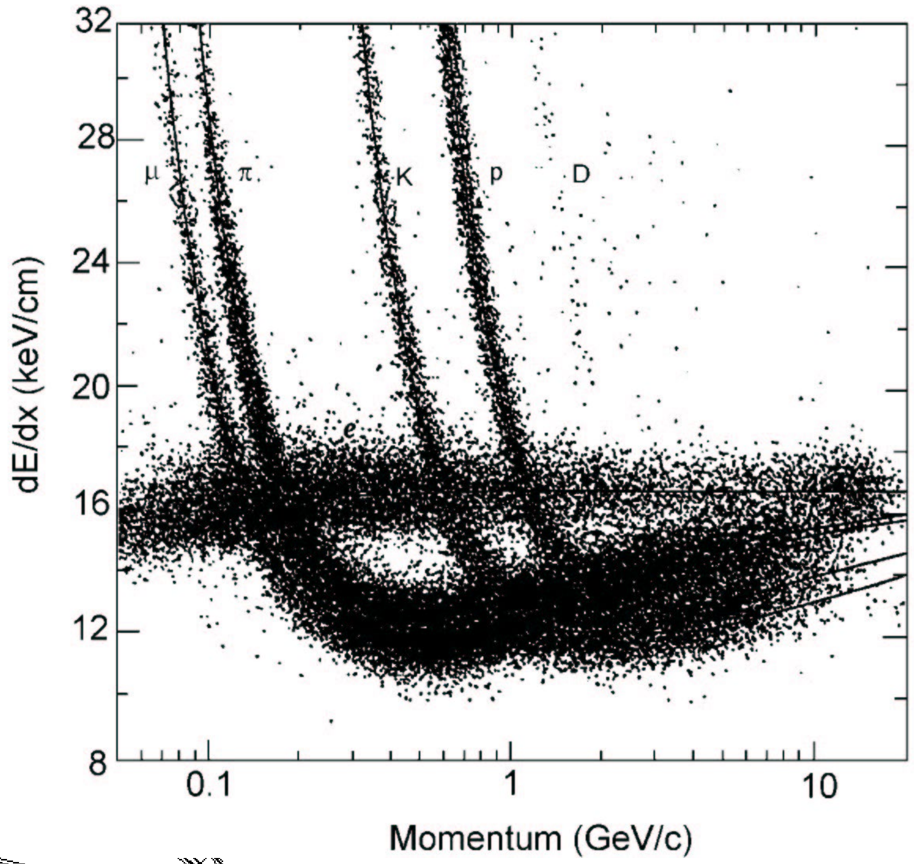

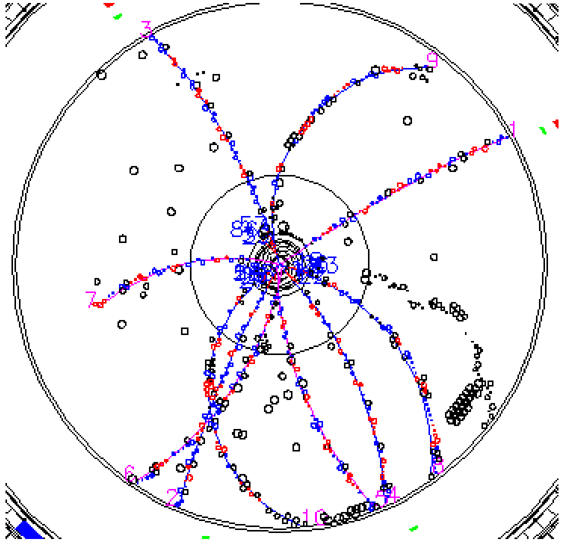

dE/dx - distribution

- dE/dx distribution has long tails due to delta electrons – Landau distribution, not Gaussian
- to improve the resolution average of many samples is taken and about 30% of largest ones are discarded

(B. Adeva et al., NIM A 290 (1990) 115)

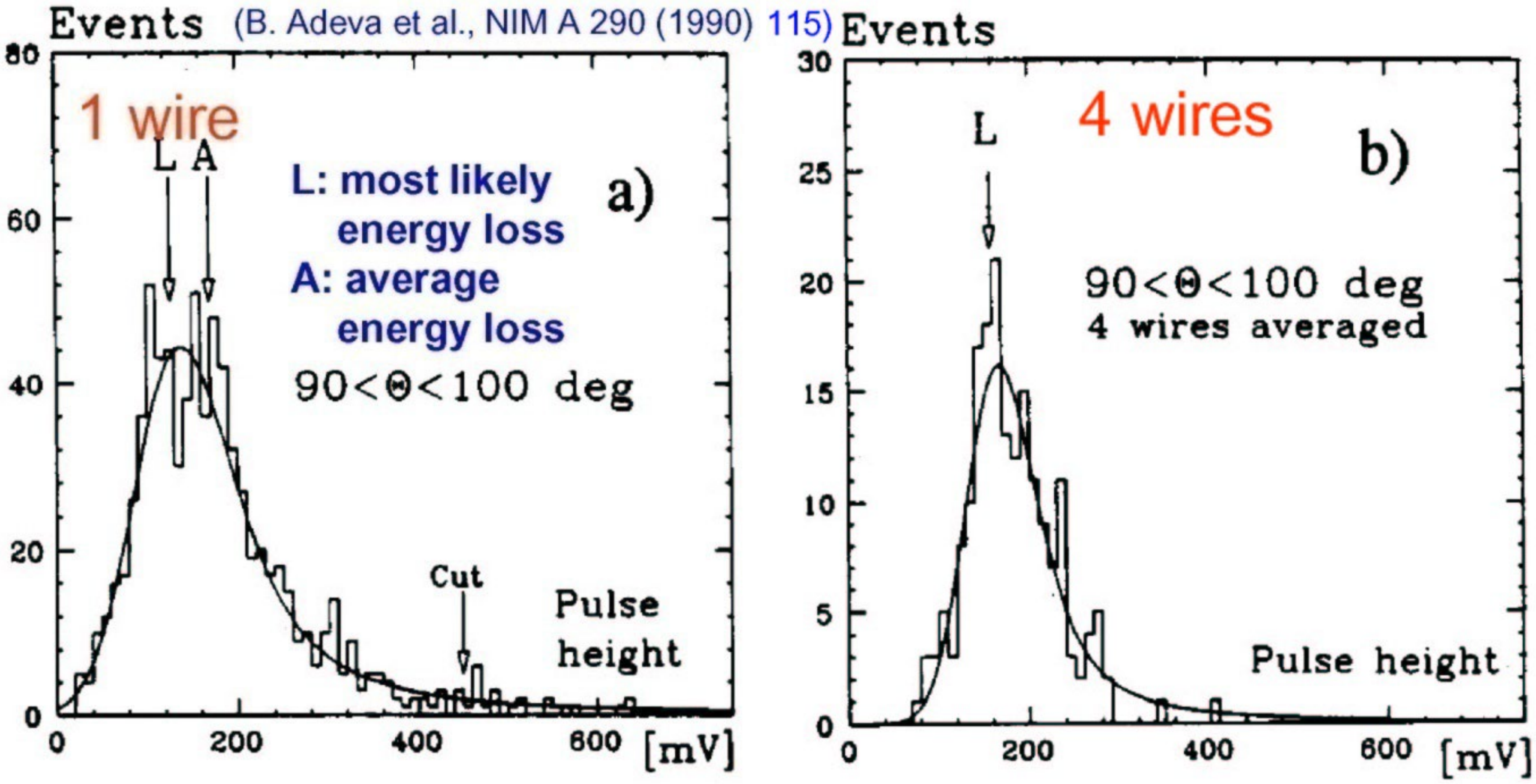

dE/dx - examples

- large drift chamber - Belle

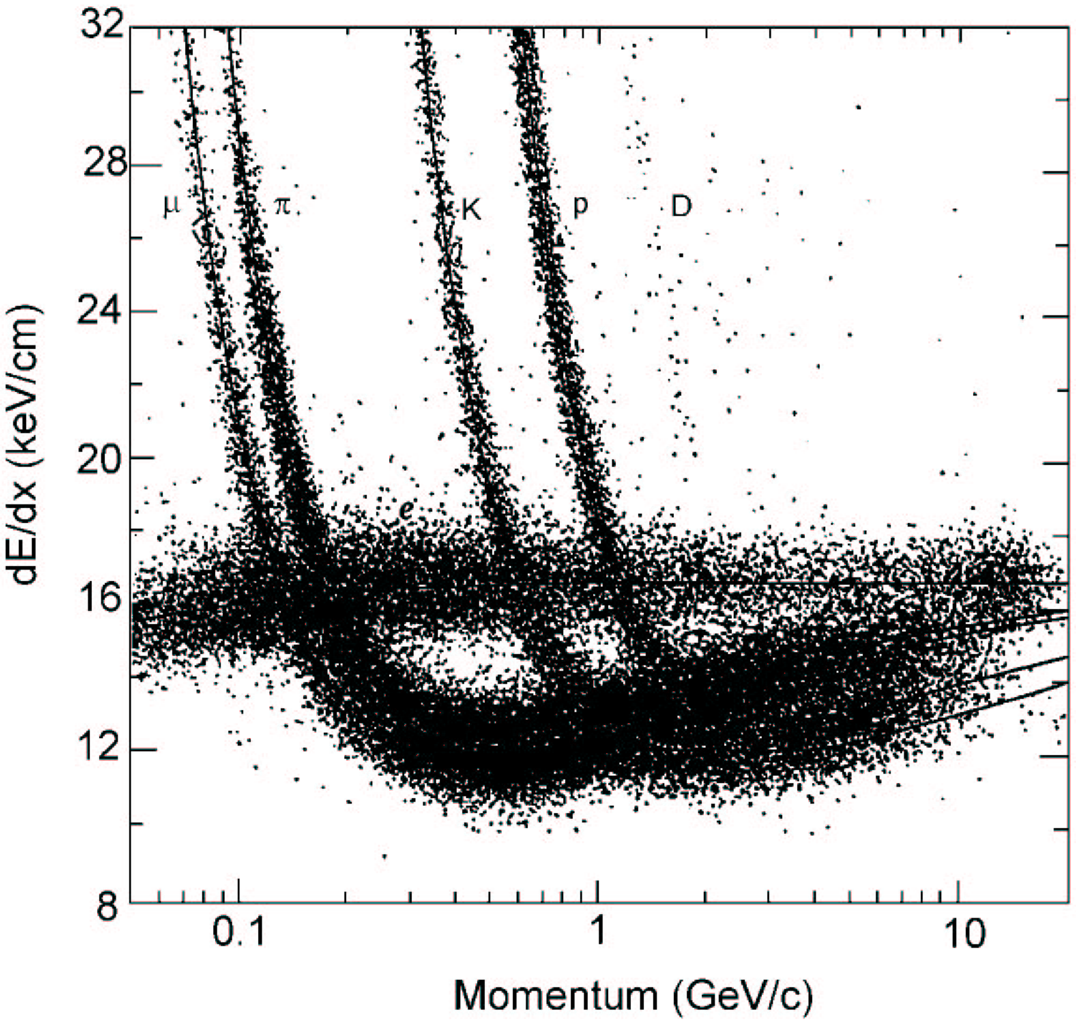

- large TPC chamber - ALICE

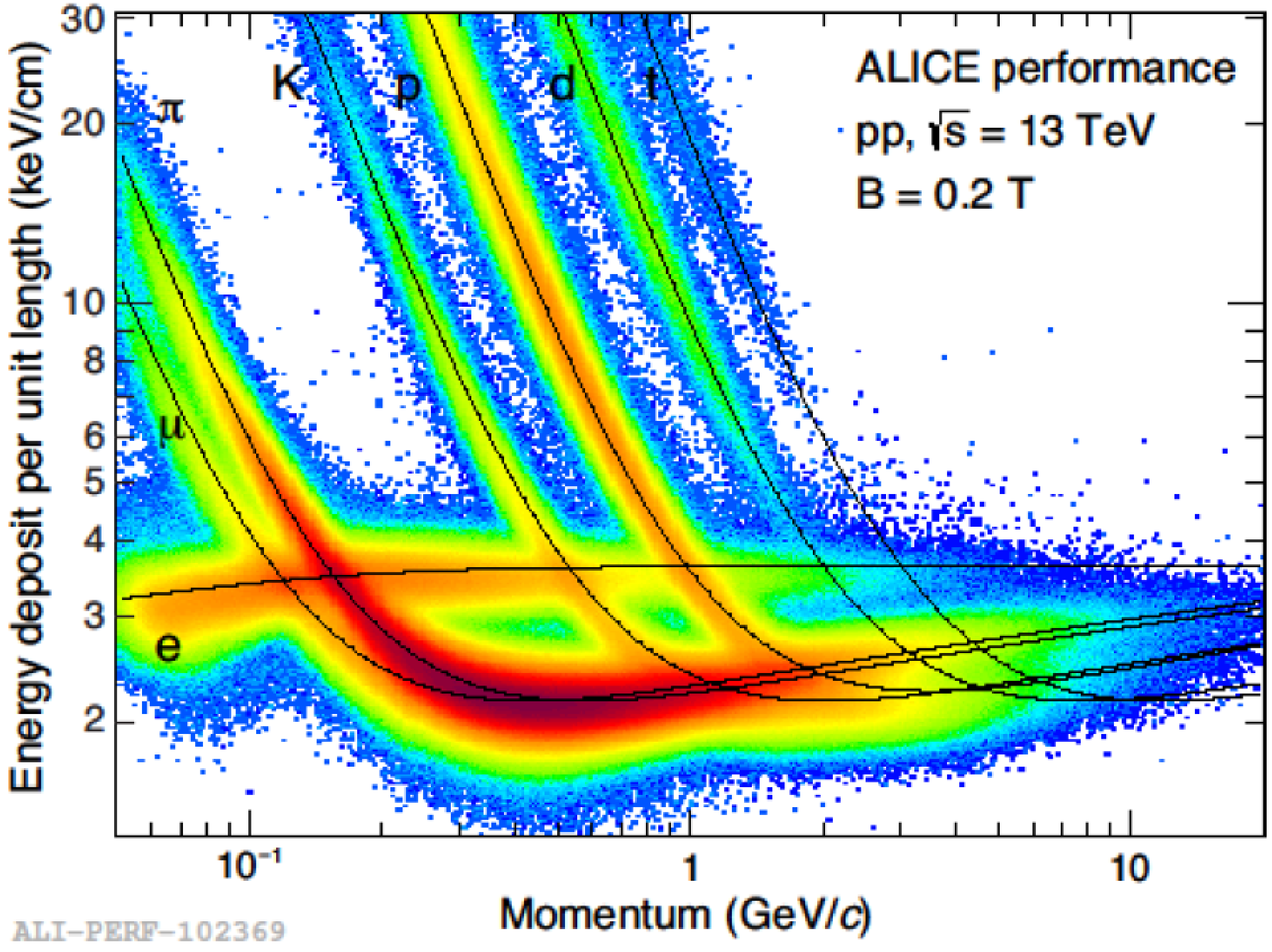

Cluster counting – dN/dx (SuperB)

- Number of clusters per track follows Poissonian statistics → better PID performance
- Timing of individual clusters in single cell → better tracking
- Single cell prototype with gas mixture 90%He+10%iC_4H_{10}
- Beam test with 210 MeV e,μ,π
- Combination of dN/dx and dE/dx → improved performance
- Waiting for large scale implementation

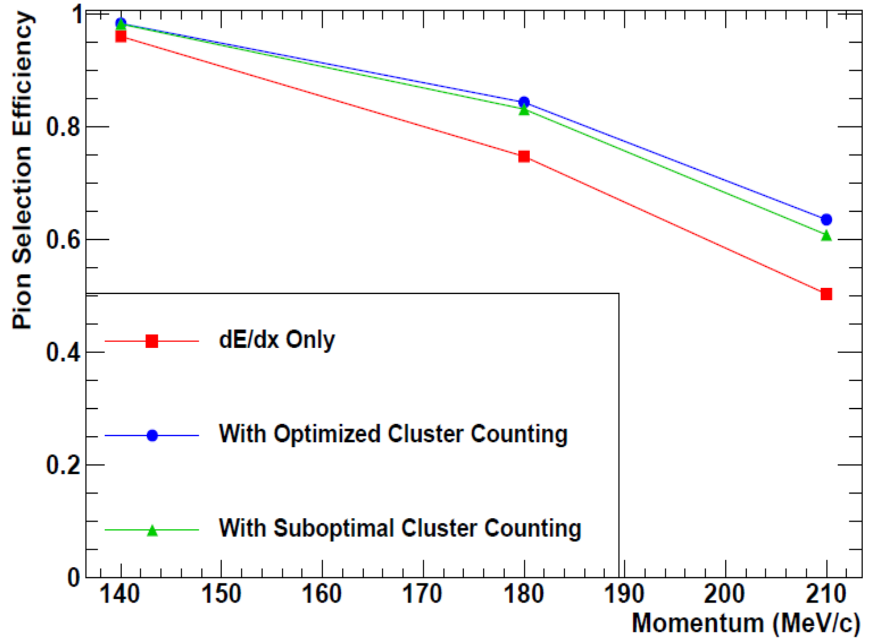

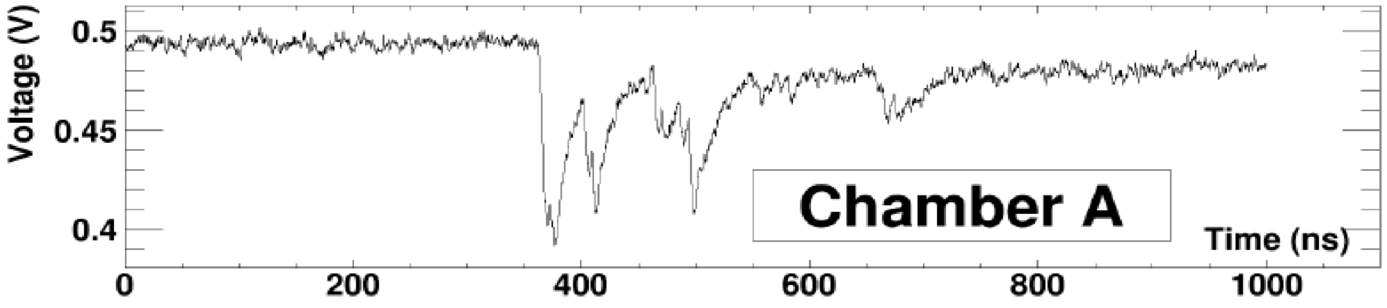

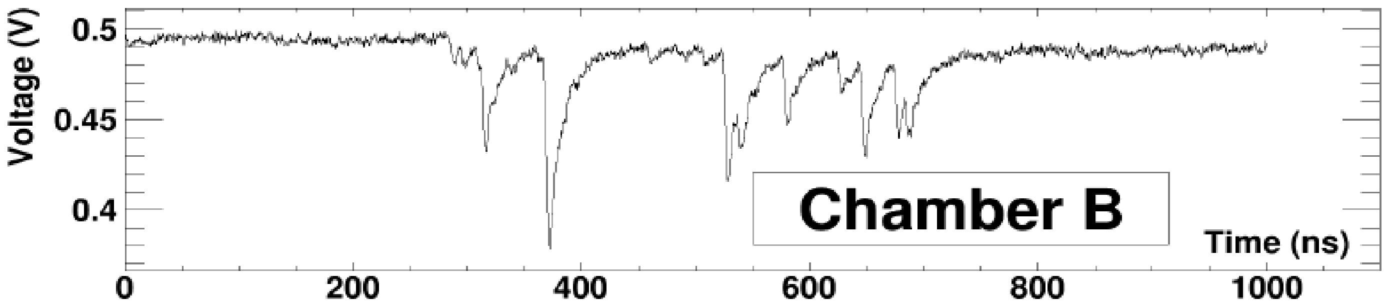

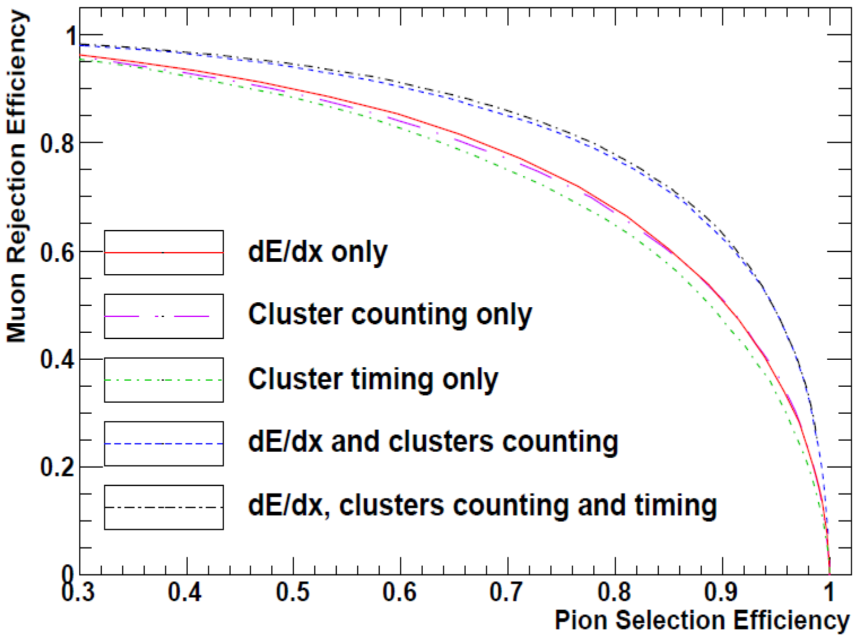

J.F.Caron et al. arXiv:1307.8101

Outline:

- Why PID?
- TOF detectors
- Specific ionization loss - dE/dx
- **Transition radiation detectors (TRD)**
- Cherenkov based PID devices
  - Threshold detectors
  - RICH detectors
  - DIRC type detectors

Transition Radiation

- when charged particle travers the boundary of two materials electric field abruptly changes leading to emission of EM waves
- X rays emitted at the boundary of two media with different refractive indices (relativistic particles)
- emission angle $\theta \approx 1/\gamma$
- emission rate depends on γ (Lorentz factor): becomes important at $\gamma \approx 1000$
- electrons at 0.5 GeV
- pions, muons above 100 GeV
- In between: discrimination of electrons vs pions, mions

$\epsilon_1, n_1 \neq \epsilon_2, n_2$

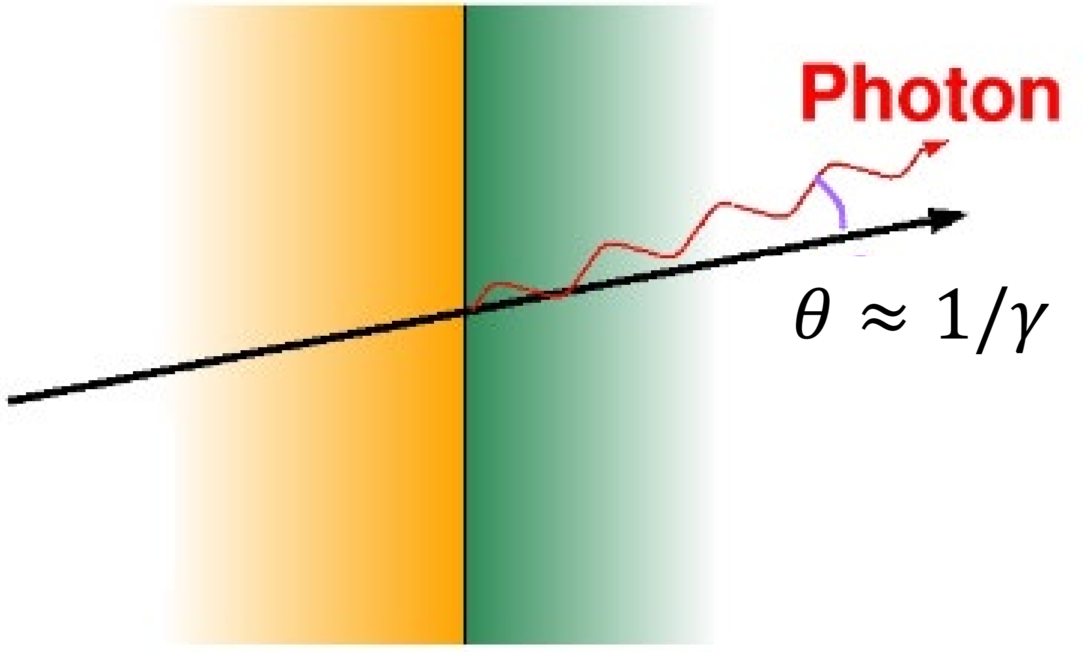

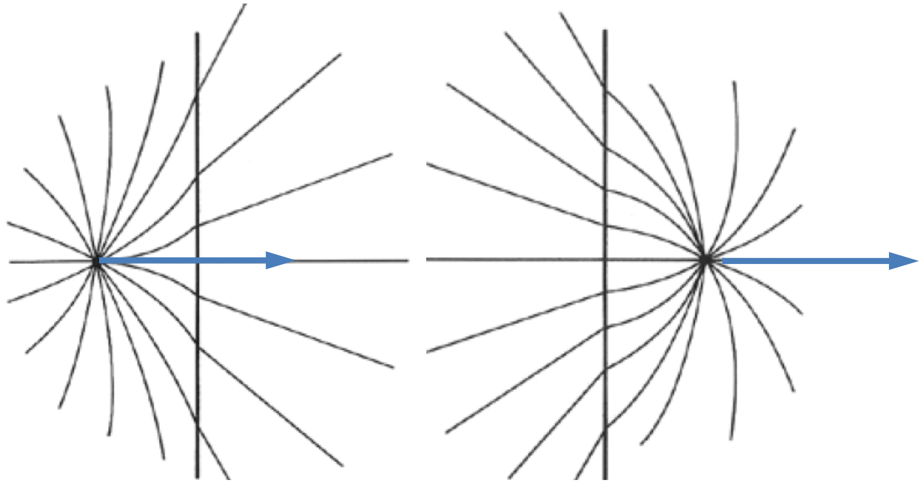

$\epsilon_1 > \epsilon_2$

Transition Radiation Detector (TRD)

- emission at small angle ($\theta \approx 1/\gamma$), photons propagate along the track – detected in tracking detectors
- many boundaries required for measurable output
  - stacks of thin foils or
  - porous materials – foam with many boundaries of individual 'bubbles'

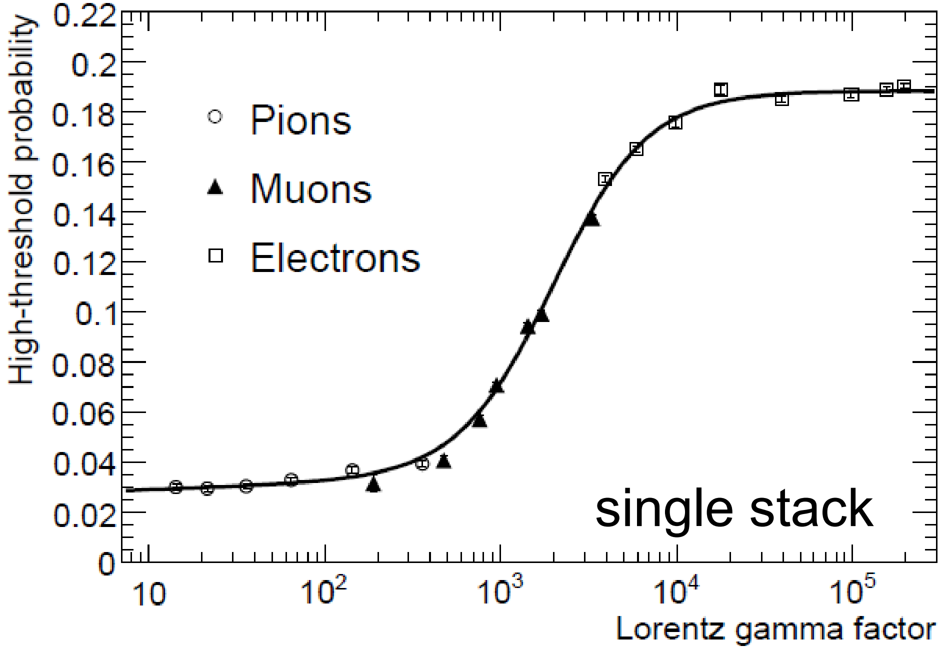

- detection of X rays (~10keV): high Z gas used in gaseous detector (mixture with Xe)
- repeated many times to detect few TR photons

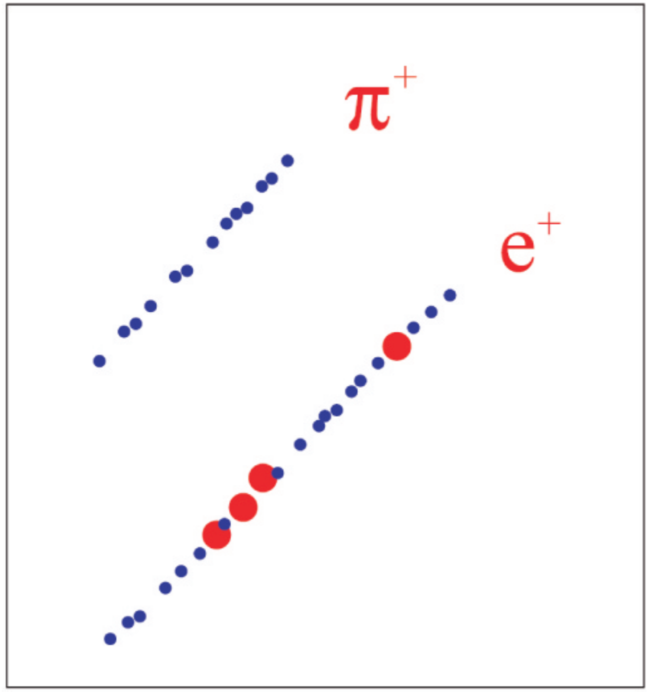

- X rays detected by localized deposition of energy contrary to ionization loss, which is spread out along the track:
- high threshold – X ray (larger red dots)
- low threshold – ionization loss (smaller blue dots)

ATLAS TRD detector

- **ATLAS TRT** (Transition Radiation Tracker) in Inner Detector
- tracking + electron ID
- ~15 polypropylene fibers/foils - fibers (barrel) and foils (end-cap)
- 70% Xe + 27% CO_2 + 3% O_2
- straw tube type (4mm dia.) - faster

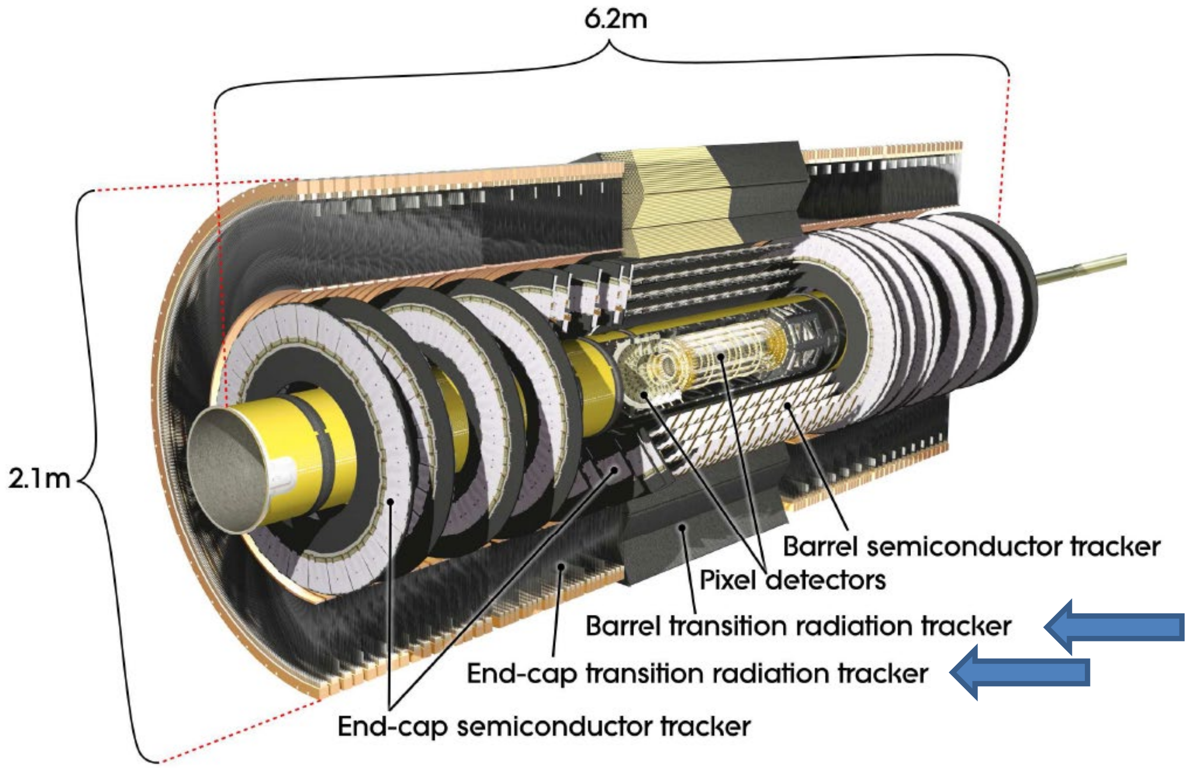

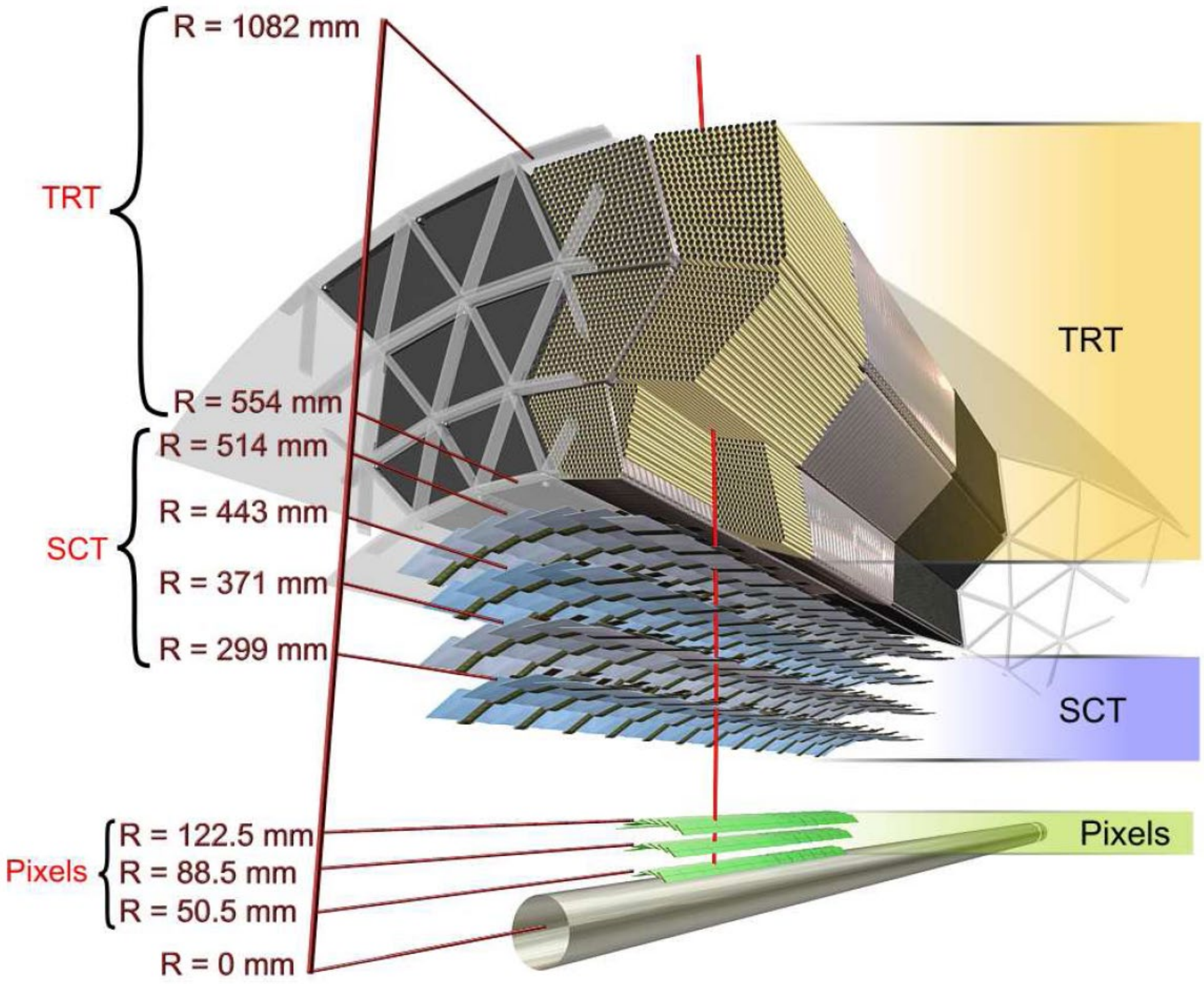

NIM A 540 (2005) 140

ATLAS TRD detector

- **ATLAS TRT** (Transition Radiation Tracker) in Inner Detector
- tracking + electron ID
- ~15 polypropylene fibers/foils - fibers (barrel) and foils (end-cap)
- 70% Xe + 27% CO_2 + 3% O_2
- straw tube type (4mm dia.) - faster

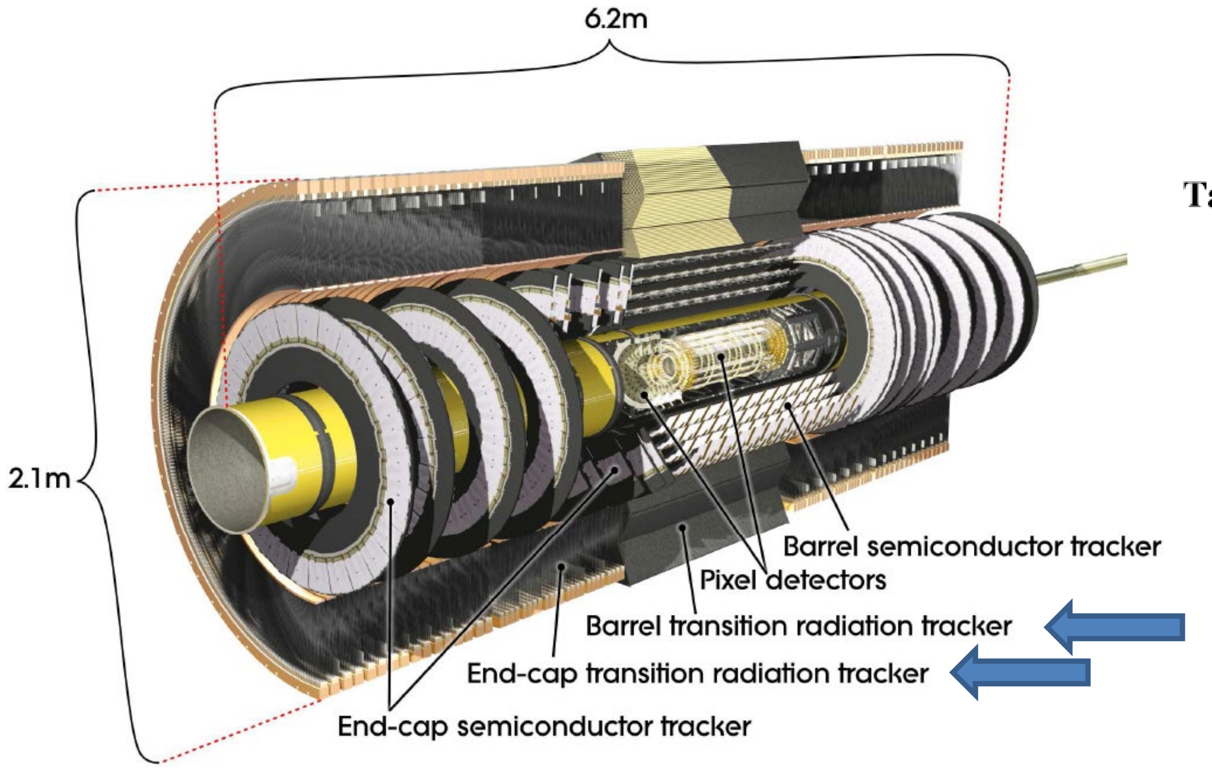

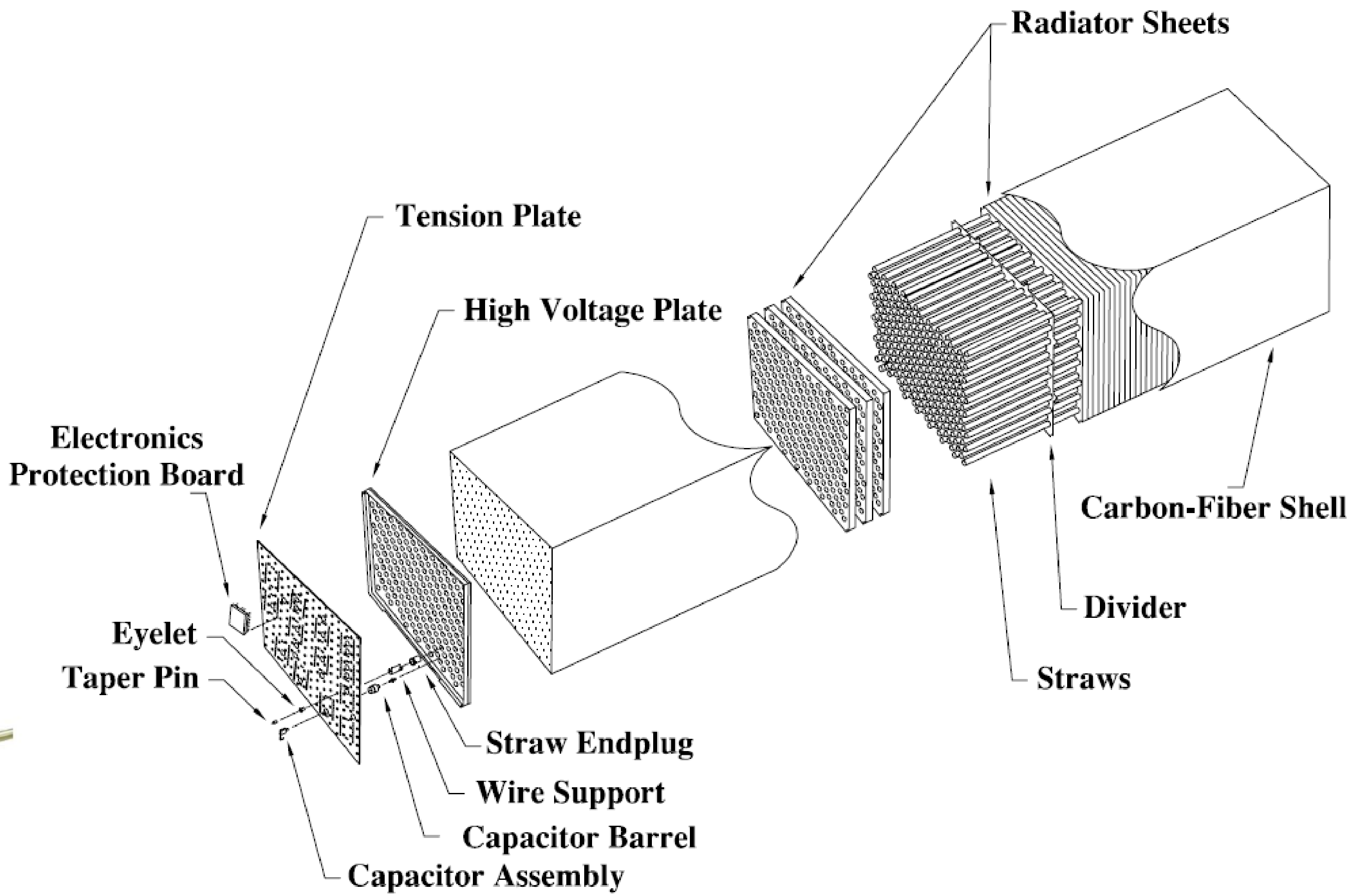

NIM A 540 (2005) 140

ATLAS TRD detector

- few percent pion misid. at 90% electron efficiency

- X-ray probability for single straw

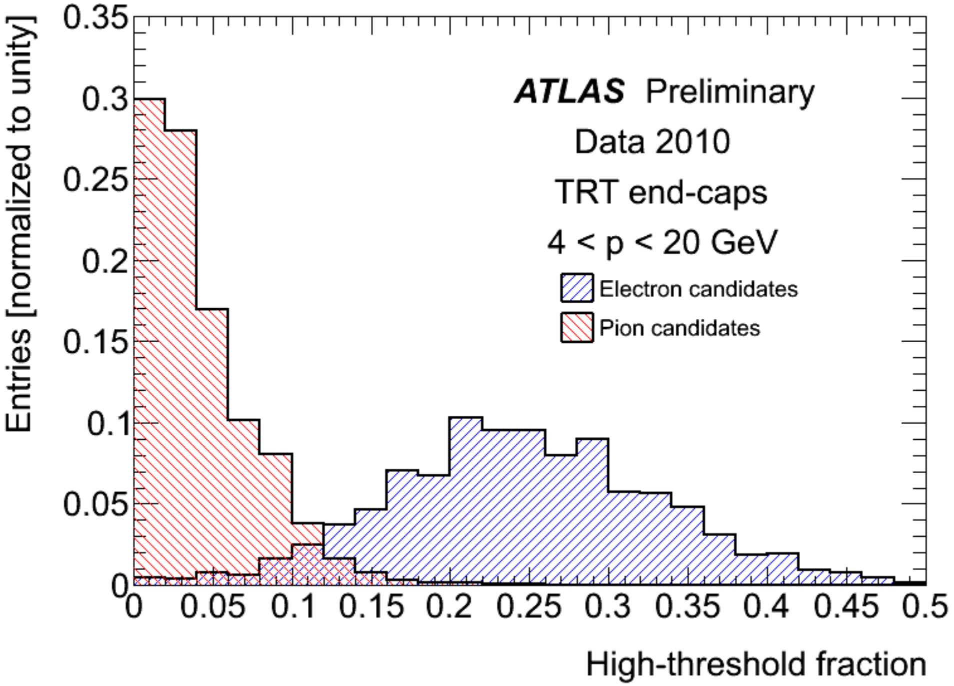

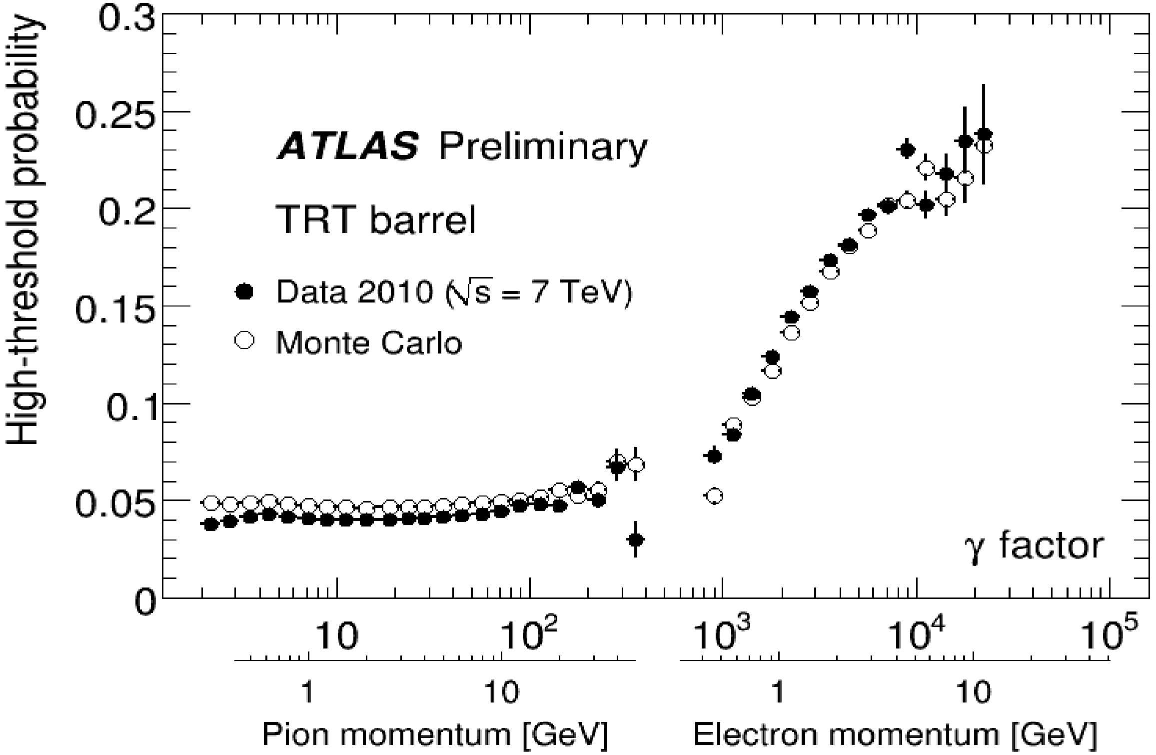

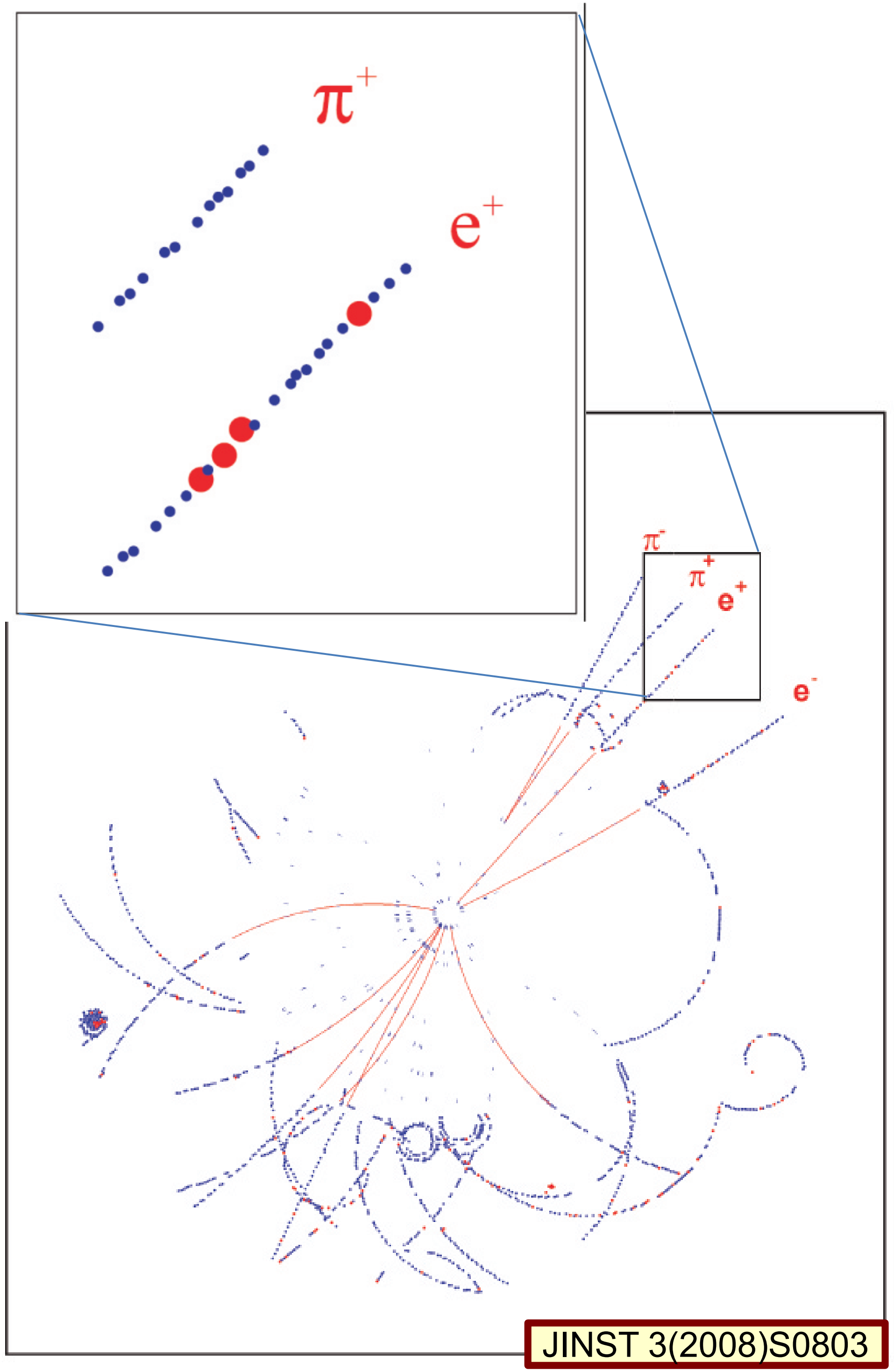

JINST 3(2008)S0803

ALICE TRD detector

- tracking + electron ID
- ~100 foils traversed
- 85% Xe + 15% CO_2
- drift chamber type – better ID

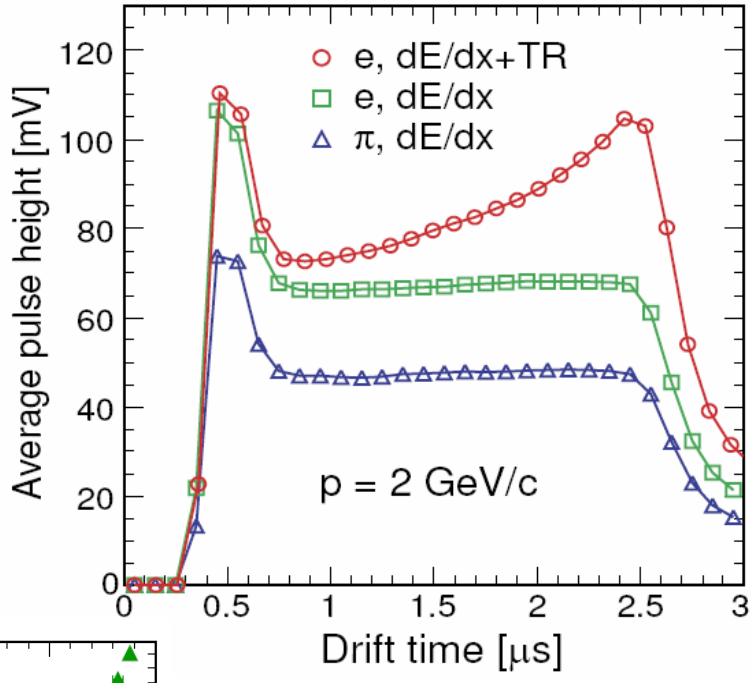

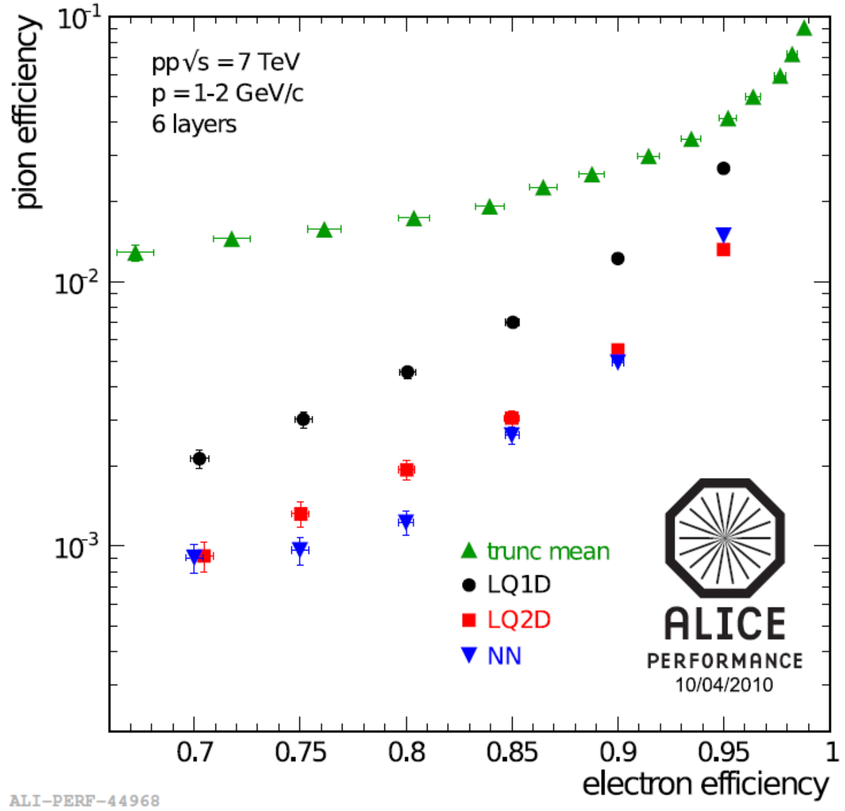

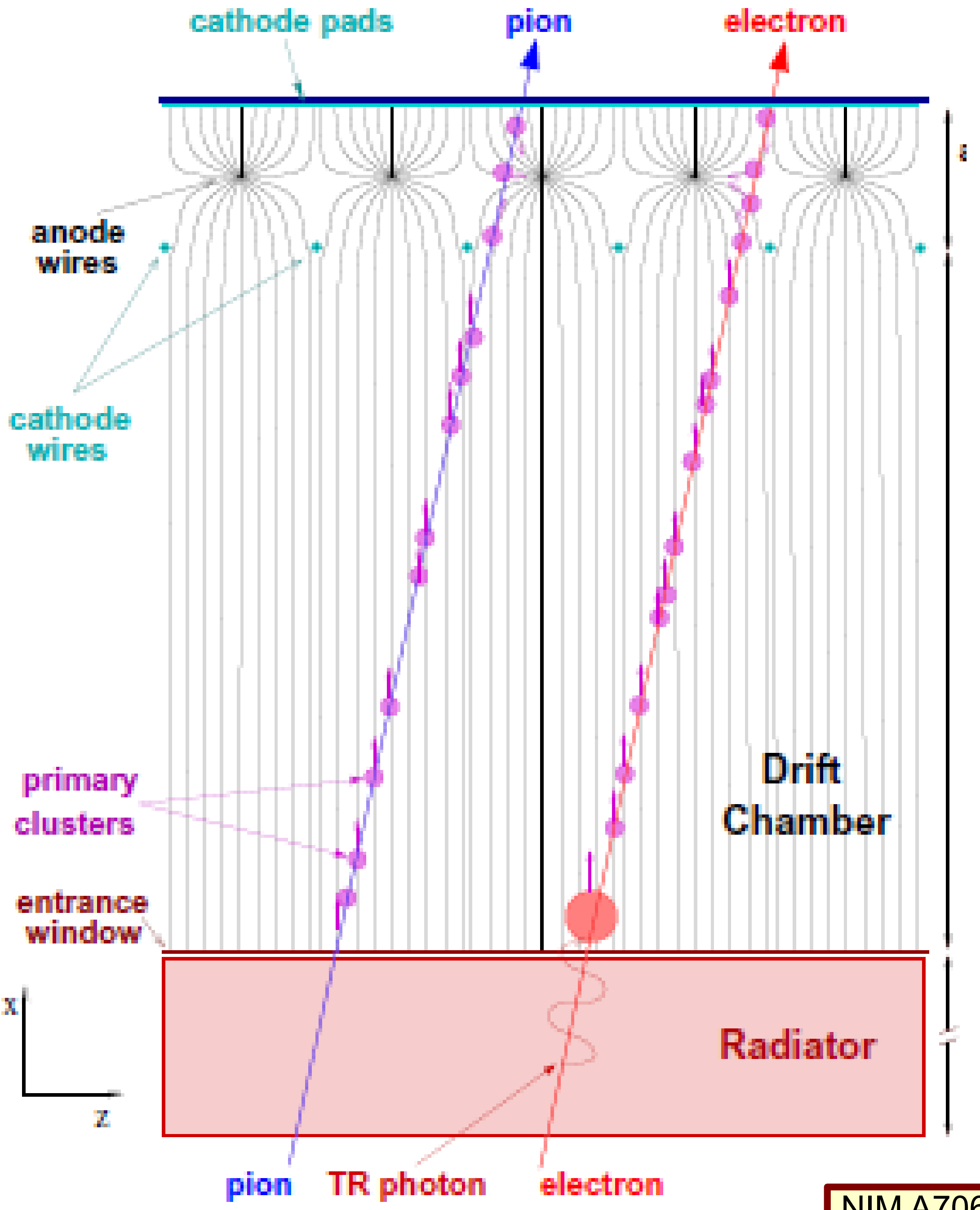

NIM A706(2013) 16

PART II

Outline:

- Why PID?
- TOF detectors
- Specific ionization loss - dE/dx
- Transition radiation detectors (TRD)
- **Cherenkov based PID devices**
  - Threshold detectors
  - RICH detectors
  - DIRC type detectors

Cherenkov radiation

- Cherenkov radiation is electromagnetic shock wave phenomena
- threshold - radiation is emitted when charged particle moves through the medium faster than the speed of light

$$v > \frac{c}{n} \rightarrow \beta = \frac{v}{c} > \frac{1}{n}$$

$$p_{thr} = \frac{mc}{\sqrt{n^2 - 1}} \approx \frac{mc}{\sqrt{2(n-1)}}, \qquad (n-1) \ll 1$$

- Cherenkov angle - angle between the particle and photon momenta directions depends on particle velocity

$$cos\vartheta_C = \frac{1}{\beta n} < \frac{1}{n}$$

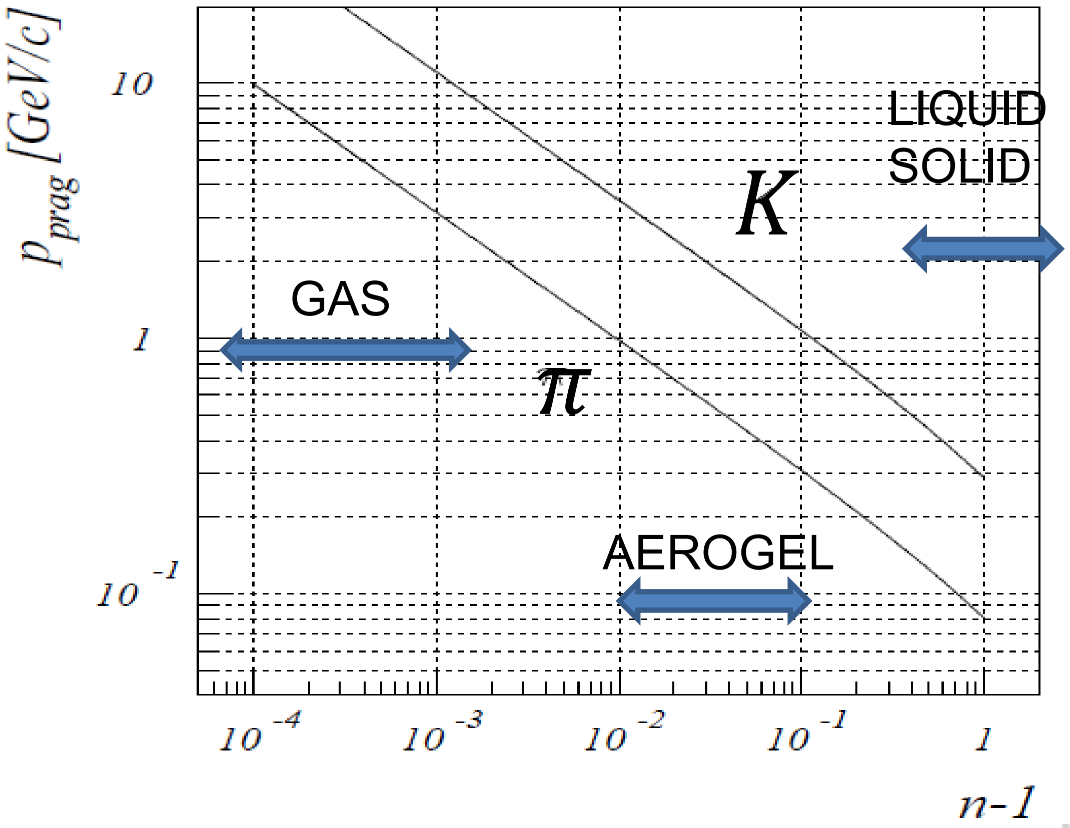

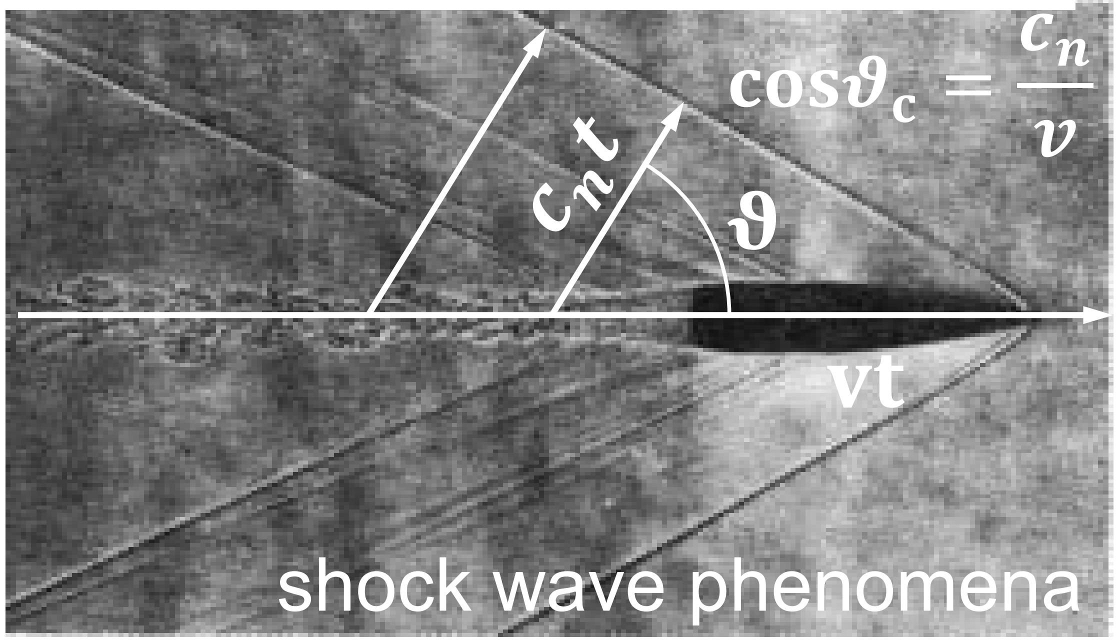

Cherenkov angle - examples

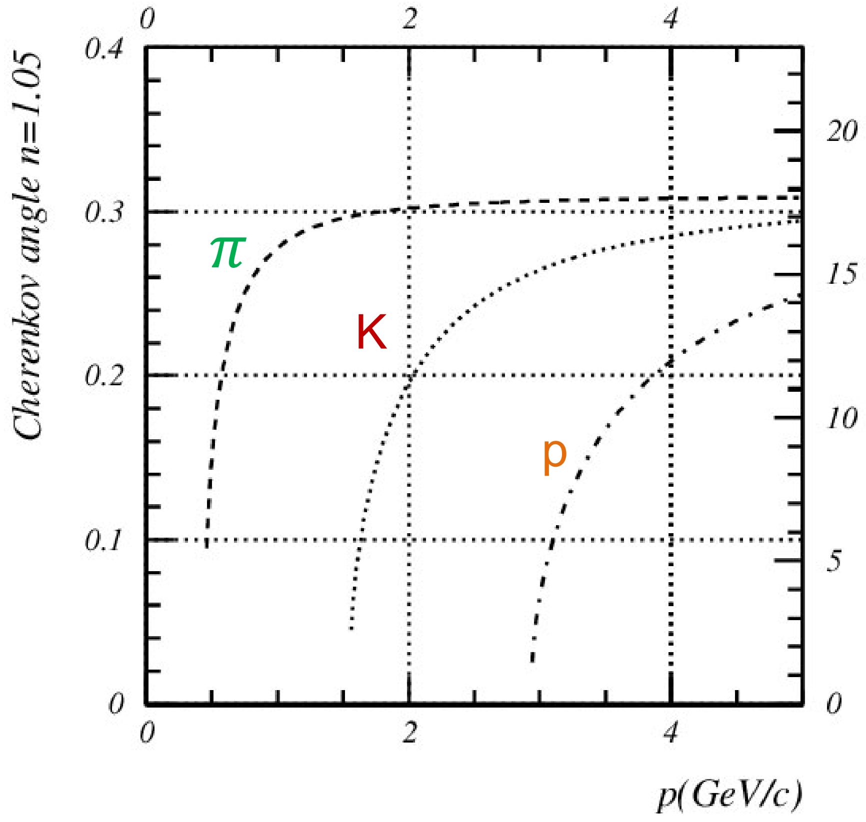

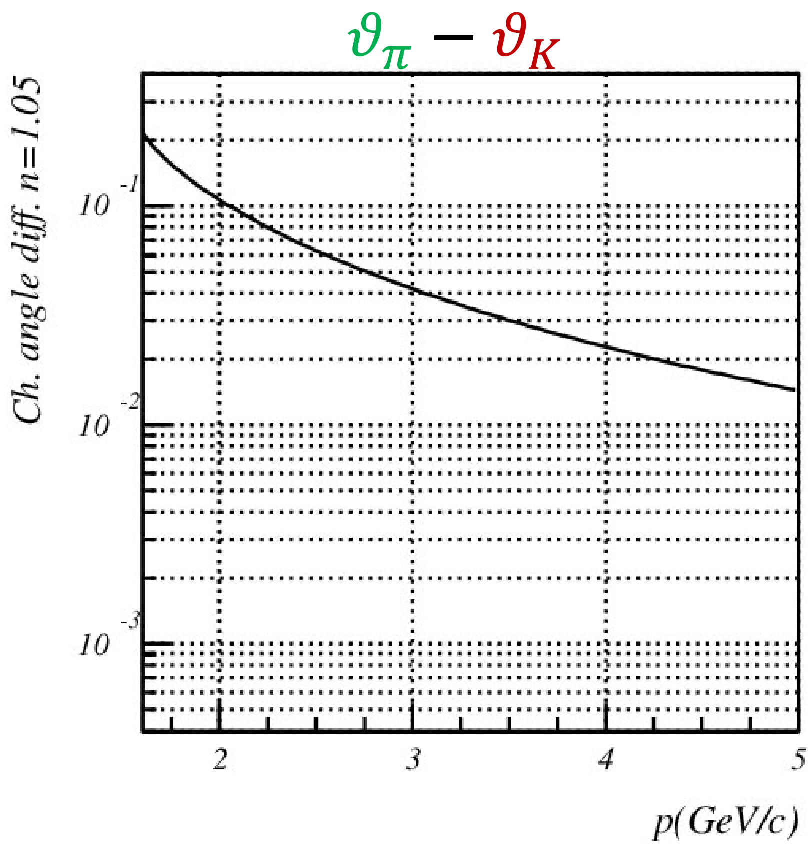

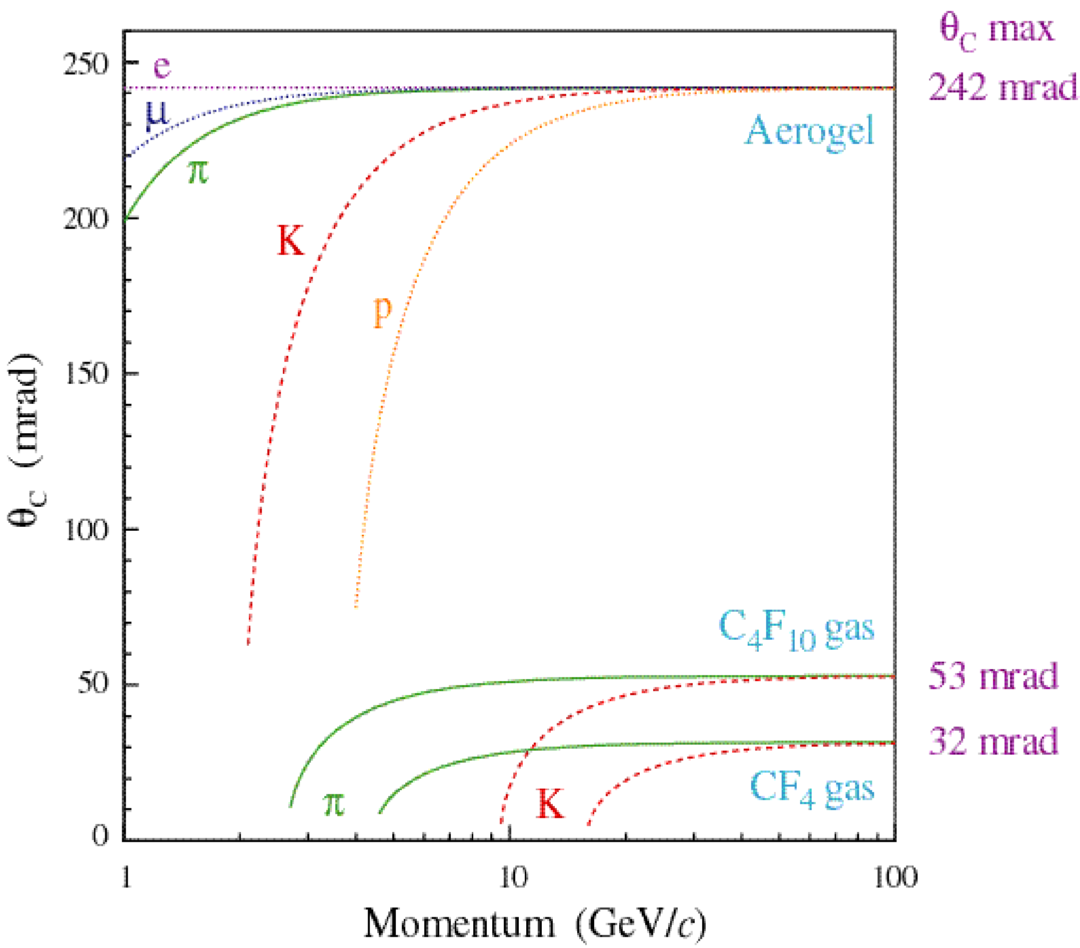

- an aerogel radiator example, candidate for ARICH

- an example from LHCb RICH I and II radiators

Cherenkov radiation

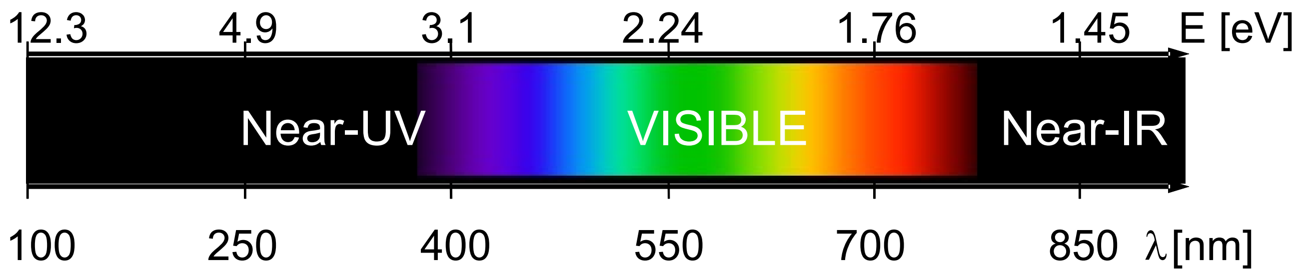

- number of photons per unit photon energy per unit length - depends on:
  - refractive index → Cherenkov angle
  - path length
  - photodetector spectral response

$$\frac{d^2N}{dEdl} = \frac{\alpha z^2}{\hbar c} sin^2\vartheta_C = \frac{\alpha z^2}{\hbar c}\left[1 - \frac{1}{\beta^2 \mathrm{n}^2(\mathrm{E})}\right] \approx \frac{370}{eVcm} sin^2\vartheta_C$$

Photon energy:

$$E_\gamma = h\nu = \frac{hc}{\lambda} \approx \frac{1239\ \mathrm{eV \cdot nm}}{\lambda}$$

- visible range 400 nm – 780 nm → 3.1 - 1.6 eV, $\Delta E_\gamma \approx 1.5\ eV$

- transformed to wavelength dependence

$$\frac{dN}{d\lambda} = hc\frac{dN}{dE}\frac{1}{\lambda^2}$$

→ more photons in blue and UV part of the spectrum

- prompt emission – no raise and decay time constants as with scintillators

→ enables precise time measurements

- light is polarized – E lies in the plane defined by particle and photon momenta

Number of Cherenkov photons - examples

	$(n-1)\cdot 10^6$ $(7\,eV)$	$\Delta n \cdot 10^6$ $(6.5\,eV - 7.5\,eV)$	$p_{prag,\pi}$ (GeV/c)	$p_{prag,K}$ (GeV/c)
Ar	315	21	5.70	20.15
CH_4	510	49	4.37	15.46
C_2H_6	898	90	3.29	11.65
C_4H_{10}	1500	160	2.55	9.01
CF_4	488	10	4.47	15.80
C_2F_6	793	23	3.51	12.39
C_4F_{10}	1510	53	2.54	8.98

- estimated number of detected photons $(\Delta E = 2eV, PDE = 0.1)$

$$N \approx \frac{370}{eV\,cm} sin^2\vartheta_C \Delta l \Delta E = \frac{74}{cm} sin^2\vartheta_C \Delta l$$

- for saturated ring $(n = \sqrt{2}, \mathrm{l} = 1\mathrm{cm})$

$$\mathrm{N} \approx \frac{74}{cm}\left(1 - \frac{1}{n^2}\right)\Delta l = 37$$

- approximated for gas $(n = 1.001, l = 1m)$

$$\mathrm{N} \approx \frac{74}{cm} 2(n-1)\Delta l \approx 15$$

- for aerogel $(n = 1.05, l = 1cm) \approx 7$

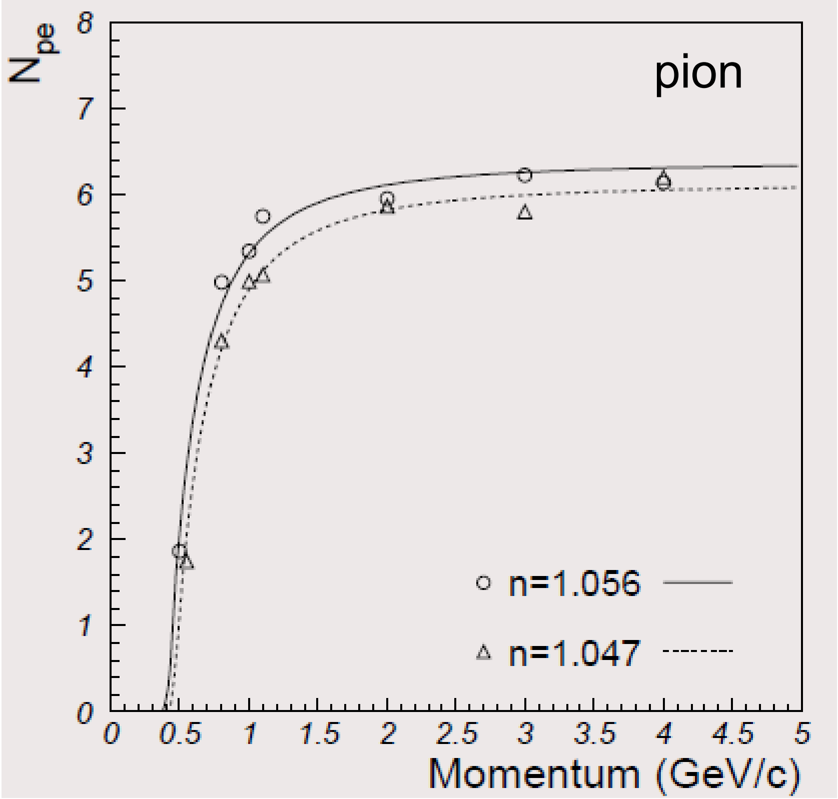

Outline:

- Why PID?
- TOF detectors
- Specific ionization loss - dE/dx
- Transition radiation detectors (TRD)
- Cherenkov based PID devices
  - **Threshold detectors**
  - RICH detectors
  - DIRC type detectors

Threshold Cherenkov counters

- ACC (Aerogel Cherenkov Counter) @ Belle (variable n=1.03,1.01,1.015, 1.02).

$$p_{thr} = \frac{mc}{\sqrt{n^2 - 1}}$$

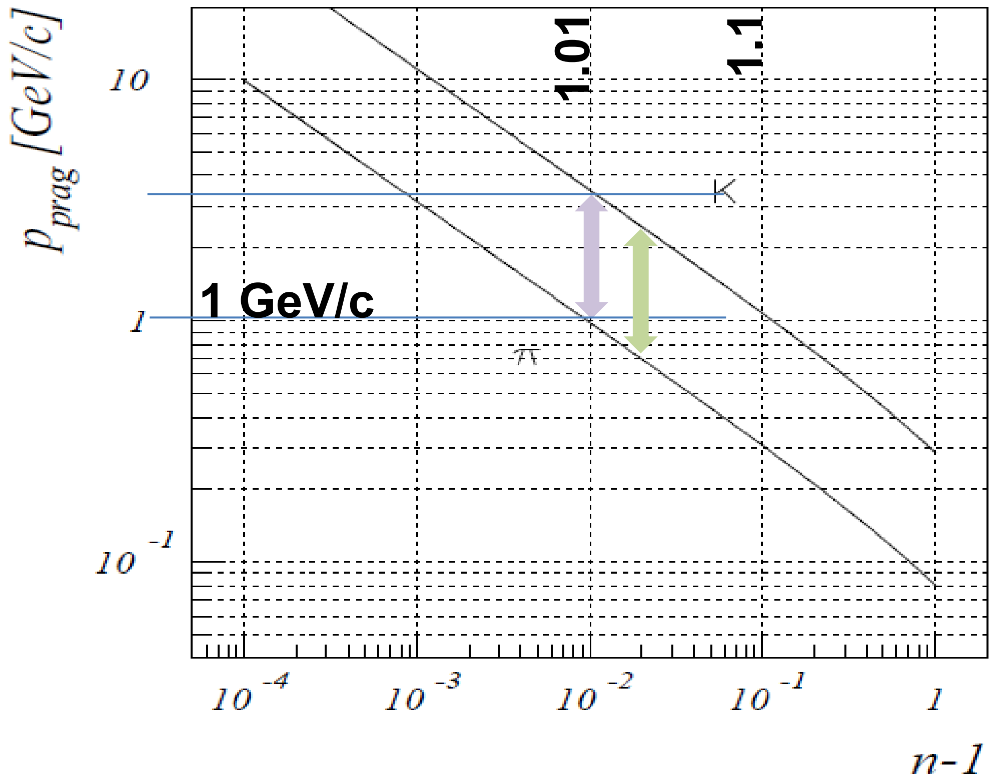

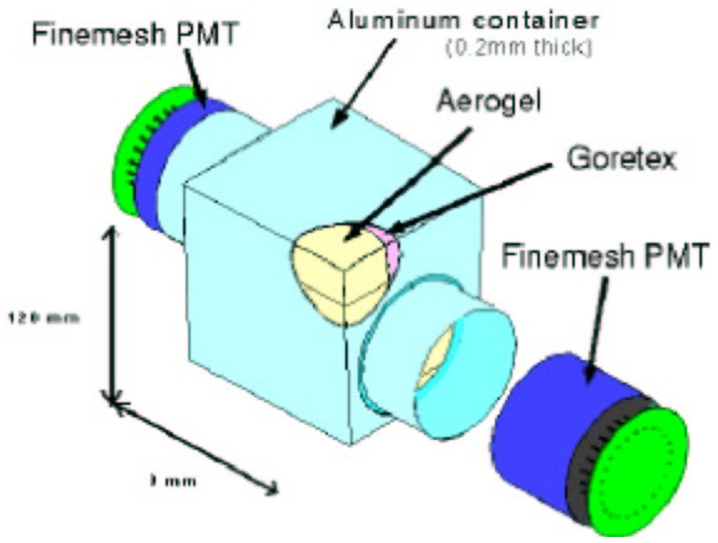

Detector unit: a block of aerogel and two fine-mesh PMTs

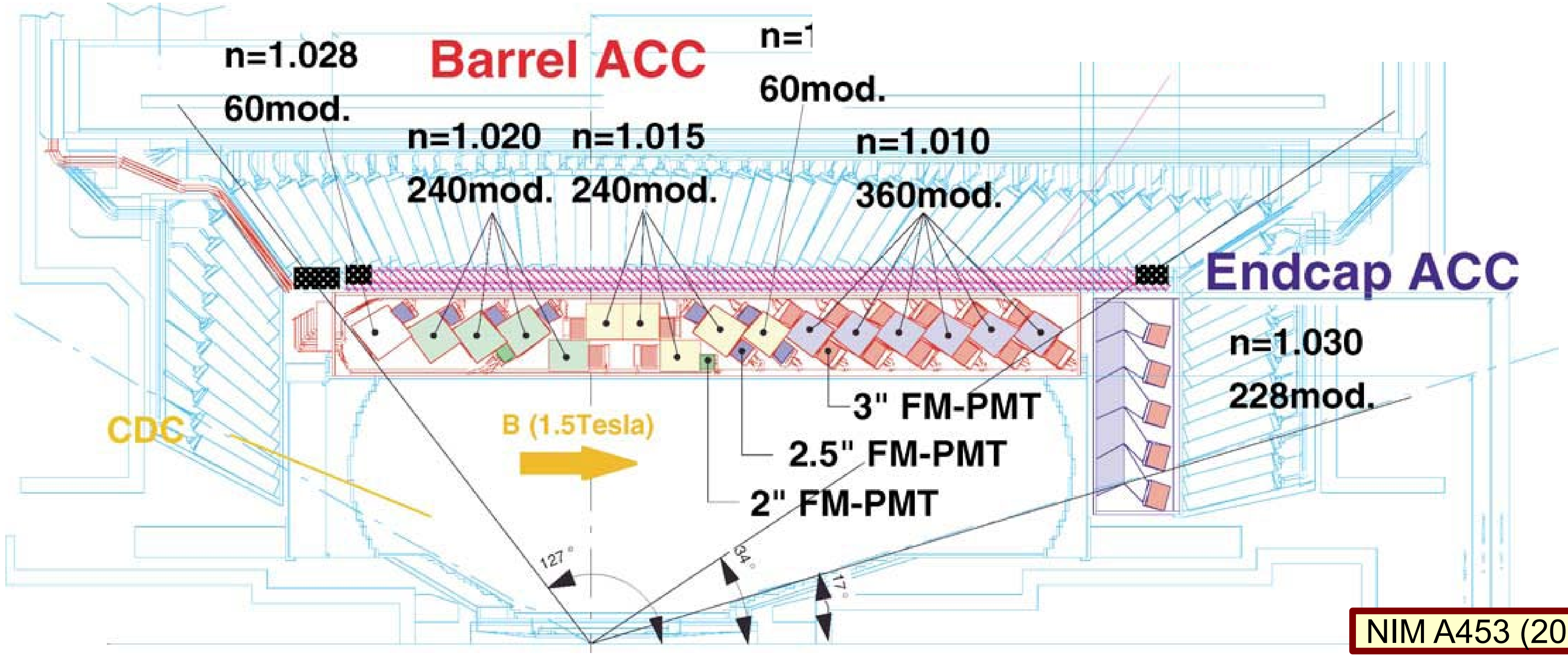

NIM A453 (2000) 321

Belle ACC performance

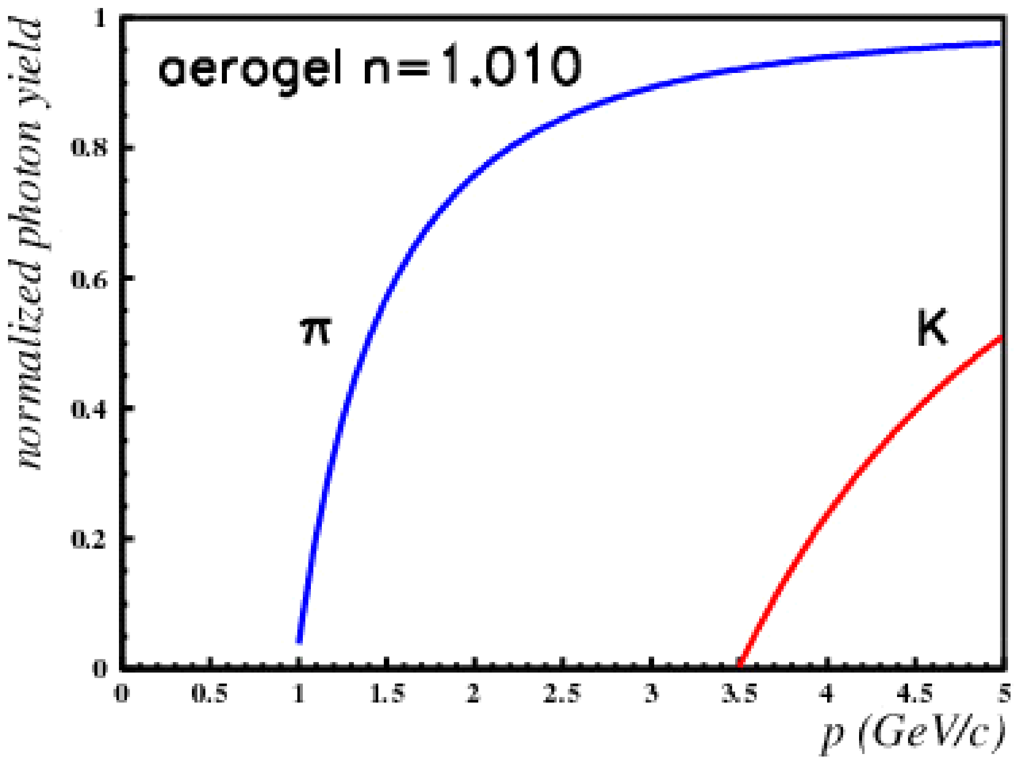

Normalized yield vs. momentum.

Yield for momentum range 2-3.5 GeV/c: expected and measured number of Ch. photons.

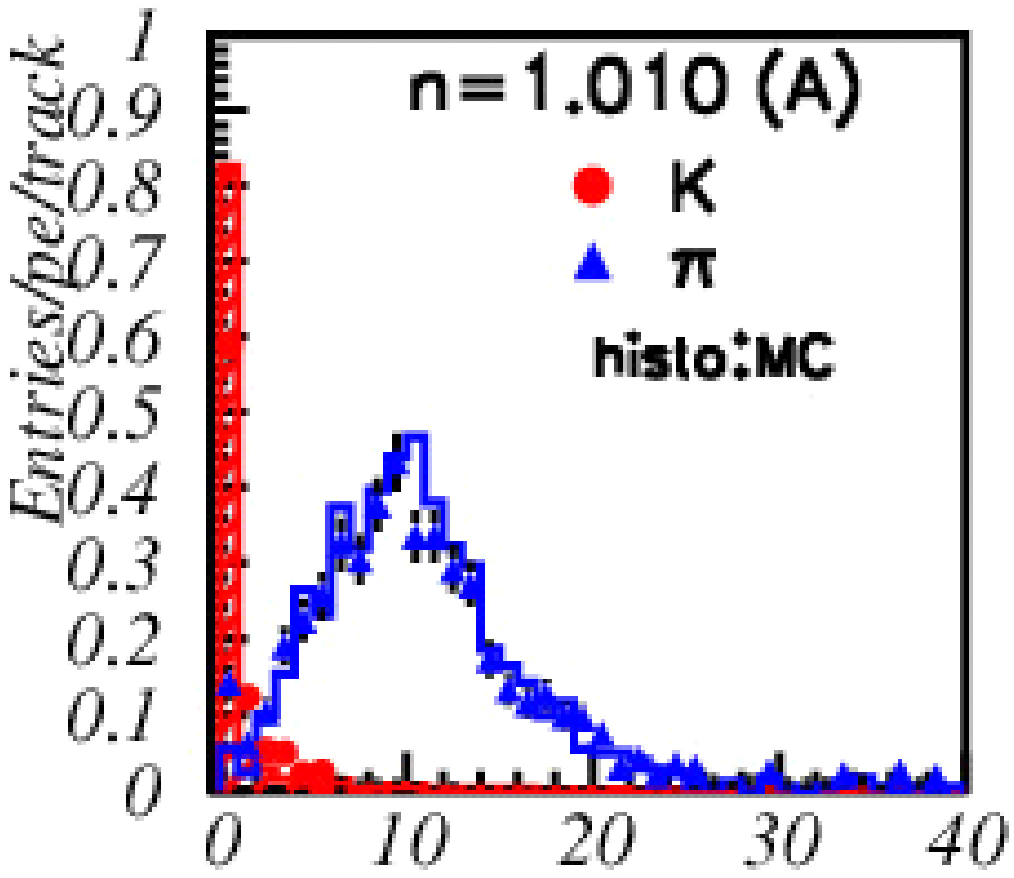

NIM A453 (2000) 321

Outline:

- Why PID?
- TOF detectors
- Specific ionization loss - dE/dx
- Transition radiation detectors (TRD)
- Cherenkov based PID devices
  - Threshold detectors
  - **RICH detectors**
  - DIRC type detectors

RICH counter basic idea

- proposed in 1977 by J. Seguinot and T. Ypsilantis

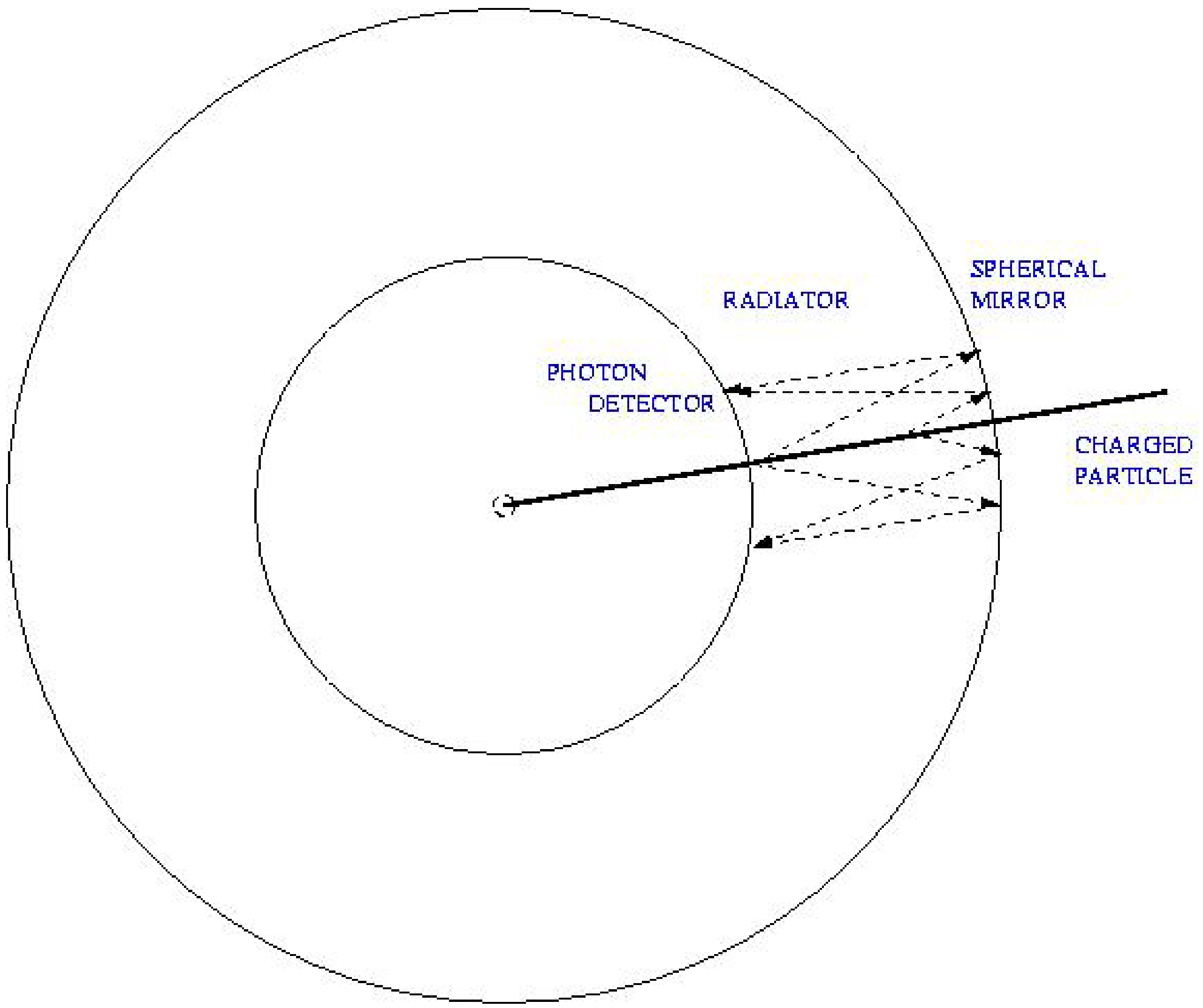

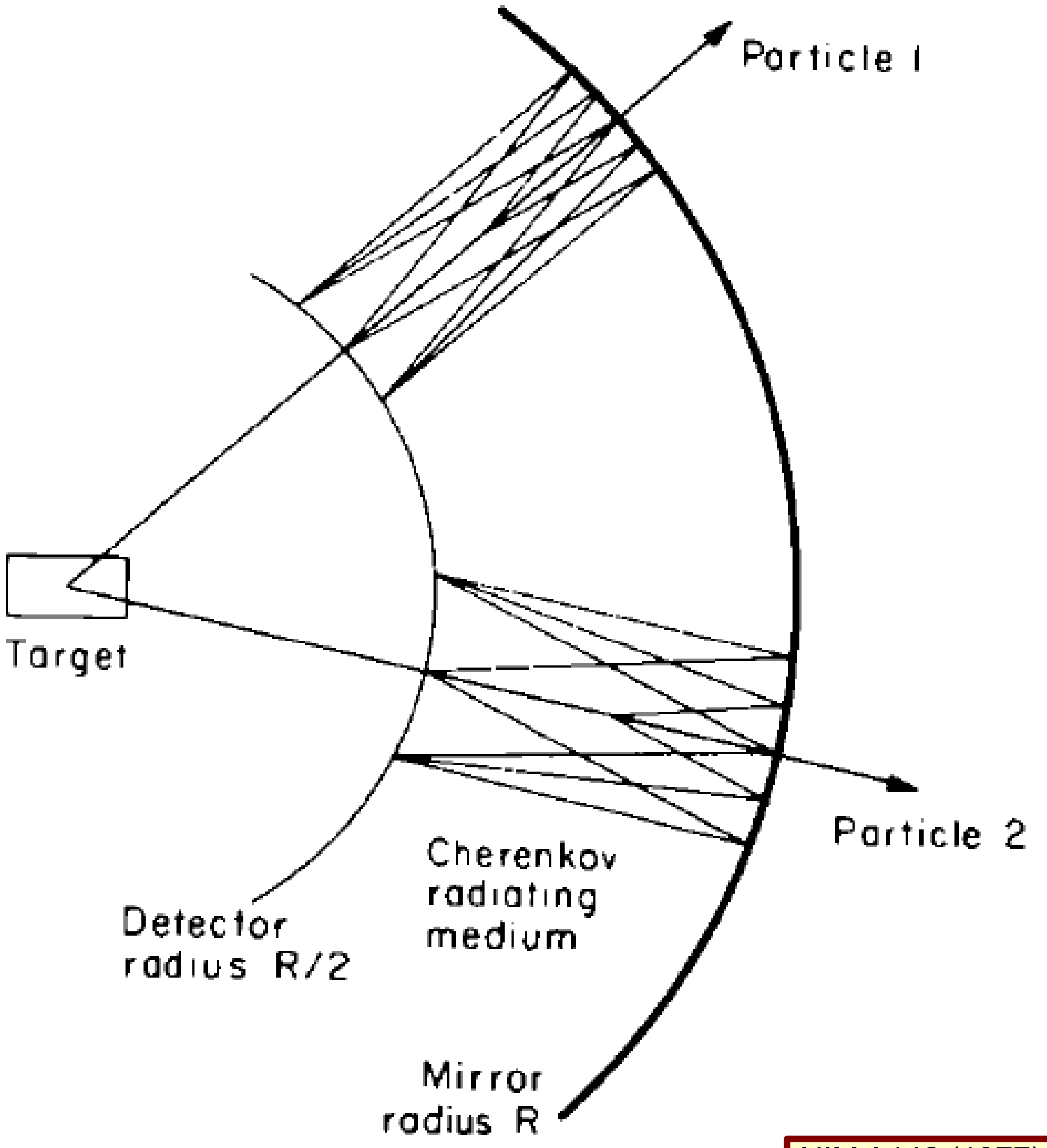

NIM A142 (1977) 377

RICH detector basic types

Ring Imaging CHerenkov counter (RICH) → measurement of Cherenkov angle → particle velocity.

Base designs:

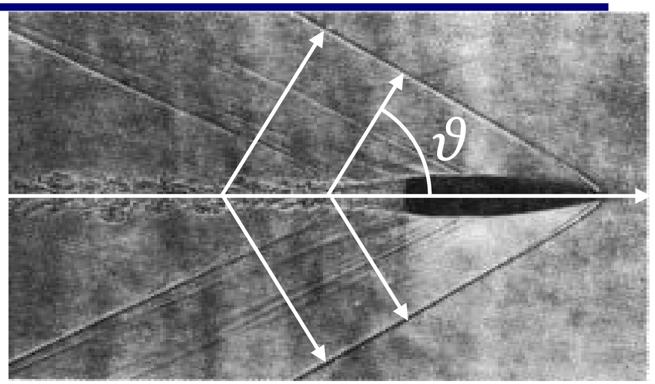

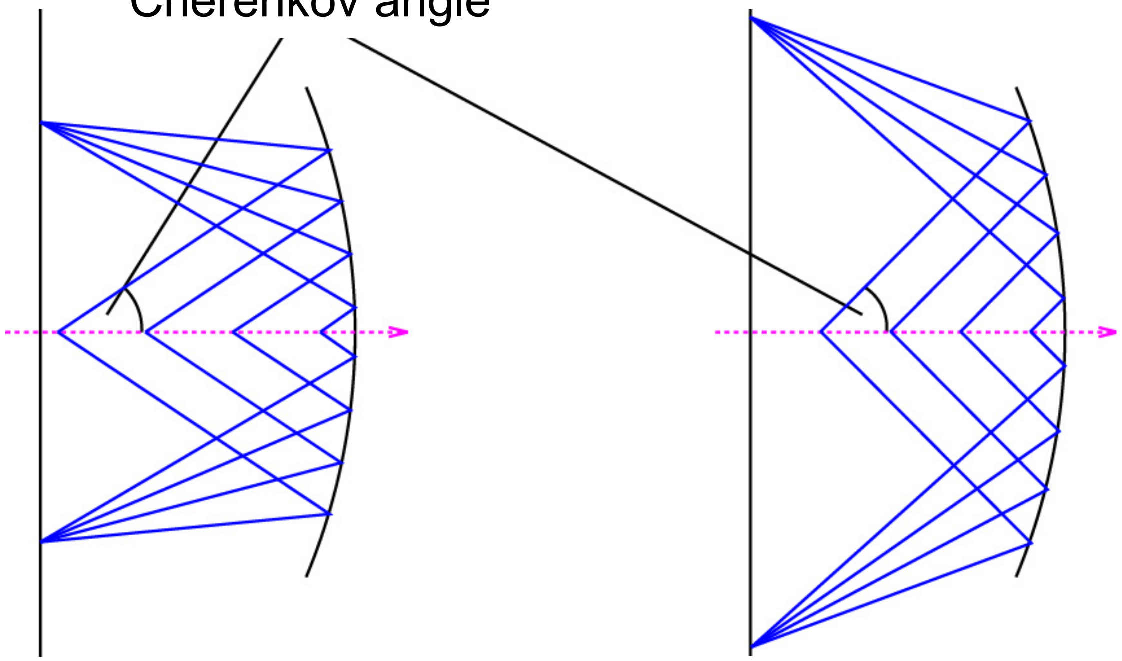

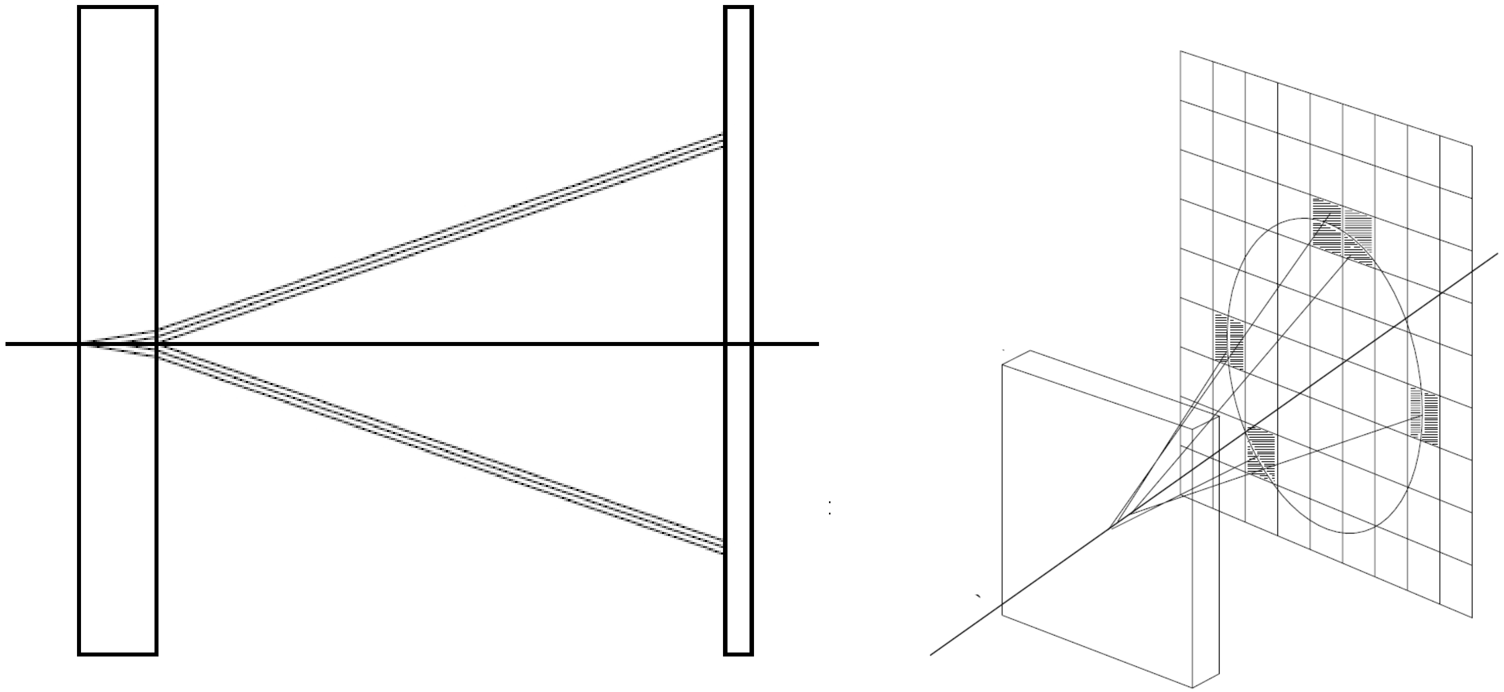

detector with focusing mirror
→ gas radiator

proximity focusing detector
→ solid or liquid radiator

RICH photon detection

RICH counter: measure photon impact point on the photon detector surface

→ detection of single photons with:

- sufficient spatial resolution
- high efficiency and low background (few photons!)
- cover a large area (square meters)

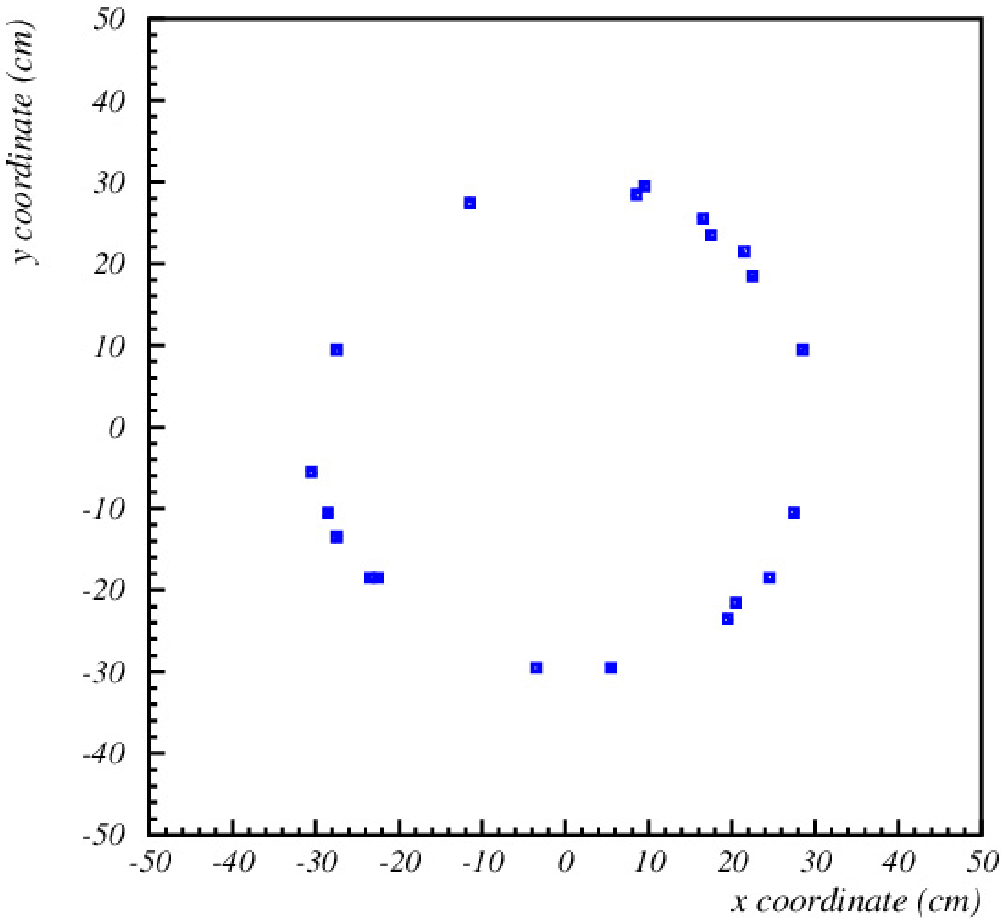

Special requirements:

- Operation in magnetic field
- High-rate capability
- Very high spatial resolution
- Excellent timing (time-of-arrival information)

Selection of photon detector is a crucial part of the detector design.

Photosensors comparison table

		Peak PDE	QE range	Gain	ENF	single photon ?	TTS	B	Rad. Hard.	Ageing
Solid state detectors	PD	$\approx 100\%$		1	1	NO	-		OK	
	APD	$\approx 80\%$	UV-IR	< 1000	> 2	NO	-	OK	OK (gain, dark count noise?)	OK
	SiPM	$\approx 60\%$		$\approx 10^6$	≈ 1.1	YES (dark counts?)	$\approx 50ps$			
Vacuum detectors	**PMT**			$\approx 10^7$	≈ 1.1		$\approx 200ps$	$\approx 0.1\ mT$		
	MA-PMT	$\approx 35\%$		$\approx 10^7$	≈ 1.1		$\approx 150ps$	$\approx 10\ mT$		OK
	MESH-PMT			$\approx 10^6$	$\approx 1.1 - 2$	YES	$\approx 100ps$	$\approx 2\ T$ (axial)	HIGH (window?)	
	MCP-PMT	$\approx 25\%$	UV-IR	$\approx 10^6$	$\approx 1.1 - 2$		$\approx 20ps$	$\approx 2\ T$ (axial)		OK? (ALD)
	VPT	$\approx 25\%$		≈ 10	≈ 2	NO	-	$\approx 2\ T$ (axial)		OK
Hybrid detectors	**HPD**	$\approx 40\%$		≈ 5000	≈ 1	YES	-	OK (axial)	OK	OK
	HAPD	$\approx 40\%$		$\approx 10^5$	≈ 1	YES	$\approx 30ps$ (@high gain)		OK (DC noise?)	
Gaseous detectors	**CsI MWPC**	$\approx 25\%$	UV	$\approx 10^5$	≈ 2	YES	$\approx 10ns$	OK	HIGH	IBF?
	CsI MPGD	$\approx 20\%$	UV	$\approx 10^6$	$\approx 1.2 - 2$	YES	$\approx 100ps$			

RICH basic reconstruction

- from the known track and photon ring a Cherenkov angle can be reconstructed

- error for single photon Cherenkov angle comes mainly from:
  - track error,
  - dispersion, variation of phase refractive index
  - unknown emission point along the track in the radiator
  - detector granularity – pad size

$$\sigma_{\vartheta_c,single} = \sigma_{\vartheta,tr.e.} \oplus \sigma_{\vartheta,disp.} \oplus \sigma_{\vartheta,emiss.p.} \oplus \sigma_{\vartheta,ph.det.res.}$$

- Cherenkov angle resolution per track reduces with square root of the number of detected photons

$$\sigma_{\vartheta,track} = \frac{\sigma_{\vartheta_c}}{\sqrt{N}}$$

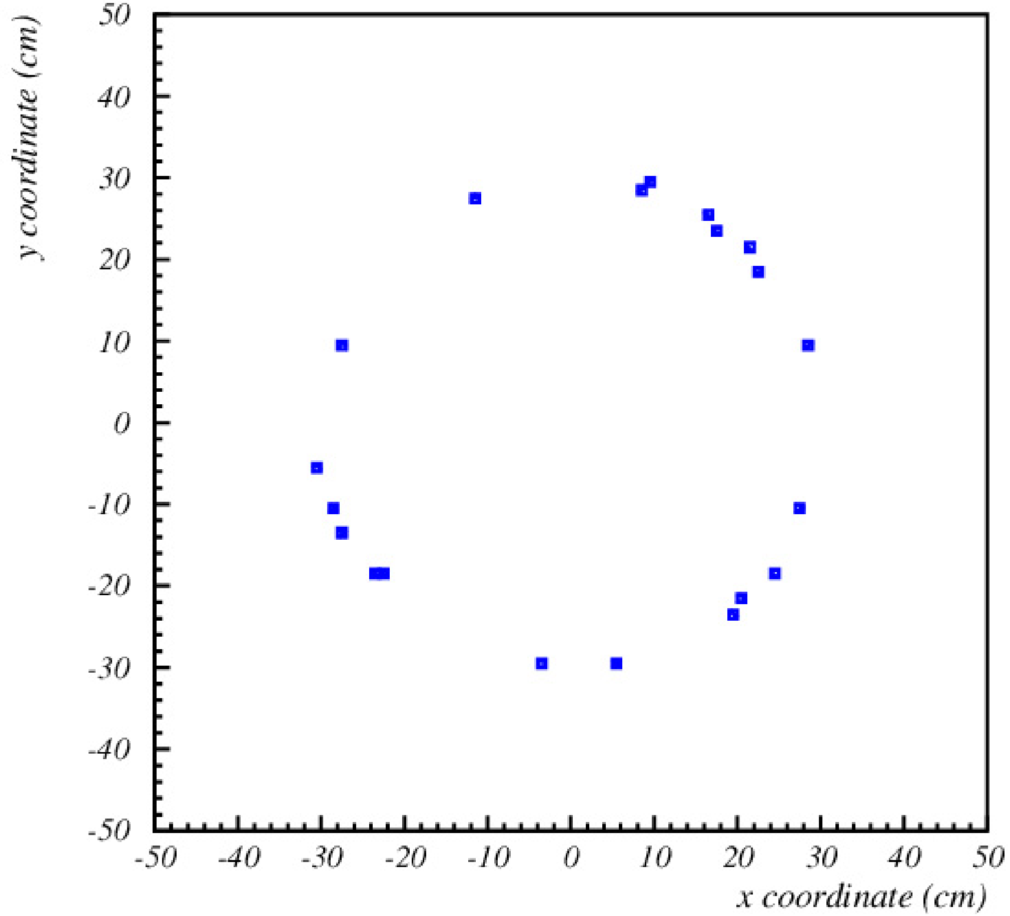

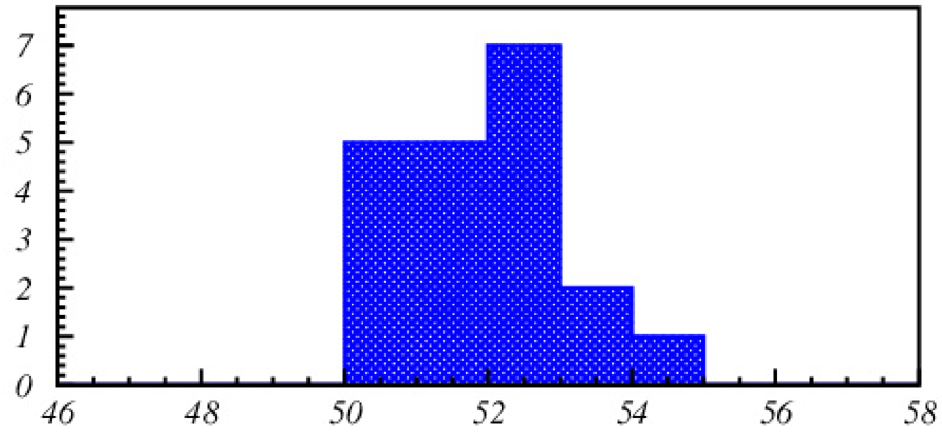

Cherekov angle distribution (mradian)

RICH – reconstructed Cherenkov angle

- example of a reconstructed Cherenkov angle vs. track momentum distribution
- bands corresponding to different particle types are clearly visible
- π/K separation up to ~ 50 GeV/c

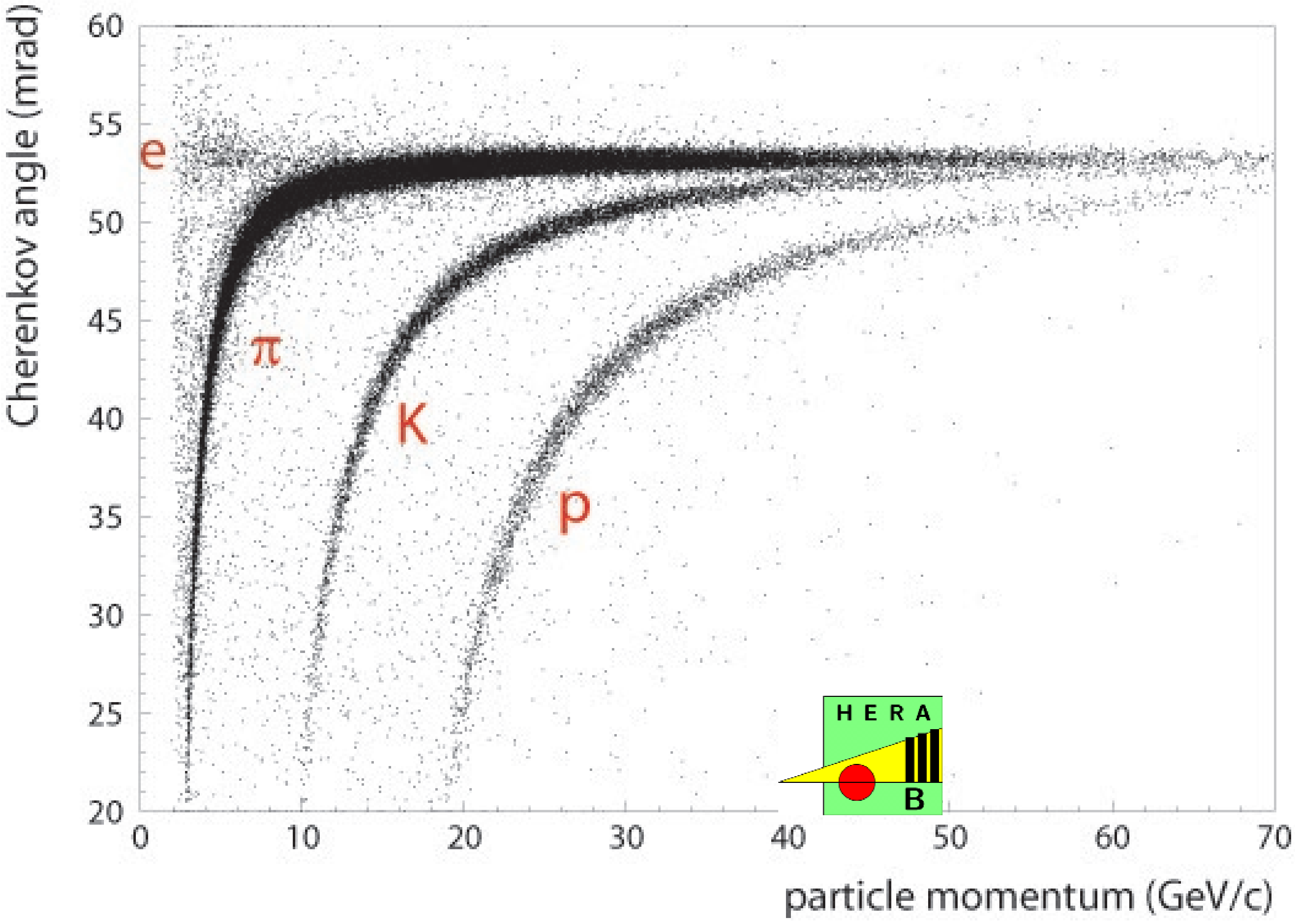

Early RICH detectors

- Detection of photons by gaseous detectors:
- photosensitive substance (TMAE, TEA) added to gas or deposited on one cathode (CsI)
- works in magnetic field
- low initial costs
- only UV transparent materials and high purity gas (not for aerogel)

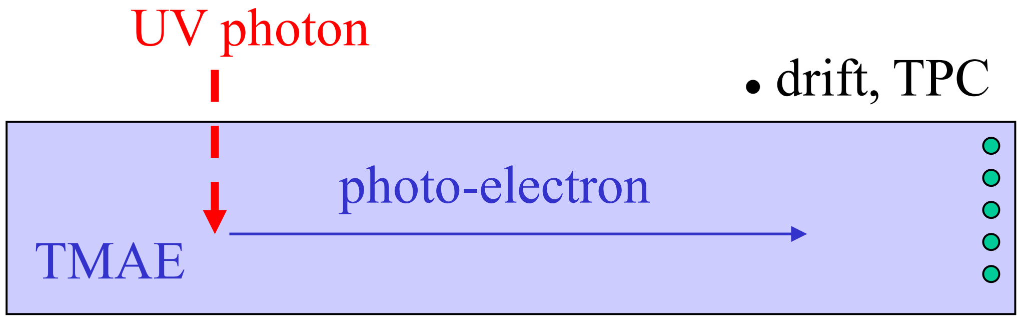

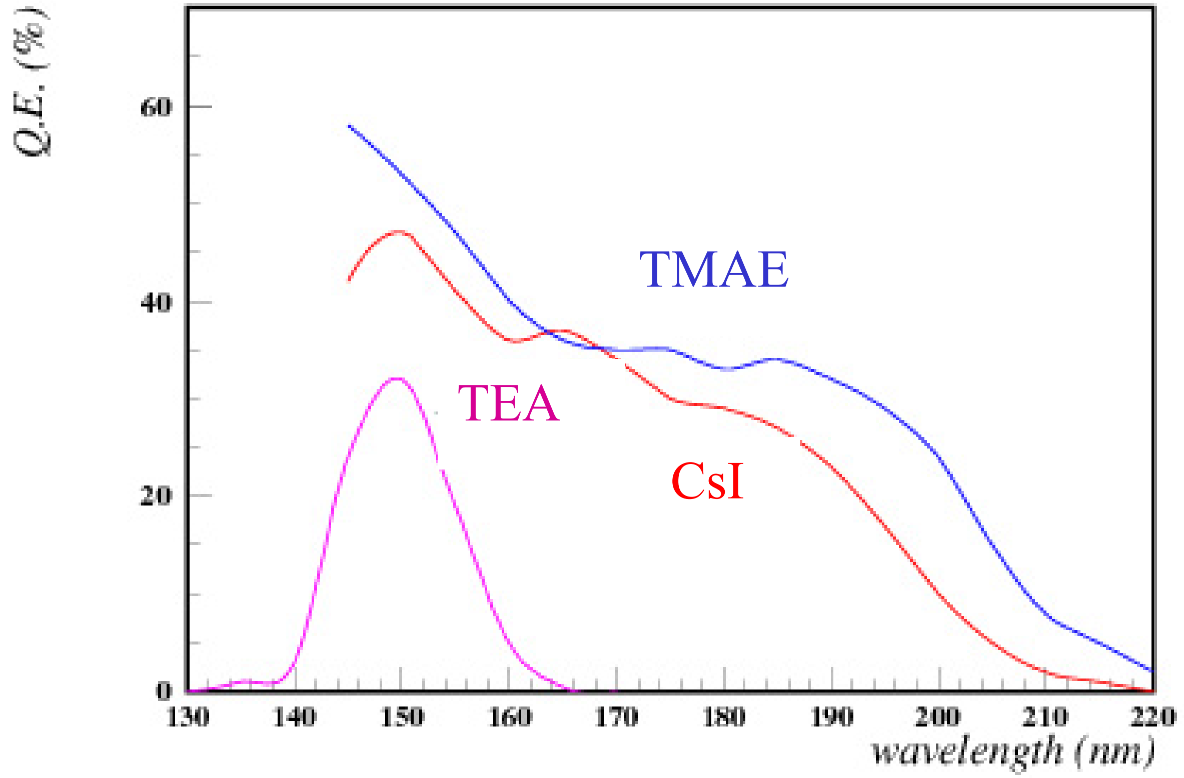

- DELPHI, SLD, OMEGA RICH counters based on TMAE:
- long absorption length → thick wire chamber detector – TPC (UV photon → photo-electron → detection of a single electron in a TPC)
- slow – low rate
- aging

Early RICH detector

OMEGA, DELPHI RICH counters based on TMAE

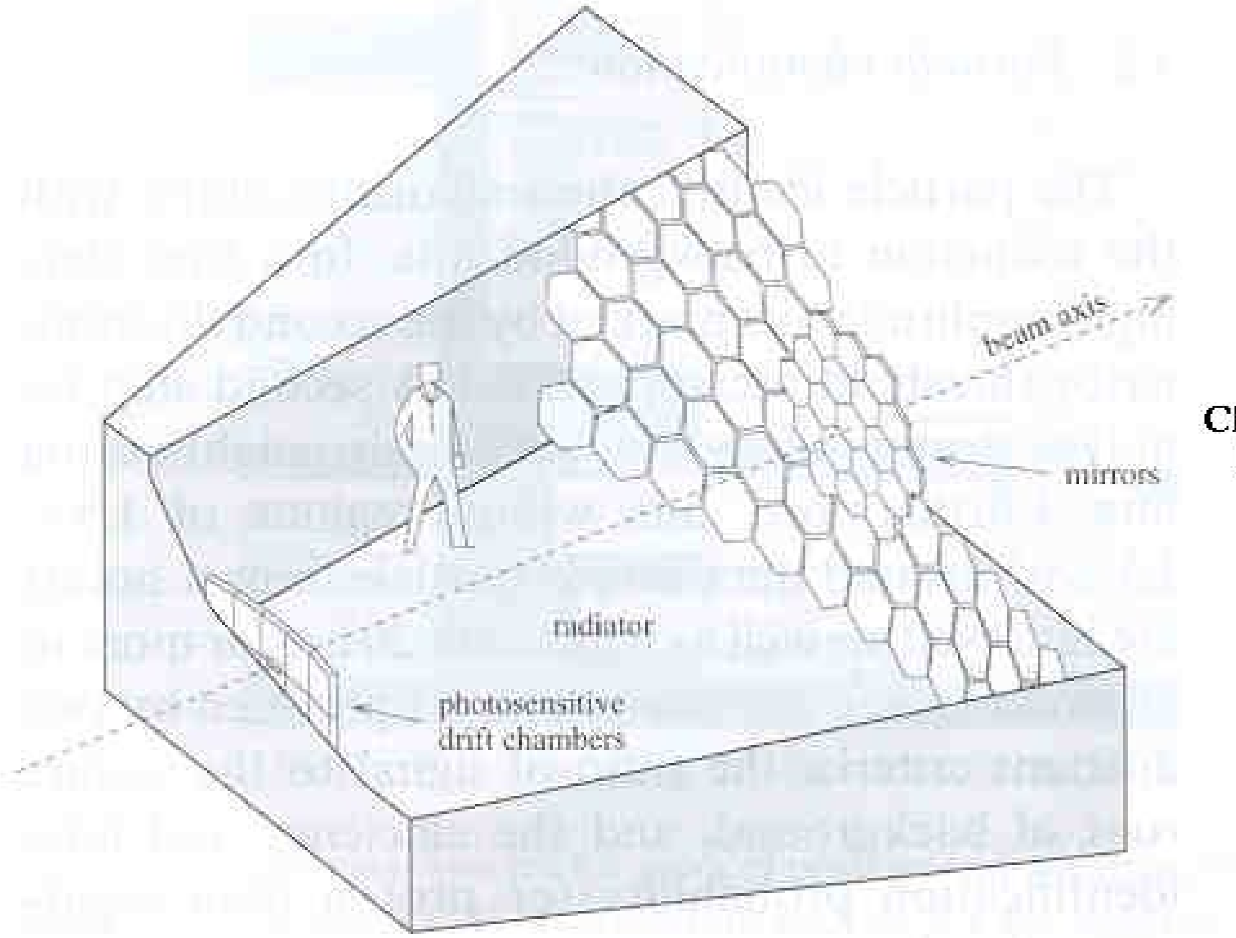

• OMEGA

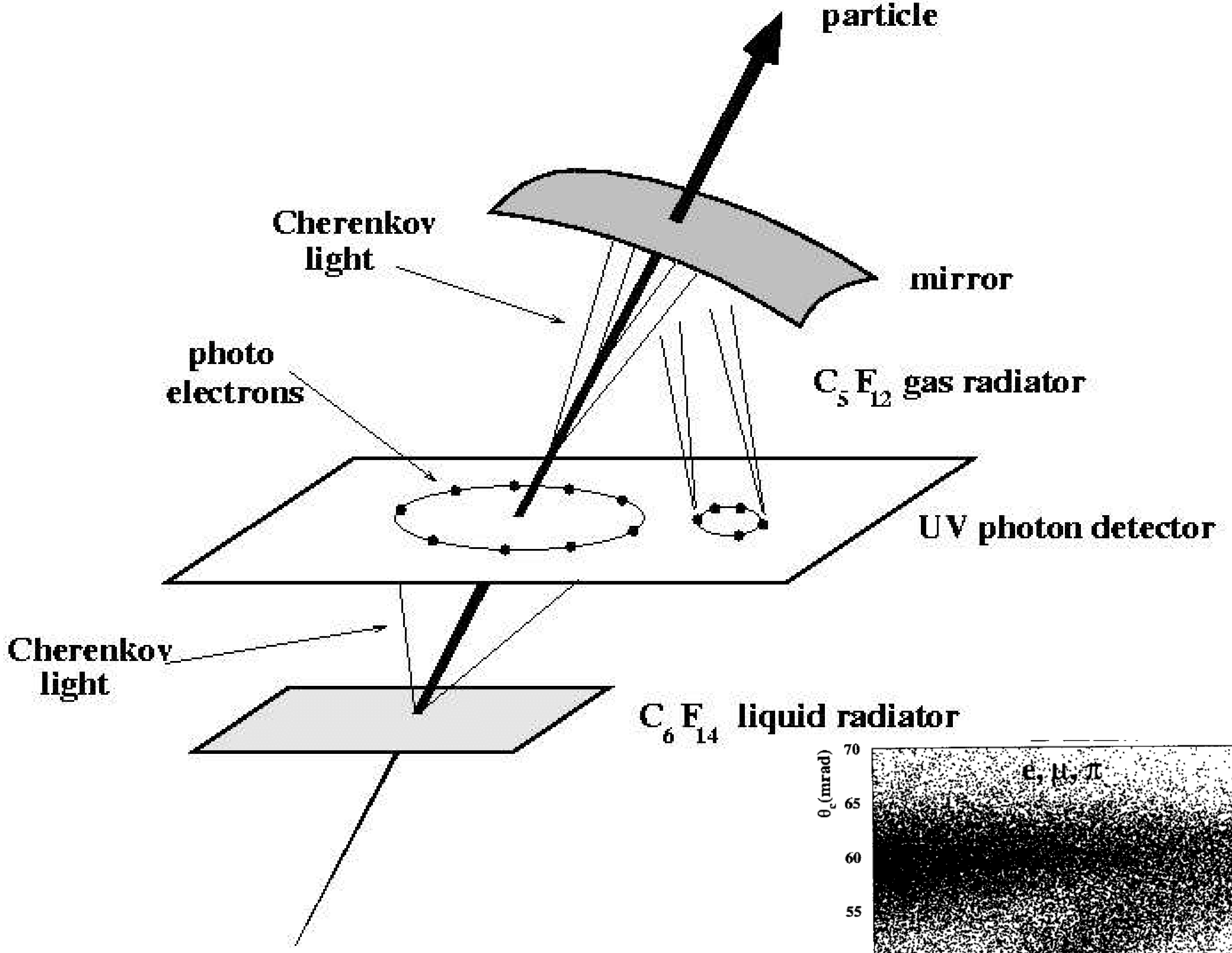

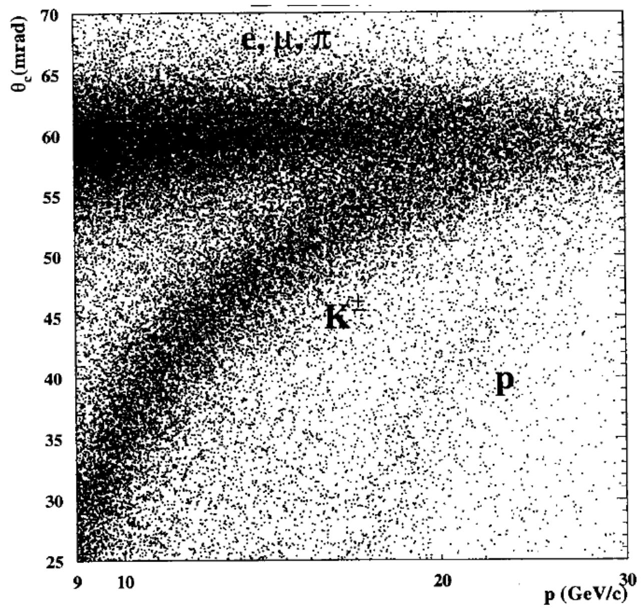

• DELPHI (dual radiator)

Faster wire chambre based RICH detectors

Thin multi-wire proportional chamber with cathode pad readout → short drift distance → fast detector

CLEO RICH:

- TEA → short absorption length
- sensitive only below 160 nm
- aging

- HADES, COMPASS, ALICE RICH:
- thin CsI layer over photocathode pads
- high-rate instabilities

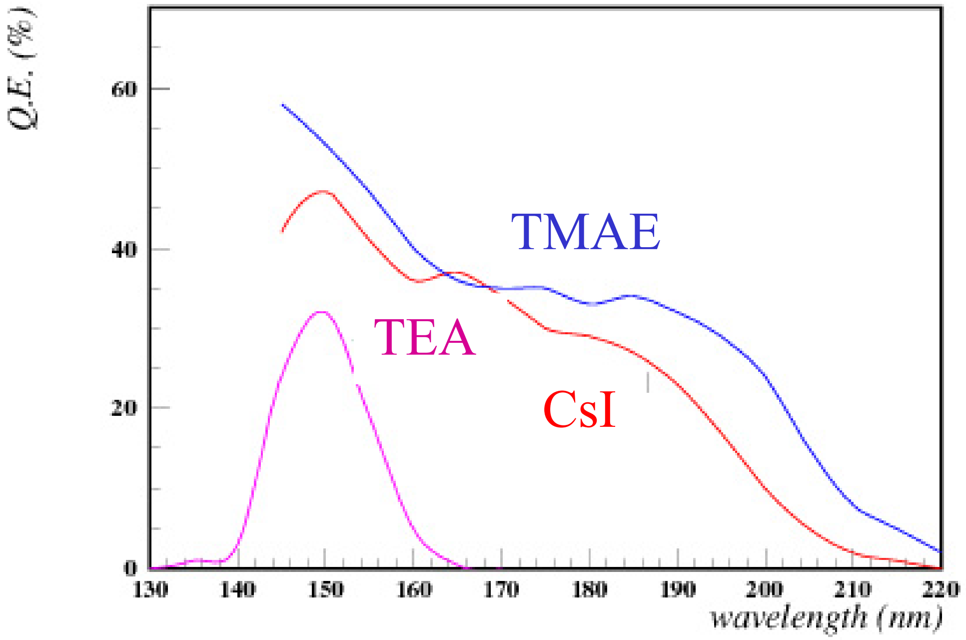

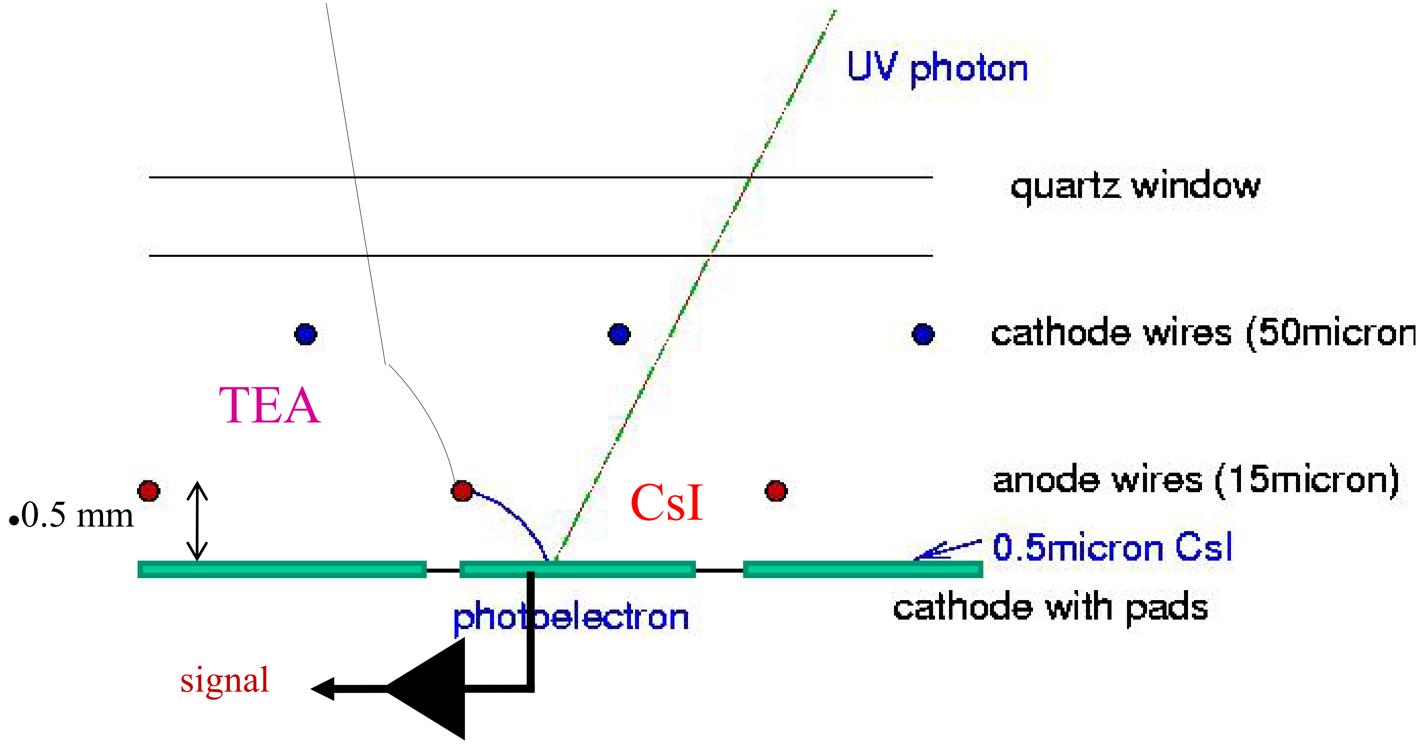

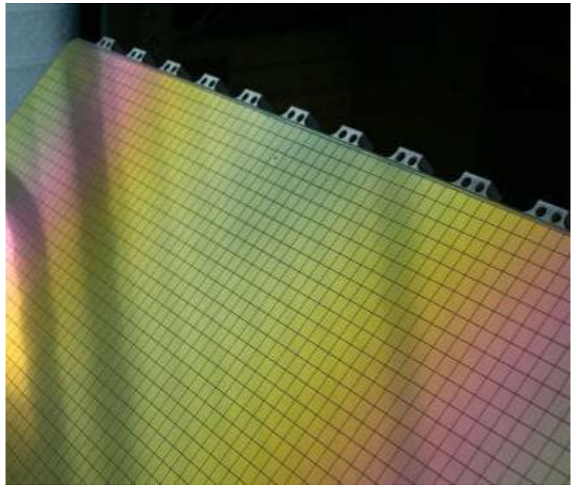

ALICE CsI RICH

ALICE experiment uses MWPCs with CsI photocathode for high momentum PID:

- proximity focusing configuration
- liquid radiator C_6F_{14} (15 mm, n=1.2989@175nm)
- CH_4 gas, gain ~ $4*10^4$
- 300nm CsI reflective photocathode, QE~25%@175nm

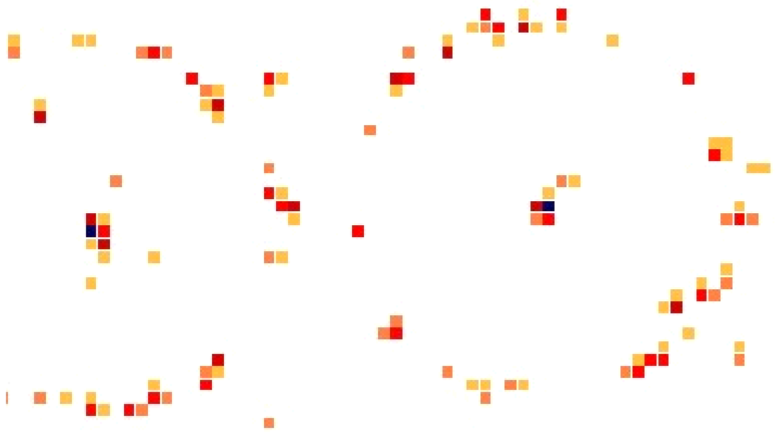

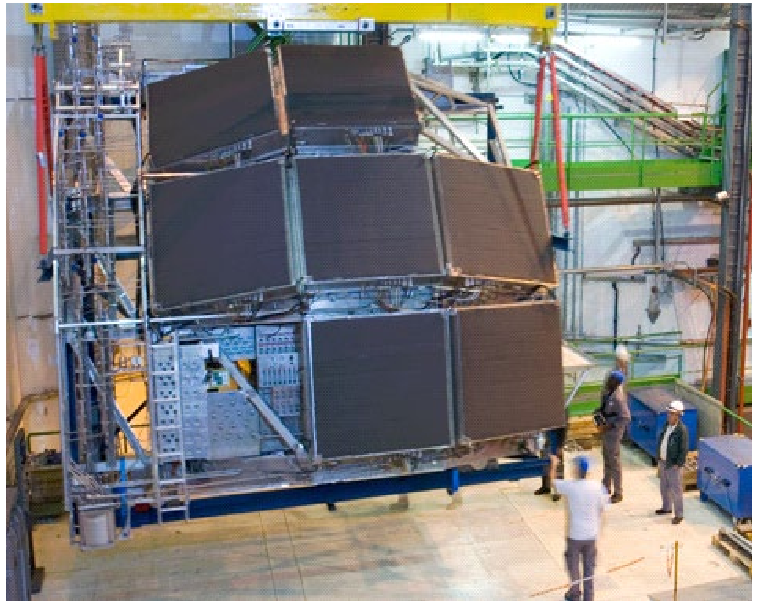

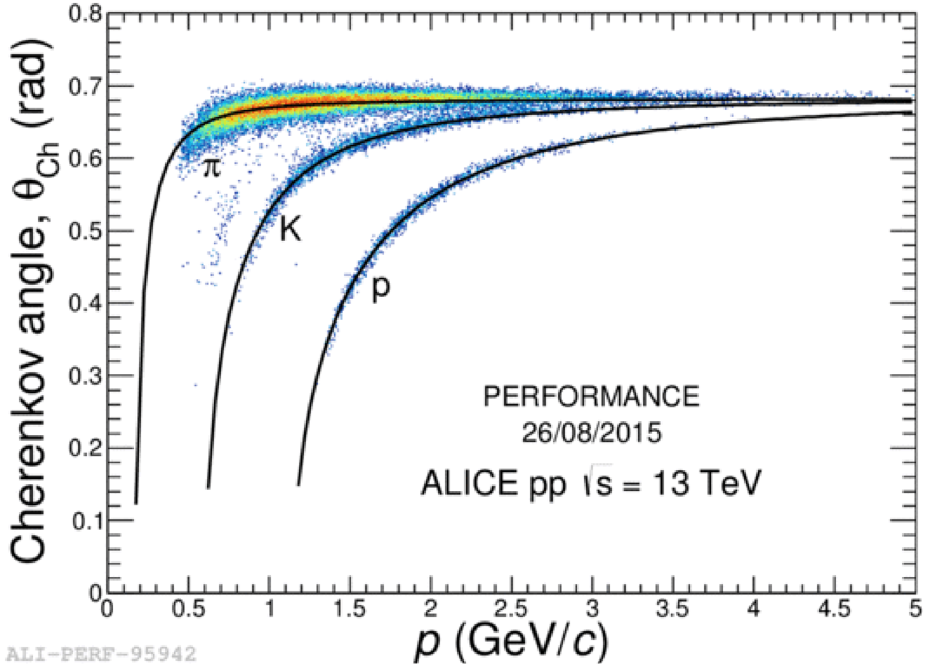

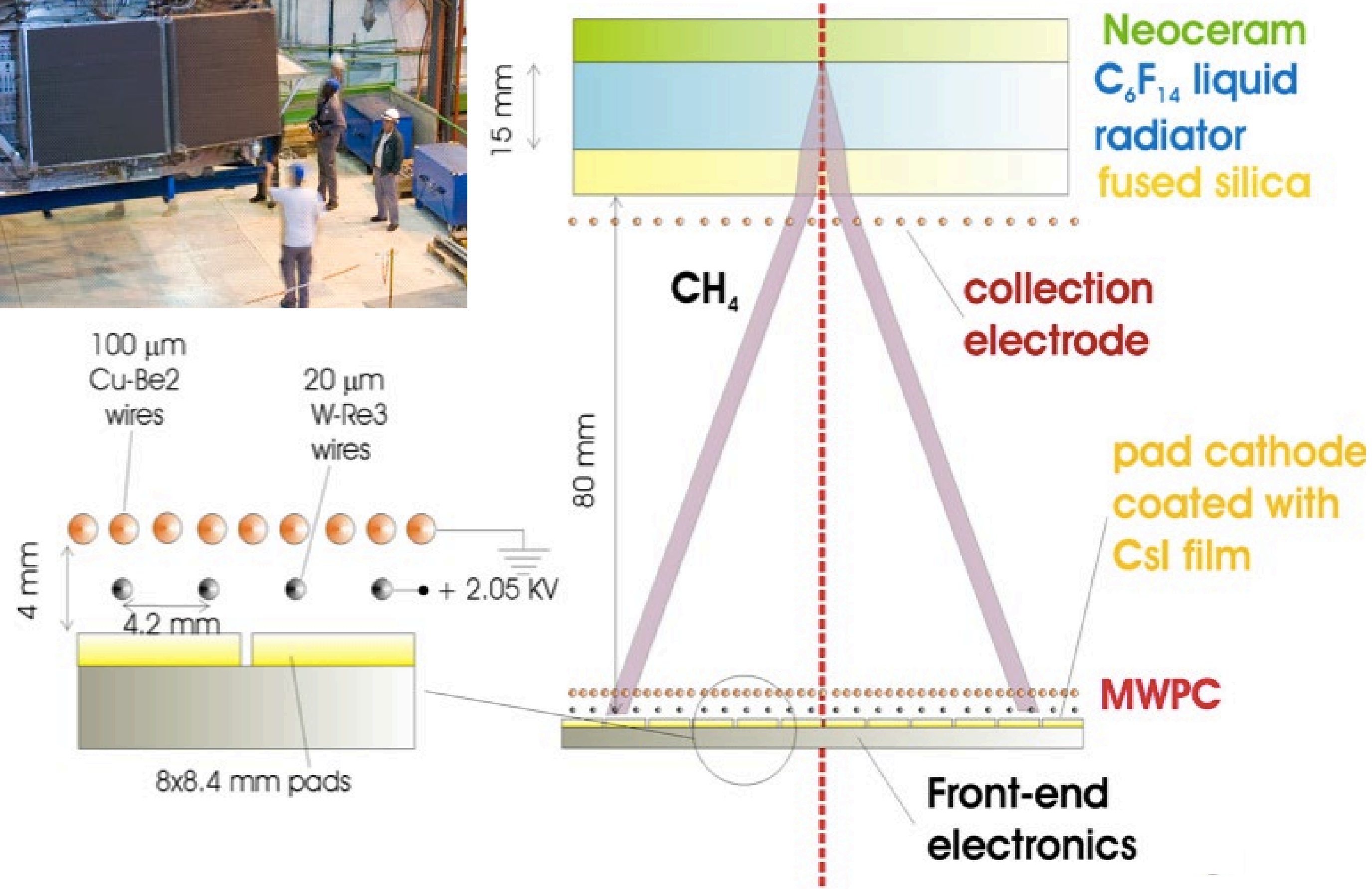

JINST 3(2008)S08002

COMPASS RICH-1 upgrade:

- THGEM + CsI – new development in gaseous photo detectors
- ~ 10 photons for saturated ring
- resolution ~1.8 mrad ...

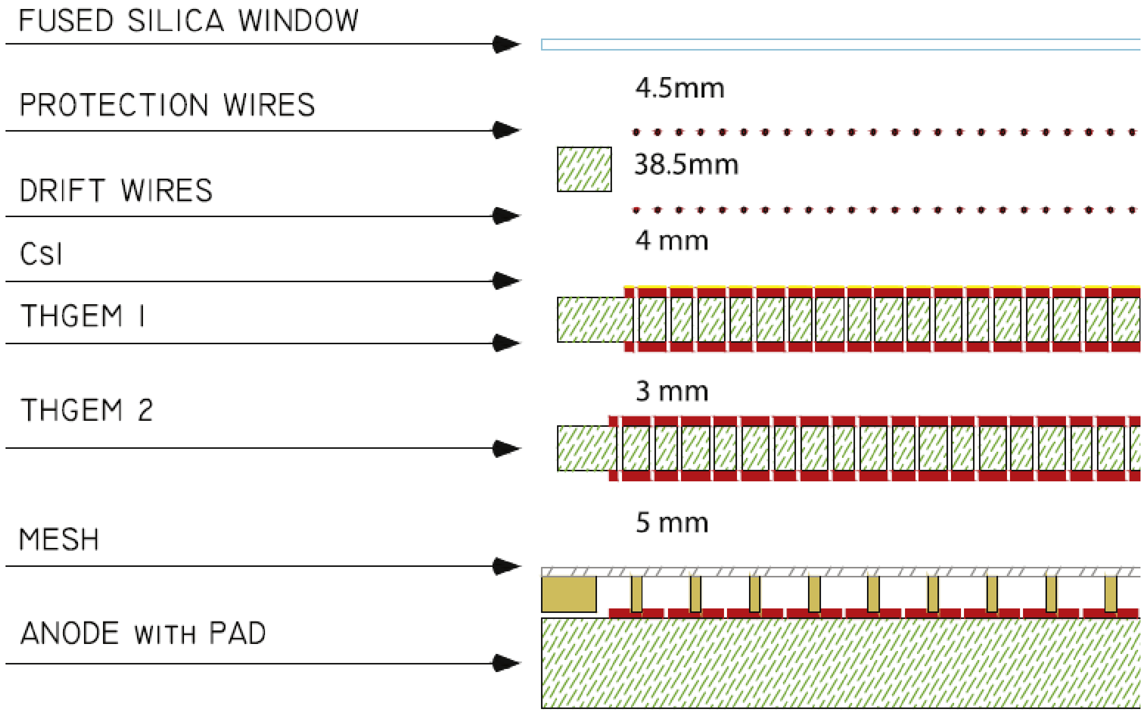

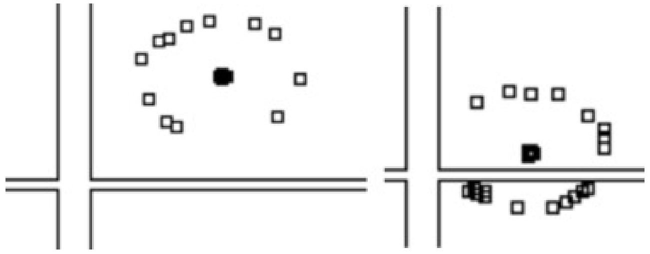

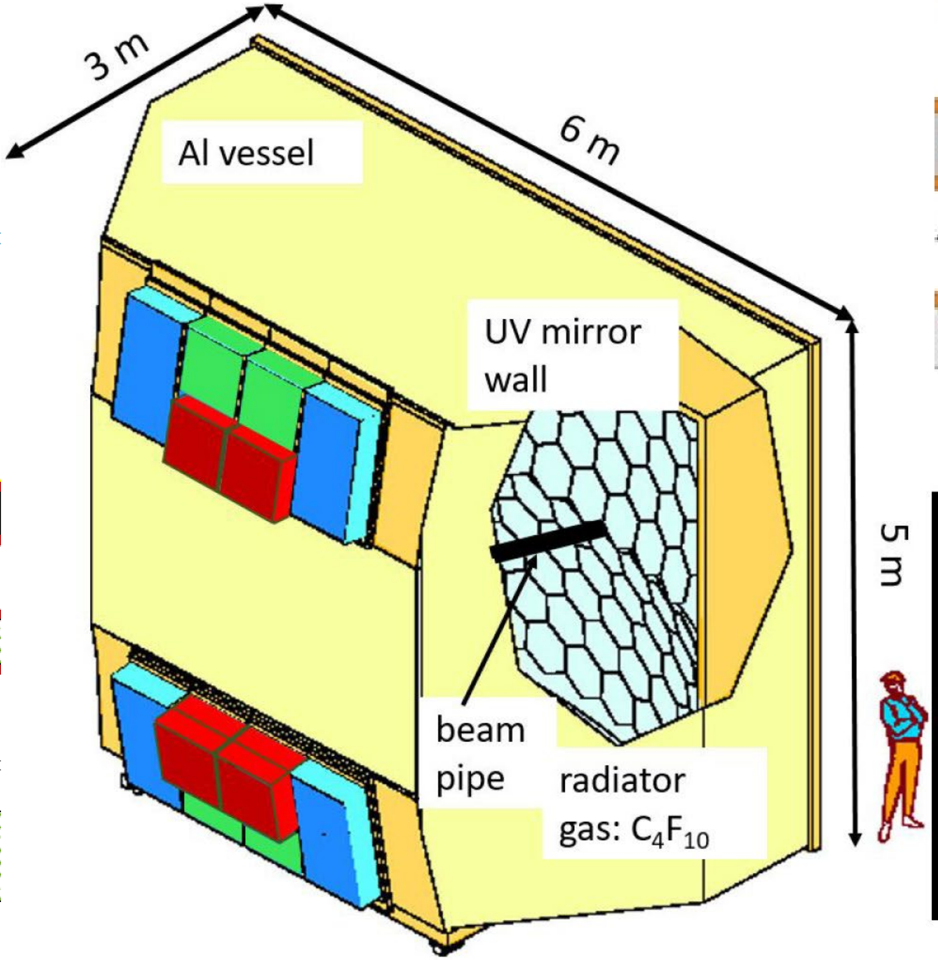

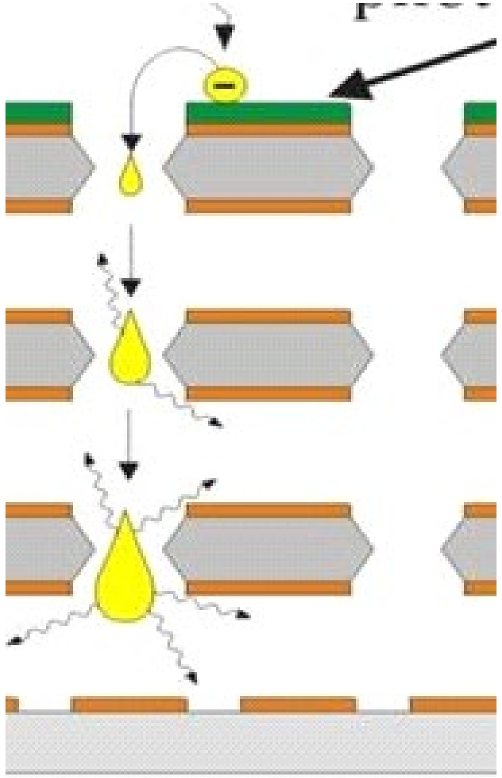

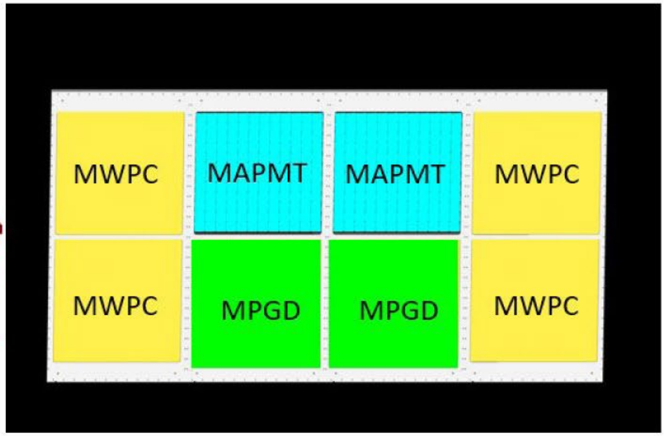

NIMA 952 (2020) 161832

Vacuum based photon detectors - PMTs

- operation at high rates over longer periods
- sensitivity for visible light – compatible with aerogel radiator
- does not work in magnetic field

- **HERMES** RICH (SELEX, PHENIX):
- dual radiator C_4F_{10} (n=1.00137 @ 633nm)+ aerogel (n=1.03 @ 633nm)
- single channel PMTs (¾ inch, Philips XP1911/UV)

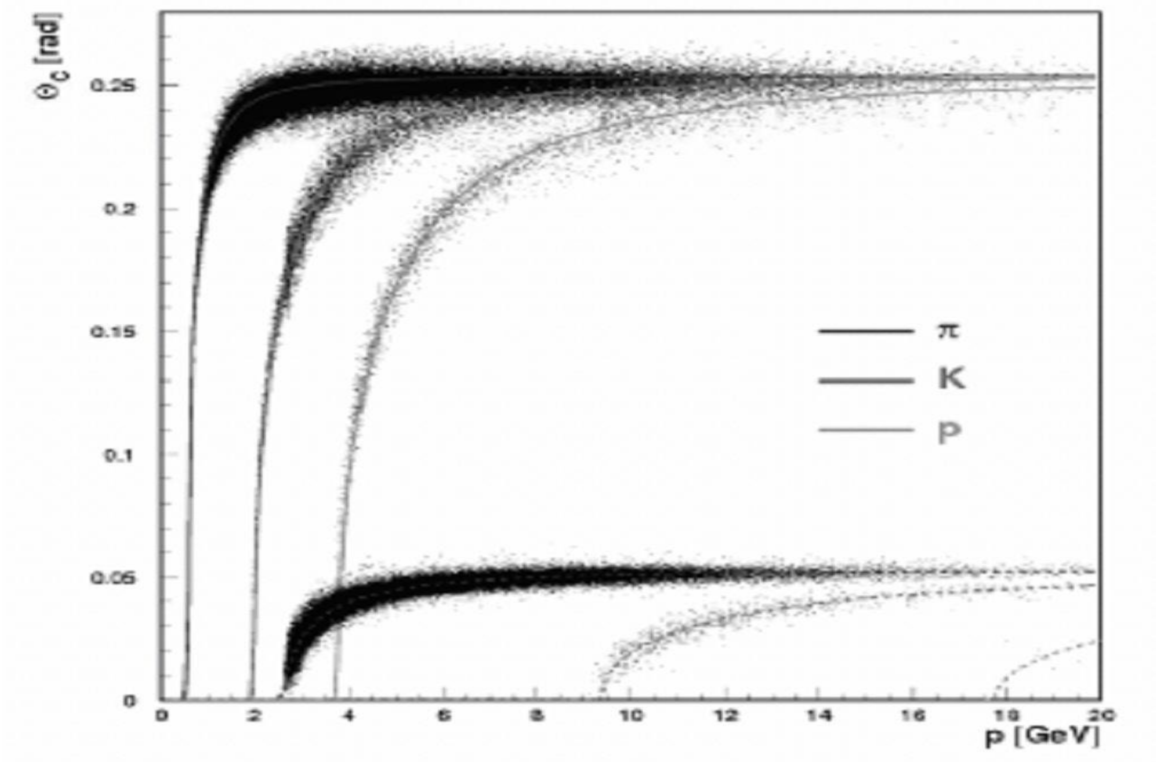

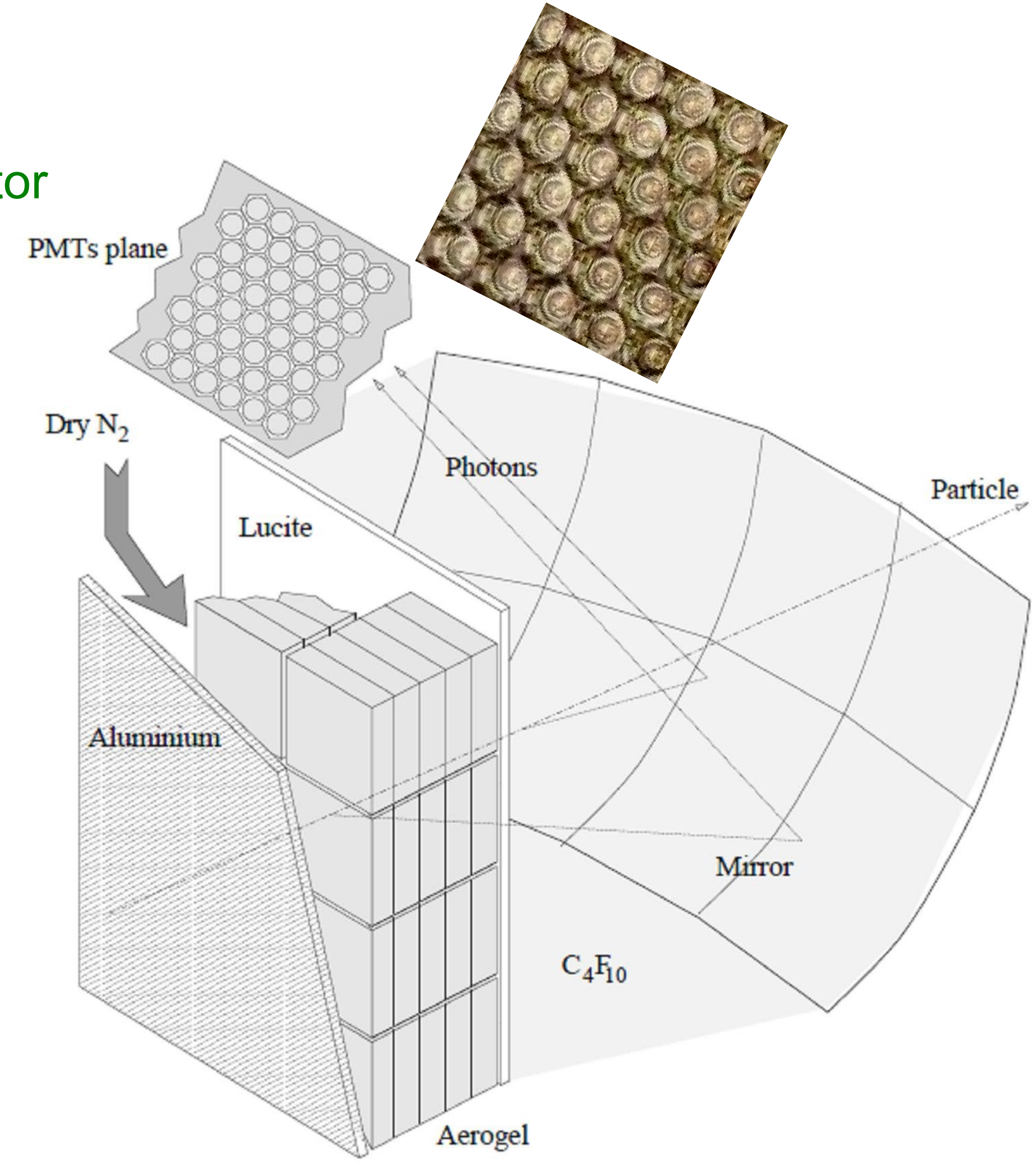

NIMA 479 (2002) 511

Multi-anode PMTs

- smaller pad size → better resolution

HERA-B RICH:

- high-rate operation (>1MHz/cm^2) → wire chamber prototypes(CsI,TMAE) abandoned
- multi-anode PMTs (Hamamatsu R5900-M16(M4)) → first use on large scale
  - excellent single photoelectron detection
  - low noise (few dark counts/s/ch.)
  - low cross-talk (< 1%)
  - low active area ration (<50%) → imaging light concentrators (area ratio 4:1)

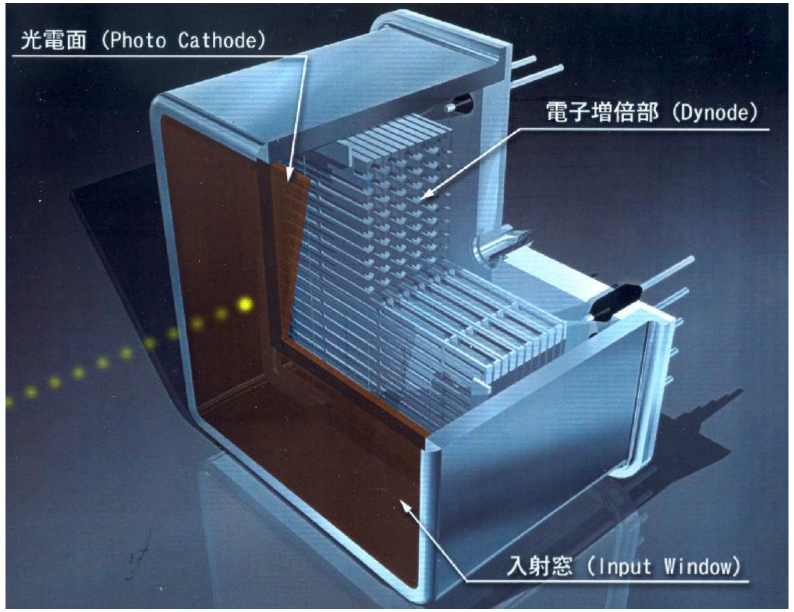

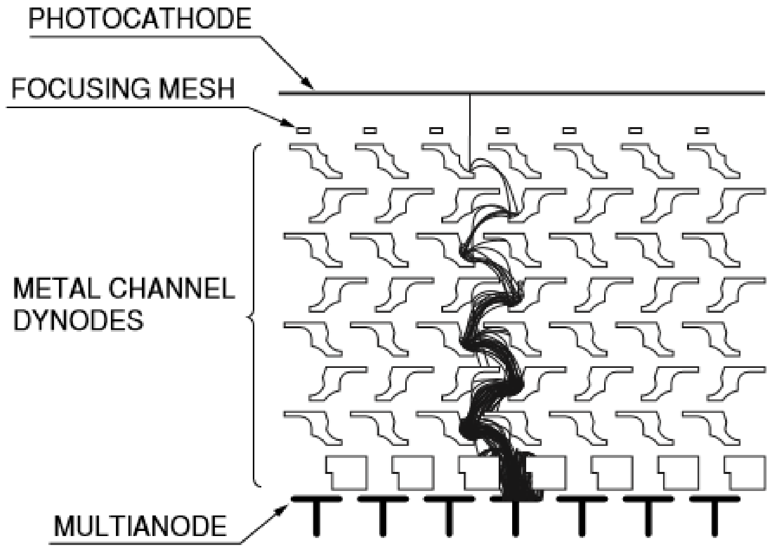

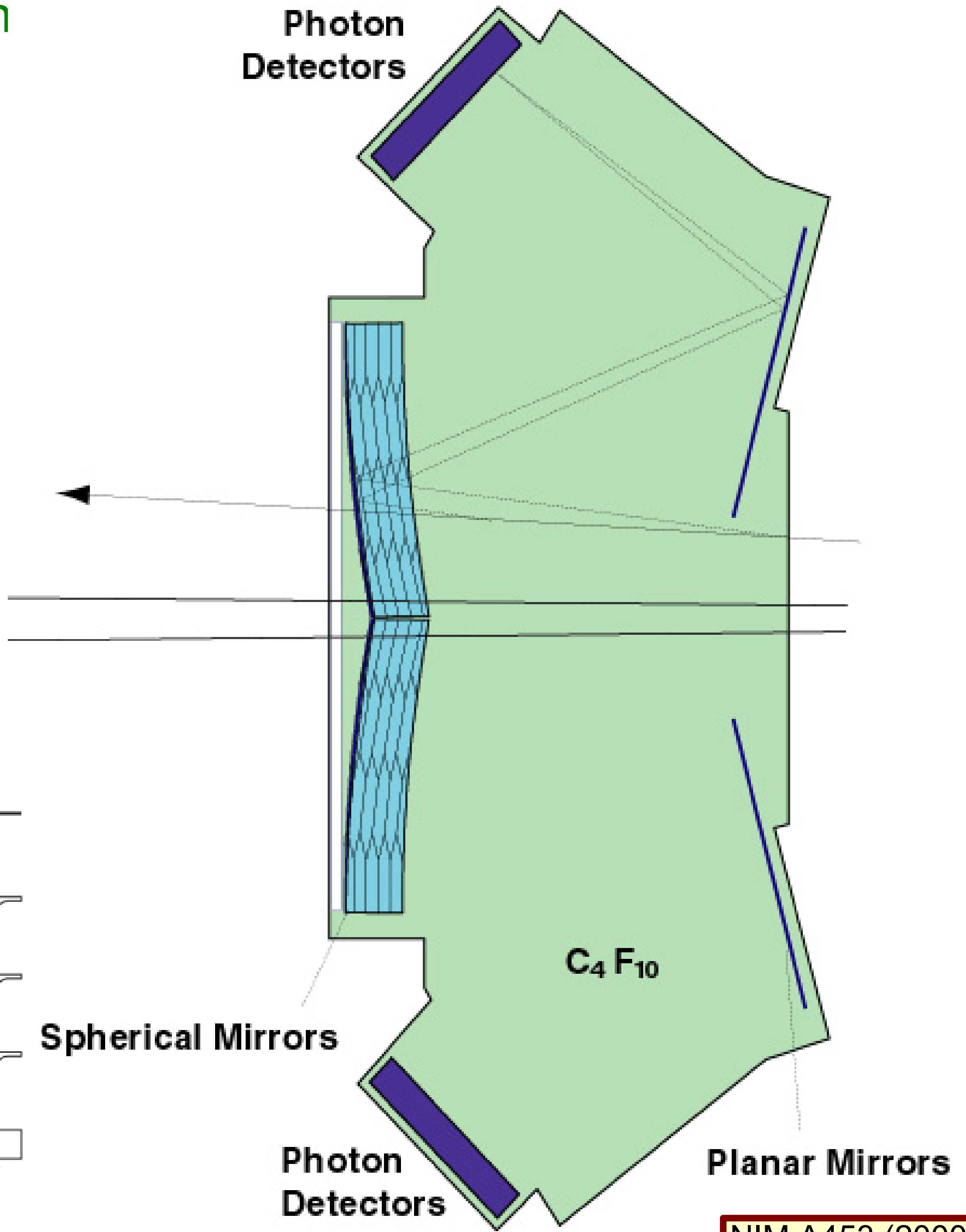

NIM A453 (2000) 289

The HERA-B RICH lens demagnification

- imaging light concentrators:
  - two lens system
  - demagnification factor 2
  - area ratio 4:1
  - limited angular acceptance ≈ 150 mrad (saturated Cherenkov angle ≈ 53 mrad)
- injection moulded plastic lenses

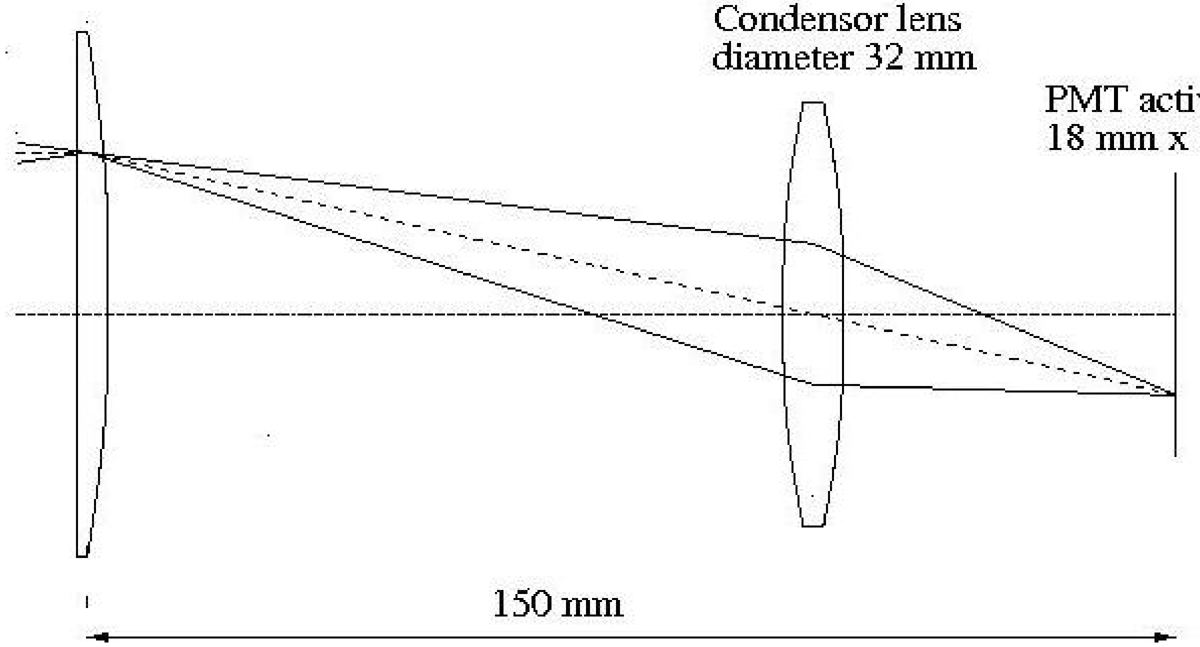

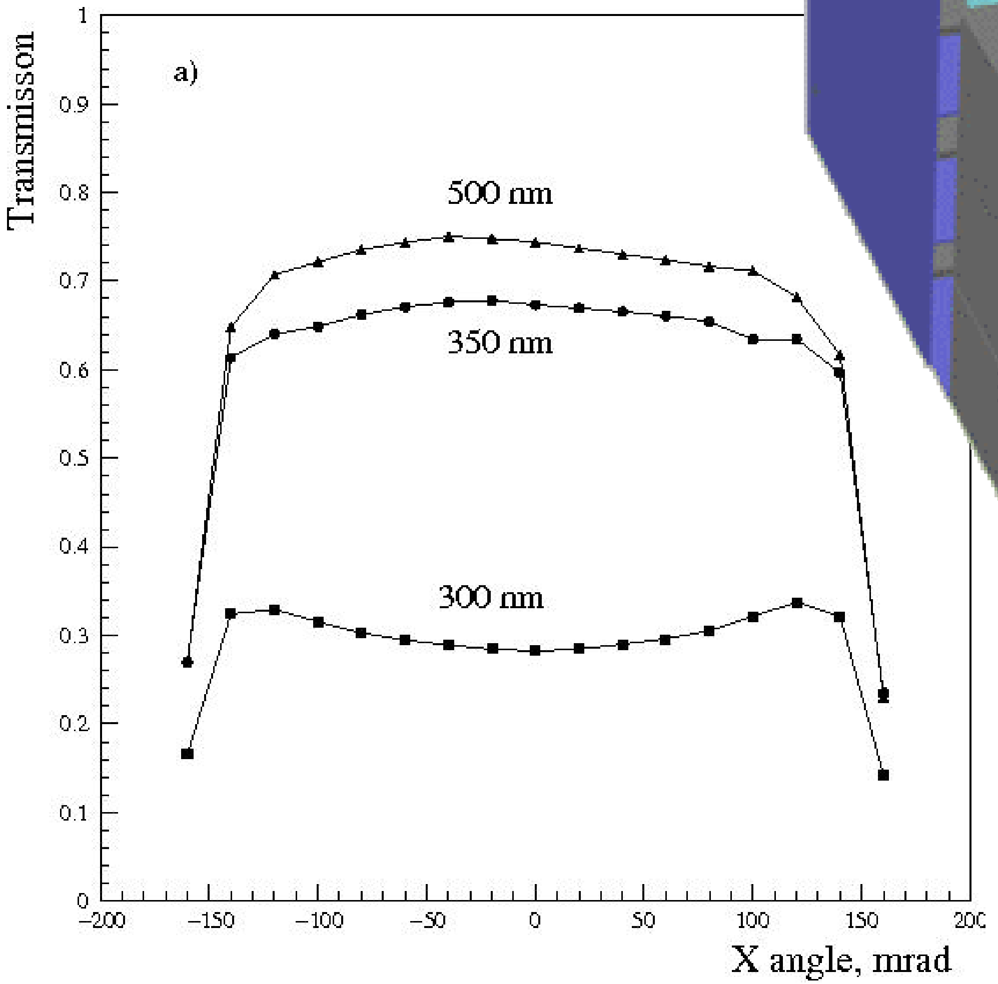

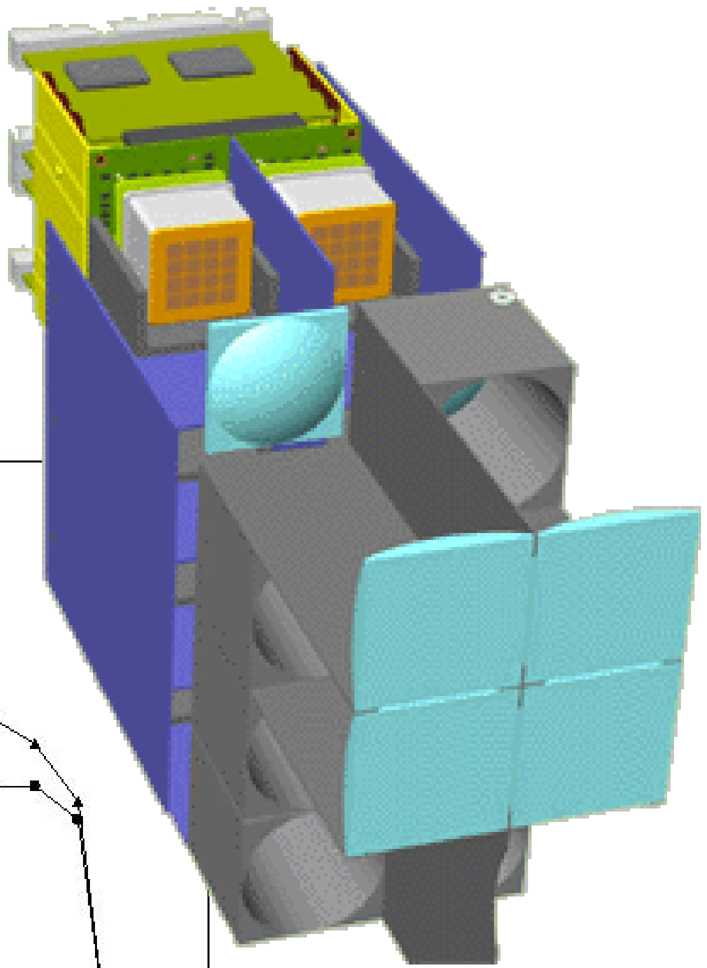

The HERA-B RICH performance

- low noise (few hits per event)
- ~ 30 ph./ring(saturated)

- good performance even at high occupancy events (typical)

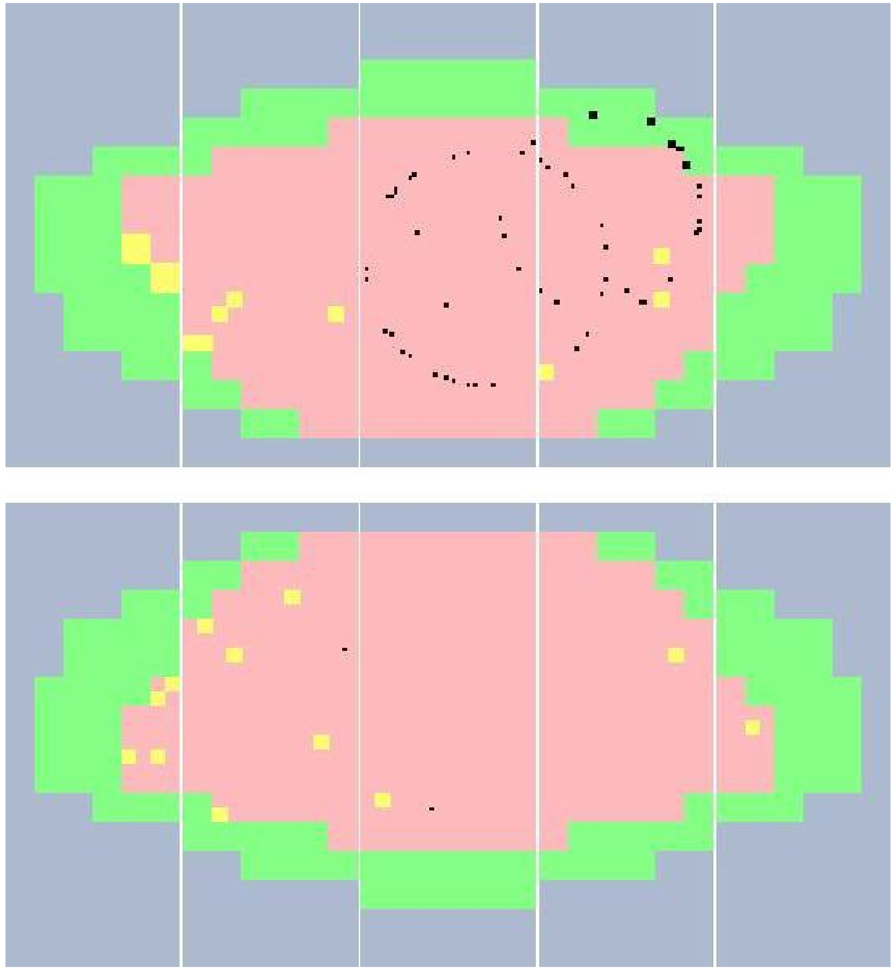

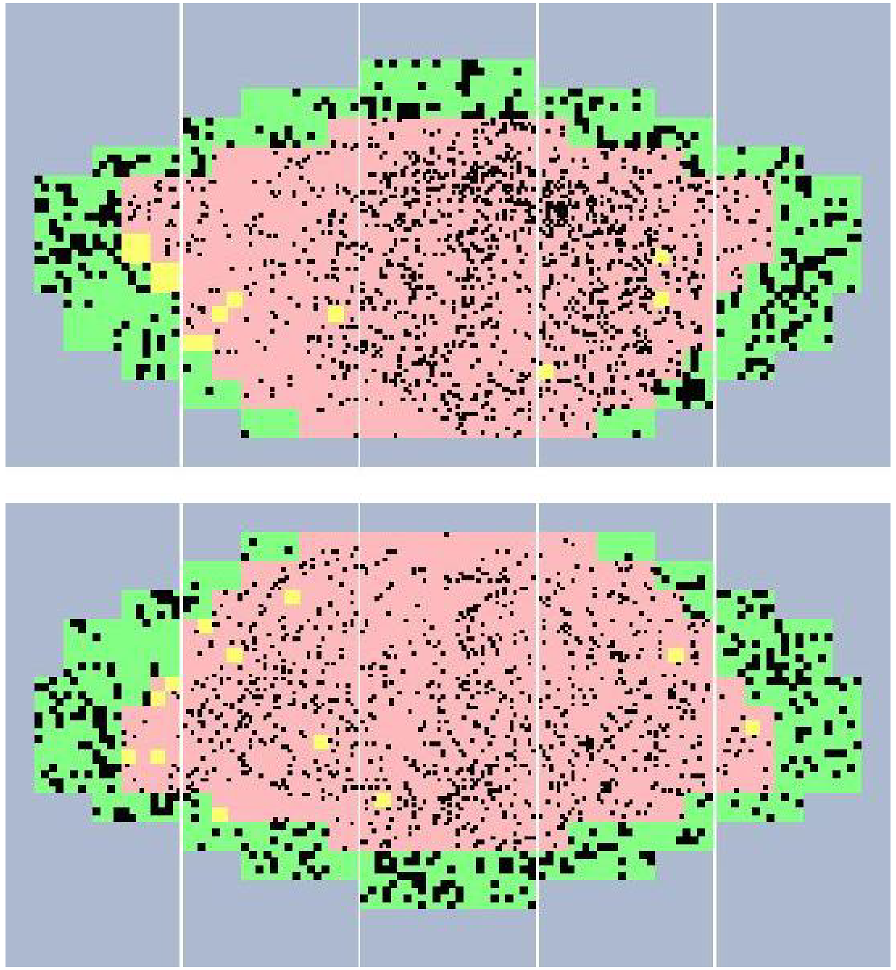

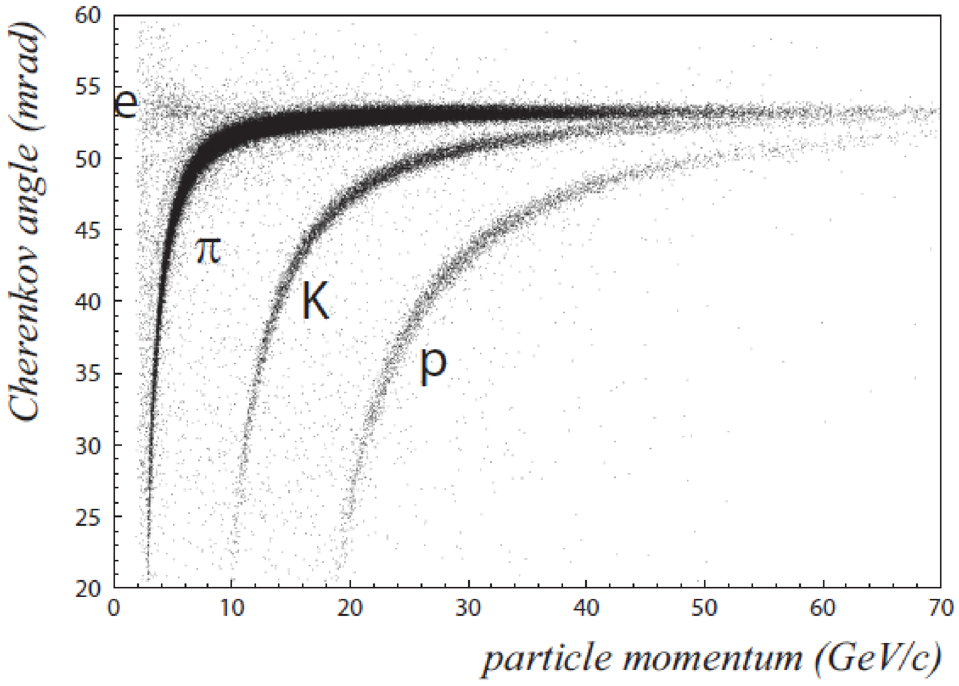

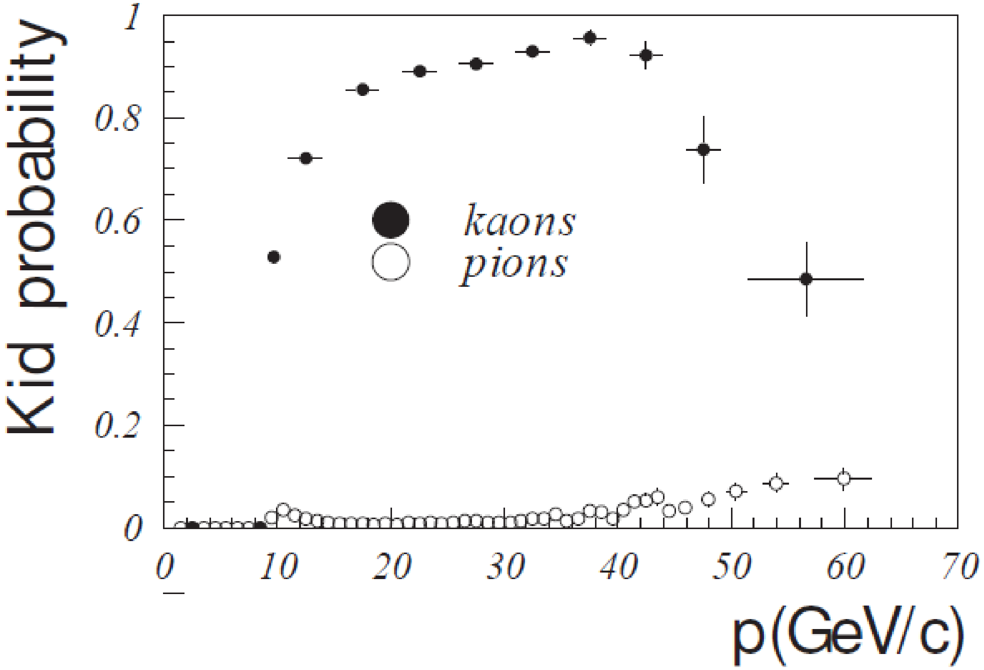

COMPAS RICH upgrade:

- CsI in central (high occupancy) part replaced with multi-anode PMTs
- similar imaging light concentrator system used
- UV extended PMTs and optics (down to 200 nm)
- area demagnification 7:1
- 60 ph. for saturated ring, resolution 0.3 mrad ...

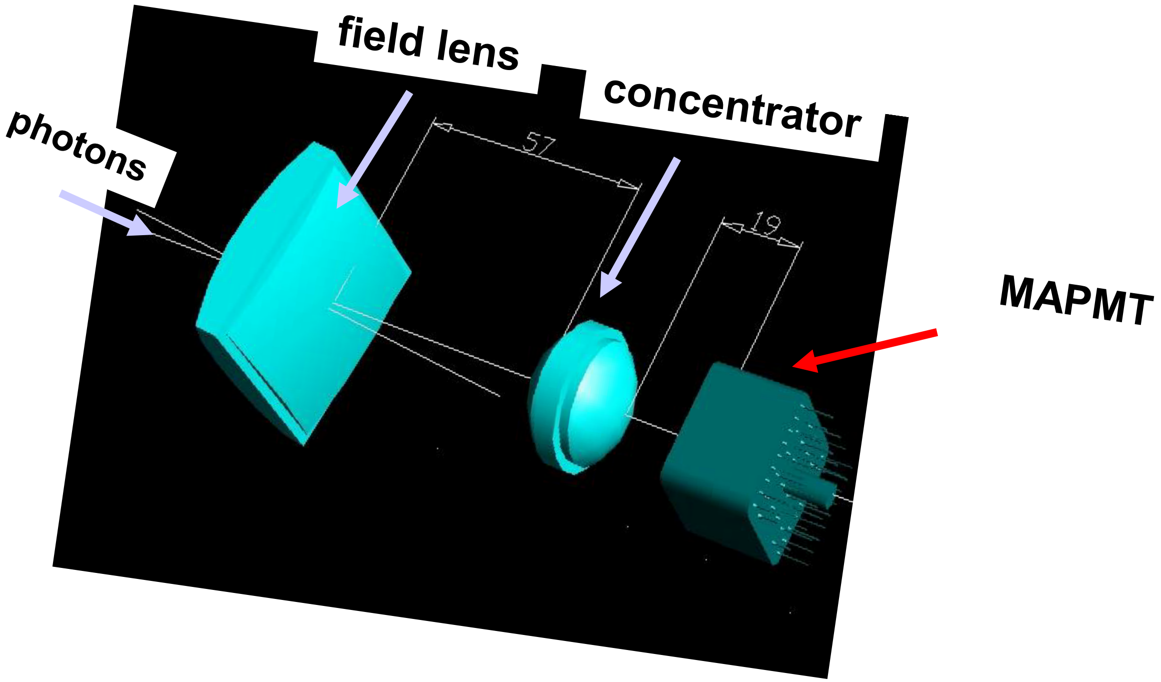

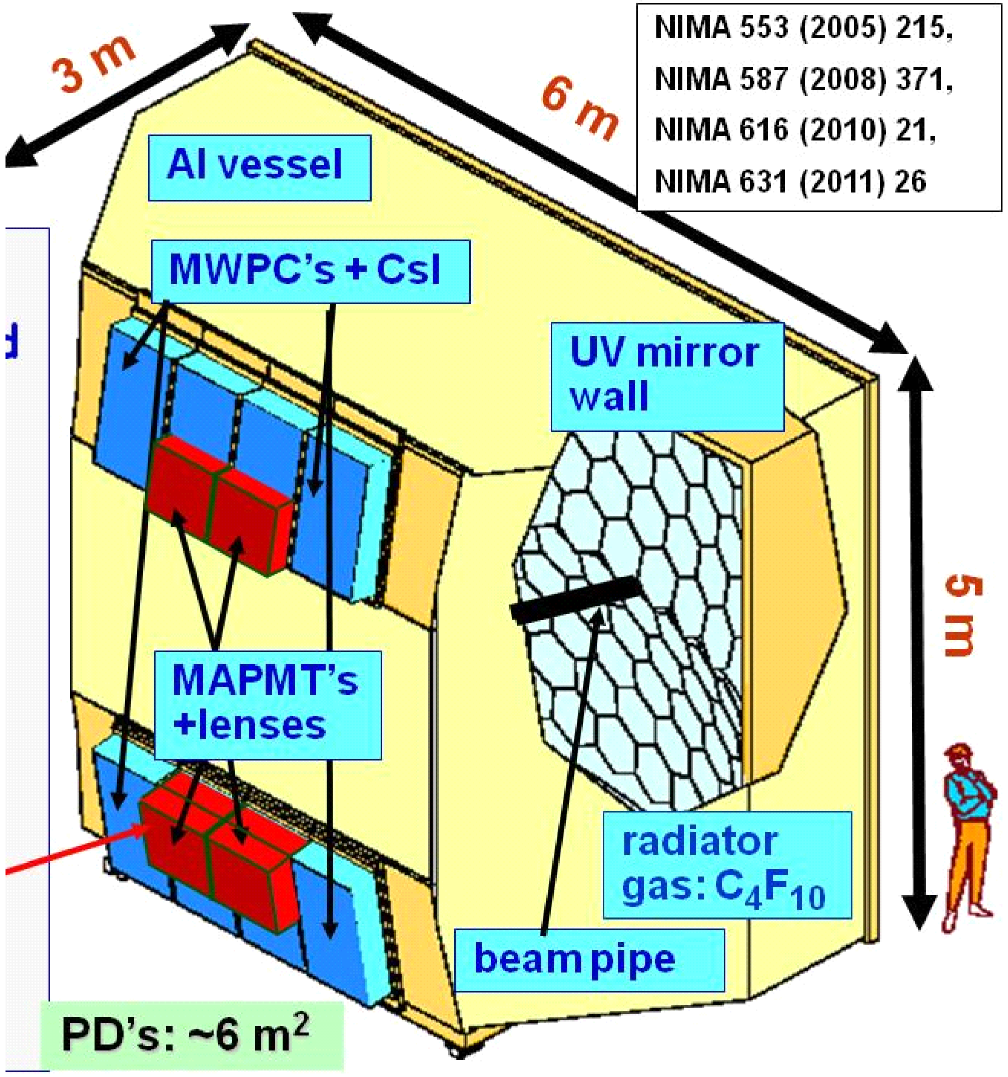

LHCb RICH 1&2 with HPDs

- 2 RICHs with 2(~~3~~) radiators (~~aerogel~~, C_4F_{10}; CF_4)
- Hybrid Photon Detector introduced
- electron optics → 5x demagnification
- sensitive to magnetic field
- HV ~20kV, gain ~5k
- CERN+DEP-Photonis (replaced with MaPMTs)

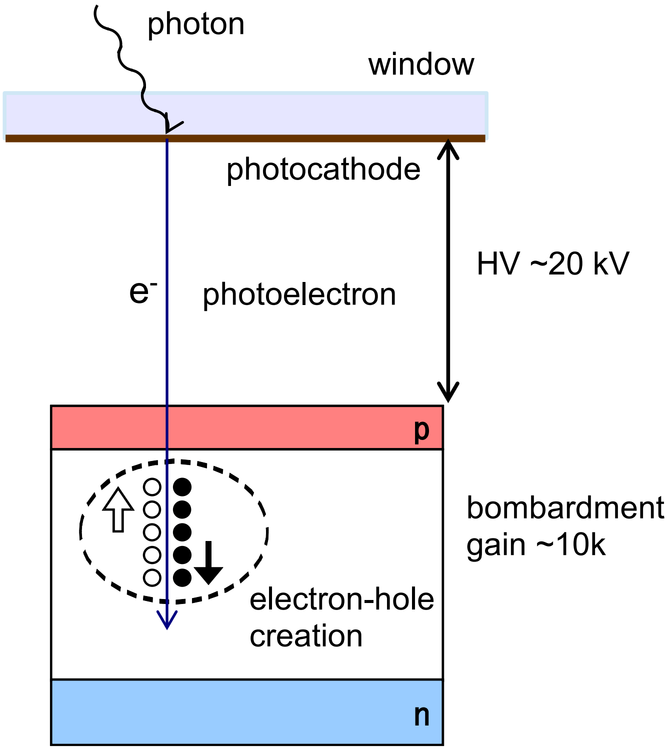

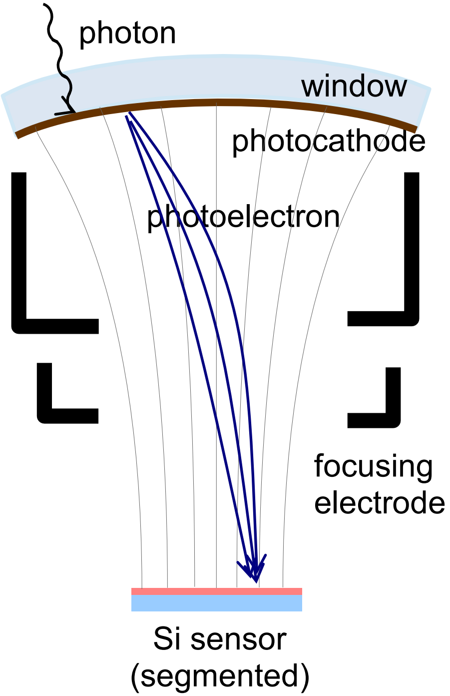

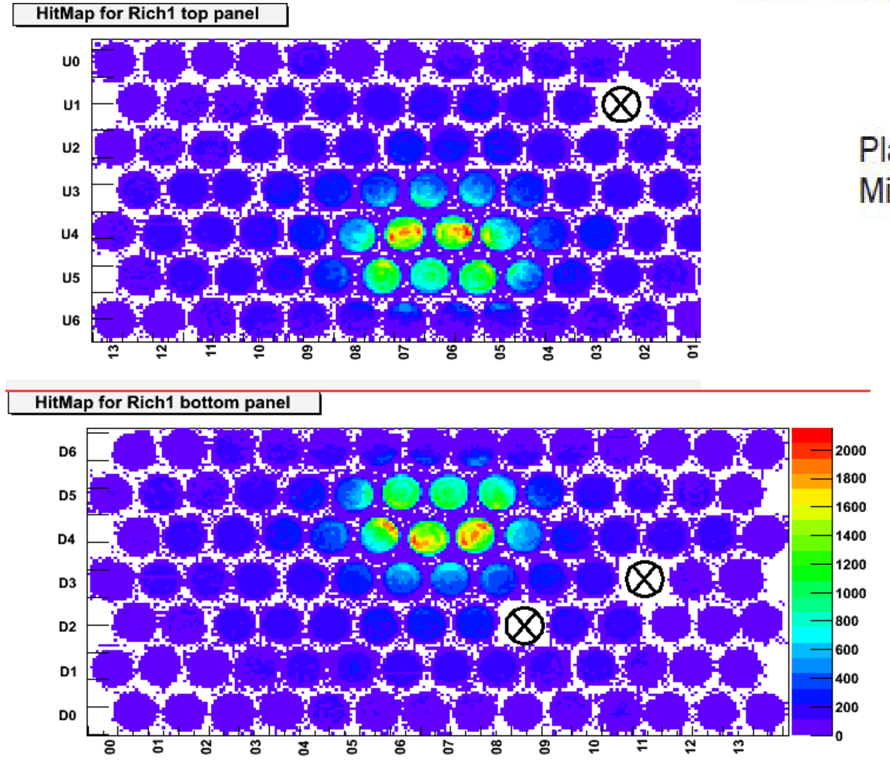

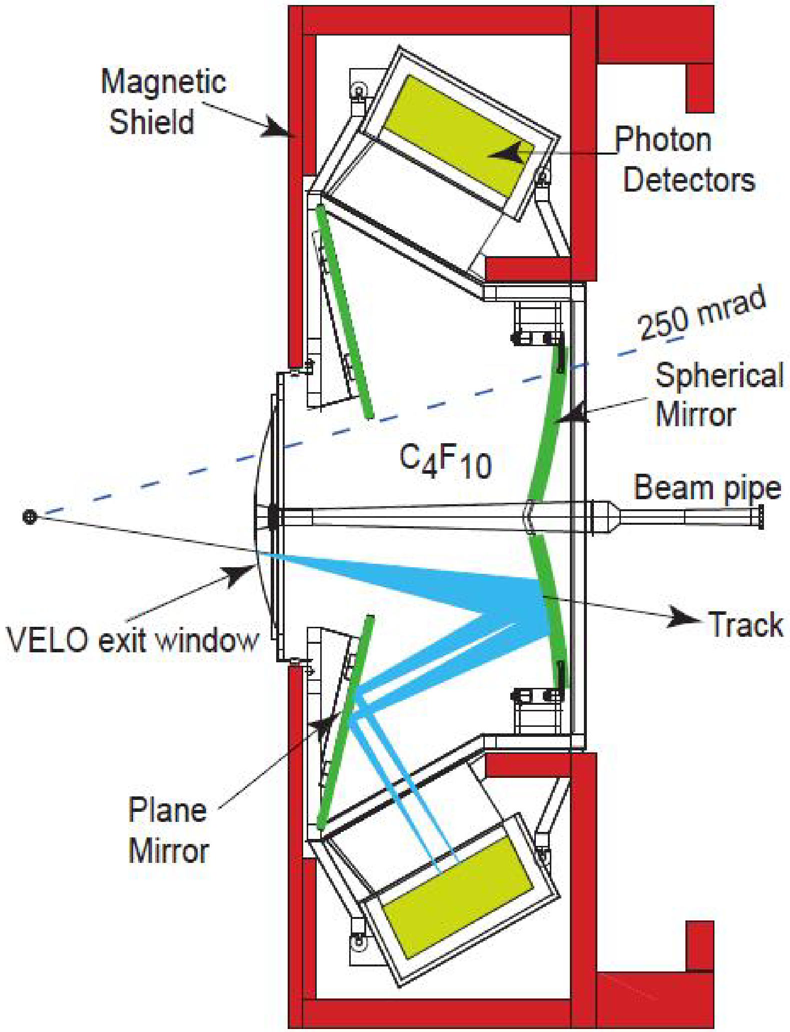

RICH 1

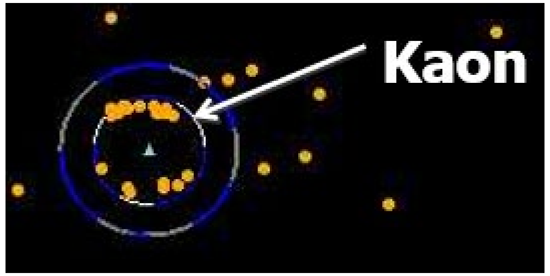

NIM A 603 (2009) 287

Belle II spectrometer

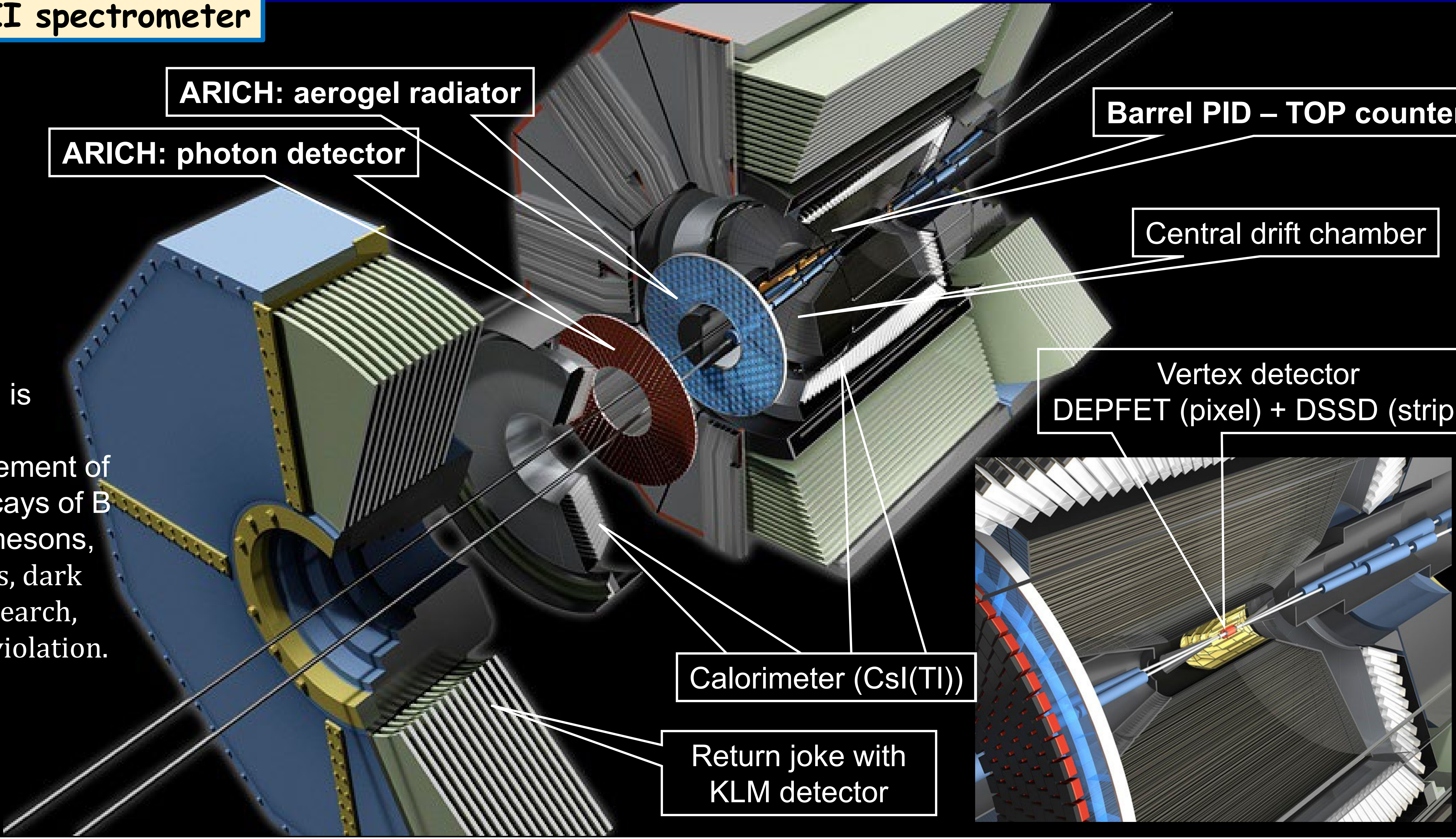

The aim is precise measurement of rare decays of B and D mesons, τ leptons, dark matter search, and CP violation.

Proximity focusing Aerogel Ring Imaging CHerenkov detector (ARICH) components:

- double layer focusing aerogel radiator (20 mm each)
- 160 mm expansion gap
- photon detector - Hybrid Avalanche Photo Detectors (HAPD)

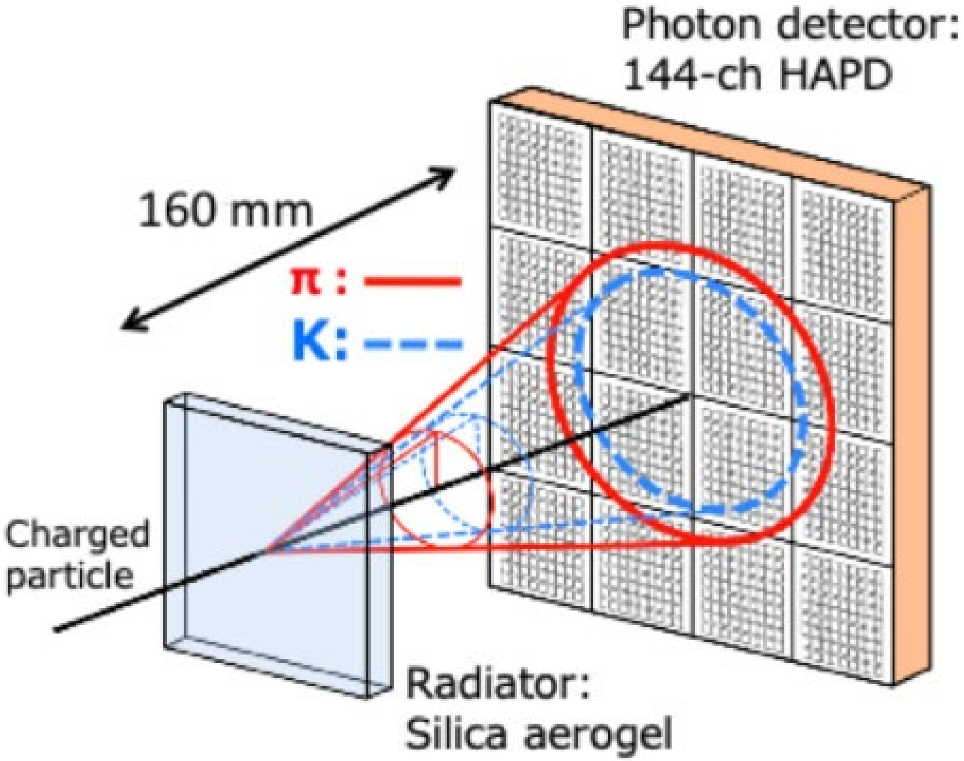

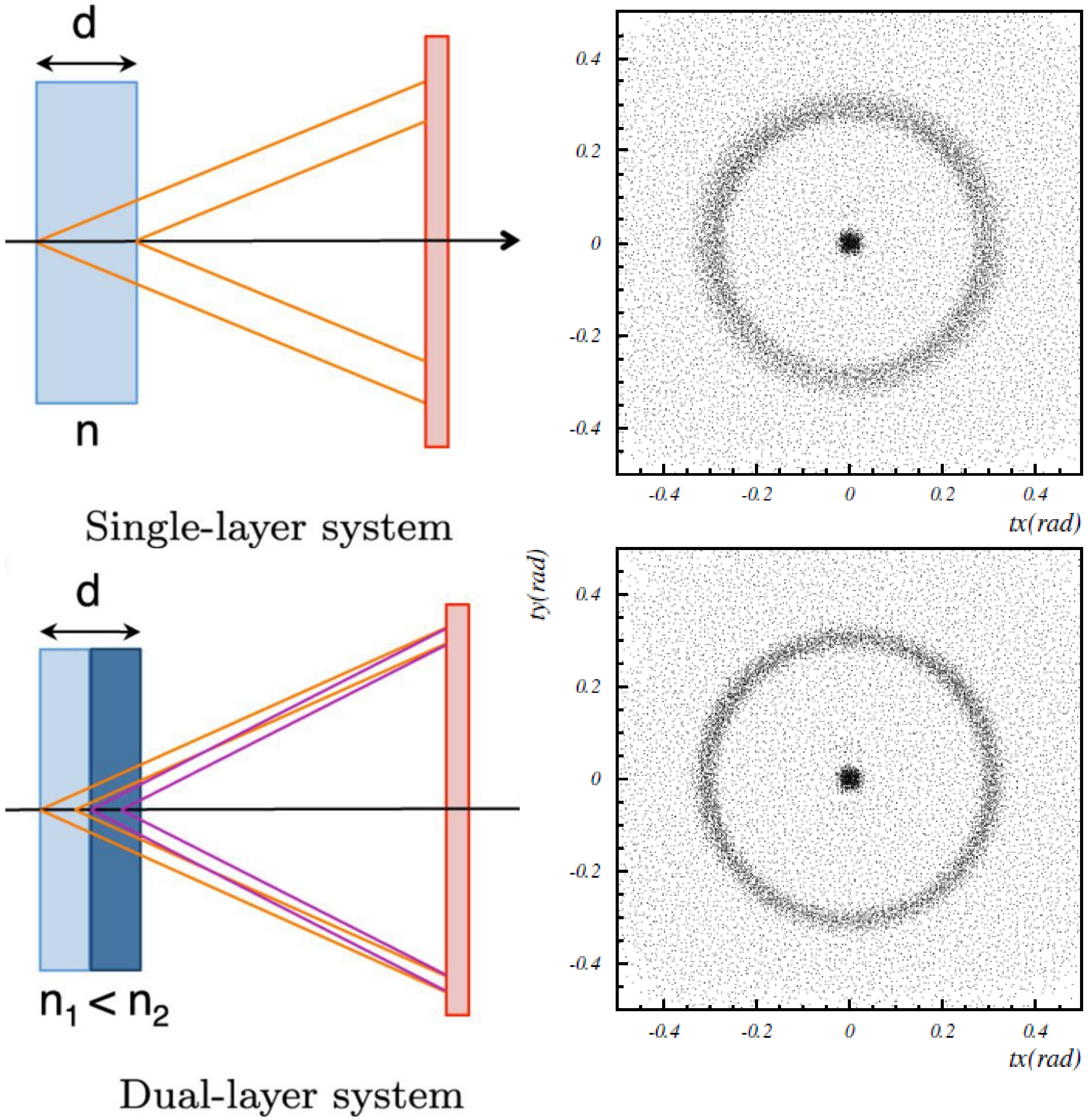

Single photon Cherenkov angle resolution

- Two main contributions to single photon resolution (n=1.05)

$$\tan \sigma_{\vartheta_c} \approx \frac{r}{l}$$

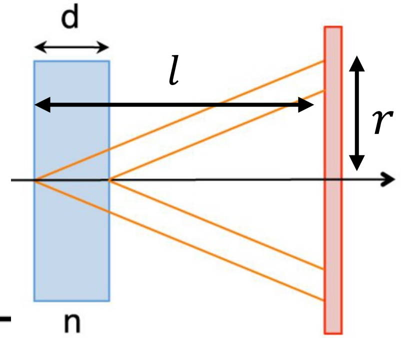

- pad size a (~6mm), position resolution $\frac{a}{\sqrt{12}}$

$$\sigma_{\vartheta,r} \approx \frac{cos^2\vartheta_c}{\left(l-\frac{1}{2}d\right)}\frac{a}{\sqrt{12}} \approx 8 \text{ mrad}$$

- aerogel thickness d, emission point uncertainty $\frac{d}{\sqrt{12}}$

$$\sigma_d \approx \frac{cos\vartheta_c sin\vartheta_c}{\left(l-\frac{1}{2}d\right)}\frac{d}{\sqrt{12}} \approx \text{Ad} = \text{d} \cdot 4 \text{ mrad/cm}$$

- single photon resolution

$$\sigma_{\vartheta_c} = \sigma_{\vartheta,a} \oplus \sigma_{\vartheta,d}$$

$$\sigma_{\vartheta_c}^2 \approx \sigma_{\vartheta,r}^2 + (Ad)^2$$

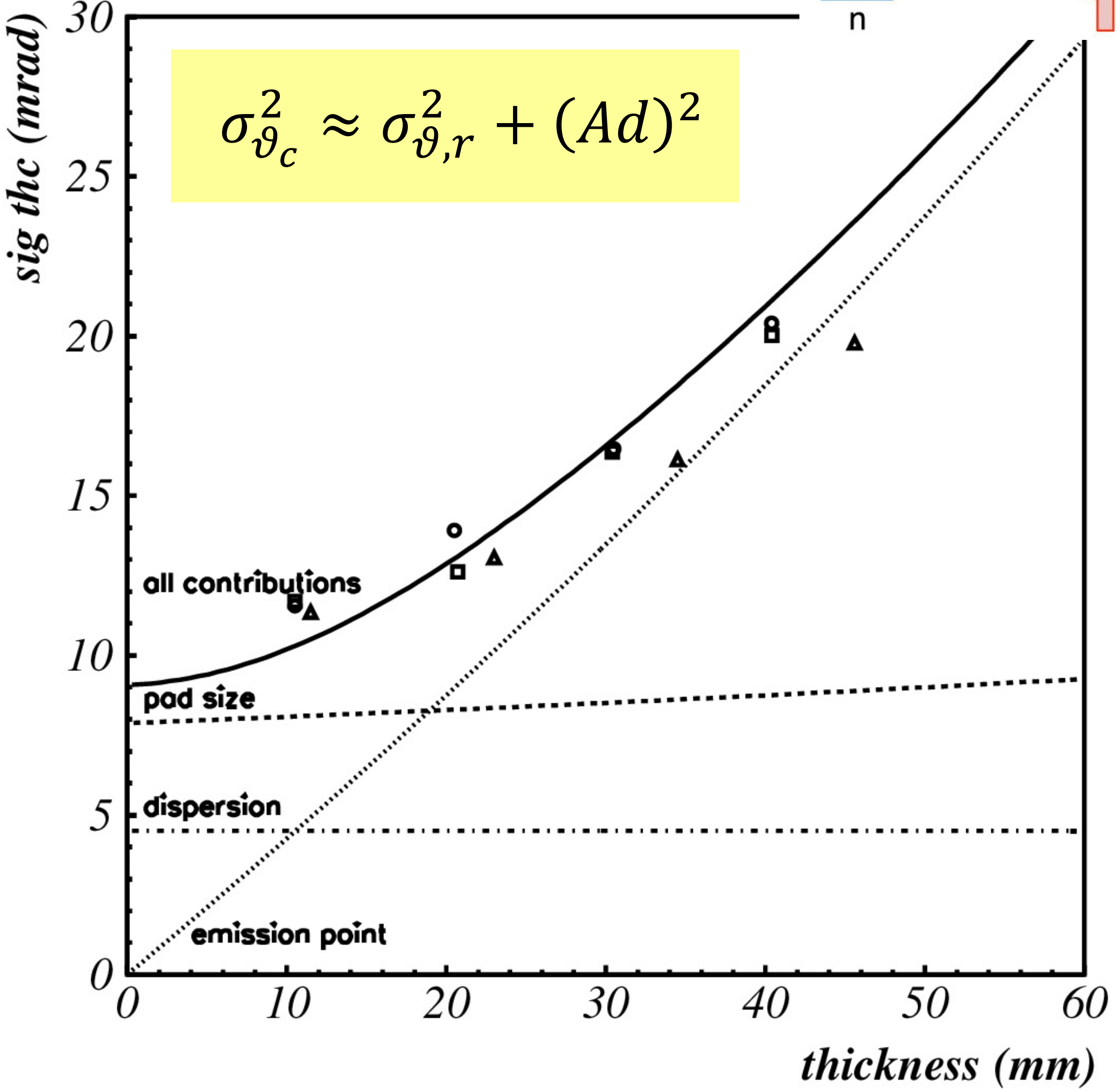

Aerogel thickness optimization

- Single track Cherenkov angle resolution

$$\sigma_{track} = \frac{\sigma_{\vartheta_c}}{\sqrt{N}}$$

- with no attenuation ($N = Bd$)

$$\sigma_{track}^2 \approx \frac{\sigma_{\vartheta,r}^2 + (Ad)^2}{Bd}$$

- minimum at

$$d_{min} = \frac{\sigma_{\vartheta,r}^2}{A} \approx 2cm$$

- minimum sigma (data)

$$\sigma_{track} \approx \frac{14mrad}{\sqrt{6}} = 5.7mrad$$

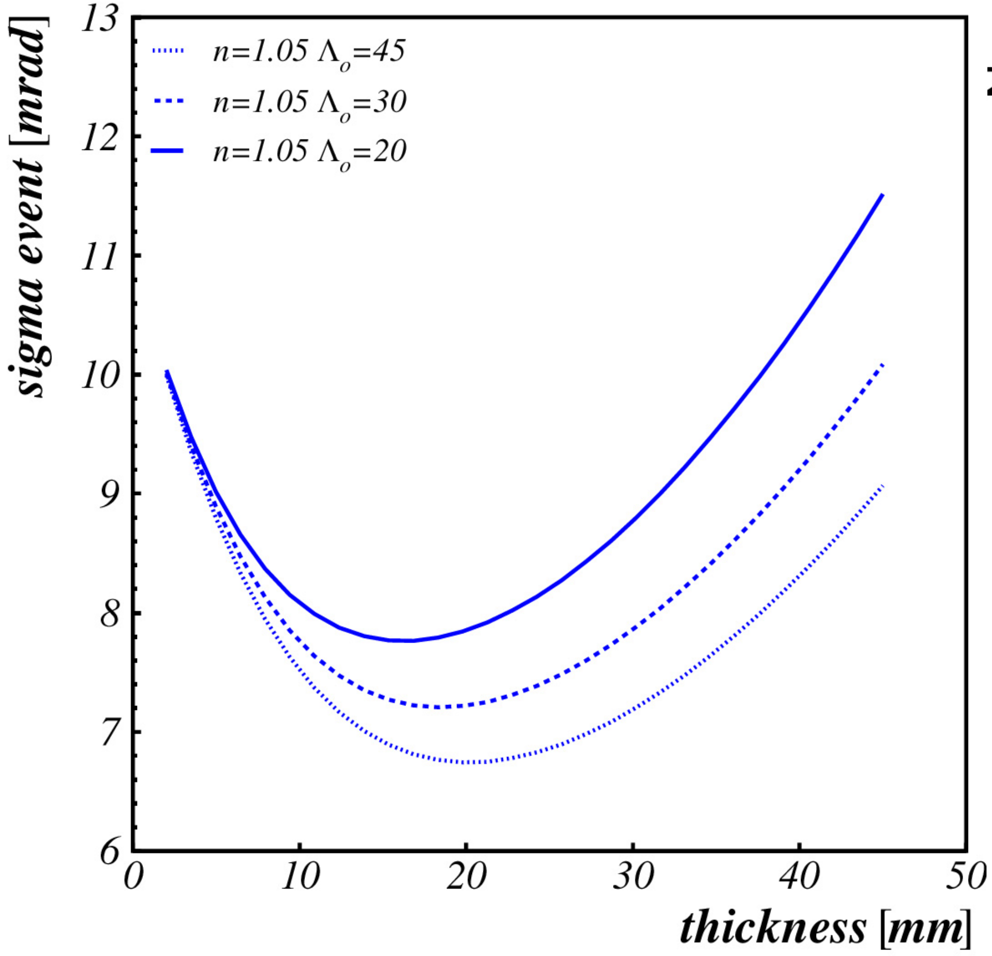

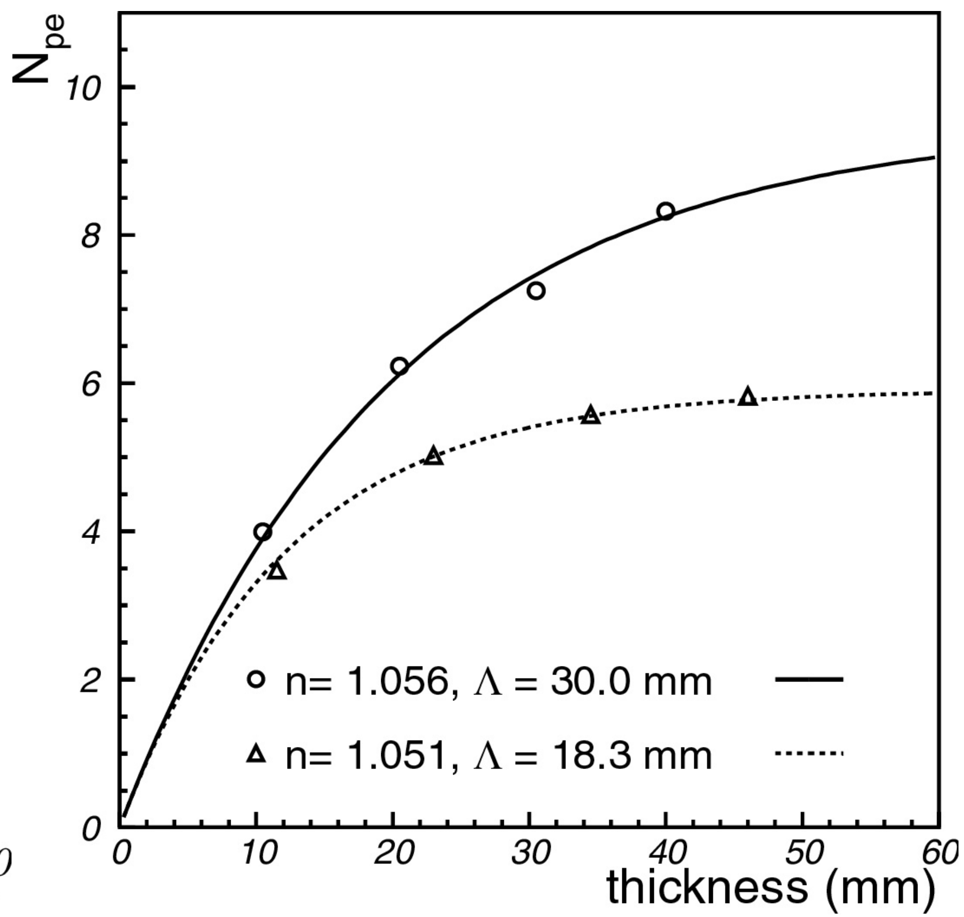

Proximity focusing aerogel RICH

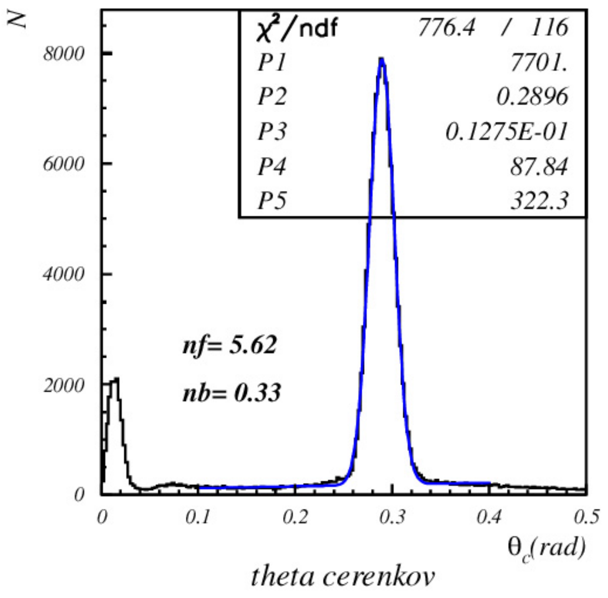

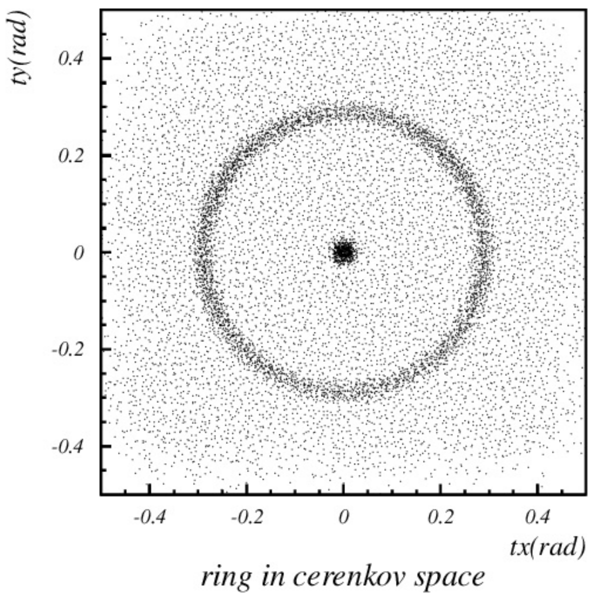

- Typical distributions for 2cm sample, obtained in the pion beam tests → N_{ph}, ϑ_C

Cherenkov angle resolution per track is optimal at ~ 2cm

- Radiators of different thicknesses and refractive indices were tested (2001,2003)

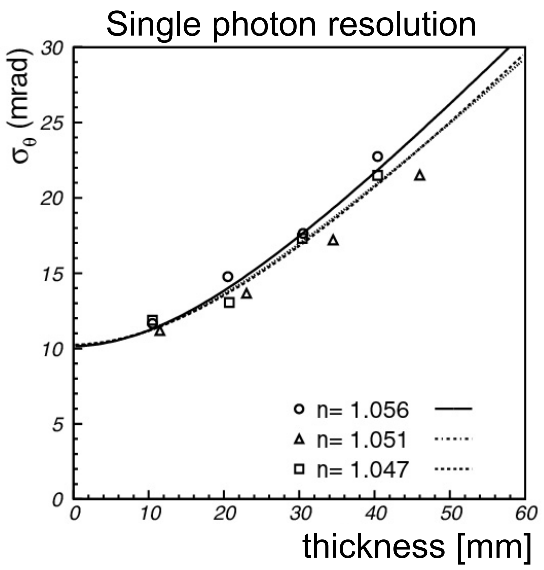

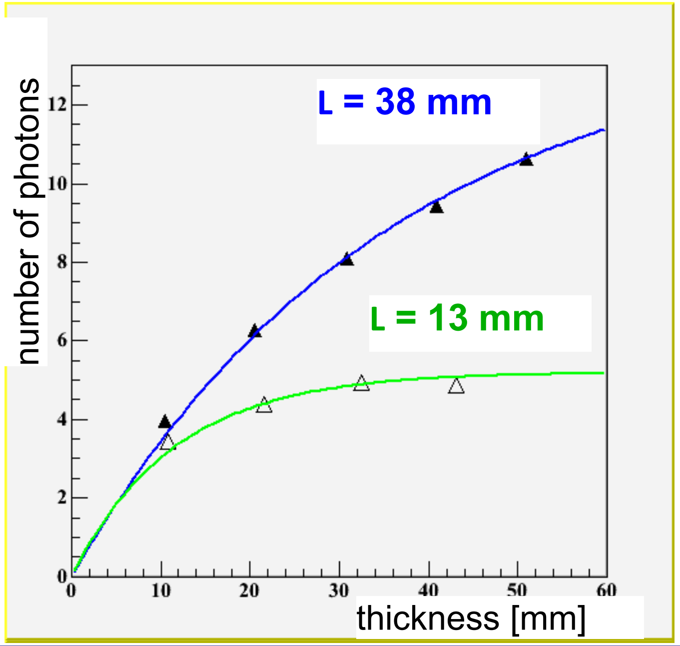

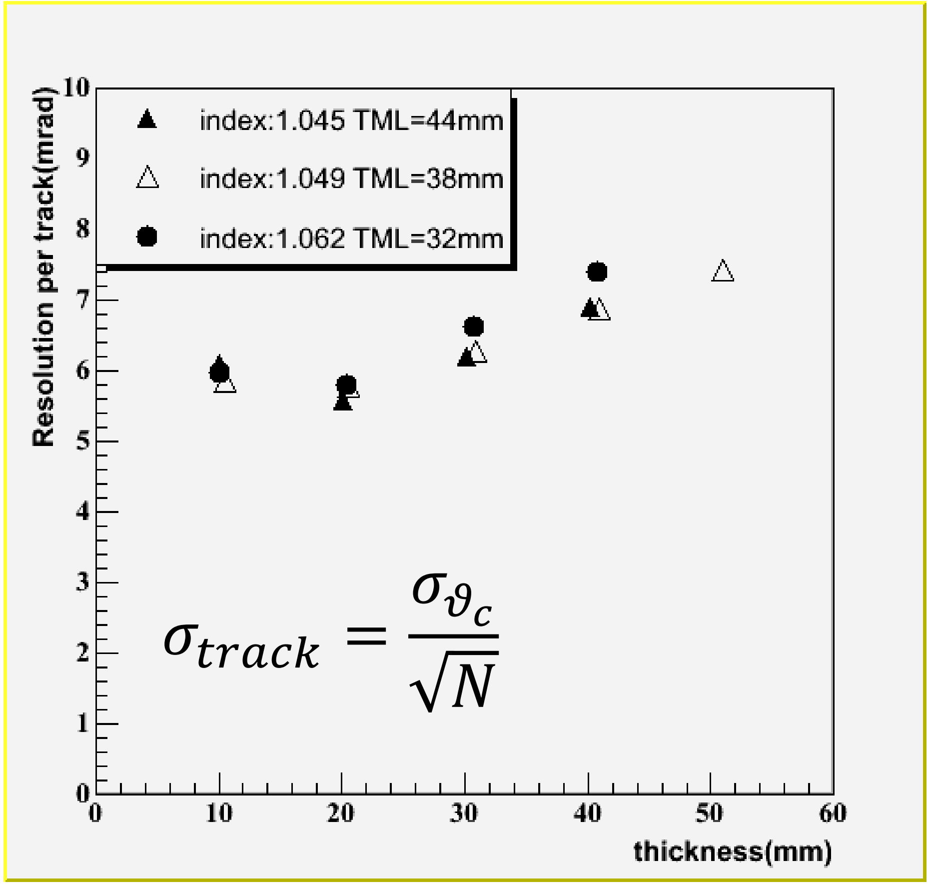

Aerogel radiator

- two layers of $20\ mm$ thick hydrophobic aerogel :
  - upstream, $\mathrm{n} \approx 1.045, \lambda_{400\ nm} \approx 47\ \mathrm{mm}$
  - downstream, $n = 1.055\ , \lambda_{400nm} \approx 37\ \mathrm{mm}$
- 4 segmented rings, 2×124 tiles
- all but exit surface of each pair covered by black paper
- each pair fixed by two black strings running radially
- completed in December 2016

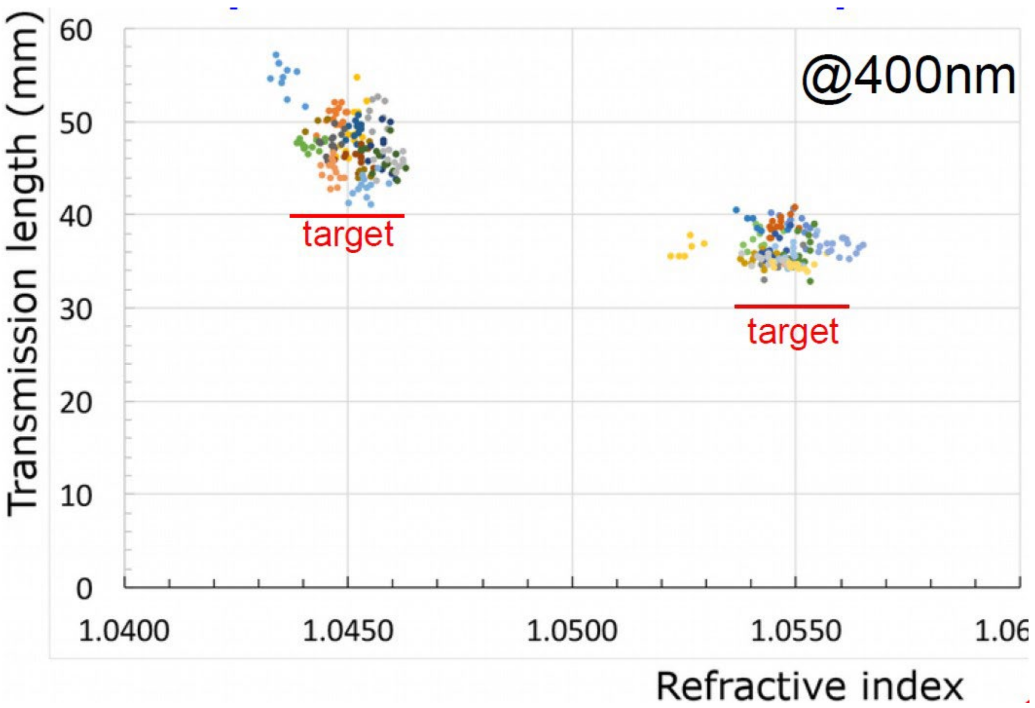

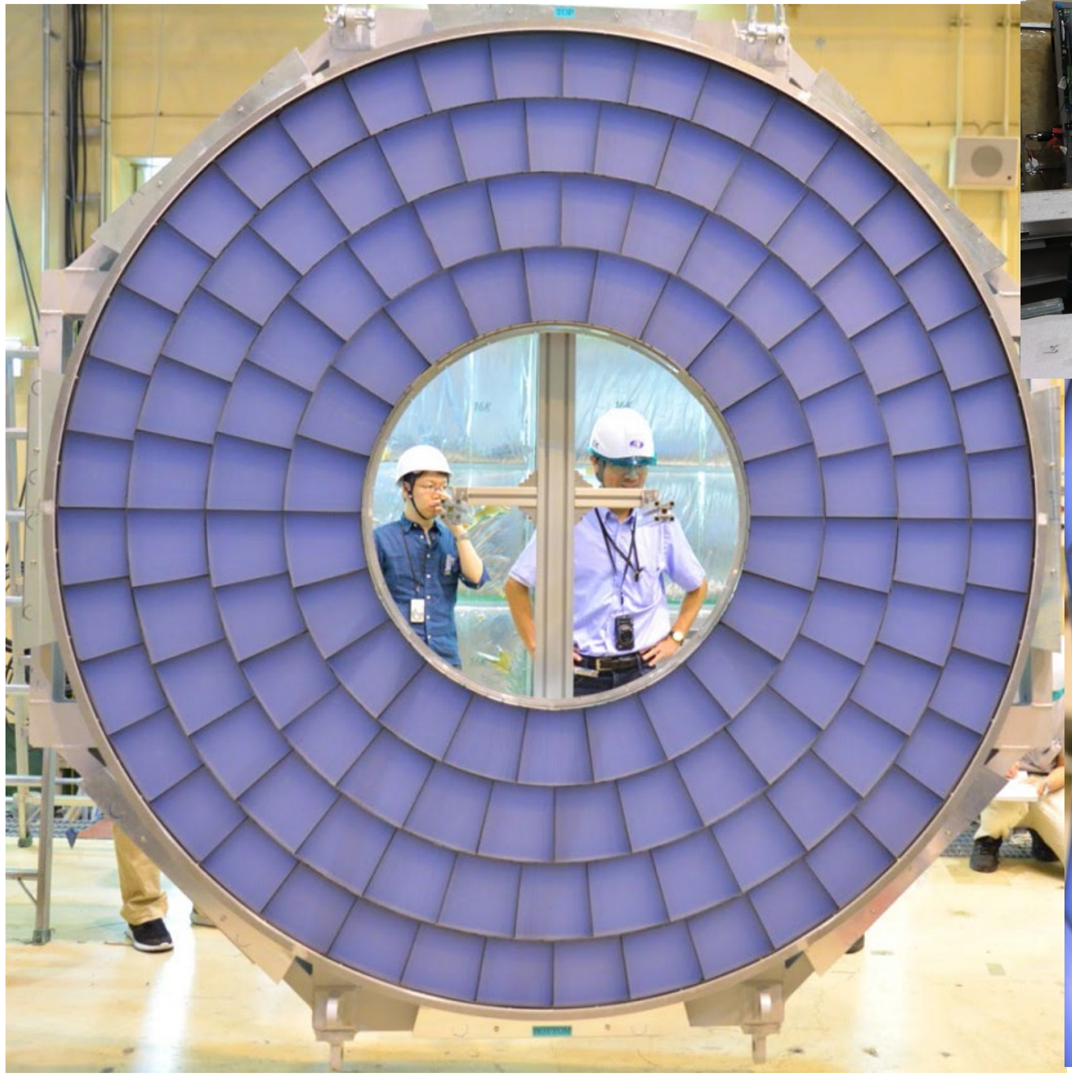

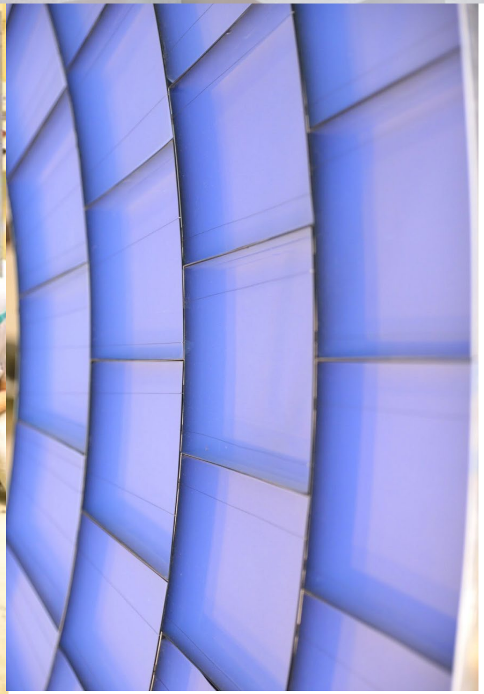

Photon detector - HAPD

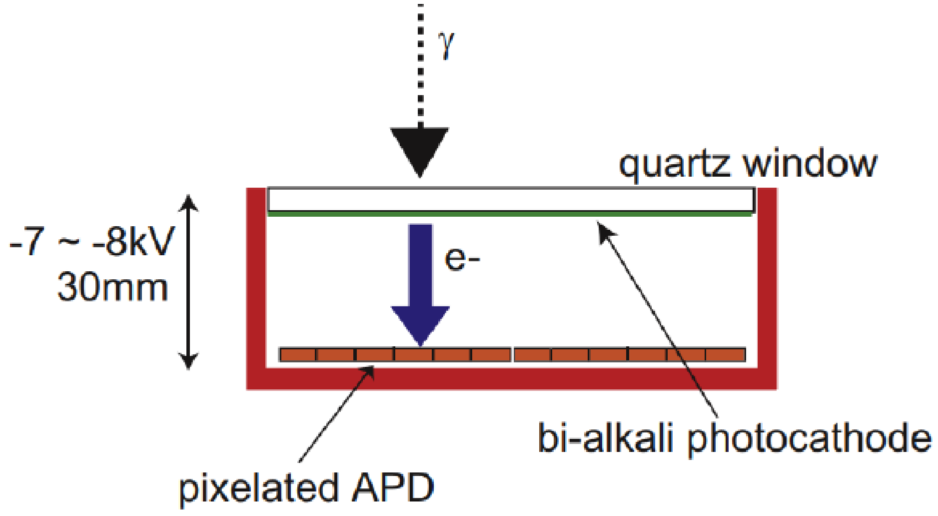

HAPD properties:

- size: $73 \times 73 \times 28\ \mathrm{mm}^3$
- 2×2 APDS with 6×6 channels, $4.9 \times 4.9\ \mathrm{mm}^2$ @ 5.1mm pitch
- $< QE_{400nm} > \approx 32\ \%$
- combined gain $\approx 70\mathrm{k}$
- channel capacitance $80\ \mathrm{pF}$
- operation in $\mathrm{B} = 1.5\ \mathrm{T}$
- radiation tolerance $\approx 10^{12}\ \frac{n_{1MeV}}{\mathrm{cm}^2}$

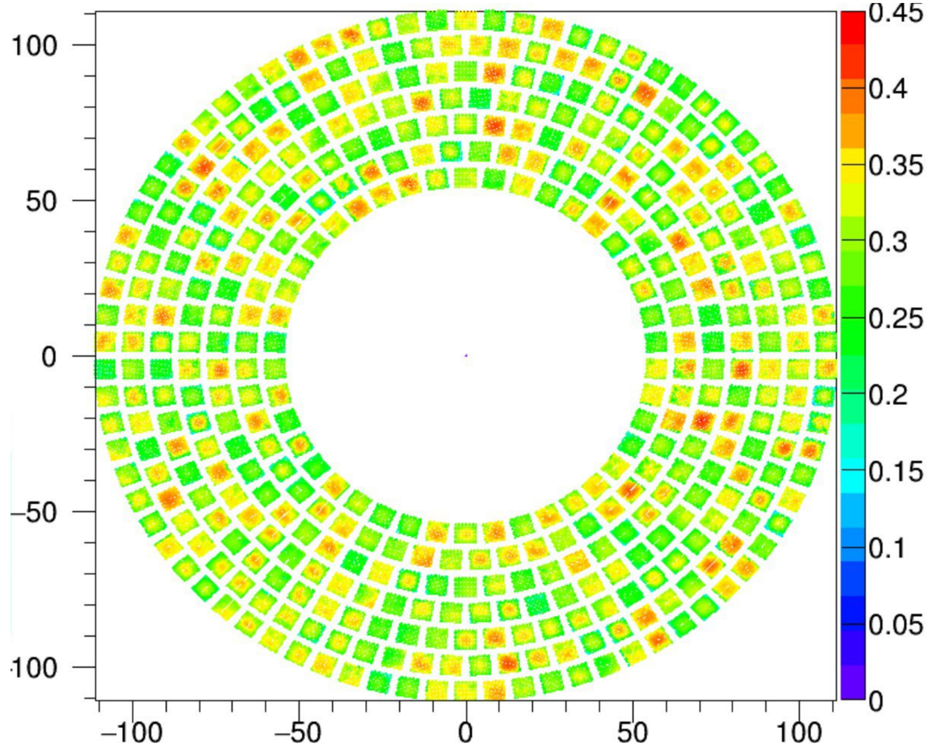

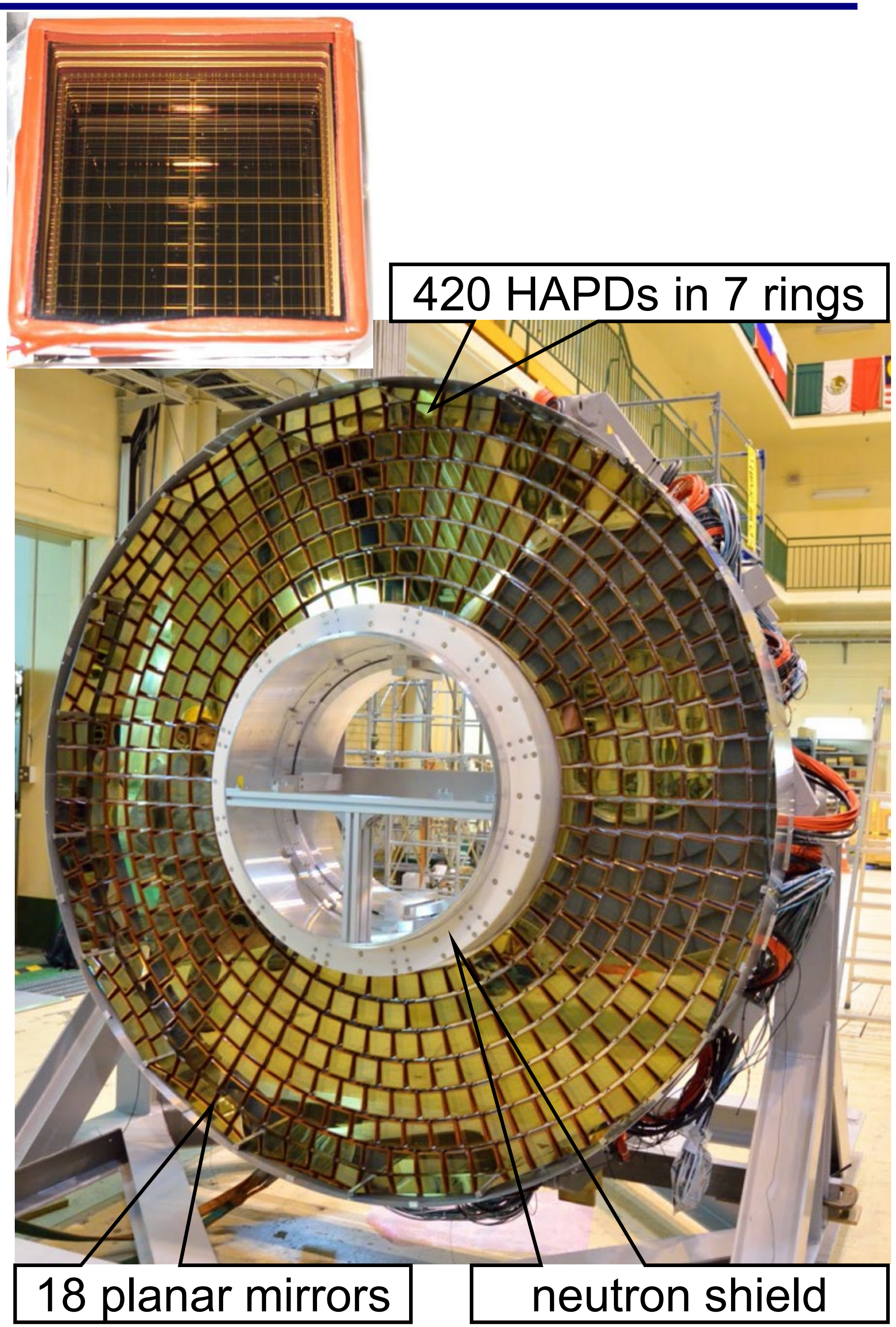

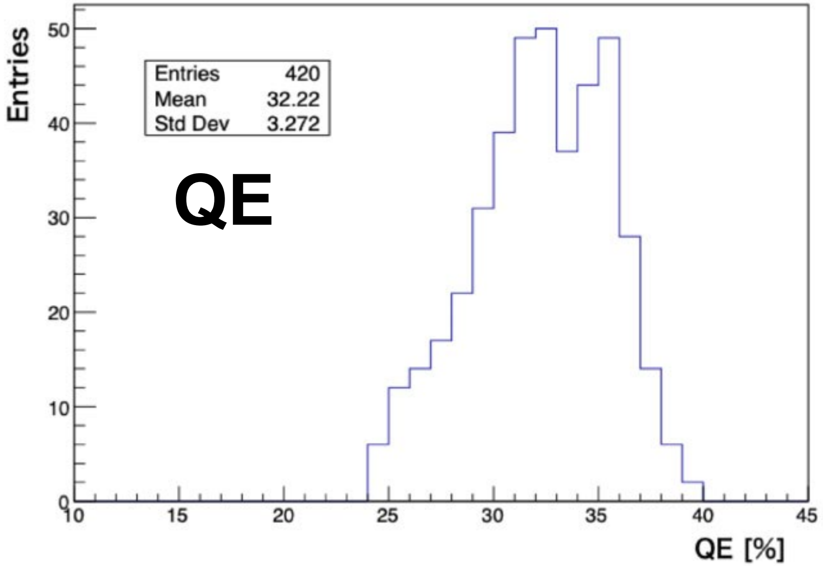

ARICH Cherenkov angle

- ARICH is aligned by maximising the agreement between expected and measured photon
- After alignment, a very good agreement is achieved between expected and measured Cherenkov angle distributions.

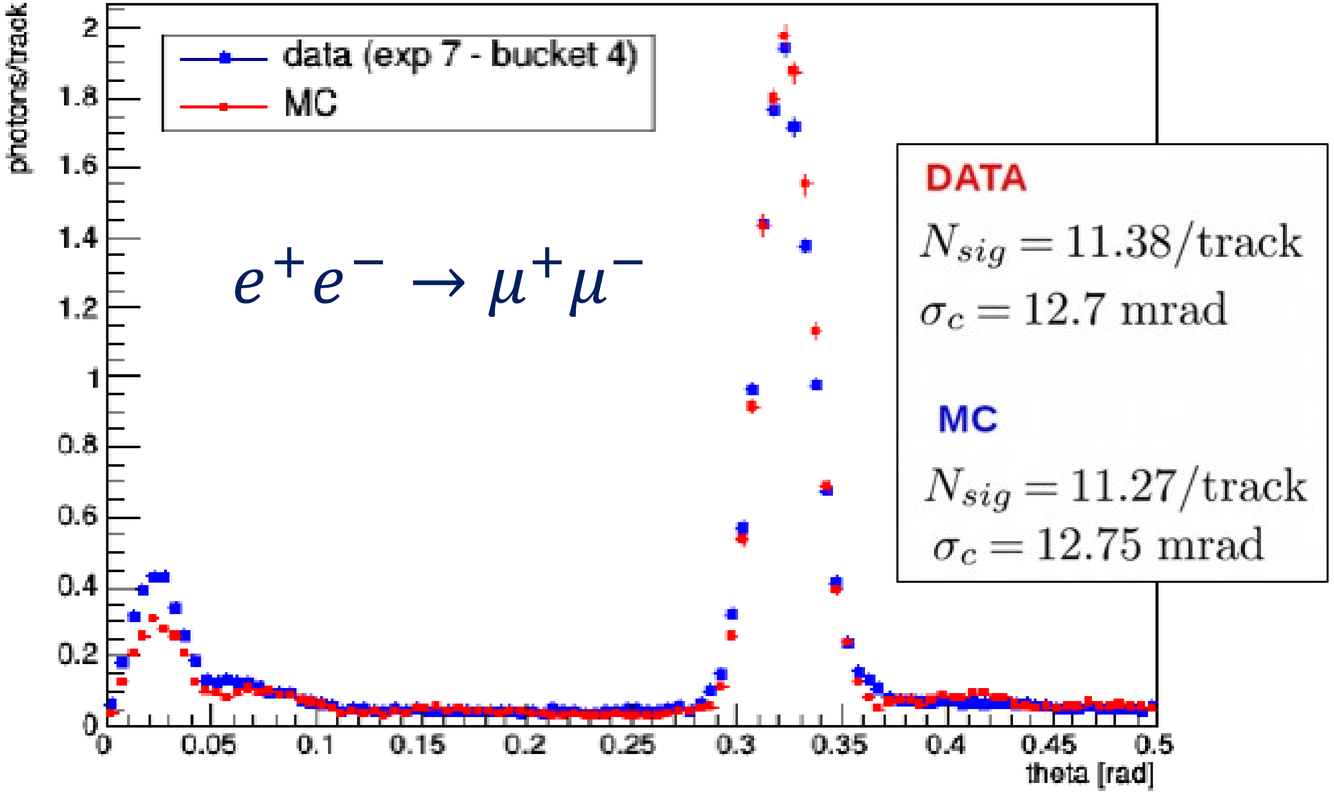

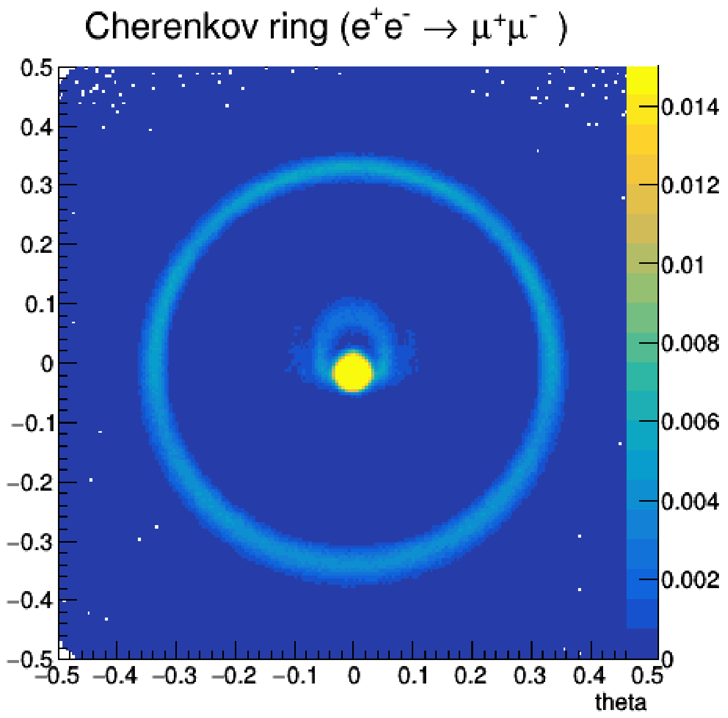

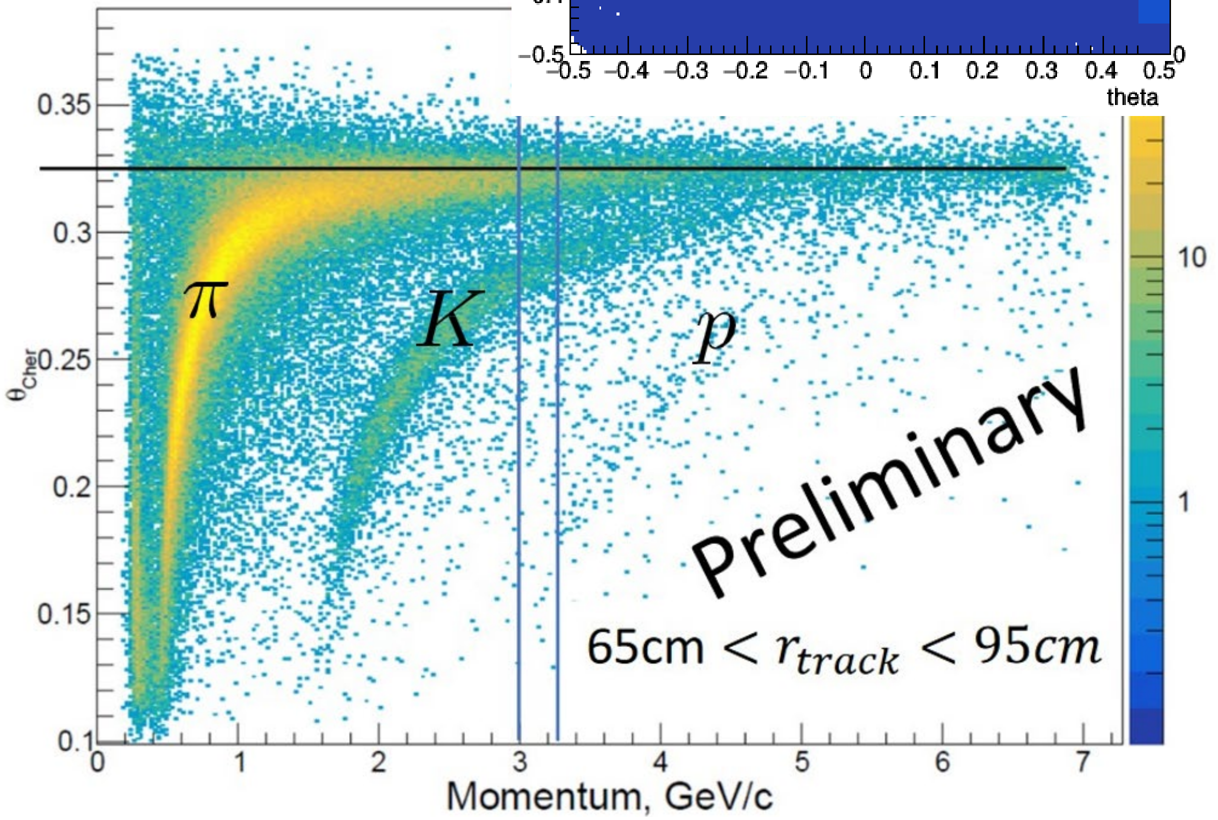

ARICH rings

- two pion ring examples
- compared with expected Cher. angle distribution

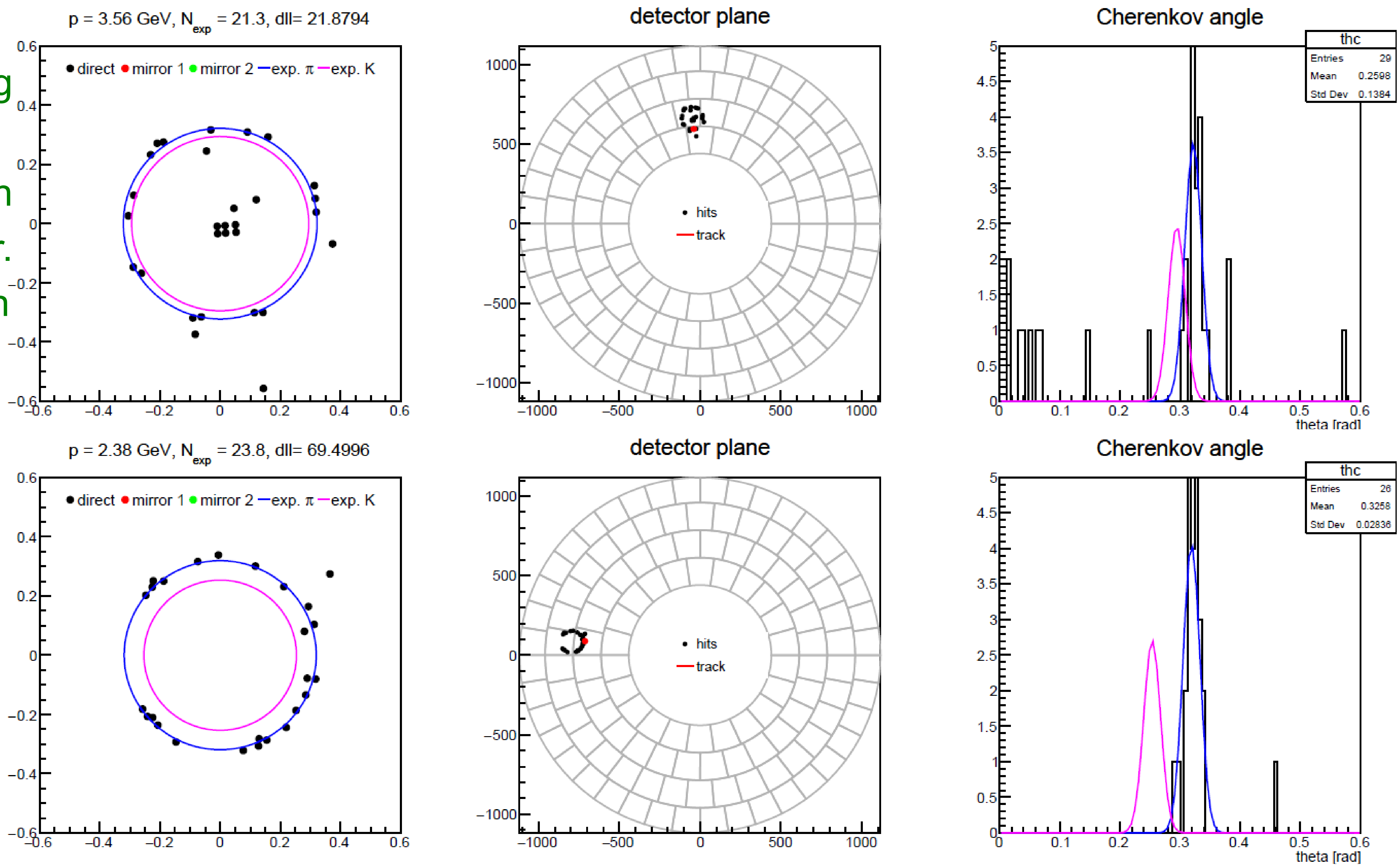

PID capability: Likelihood calculation

- PDF of Cherenkov photons from both radiators and uniform background for mass hypothesis m can be approximated as a function of Cher. angle (ϑ) and by

$$n_{cf}(\vartheta, m) \approx \left(\frac{\bar{N}_1}{\sqrt{2\pi}\sigma_1} e^{-\frac{(\vartheta - \vartheta_1(m))^2}{2\sigma_1^2}} + \frac{\bar{N}_2}{\sqrt{2\pi}\sigma_2} e^{-\frac{(\vartheta - \vartheta_2(m))^2}{2\sigma_2^2}} \right)$$

$$n_{bf}(\vartheta, m) \propto \vartheta$$

- likelihood function – Poisson distribution of hits on each pad with mean value $\bar{n}_i(m)$

$$\mathcal{L}(m) = \prod_{nohiti} e^{-\bar{n}_i(m)} \cdot \prod_{hiti} \left(1 - e^{-\bar{n}_i(m)}\right)$$

$$\ln \mathcal{L}\ (m) = -\sum_{nohiti} \bar{n}_i(m) + \sum_{nohiti} \ln\left(1 - e^{-\bar{n}_i(m)}\right) = -\sum_{nohiti} \bar{n}_i(m) - \sum_{hiti} \bar{n}_i(m) + \sum_{hiti} \bar{n}_i(m) + \sum_{hiti} \ln\left(1 - e^{-\bar{n}_i(m)}\right)$$

$$\ln \mathcal{L}\ (m) = -\bar{N}(m) + \sum_{hiti} \left(\bar{n}_i(m) + ln\left(1 - e^{-\bar{n}_i(m)}\right)\right)$$

- summation is needed only over the pixels with hit

PID capability: π/K separation power with $D^{*\pm}$ decays

- π, K identified by π_{slow} charge

$$D^{*+} \to D^0\ \pi^+_{\rm slow}, \quad D^0 \to K^-\ \pi^+$$

$$D^{*-} \to \bar{D}^0\ \pi^-_{\rm slow}, \quad \bar{D}^0 \to K^+\ \pi^-$$

- Apply selection criteria on

$$R[K/\pi] = \frac{\mathcal{L}_K}{\mathcal{L}_K + \mathcal{L}_\pi}$$

$\mathcal{L}$ - likelihood for given id. hypothesis

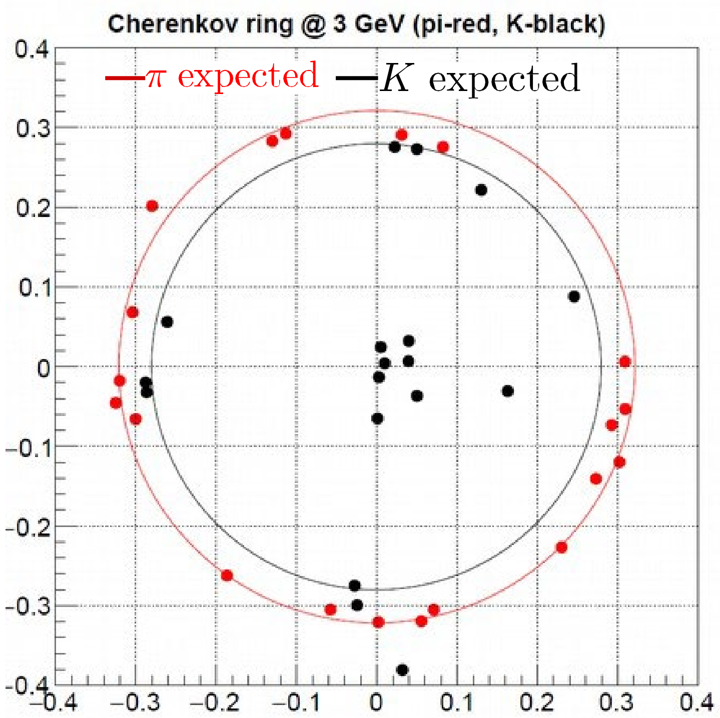

D^0 mass peak

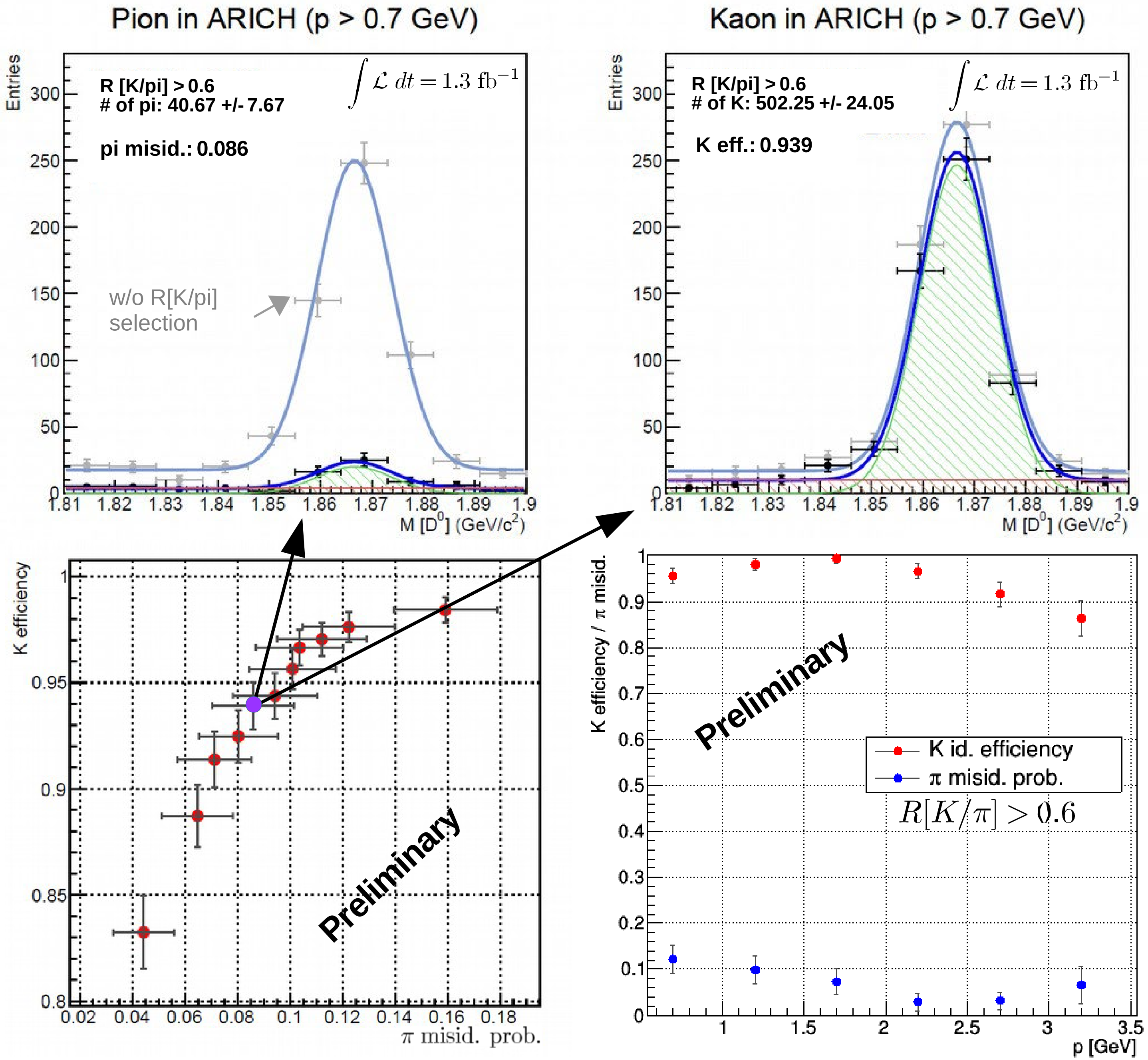

Photon detectors: SiPM

- immune to magnetic field
- high photon detection efficiency (PDE)
- good timing properties (< 300ps FWHM)
- no high voltage
- low material budget
- high noise rate ~ 0.1MHz/mm^2
- radiation damage - increase of dark noise

Possible candidate:

- array of Hamamatsu S10362-11-100P

Improve signal to noise ratio by:

- narrow time window
- use of light concentrators

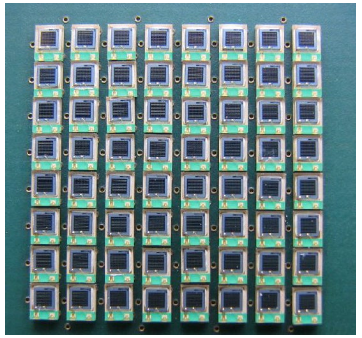

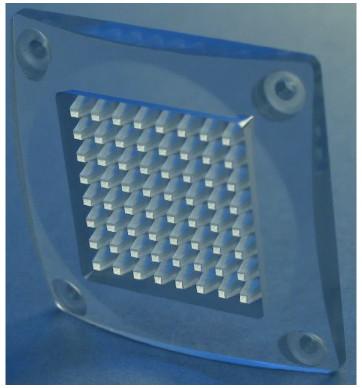

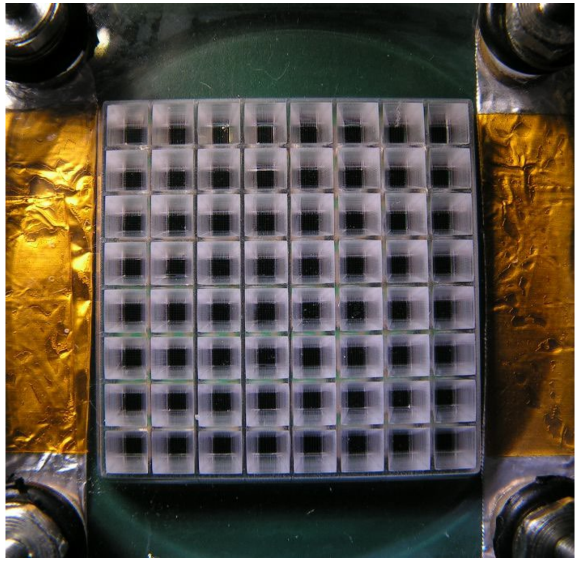

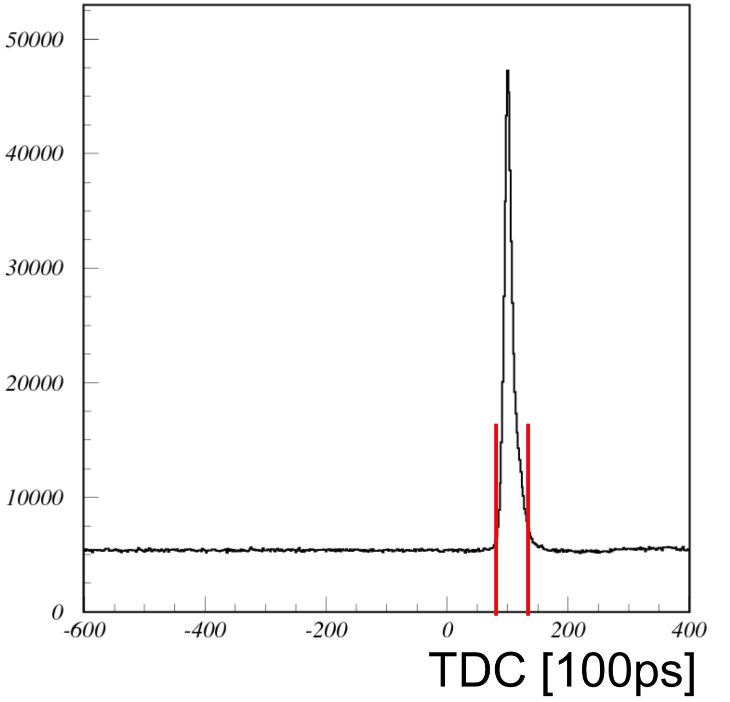

- beam test result (1cm,n=1.03)

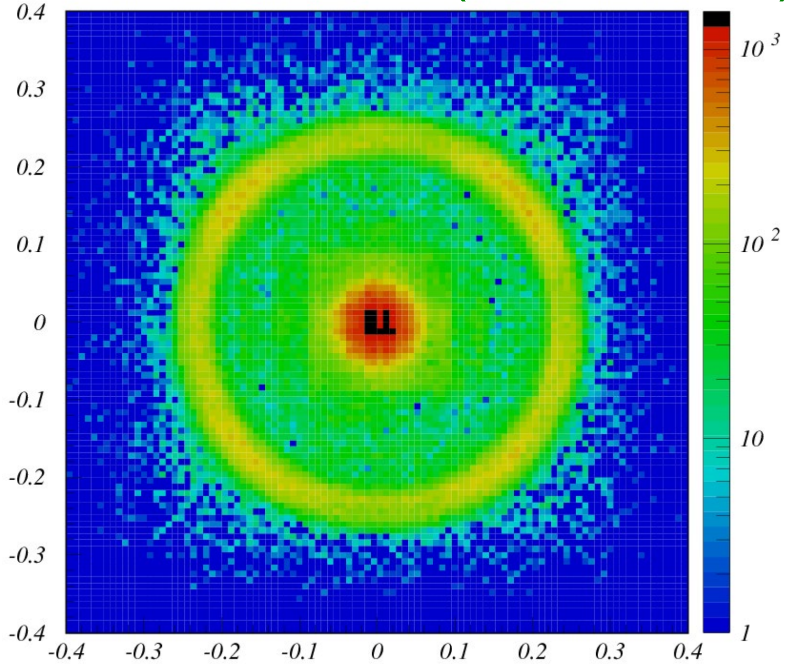

NIM A613 (2010) 195

EIC mRICH

- radiator: aerogel + Fresnel lens
- photosensor: SiPM

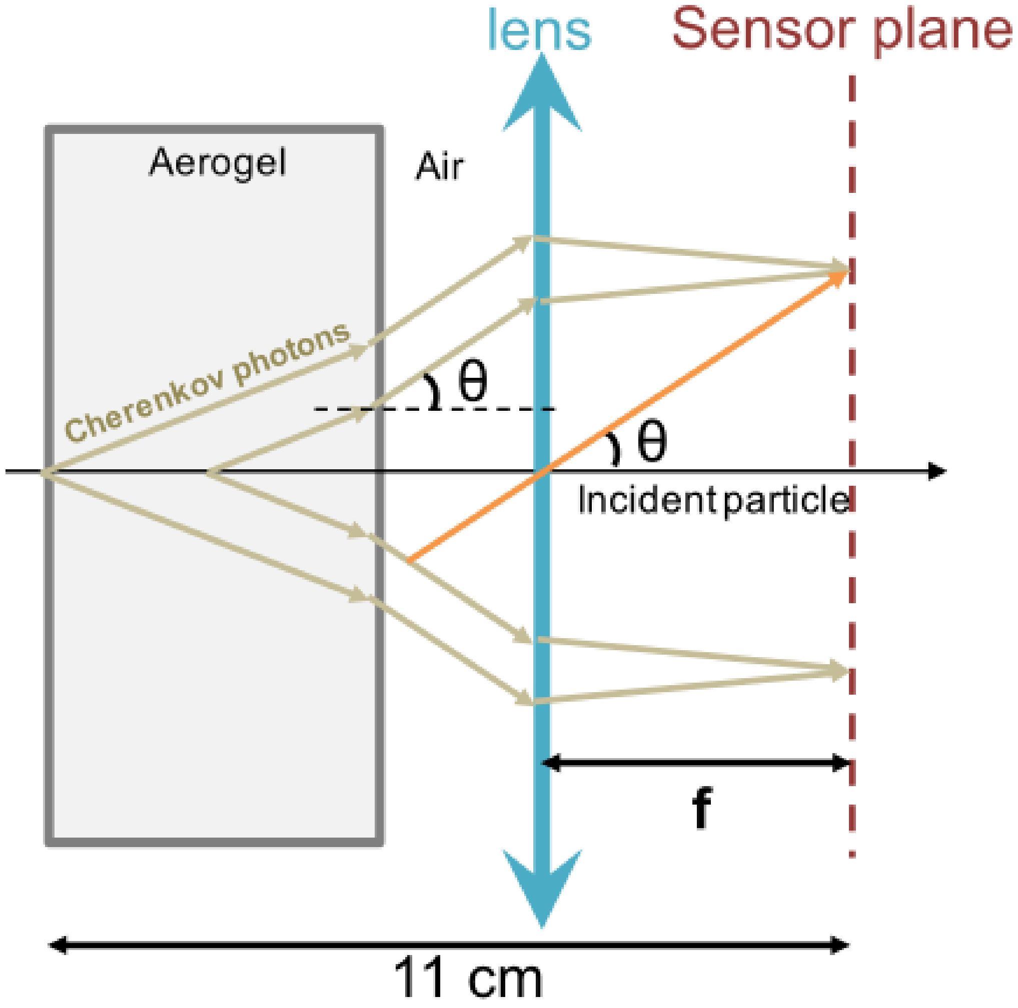

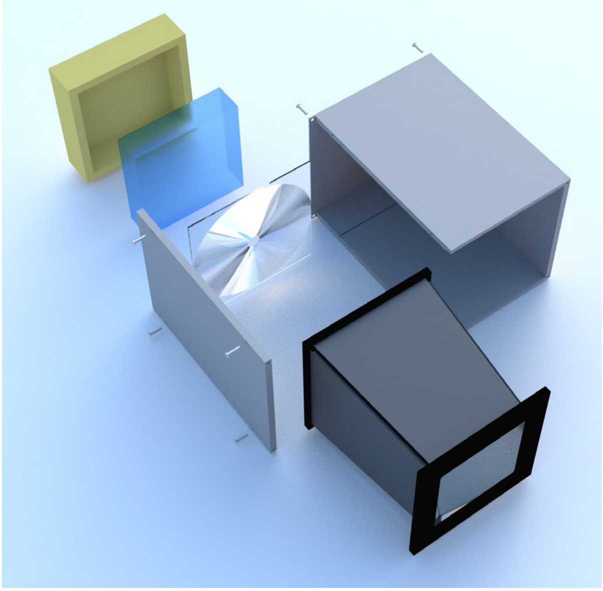

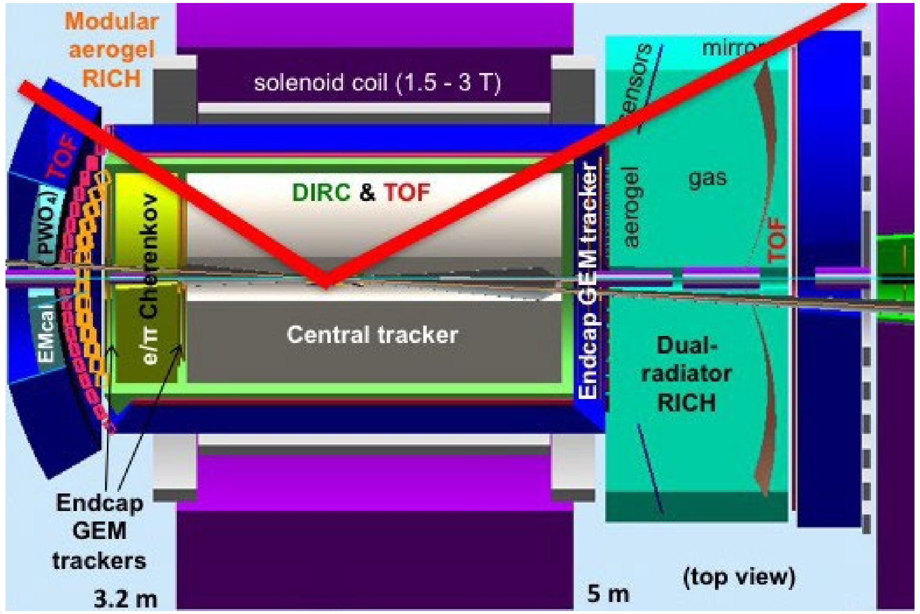

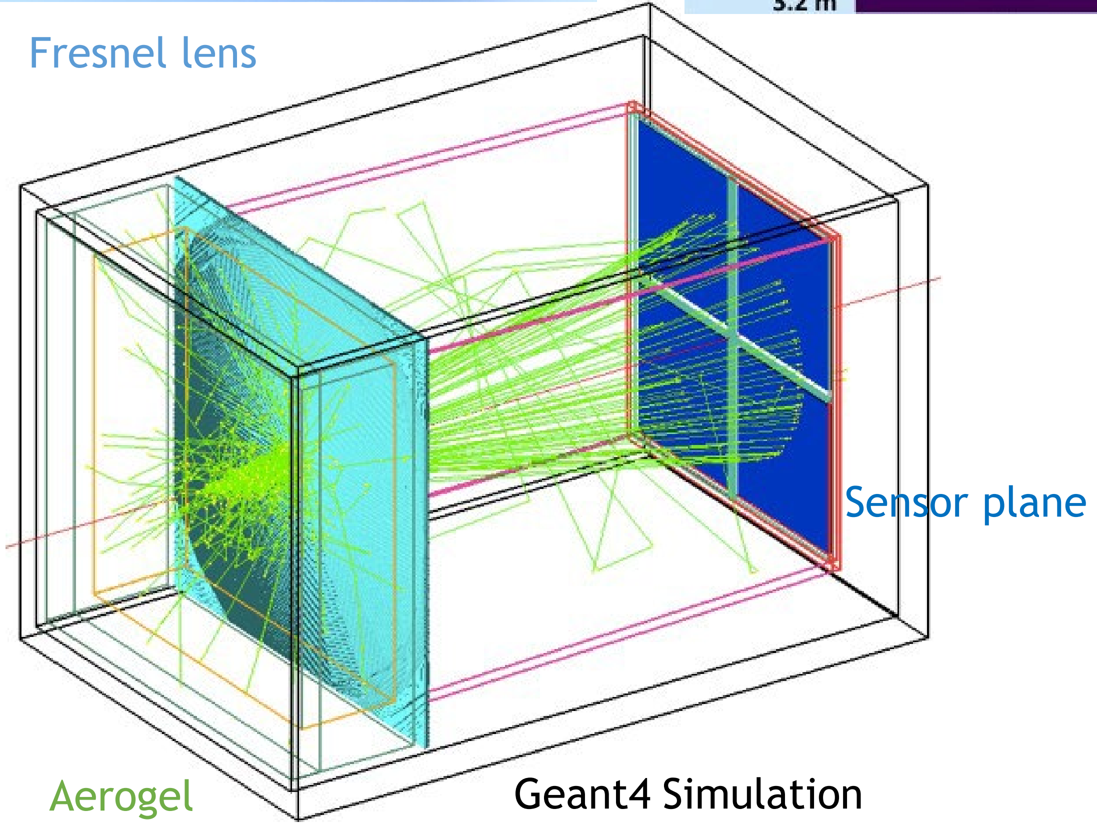

Outline:

- Why PID?
- TOF detectors
- Specific ionization loss - dE/dx
- Transition radiation detectors (TRD)
- Cherenkov based PID devices
  - Threshold detectors
  - RICH detectors
  - **DIRC type detectors**

DIRC detector @ BaBar

- quartz bar as radiator and light guide
- water filled expansion volume with PMTs outside magnetic field

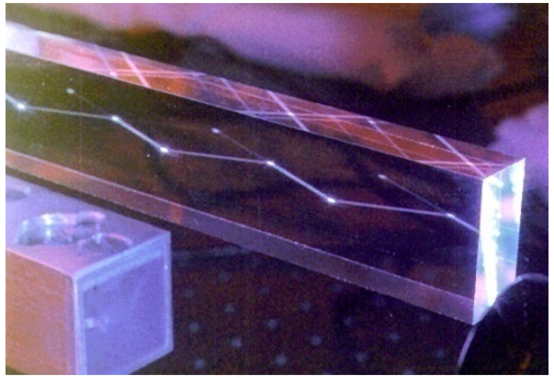

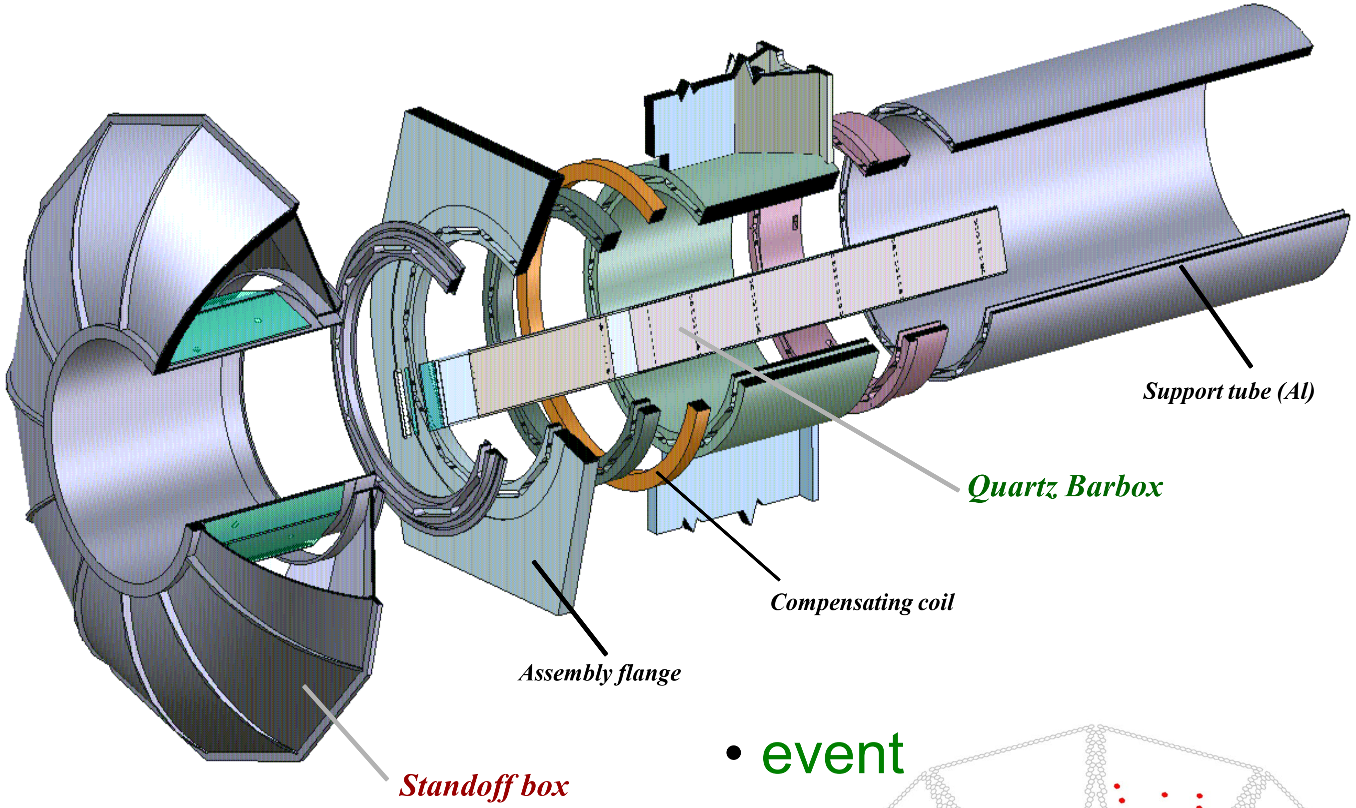

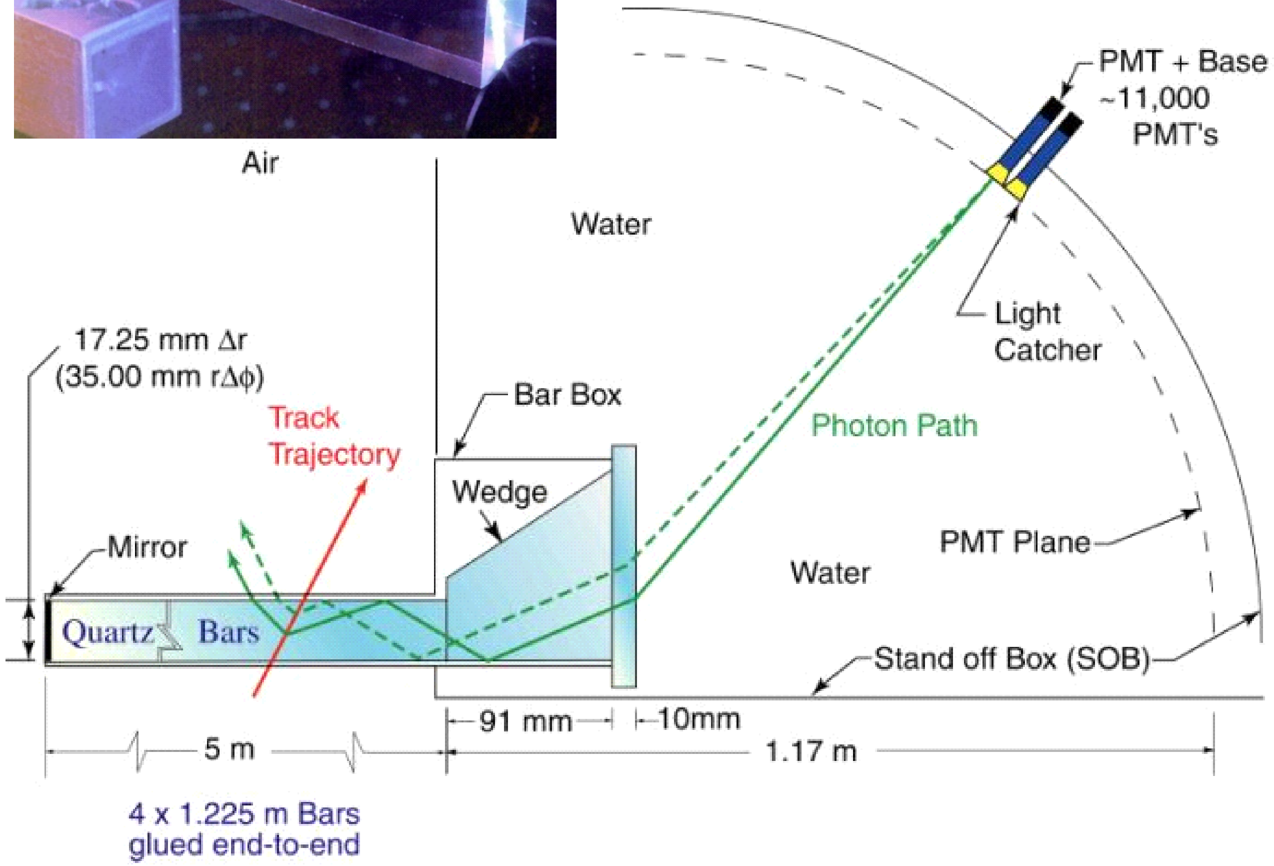

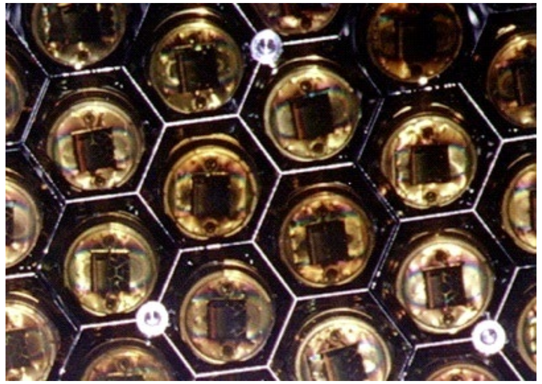

- event

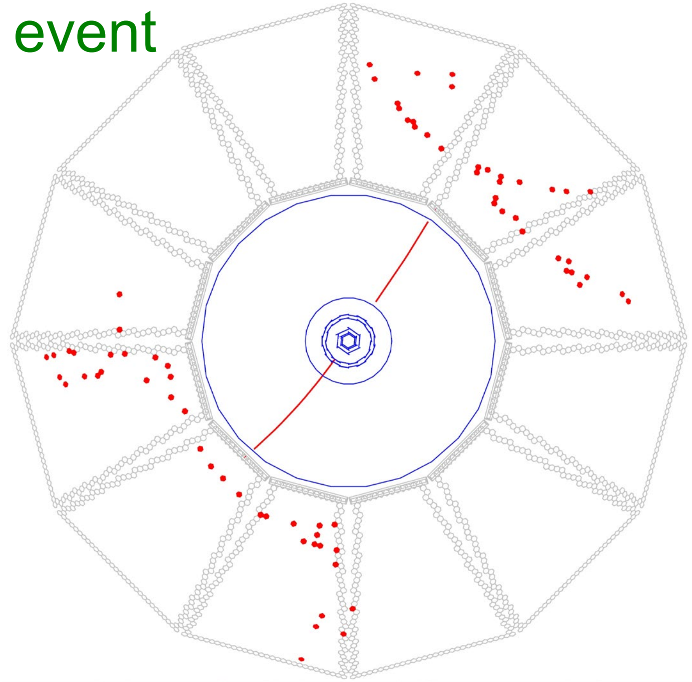

NIM-A479(2002)1

DIRC performance

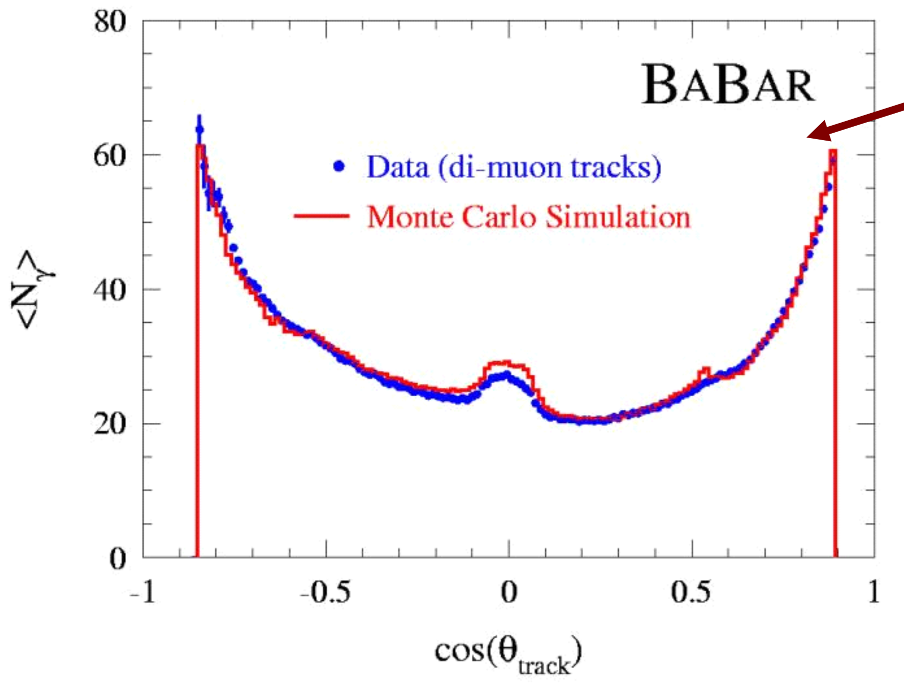

Lots of photons

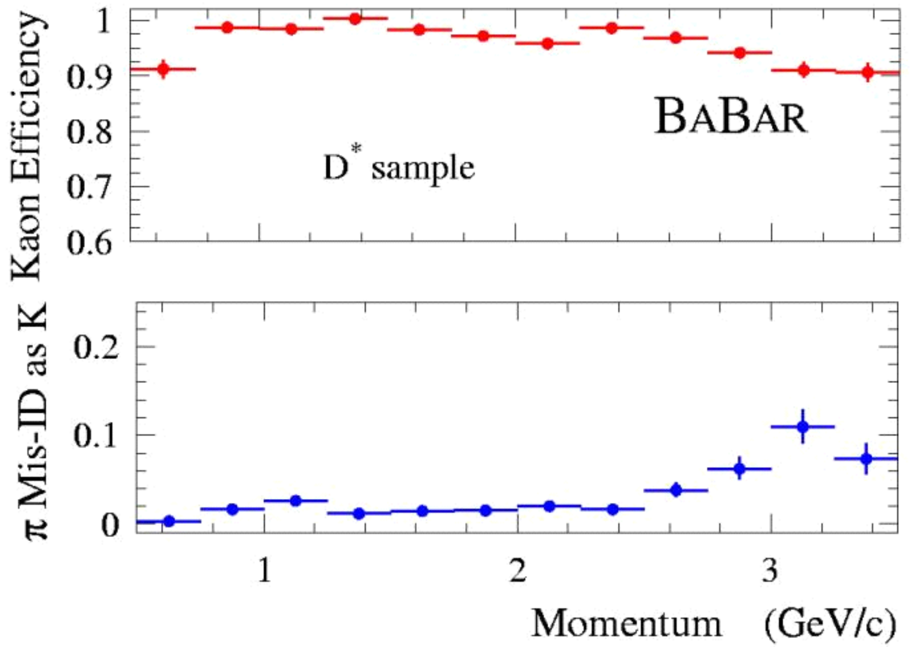

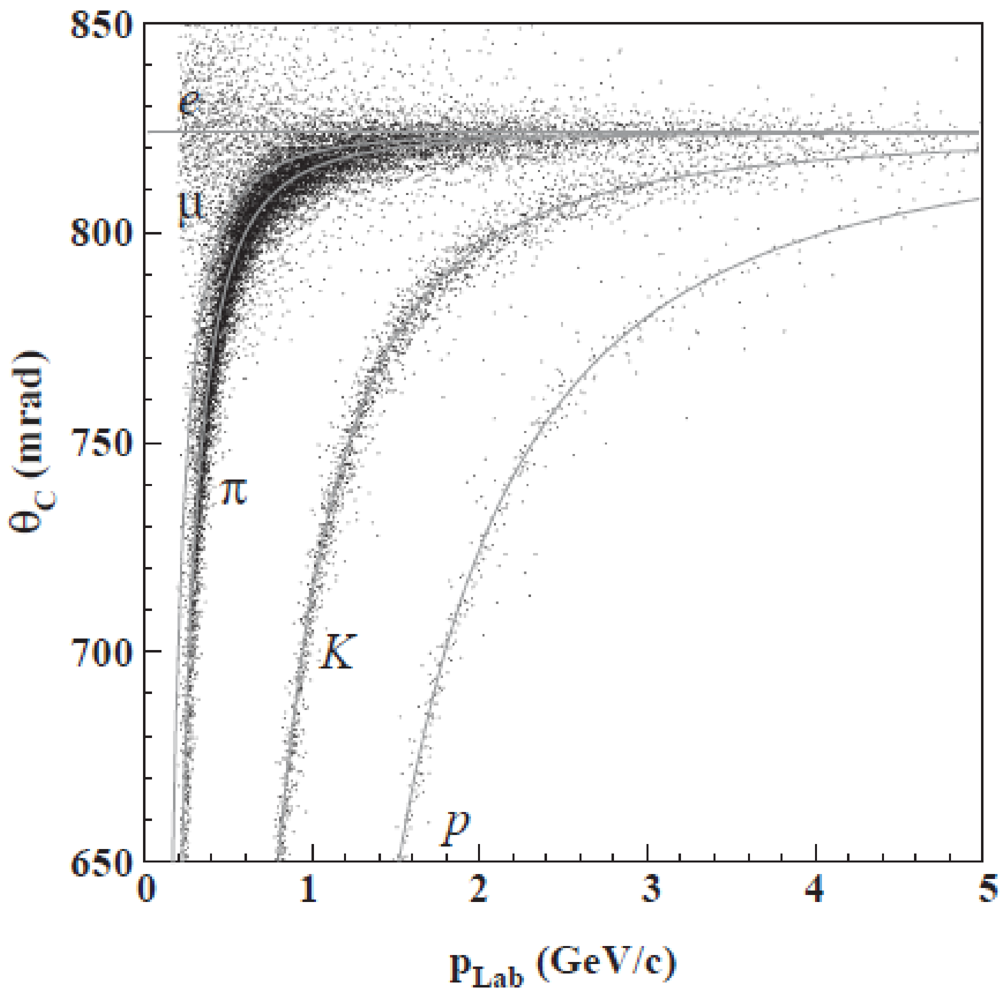

Excellent π/K separation

NIM A538 (2005) 281, NIM A553 (2005) 317

FDIRC design

Focusing DIRC (SuperB R&D)

• additional wedge and expansion volume with mirror made from quartz → smaller volume less sensitive to neutrons

• flat-panel PMT Hamamatsu H8500 for photon detection → better time resolution

Background suppression x25 (volume) x10 (timing).

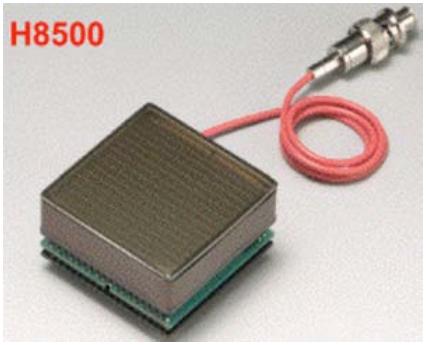

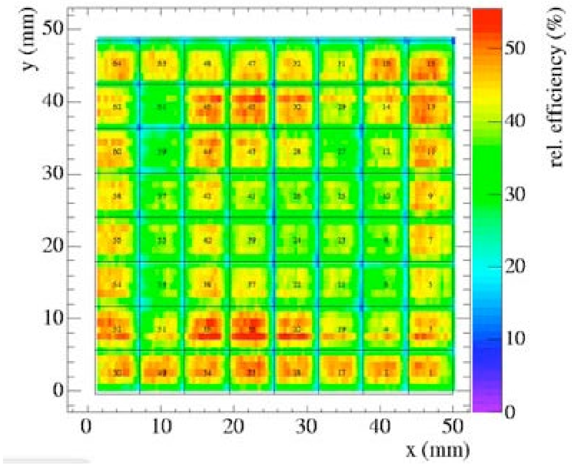

Ray tracing:

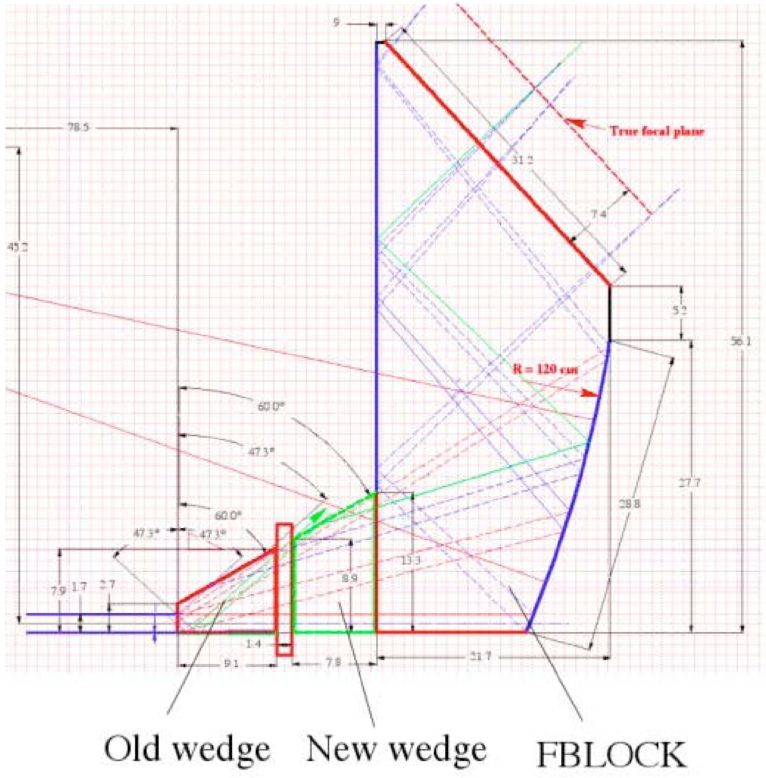

Geant 4 model:

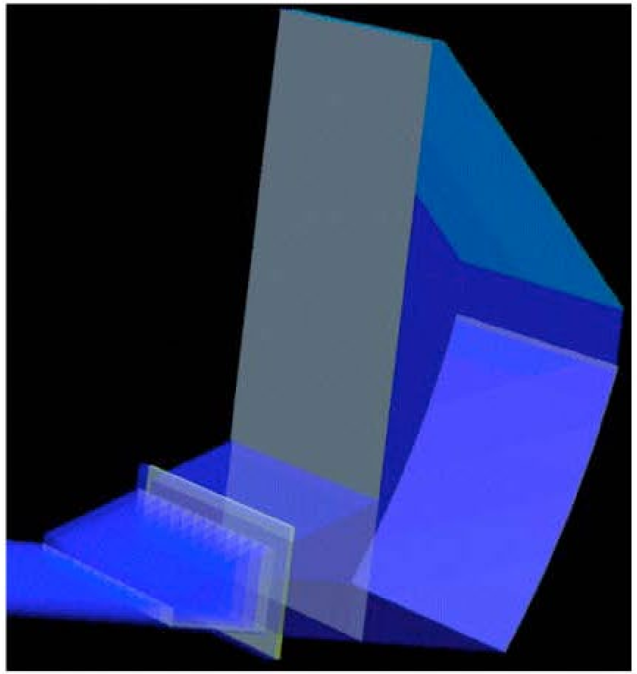

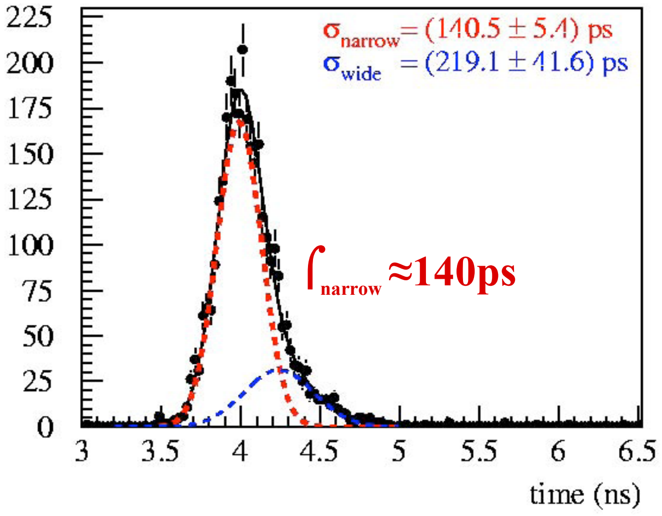

SLAC-PUB-13464, 2008

FDIRC chromatic error correction

- correlation between the propagation time (L/c_g) and Cherenkov angle ($cos\vartheta_c = c/vn$) is used to improve the angular resolution

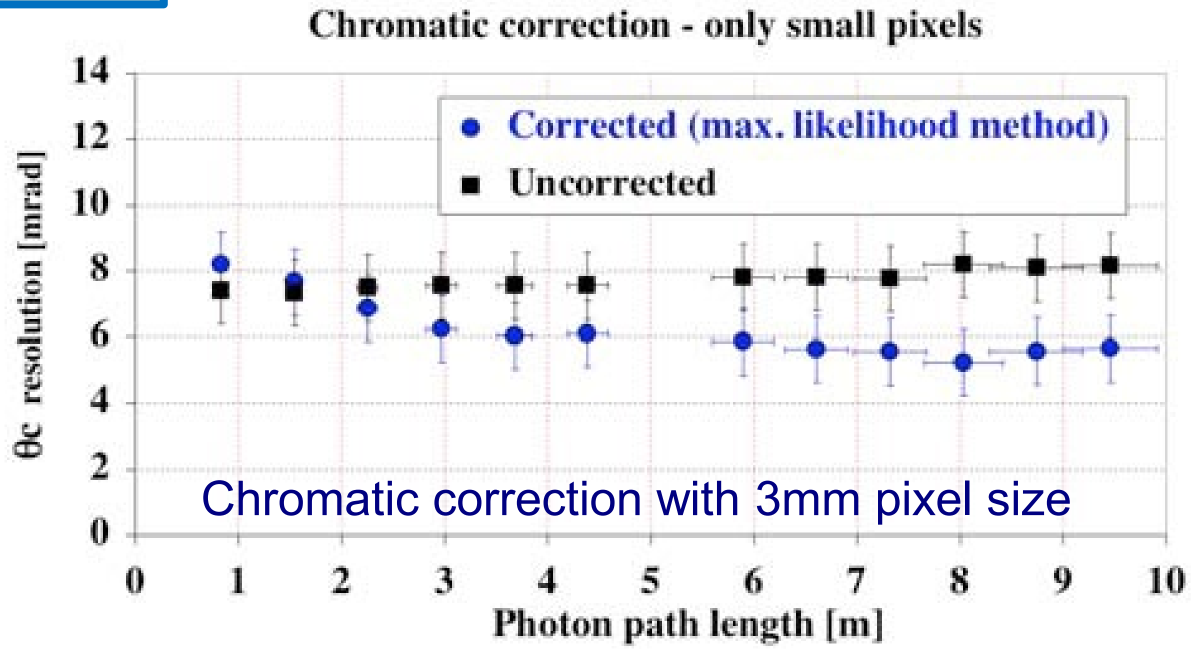

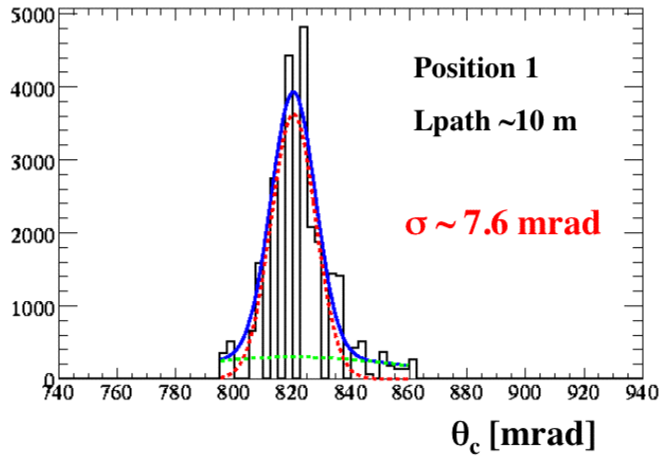

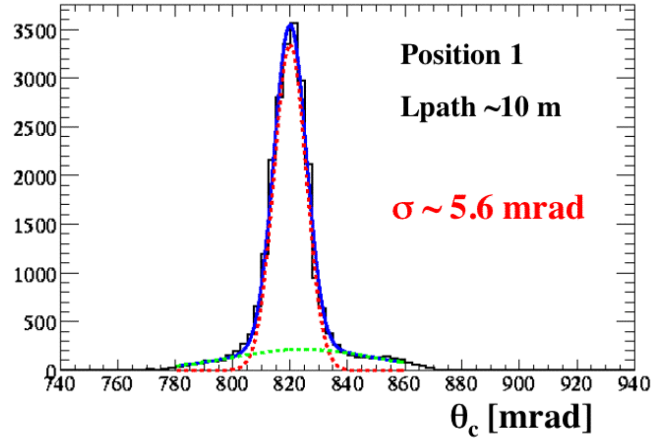

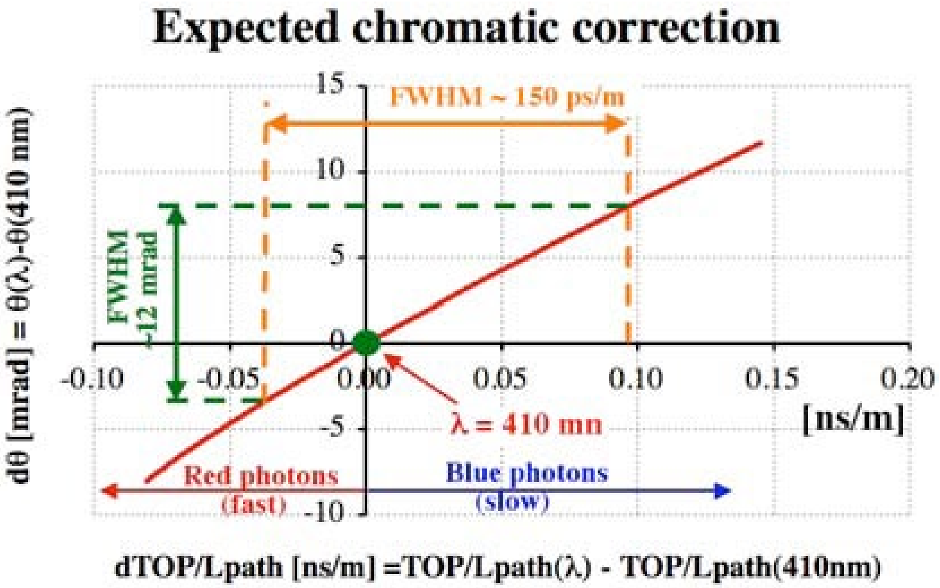

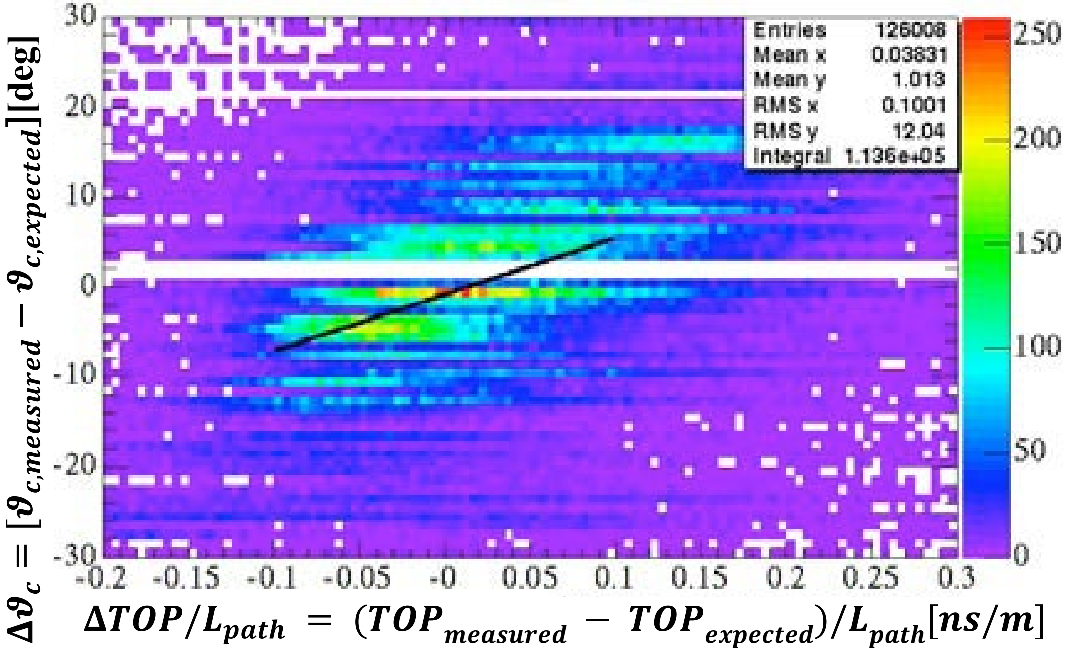

Phase vs group light speed – refractive index of quartz

- group velocity is lower than phase velocity
- variation of group refractive index $n_g(\lambda)$ is larger than variation of phase refractive index $n(\lambda)$

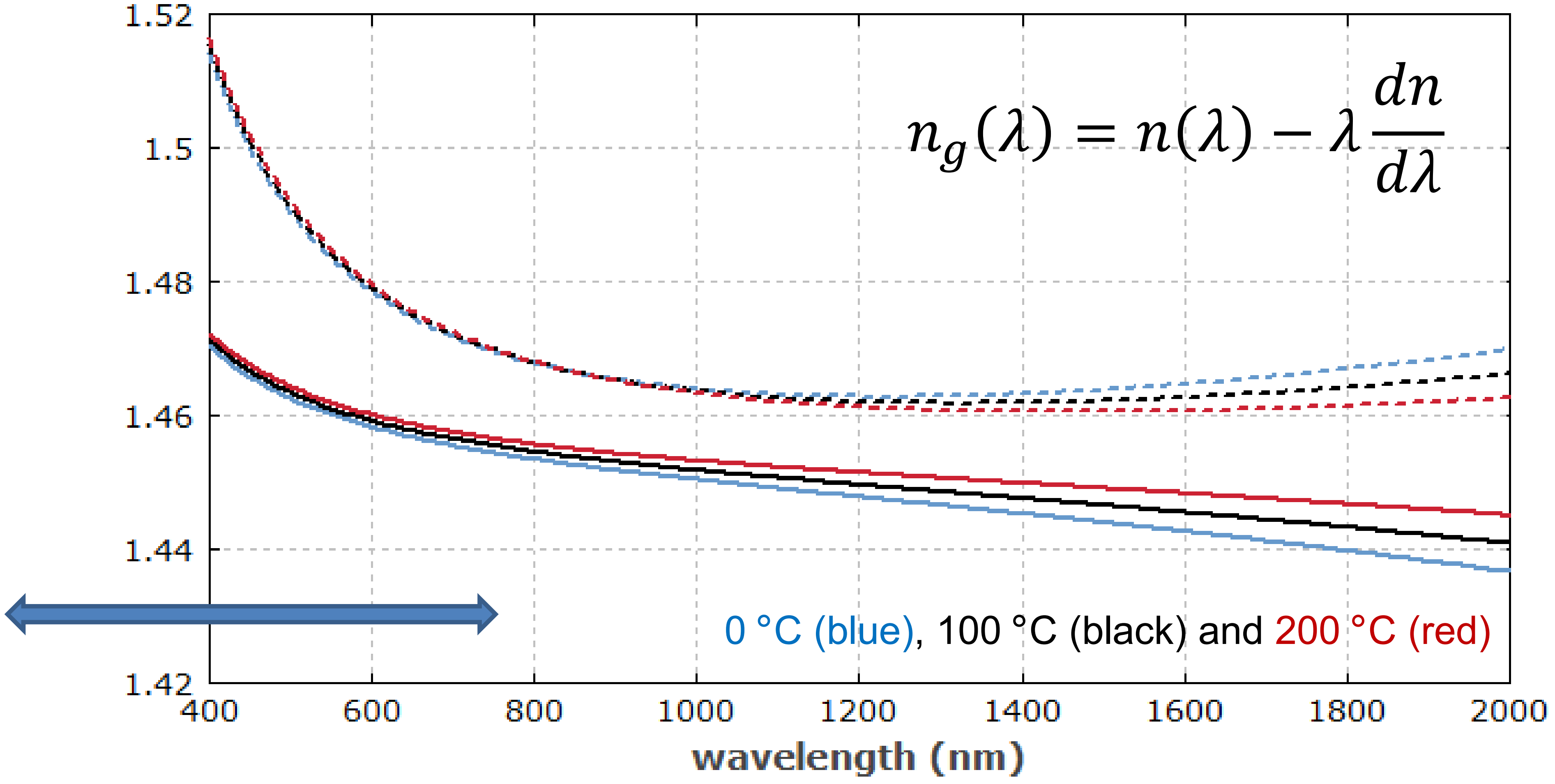

https://www.rp-photonics.com/group_index.html

TOP principle

Based on a DIRC concept:

- instead of 2D imaging → 1D + Time Of Propagation (TOP, path length)

→ **compact detector**

Linear array PMT (~5mm)
Time resolution σ ~40ps

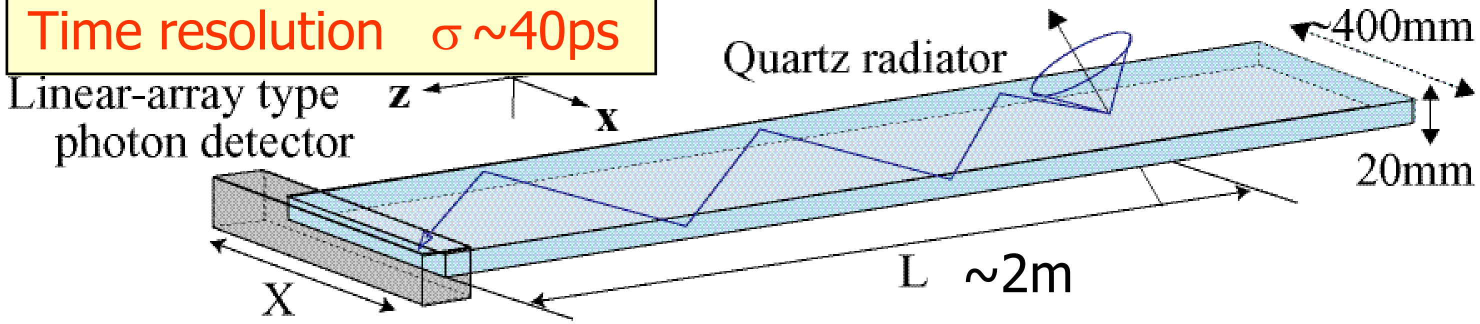

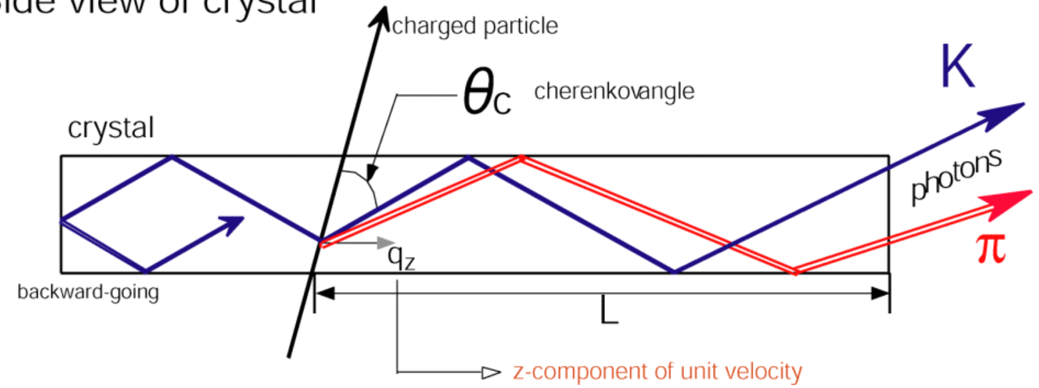

$$cos\vartheta_C = \frac{1}{\beta\, n(\lambda)}$$

$$t_{TOP} = \frac{l}{c_g(\lambda)} = \frac{l\, n_g(\lambda)}{c_0}$$

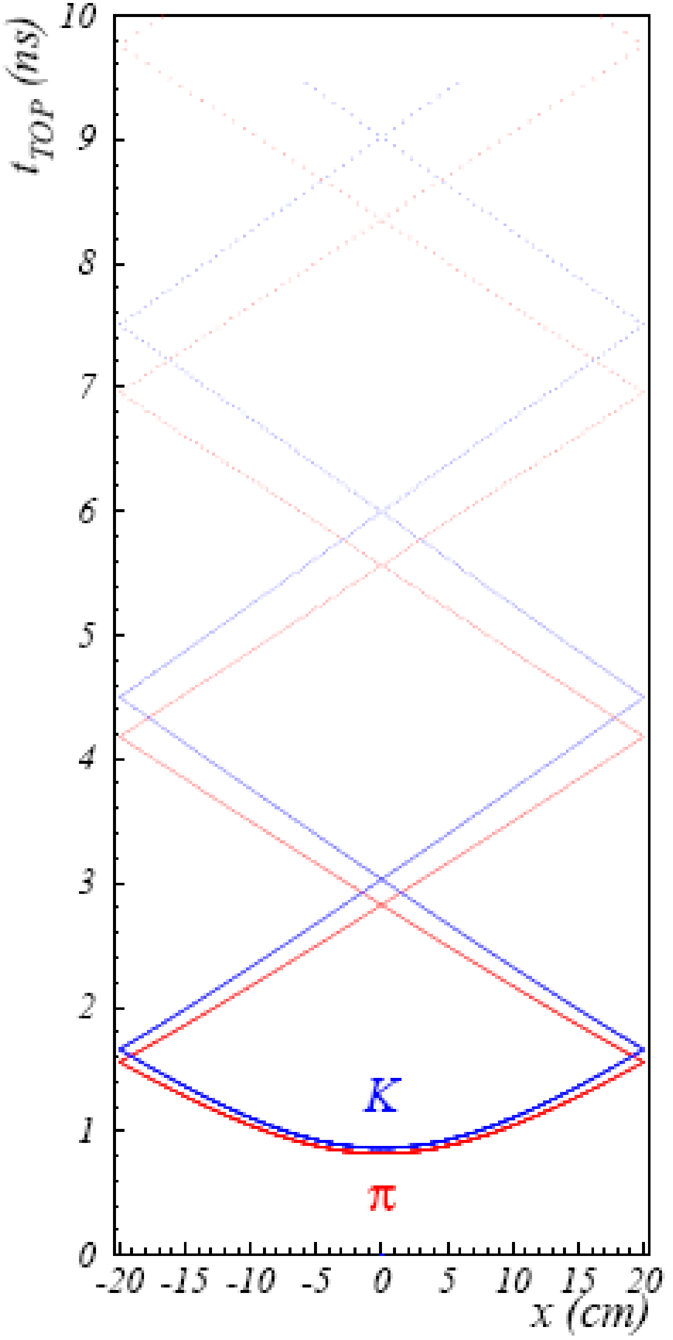

- measured time relative to bunch crossing is a combination of photon propagation time and time of flight from the interaction point to the quartz bar

Belle II TDR

Focusing TOP

Focusing TOP concept:

- focusing added for photons reflected from non instrumented side of the bar
- by focusing photons of different wavelength, that are emitted at different Cherenkov angles, are separated at the focal plane -> reduced error due to chromatic dispersion

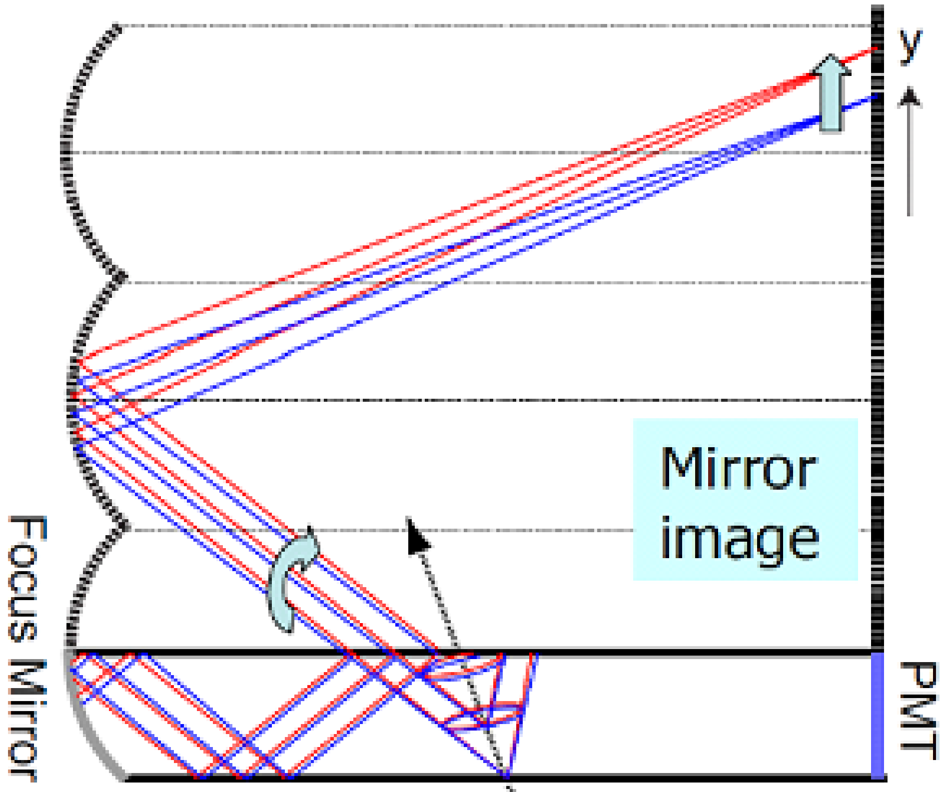

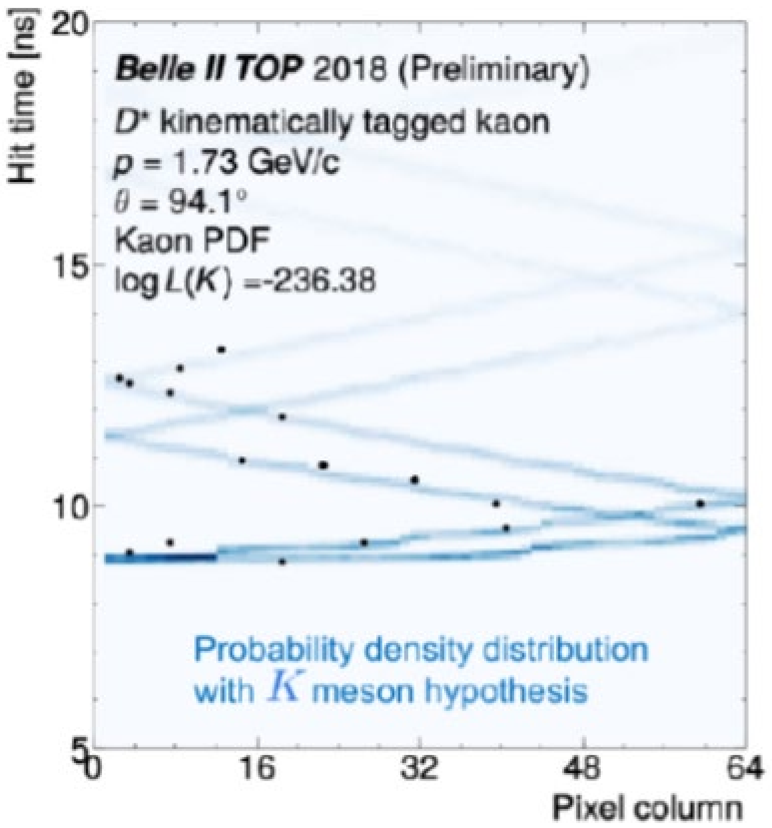

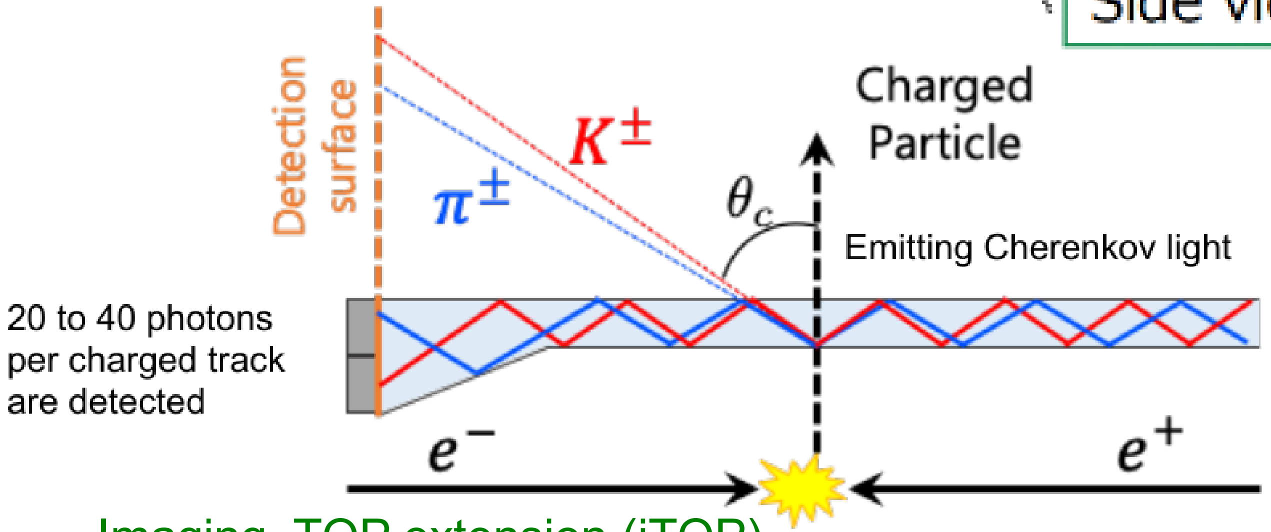

Imaging TOP extension (iTOP)

TOP radiator

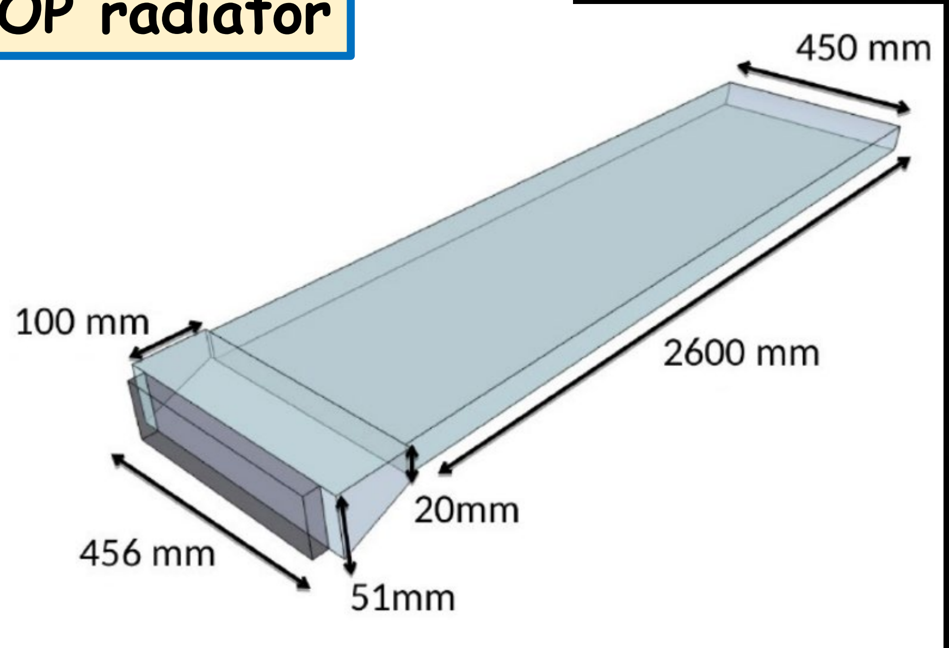

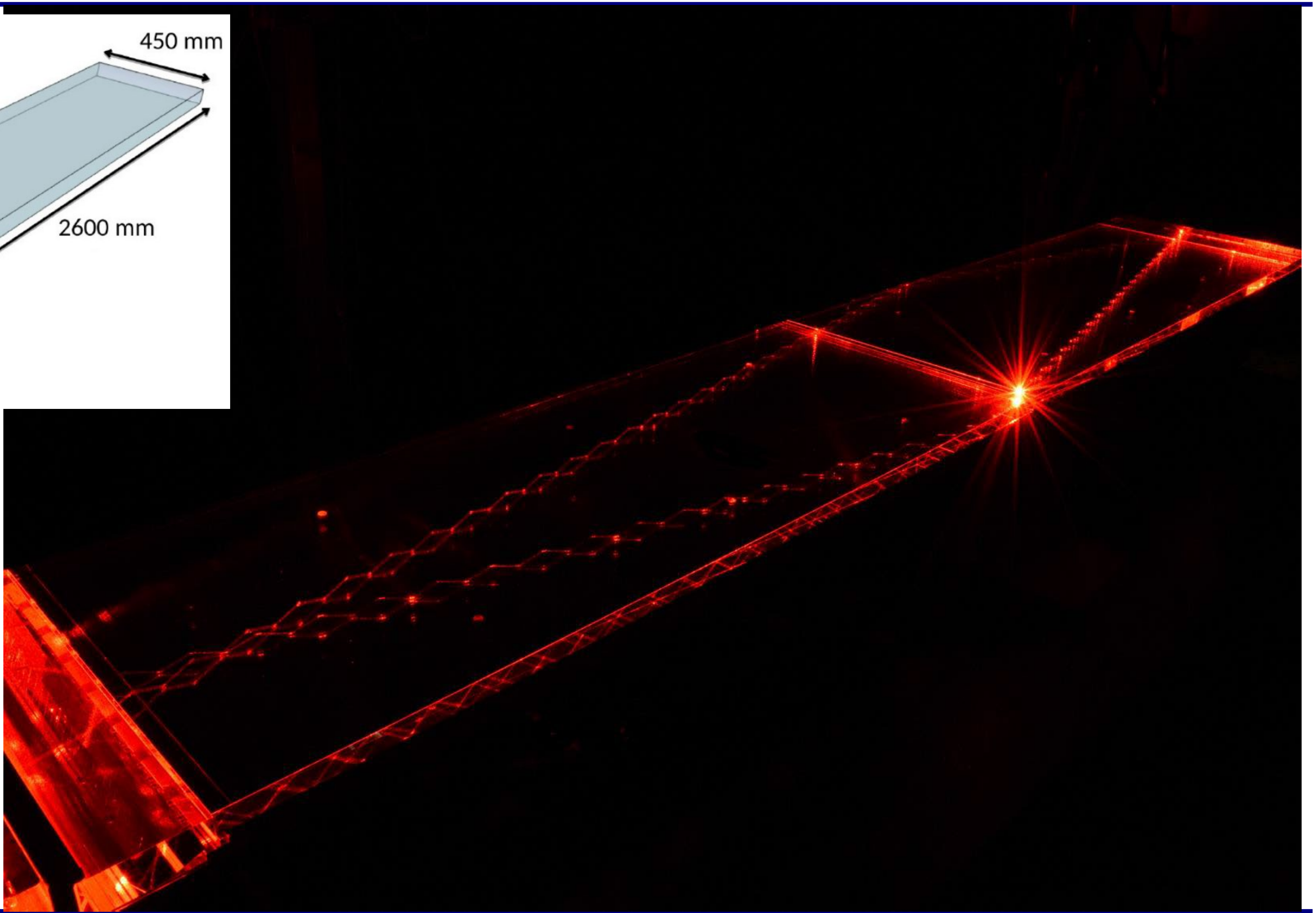

Fast photon detection: MCP-PMT (Hamamatsu SL10)

Multiandode MCP-PMT was developed in cooperation with Hamamatsu:

- bi-alkali photocathode
- gain ~1.5x10^6 @ 1.5 T
- single photon time resolution ~35ps @ 1.5T
- pad size ~5mm x 5mm (4x4 array)
- additional cut-off filter 320 nm

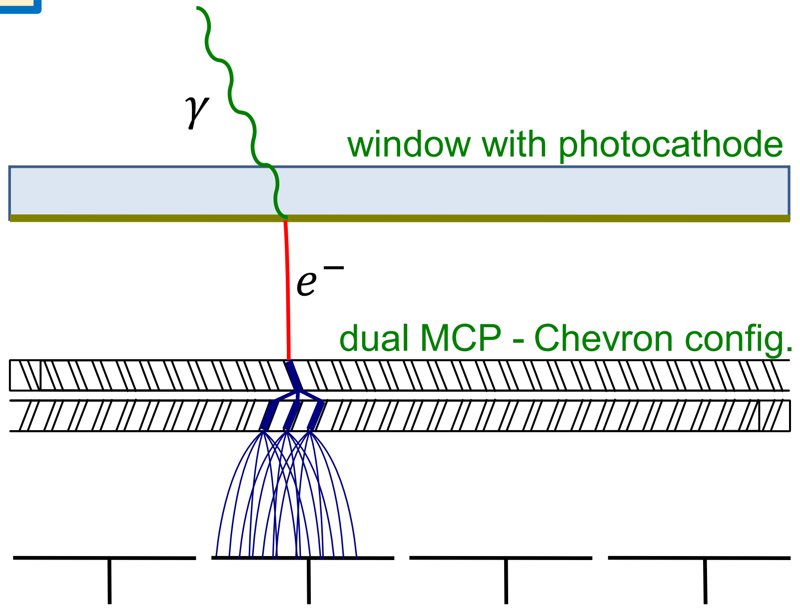

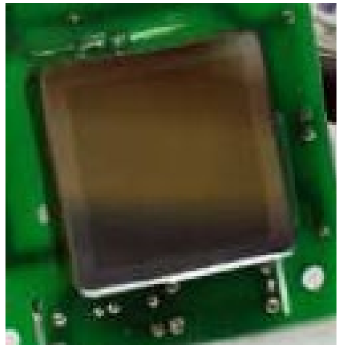

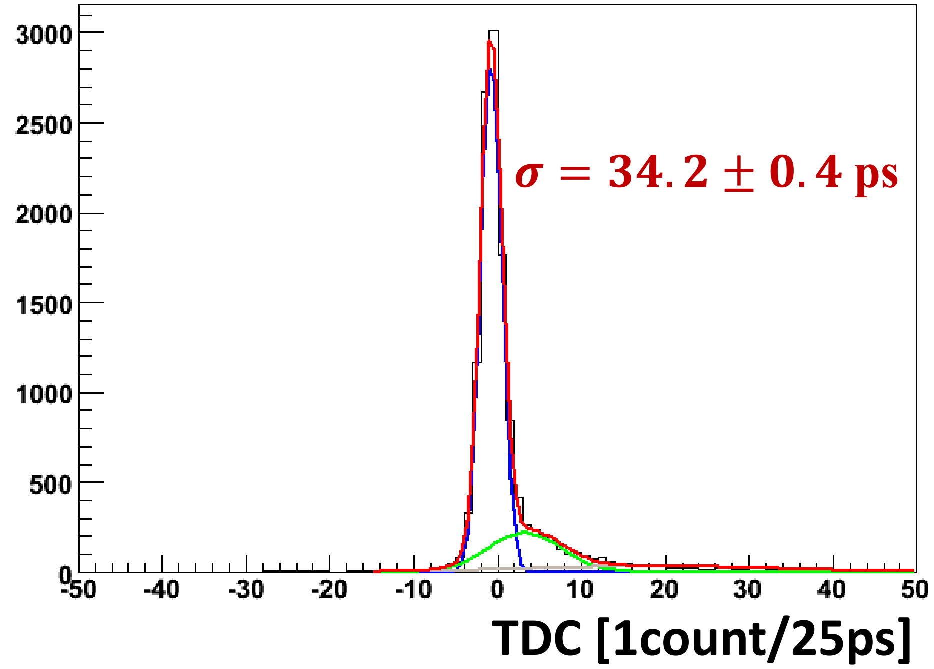

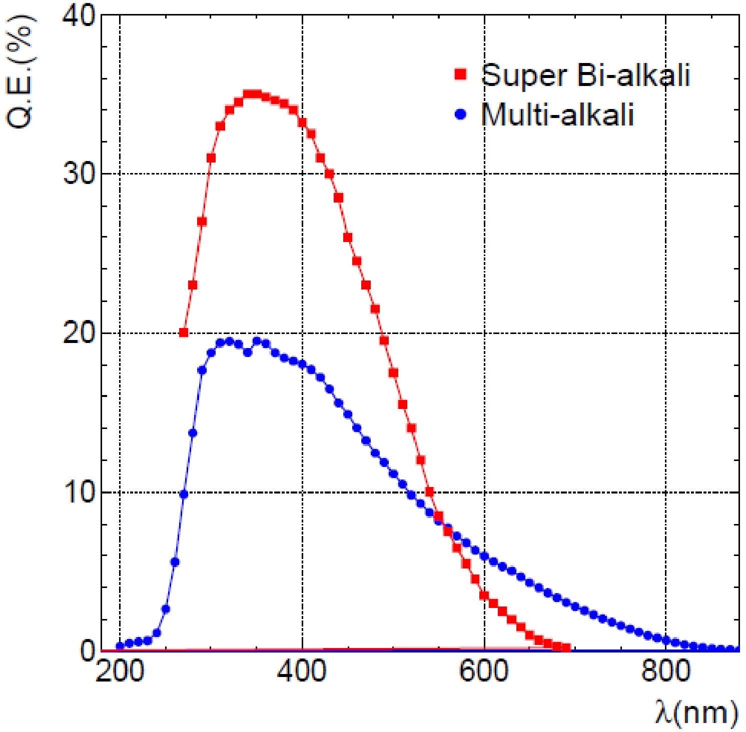

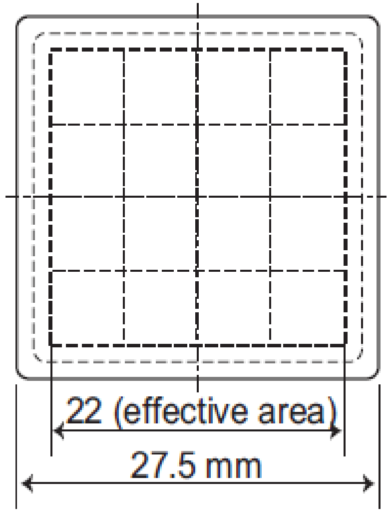

TOP – event example

- hit distribution for kinematically tagged kaon from $\mathrm{D}^{*+} \rightarrow D^0(\rightarrow K^-\pi^+)\pi^+_{slow}$ decay compared with PDFs for three different hypothesis: π, K, p ,
- hit distribution compatible with K hypothesis (highest logL)

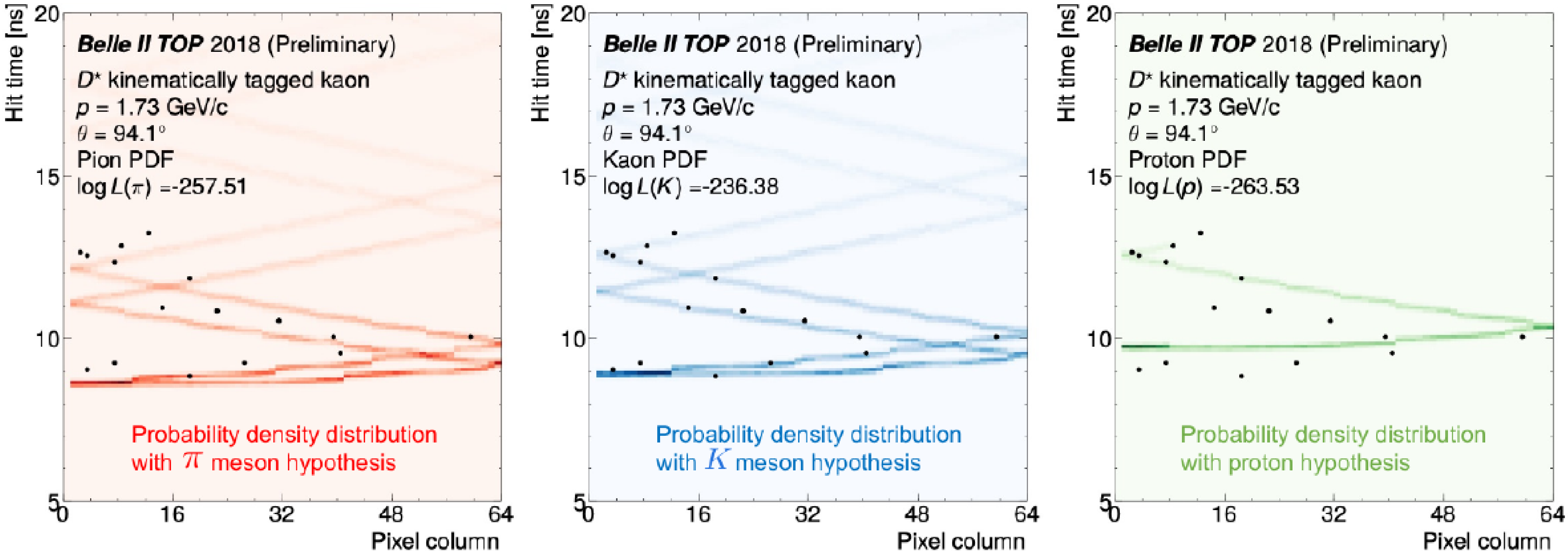

TOP – PID performance: $D^{*+} \to D^0 (\to K^- \pi^+)\pi^+$

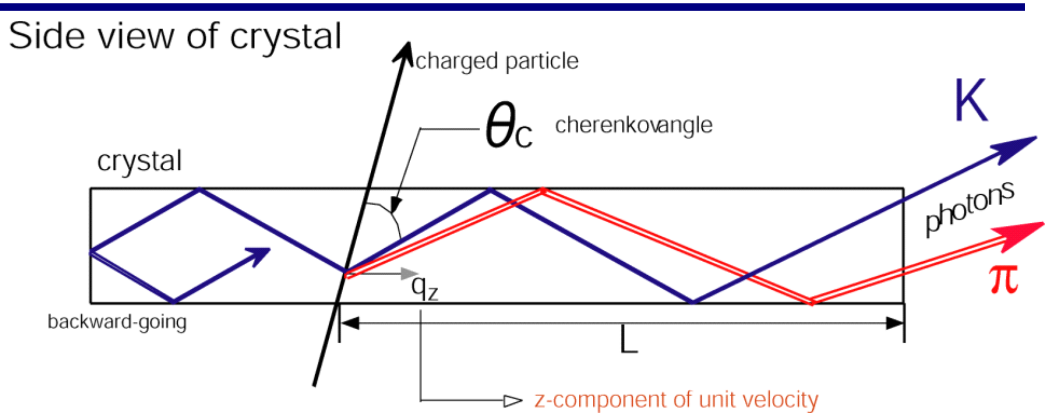

- preliminary TOP PID performance – K efficiency vs. π misidentification probability

$\mathcal{L}_K > \mathcal{L}_\pi$

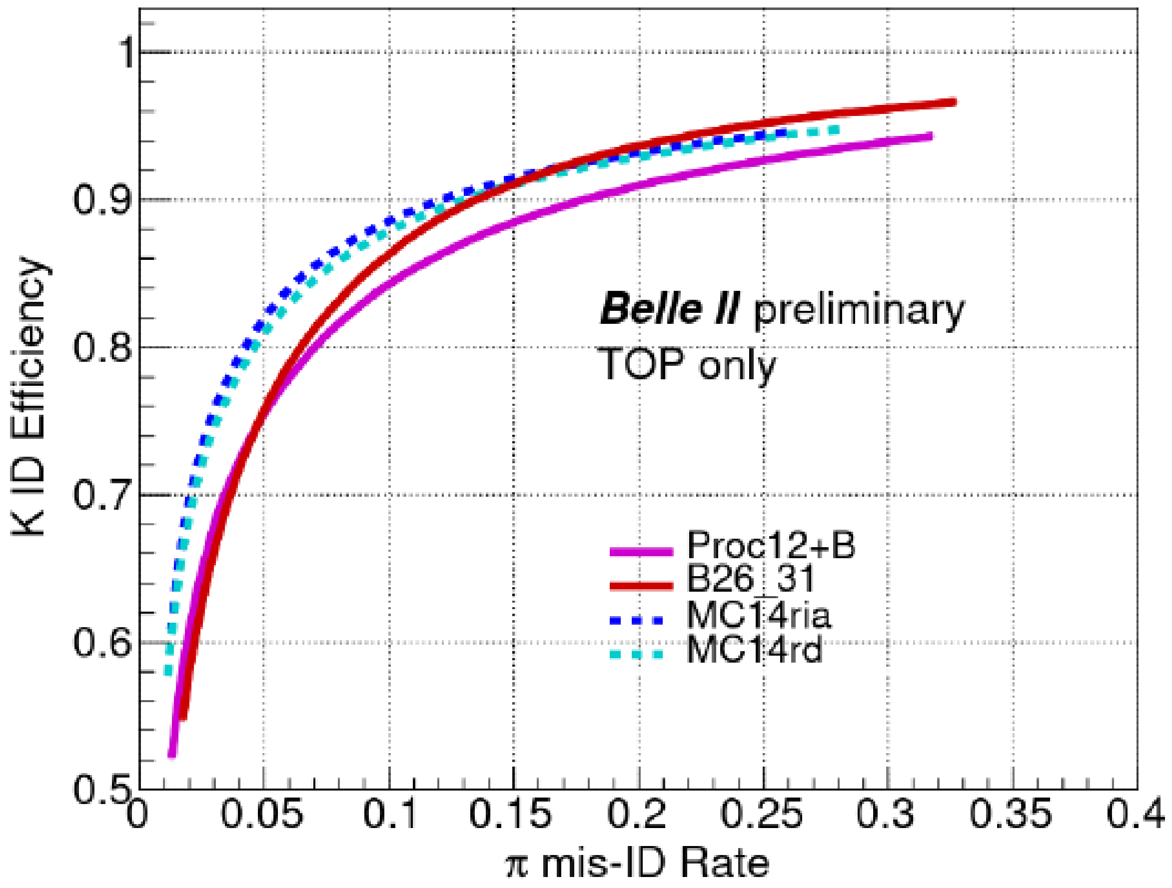

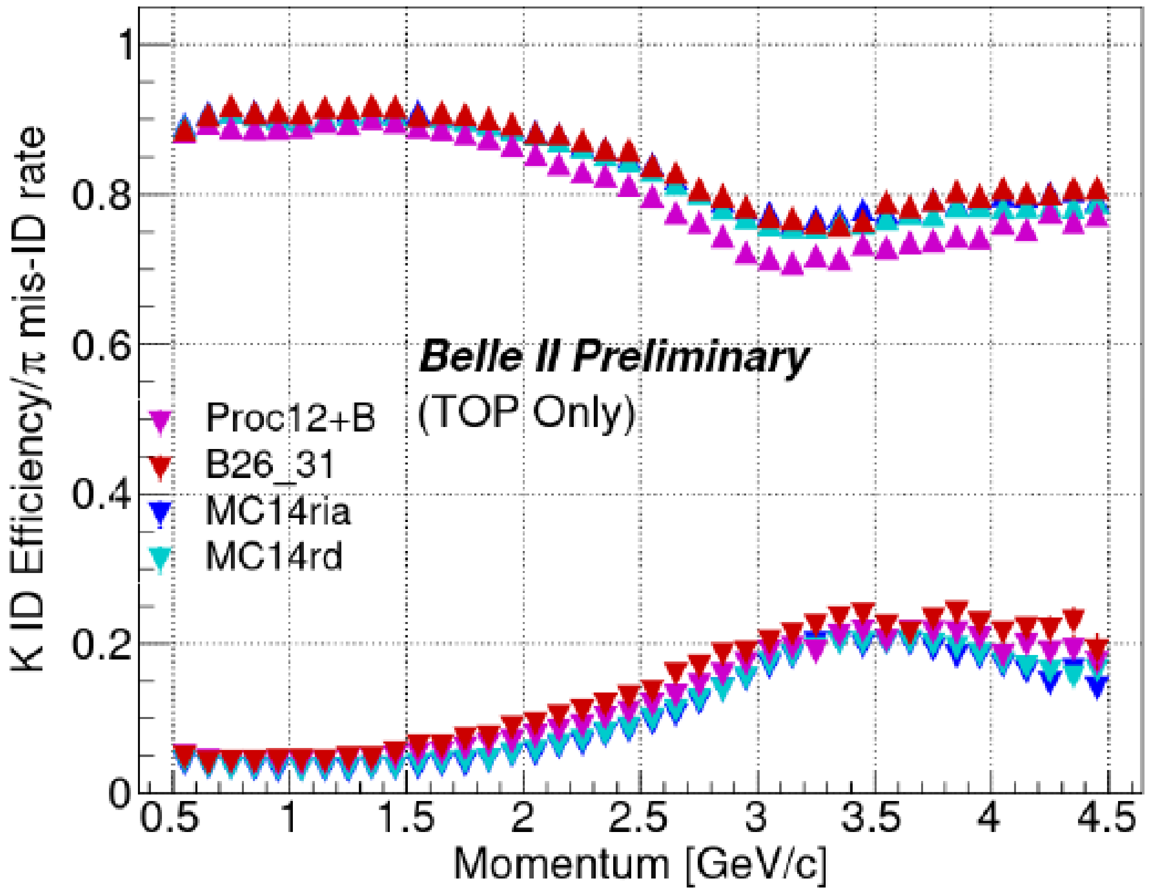

TORCH: TOP like TOF disc detector

- **TORCH** for LHCb PID upgrade
- TOF based on internally reflected Cherenkov light
- low momentum PID (< 10 GeV)
- in front of RICH2

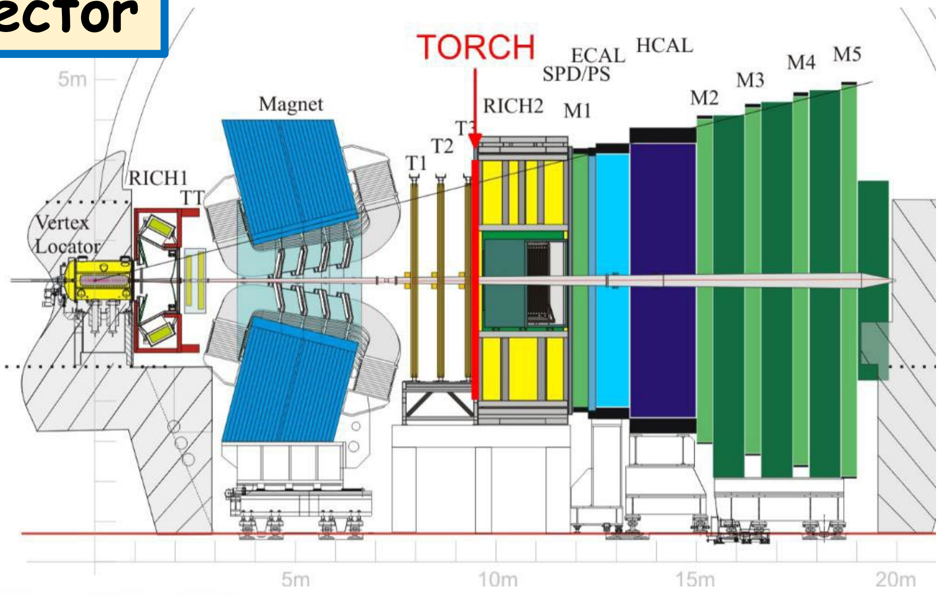

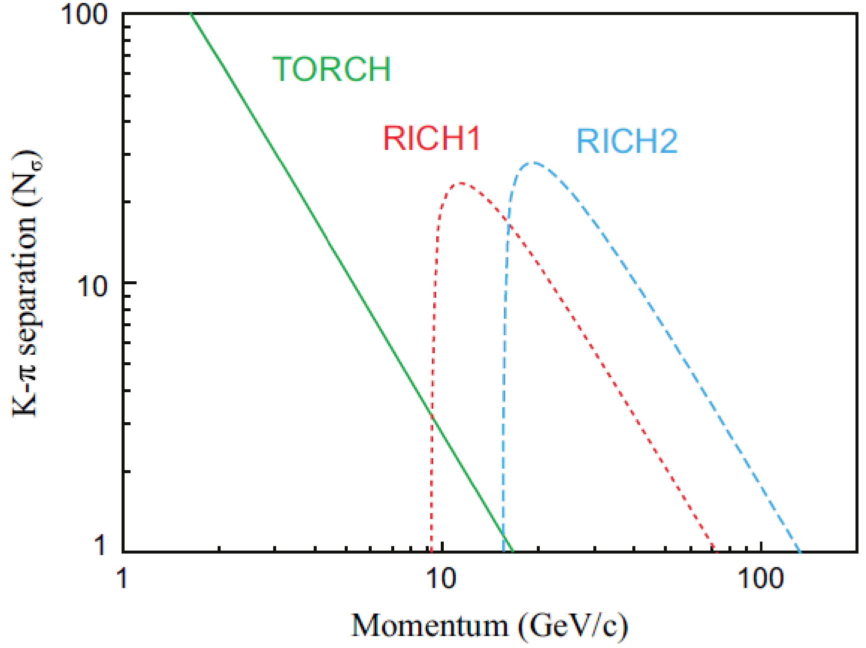

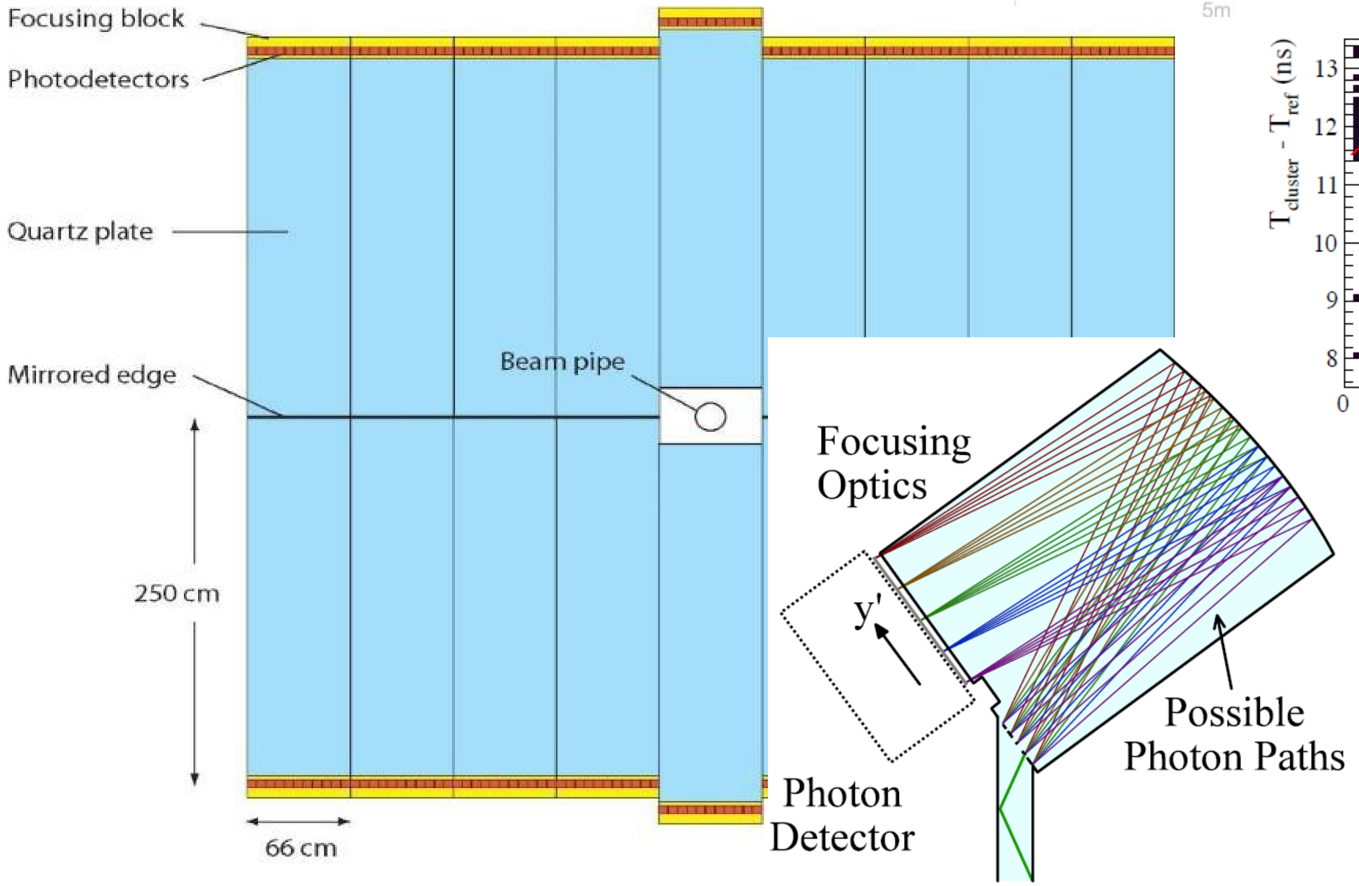

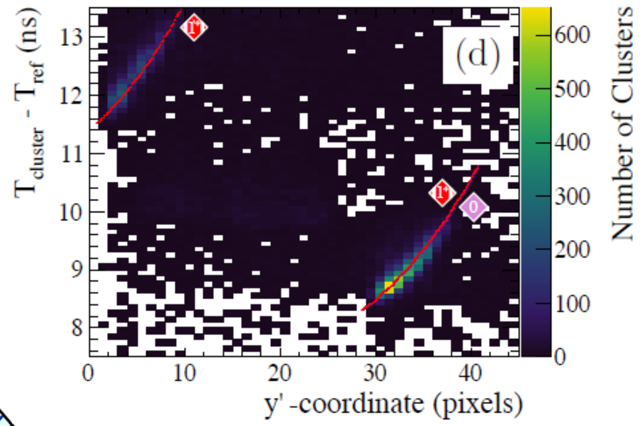

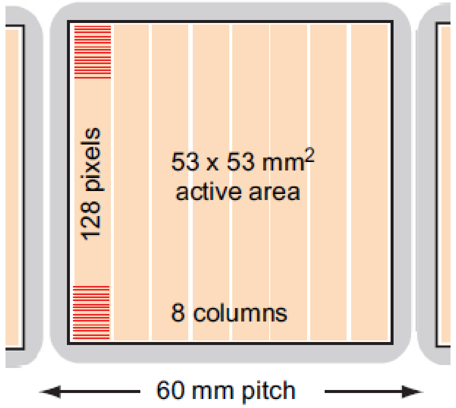

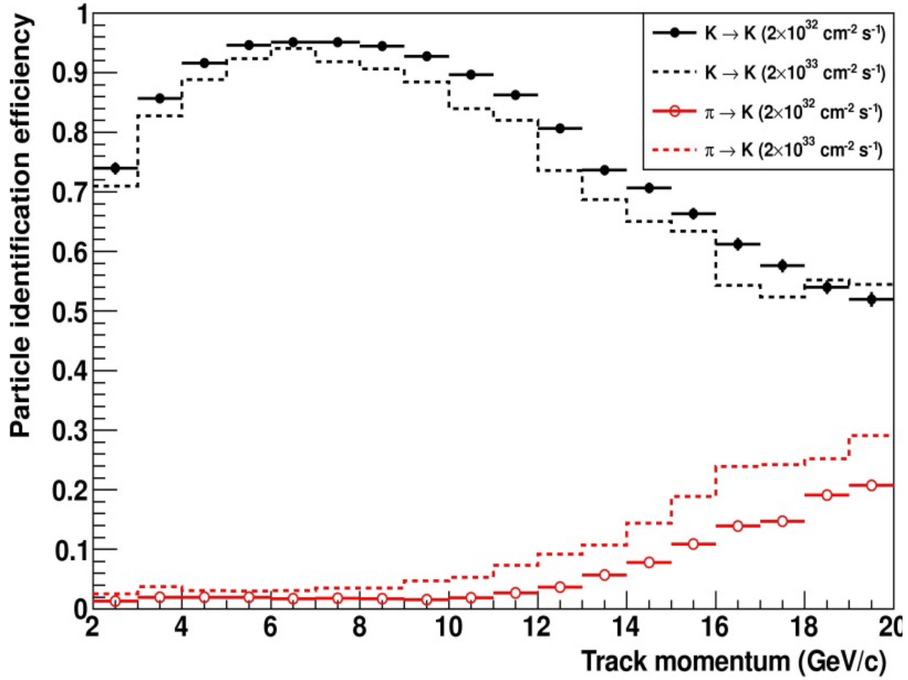

ICFA 2023 ARICH detector

- trigger: 2 cm plastic scintillator

- ARICH
- focusing radiator - two layers of 2 cm thick aerogels :
  - upstream, $n \approx 1.048$, $\lambda_{400\,nm} \approx 44$ mm
  - downstream, $n = 1.062$, $\lambda_{400nm} \approx 55$ mm

- photon detector:
  - 6x6 array of Ma-PMTS (HERA-B) at 30 mm pitch – 576 channels
  - readout electronics – Belle 2 ARICH FE boards

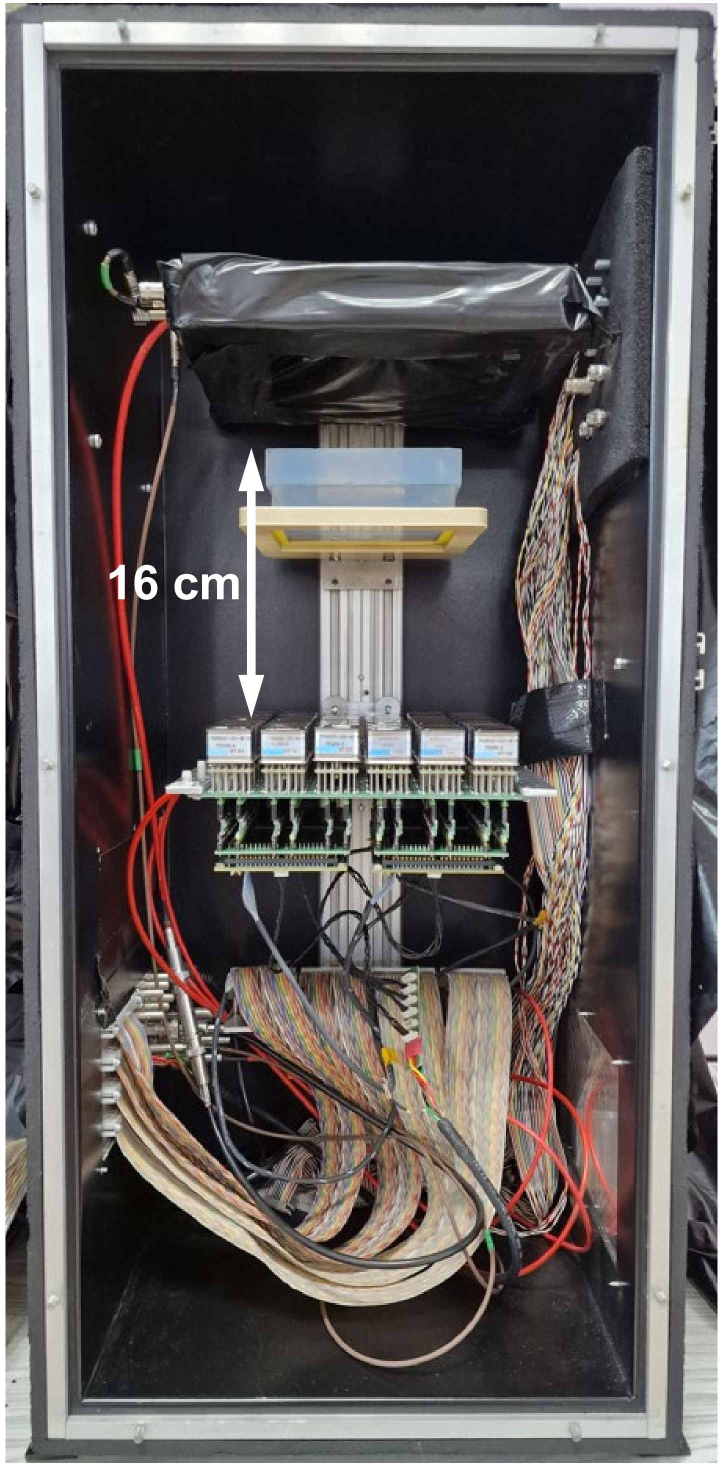

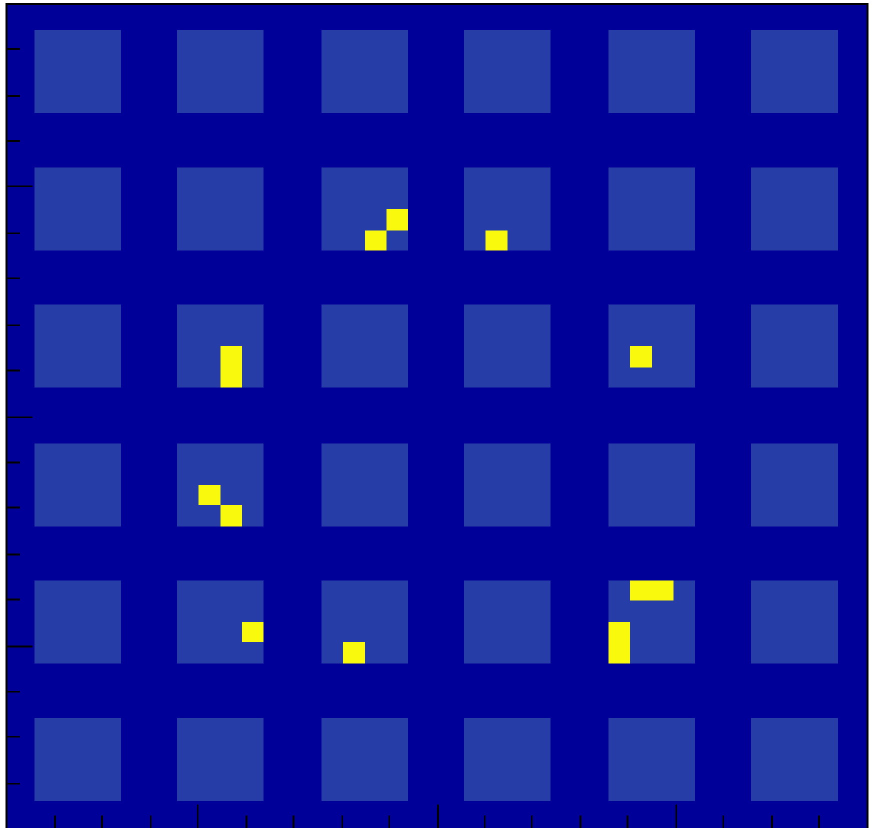

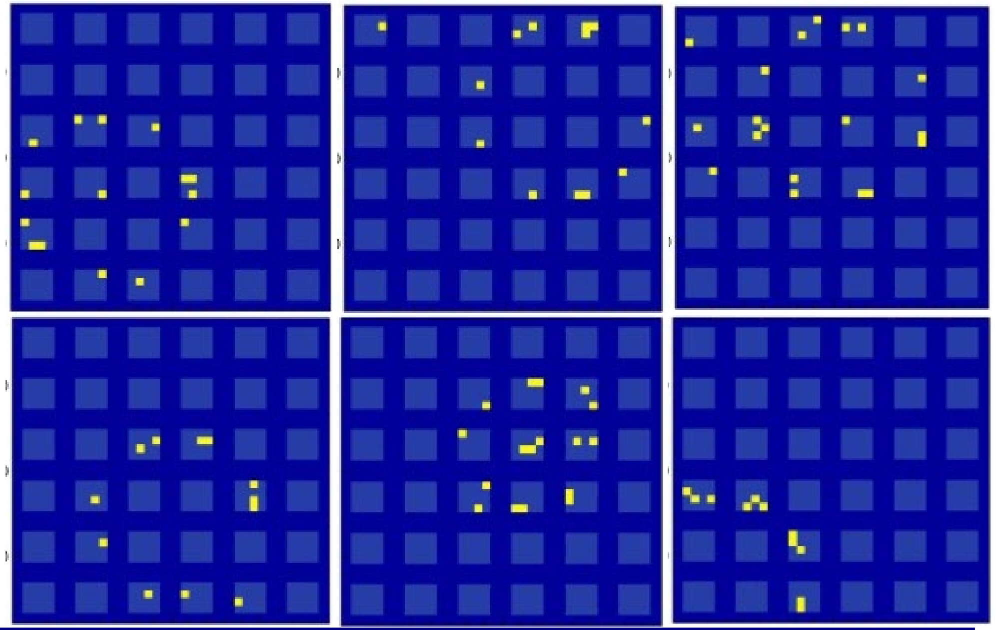

BACKUP SLIDES

Mesh PMT

Coarse mesh or fine mesh types:

- multiplication is confined in space
  - → cross-wire readout
  - → multi-anode designs
- high gain up to 10^7
- good linearity
- operation in relatively high magnetic field
  - → maximum gain at 30^o between the magnetic field and PMT axes

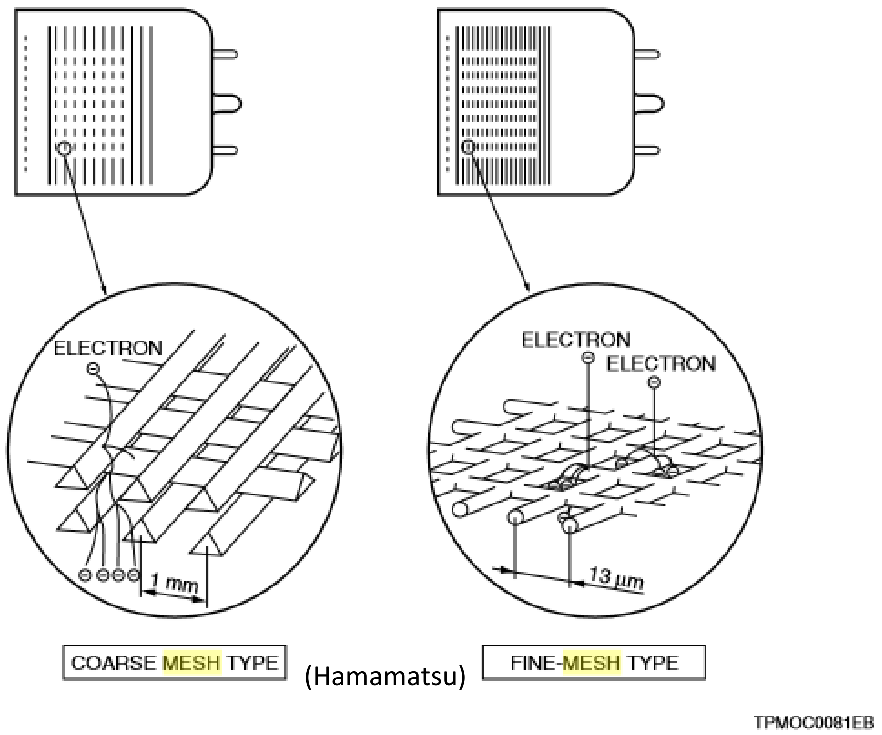

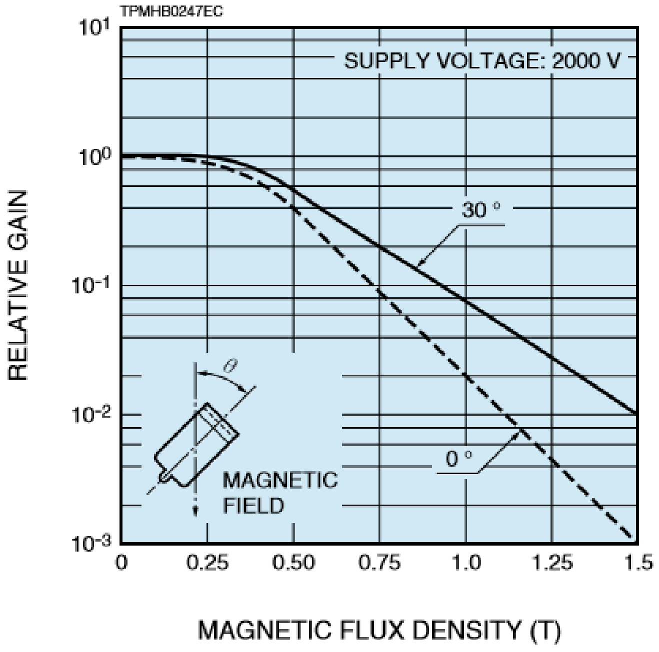

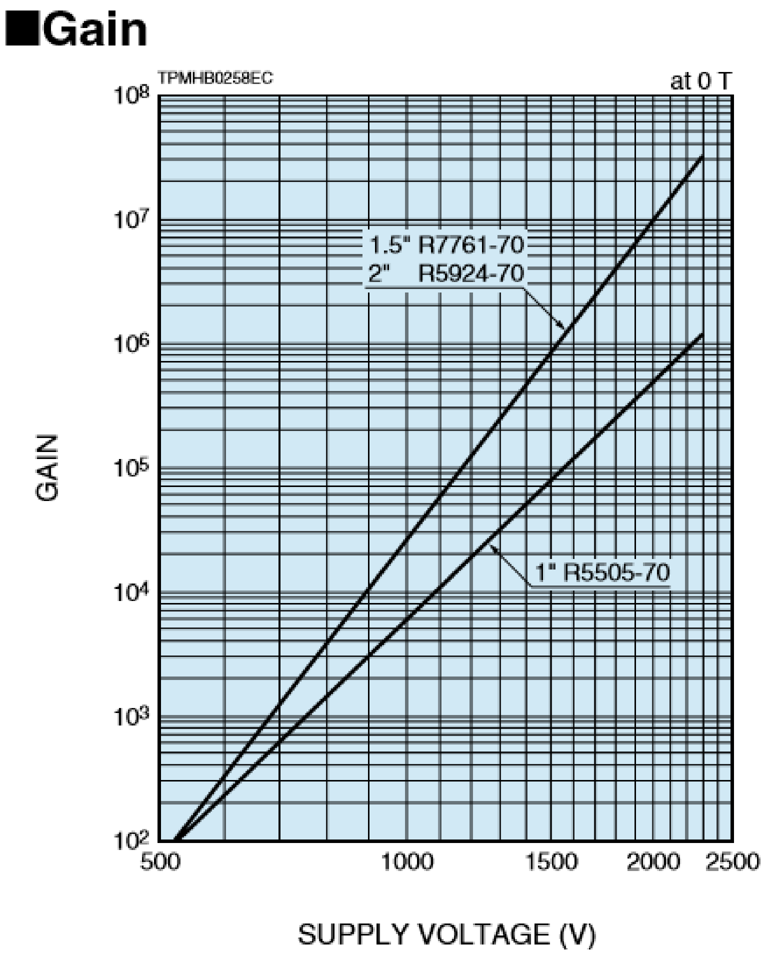

Gaseous photodetectors

Different ways to achieve photo-sensitivity:

- addition of photosensitive molecules to the counter gas (TMAE, TEA)
- solid photocathode deposited on the cathode (CsI)
- semitransparent cathode on the window (bialkali)

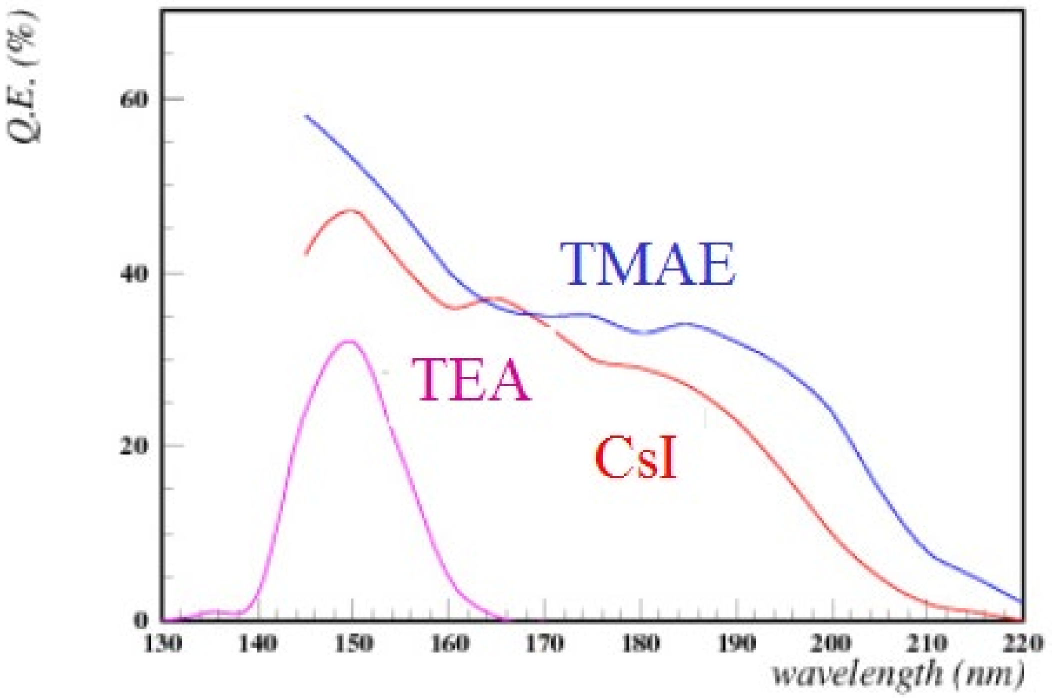

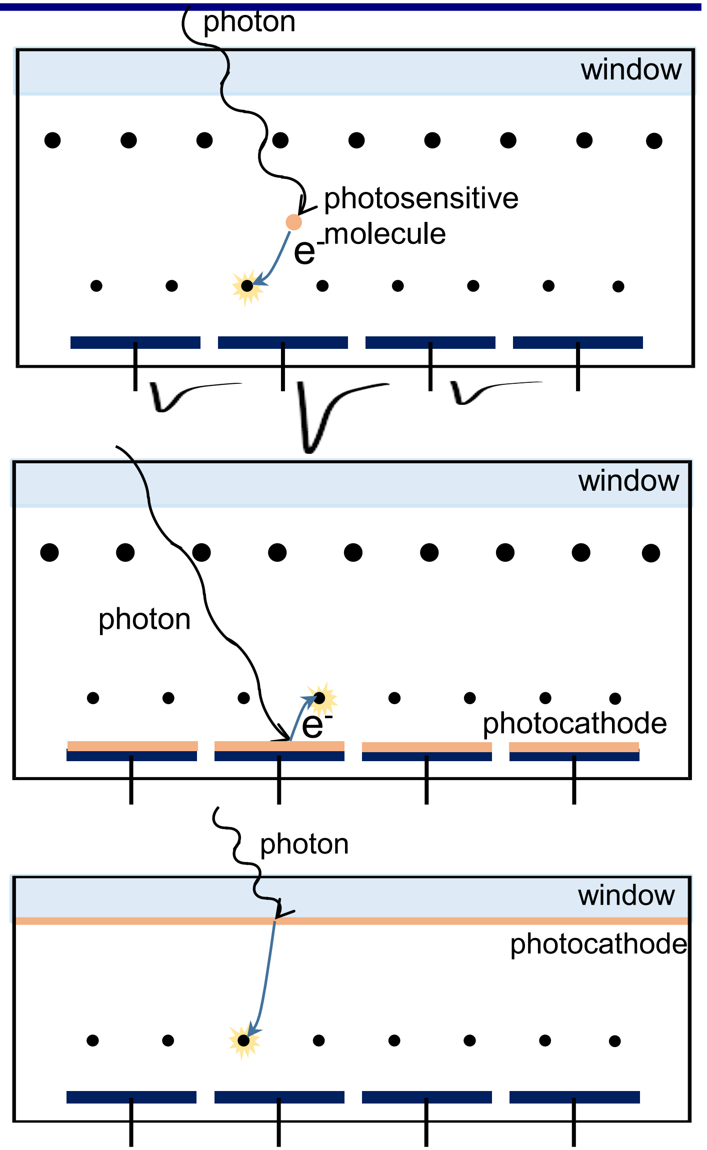

Released photoelectron drifts toward the high field region and produces the avalanche → multiplication → detectable signal

- TMAE, TEA, CsI sensitive in deep UV
- bialkali sensitive also in visible but requires very clean gas – long term operation not yet demonstrated

Difficulties:

- High gain operation (ion feedback and light emission from avalanche)
- Gas purity → UV transparency
- Aging (ion backflow, impurities)

Photosensitivity in gaseous detectors

Gaseous detectors (MWPCs, TPCs) use admixtures of photosensitive substances or solid CsI photocathode to gain photo-sensitivity in UV region.

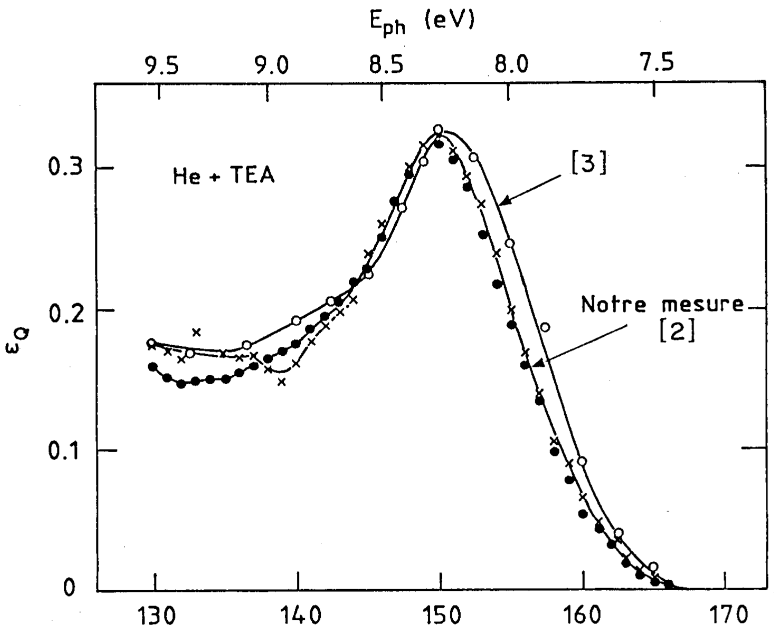

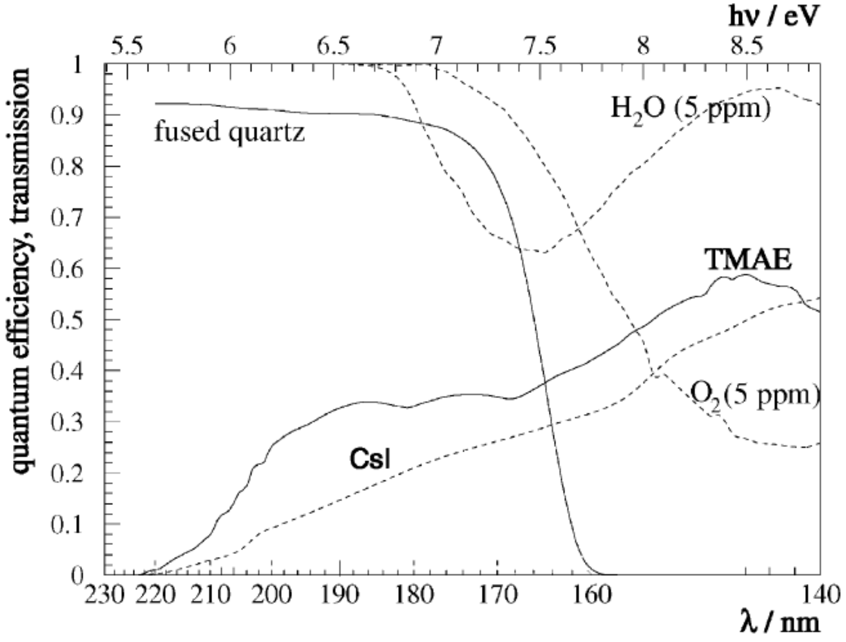

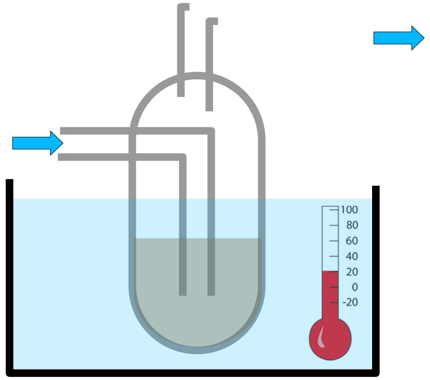

molecule	E_I [eV] (I_I [nm])	max. QE(E)	$l_{abs@293K}$ [mm]
TEA $(C_2H_5)_3N$	7.5 (164)	0.33 (8.2)	0.43
TMAE $C_2[(CH_3)_2N]_4$	5.36 (230)	0.51 (8.3)	26
DMA $(CH_3)_2NH$	8.3 (148)	0.2 (9.2)	
TMA $(CH_3)_3N$	7.9 (156)	0.27 (8.6)	

Photosensitive agent is admixed to the counting gas of a MWPC by bubbling the gas through the liquid agent at a given temperature → concentration control.

Photosensitive materials - photocathodes

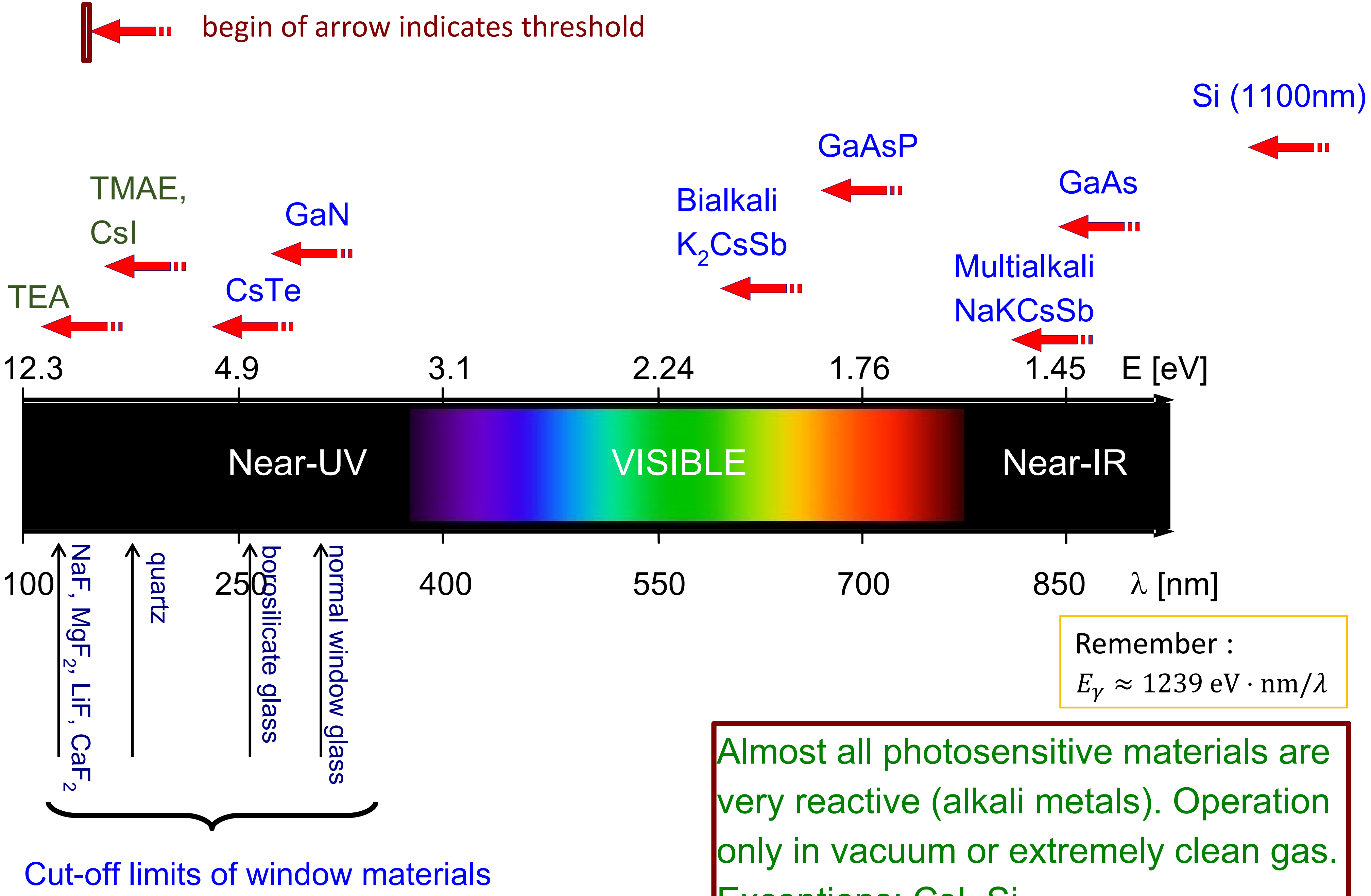

Remember :
$E_\gamma \approx 1239\ \mathrm{eV} \cdot \mathrm{nm}/\lambda$

Almost all photosensitive materials are very reactive (alkali metals). Operation only in vacuum or extremely clean gas. Exceptions: CsI, Si.

Transmission mode photo-cathodes

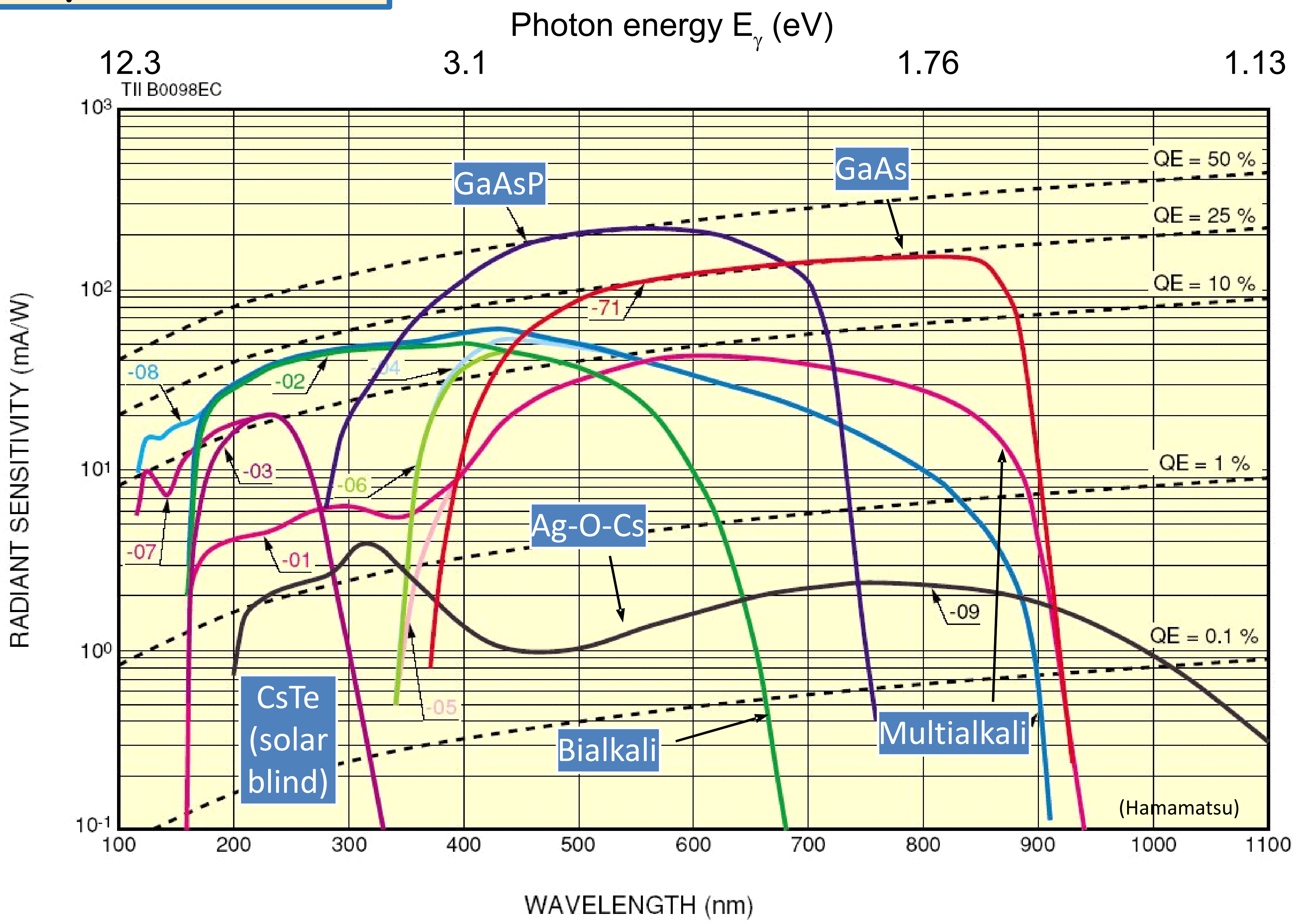

Bialkali: Sb-K-Cs, Sb-Rb-Cs, Na-K-Sb Multialkali: Sb-Na-K-Cs

Photo-multiplier tubes (PMT's)

Principle of operation:

- photo-emission from photo-cathode – QE
- collection of photoelectrons by 1st dynode - η_{col} (CE)
- Secondary emission (SE) from N dynodes:
  - dynode gain $\delta_i \sim 3 - 50$ (function off incoming electron energy);
  - total gain M:

$$\mathrm{M} = \delta_1 \cdot \delta_2 \cdots \delta_N = \prod_{\mathrm{i}=1}^{\mathrm{N}} \delta_{\mathrm{i}}$$

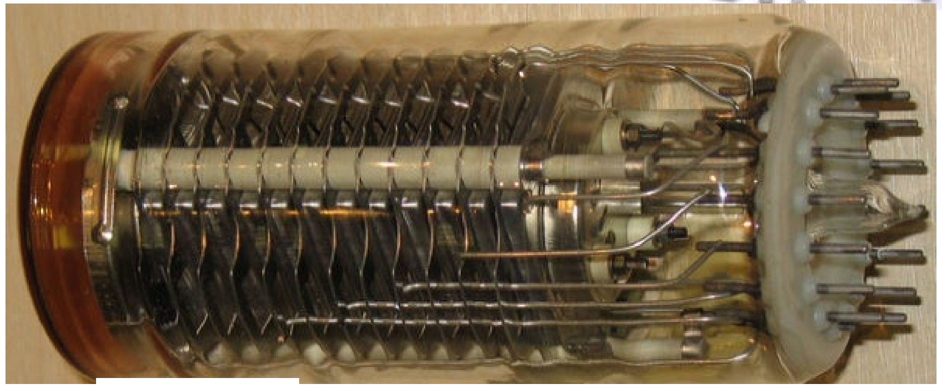

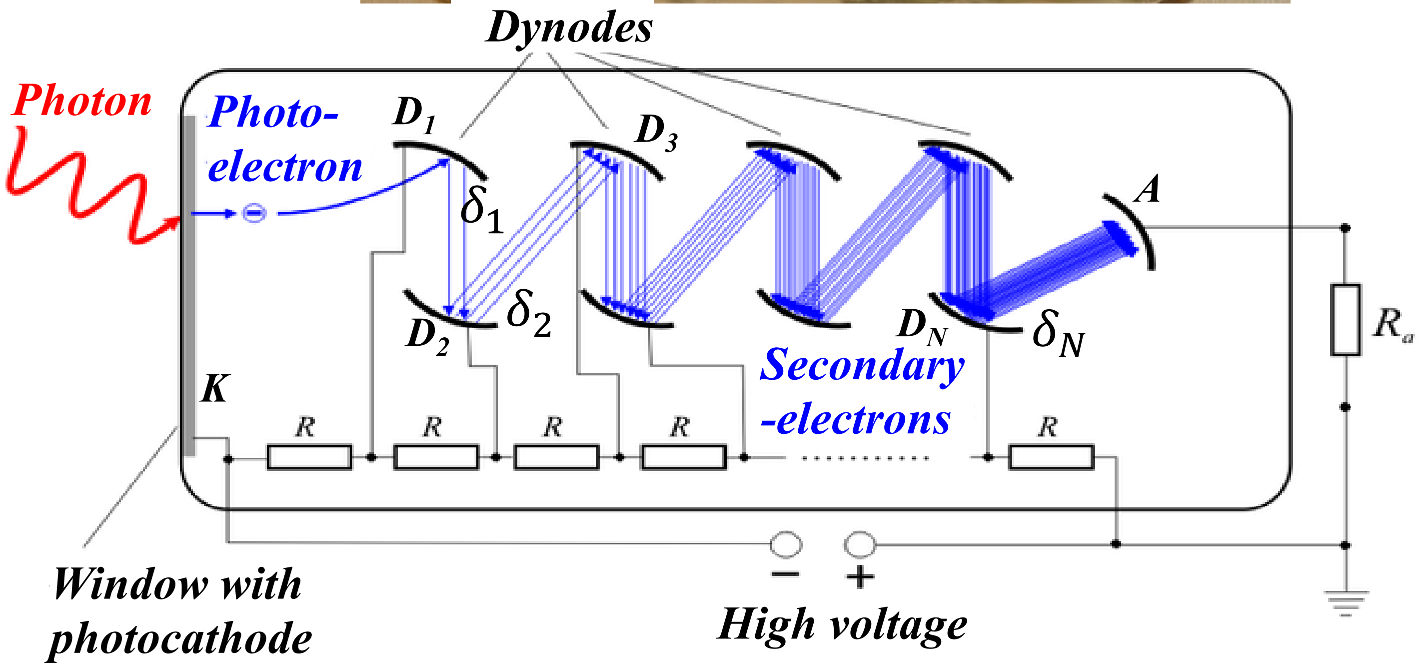

- Example:
  - 10 dynodes with
    - $\delta = 4$
    - $M = \delta^N = 4^{10} \approx 10^6$

Multi-anode PMT (MA-PMT)

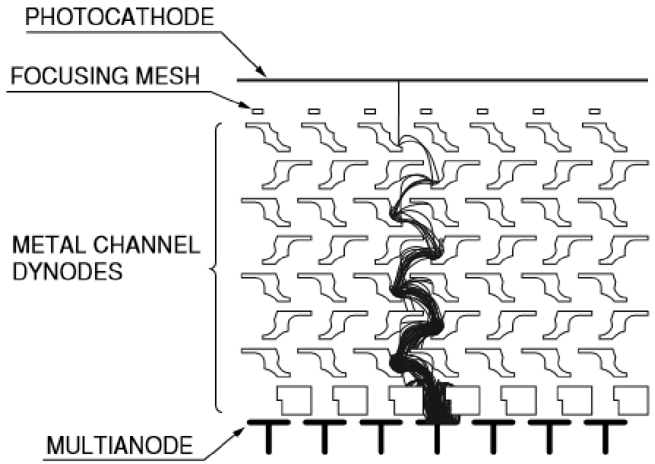

Metal channel dynode (Hamamatsu):

- multiplication is confined in a narrow channel
  → multi-anode designs
  → some tolerance to modest magnetic field
- ~ 30 mm x 30 mm
- gain up to 10^7, excellent single photon detection
- gain uniformity typ. 1 : 2.5;
- cross-talk typ. < 2% (for 2x2 mm^2 pads)
- low DCR, few counts/cm^2/s

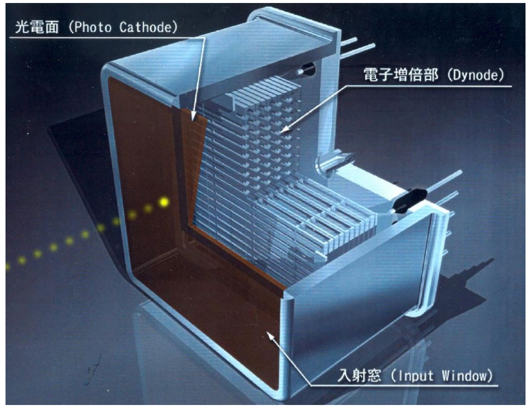

Flat-panel (Hamamatsu H8500):

- 8 x 8 channels (5.8 x 5.8 mm^2 each)
- ~ 50 mm x 50 mm
- Excellent active area coverage (89%)

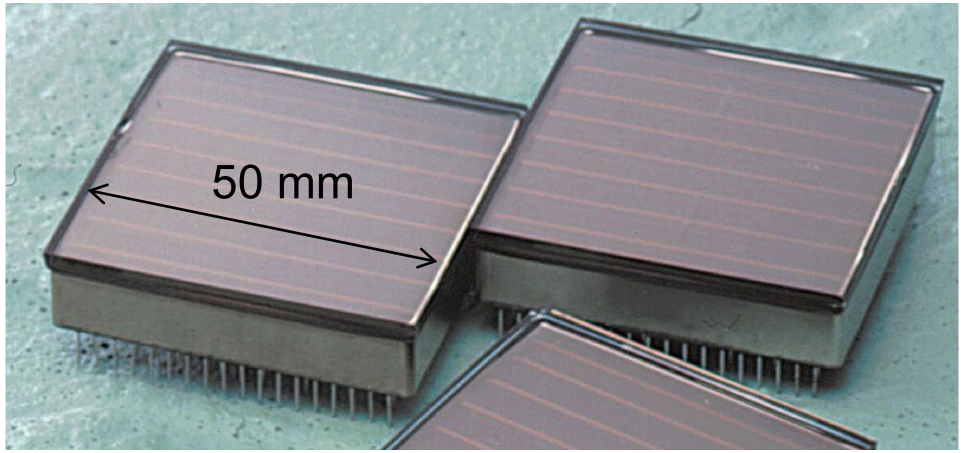

Micro Channel plate PMT (MCP-PMT)

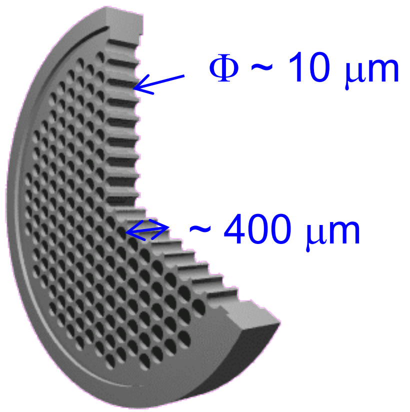

Similar to ordinary PMT – dynode structure is replaced by MCP.

Basic characteristics:

- Gain ~ 10^6 → single photon
- Collection efficiency ~ 60%
- Small thickness, high field
  → small TTS
- Works in magnetic field
- Segmented anode
  → position sensitive

MCP is a thin glass plate with an array of holes (<10-100 μm diameter) - continuous dynode structure

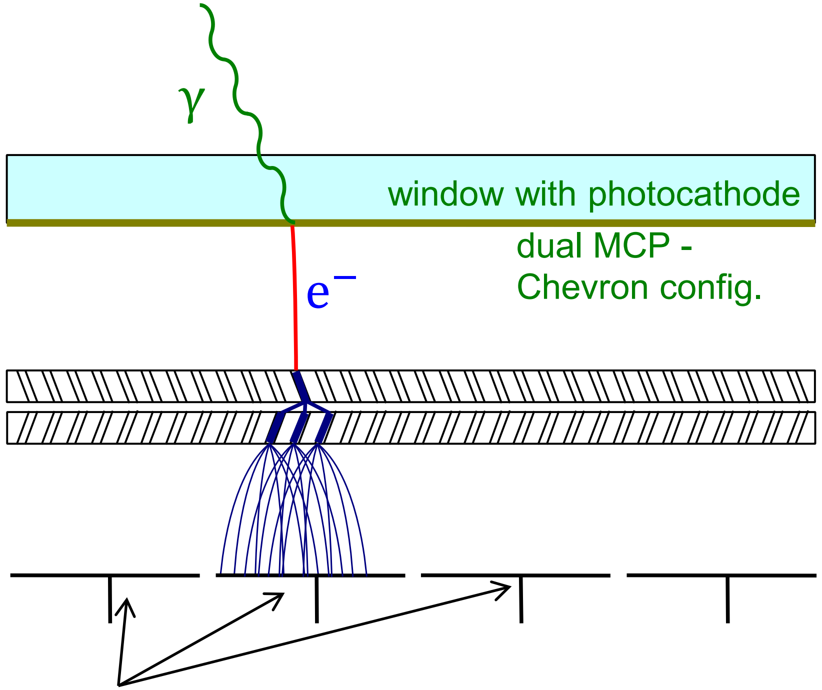

Anodes → can be segmented according to application needs

MCP gain depends on L/D ratio – typically 1000

For L/D=40

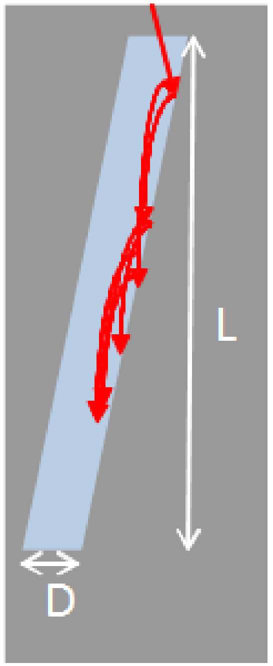

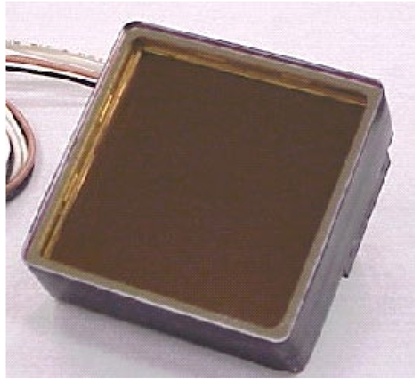

PHOTONIS

HAMAMATSU

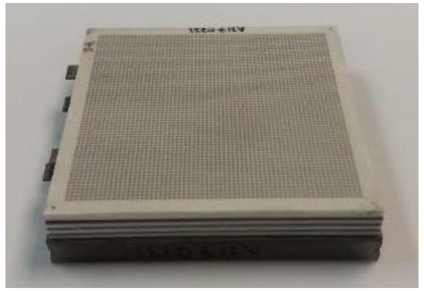

PHOTEK

Hybrid photodetector (HPD) concept

Combination of vacuum and silicon device – multiplication step in silicon. Detection steps:

- photon interacts in photocathode and produces photoelectron
- high electric field accelerates photoelectron
- on impact electron-hole pairs are generated ("bombardment" gain)

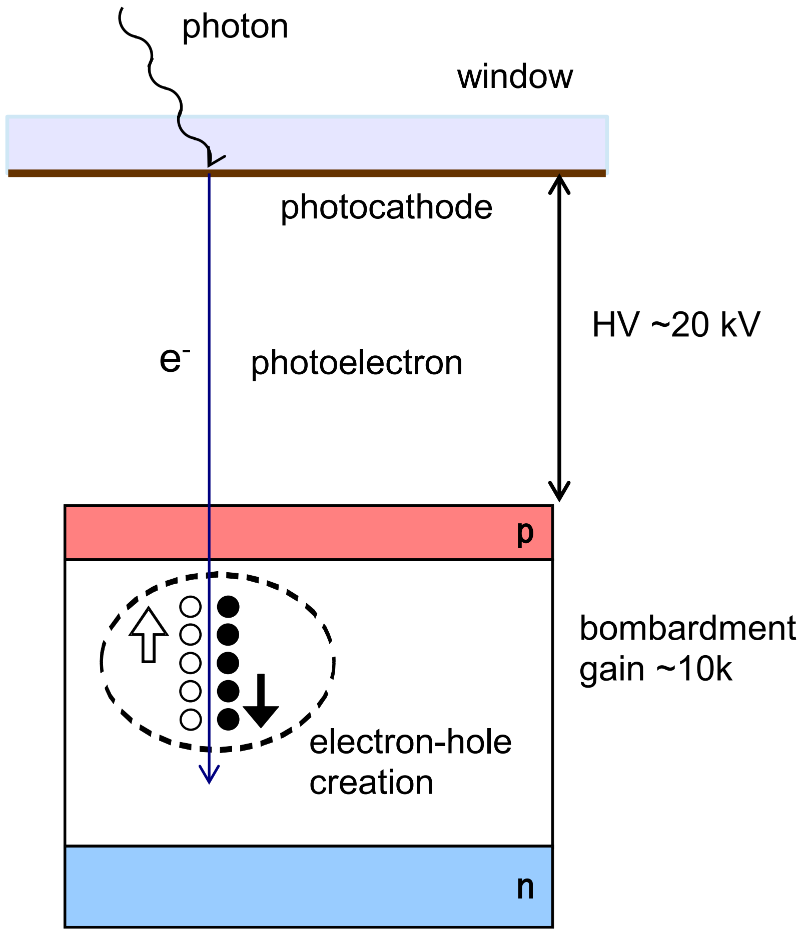

Hybrid avalanche photodetector (HAPD) concept

Combination of vacuum device and avalanche silicon diode:

- first steps equal as in HPD
  → photoelectron acceleration, electron-hole pair generation on impact
- primary electrons drift into avalanche region where they produce second multiplication (~50)
  → lower HV required
  → higher gain
  → higher capacitance → larger electronic noise
- intrinsically very fast